

**Hydrogen-powered aviation –  
techno-economics of flying with green liquid hydrogen**

A holistic evaluation of the pathway to climate-friendlier air travel

Von der Fakultät für Elektrotechnik und Informatik  
der Gottfried Wilhelm Leibniz Universität Hannover  
zur Erlangung des akademischen Grades

Doktor-Ingenieur  
(abgekürzt: Dr.-Ing.)  
genehmigte Dissertation

von Herrn  
Julian Hölzen, M. Sc.

geboren am 20.06.1992  
in Dachau, Deutschland

1. Referent: Prof. Dr.-Ing. Richard Hanke-Rauschenbach  
2. Referent: Prof. Dr. Thomas S. Spengler  
3. Referent: Prof. Dr.-Ing. Andreas Strohmayer  
Tag der Promotion: 16.02.2024



Graphic: © HyNEAT (<https://www.hyneat.de/>)

## Abstract

The aviation sector set itself the target of net-zero CO<sub>2</sub> emissions by 2050. However, there is no silver bullet such as a single technology to achieve this ambitious goal. New technologies like hydrogen (H<sub>2</sub>) propulsion do not only change future aircraft design but also fuel supply chains and operations of aircraft. In comparison to that, new fuels like drop-in synthetic kerosene imply mostly changes to the fuel production and supply infrastructure only, but might cause higher costs and lower resource efficiencies.

The time for technology decisions is now. The sector's main "workhorse" with the most take-offs and causing around 50% of all commercial aircraft emissions is the single-aisle aircraft segment. In this category, the next product launches are expected in the 2030s with final investment decisions by aircraft manufacturers already in less than 5 years. These new aircraft will shape the development of the sector's climate impact in the following 20-30 years and will determine if the 2050 net-zero target can be reached. Consequently, a holistic techno-economic investigation is undertaken for this aircraft segment to evaluate the economic competitiveness of H<sub>2</sub> propulsion concepts compared to other decarbonization options.

It is derived that H<sub>2</sub>-powered single-aisle aircraft technology alone would lead to an average 5%-increase in total direct operating costs for airlines. Therefore, major technology developments are required targeting inter alia the onboard liquid H<sub>2</sub> (LH<sub>2</sub>) tank, high-performing H<sub>2</sub> combustion engines, and safe H<sub>2</sub> fuel system integration.

Moreover, the analysis shows that the main economic uncertainty arises from the supply costs for green LH<sub>2</sub>. Demand scenarios for 2050 indicate that larger-scale supply chains for aviation use might be needed. With annual demands of 100 ktLH<sub>2</sub> or more, major national and intercontinental hub airports could take a H<sub>2</sub> hub role dominating regional H<sub>2</sub> consumption.

Regarding the supply pathways for green LH<sub>2</sub> to airports, three main options are identified: on-site, LH<sub>2</sub> off-site, or gaseous H<sub>2</sub> off-site production. In a first optimization task, it is derived that costs could reach 2.04 USD/kgLH<sub>2</sub> in a 2050 base case scenario for locations with strong renewable energy source (RES) conditions and greater LH<sub>2</sub> demands. This could lead to cost-competitive flying with H<sub>2</sub> compared to fossil kerosene in combination with emission taxes. While the main costs are caused by the RES, water electrolysis, and H<sub>2</sub> liquefaction, the costs for the LH<sub>2</sub> refueling system only mark 3–5% of the total supply costs.

If techno-economic uncertainties are reflected, the LH<sub>2</sub> cost span ranges between 1.37–3.48 USD/kgLH<sub>2</sub> at different airports with good and weaker RES conditions. For the latter, H<sub>2</sub> imports from larger H<sub>2</sub> markets/exporting countries are of special importance to achieve these costs – not only due to less performing RES locally, but also due to limited space availability.

A European-centered case study is performed to combine the optimization of green LH<sub>2</sub> supply and aircraft designs with the investigation of operational strategies in one specific air traffic network. In a 2050 scenario, it is calculated that LH<sub>2</sub> could cost around 2–3 USD/kgLH<sub>2</sub> at main European airports. Then, average total operating costs would be 3% less expensive than flying with synthetic kerosene in the considered network. Tankering, an operational strategy to save fuel costs, might only enable reduced operating costs for H<sub>2</sub>-powered aircraft in the early adoption phase when no larger-scale H<sub>2</sub> import would be available.

Finally, it is found that using LH<sub>2</sub> for aircraft propulsion might lead to lower installation requirements for RES capacity when compared to the synthetic kerosene option. This resource efficiency aspect is another important criterion for choosing the future decarbonization technology in air travel since green electricity will most likely be a constraint resource in the next decades.

## Zusammenfassung

Der Luftfahrtsektor strebt die CO<sub>2</sub>-Neutralität bis 2050 an. Jedoch gibt es zum Erreichen des Ziels bisher keine einzelne, klar überlegende Technologie. Konzepte zur Dekarbonisierung wie neue Flugzeuge mit Wasserstoff-(H<sub>2</sub>)-Antrieben erfordern nicht nur einen neuen Flugzeugentwurf, sondern auch neue Energiebereitstellungsinfrastruktur sowie neue Betriebskonzepte im Luftfahrtsystem. Im Gegensatz dazu könnten existierende Flugzeuge beim Einsatz nachhaltiger Kraftstoffe (SAF) weiter genutzt werden, wobei aber deren Wirtschaftlichkeit aufgrund hoher Kraftstoffkosten im Vergleich zu H<sub>2</sub>-betriebenen Flugzeugen geringer sein könnte.

Die Zeit zum Treffen der notwendigen Technologieentscheidungen ist jetzt. Denn eine neue Produktgeneration im „Single-Aisle“-Flugzeugsegment, das die meisten Starts und etwa 50% der Emissionen in der kommerziellen Luftfahrt ausmacht, wird schon in den 2030er Jahren erwartet. Dafür müssen die endgültigen Investitionsentscheidungen der Flugzeughersteller bereits in weniger als 5 Jahren getroffen werden. Diese neuen Flugzeuge werden die Entwicklung der Klimawirkungen des Sektors in den nächsten 20-30 Jahren prägen und darüber entscheiden, ob das Ziel der CO<sub>2</sub>-Neutralität bis 2050 erreicht werden kann. Folglich wird in dieser Dissertation eine umfassende techno-ökonomische Untersuchung für Wasserstoffantriebe in diesem Flugzeugsegment durchgeführt.

Es wird gezeigt, dass die Betriebskosten für Fluggesellschaften allein durch neue H<sub>2</sub>-betriebene Single-Aisle-Flugzeuge um durchschnittlich 5% steigen würden. Dafür sind wesentliche technologische Entwicklungen erforderlich – unter anderem leichte und kompakte Flüssigwasserstoff-(LH<sub>2</sub>)-Tanks, effiziente H<sub>2</sub>-Verbrennungsturbinen und eine sichere Integration des H<sub>2</sub>-Treibstoffsystems.

Darüber hinaus zeigt die Betriebskostenanalyse, dass die Versorgungskosten für grünes LH<sub>2</sub> die Hauptunsicherheit zur Wirtschaftlichkeit dieser Flugzeuge ausmacht. Dabei deuten 2050-Nachfrageszenarien schon darauf hin, dass möglicherweise große H<sub>2</sub>-Liefermengen für den Luftverkehr erforderlich sein könnten. Mit jährlichen Bedarfen von 100 ktLH<sub>2</sub> oder mehr könnten große nationale und interkontinentale Drehkreuzflughäfen eine besondere Rolle als H<sub>2</sub>-Hubs übernehmen und den regionalen H<sub>2</sub>-Verbrauch dominieren.

Für die Luftfahrt sind drei Bereitstellungsketten von grünem LH<sub>2</sub> von Relevanz: Vor-Ort-Produktion von LH<sub>2</sub> sowie Import von LH<sub>2</sub> oder gasförmigem H<sub>2</sub> von Produktionsorten außerhalb des Flughafens. Im Basisfallszenario 2050 ergeben sich in einer ersten Optimierung Kosten in Höhe von 2,04 USD/kgLH<sub>2</sub> an Standorten mit guten Bedingungen für erneuerbare Energieerzeugung. Dies würde zur Wettbewerbsfähigkeit von Flügen mit H<sub>2</sub> im Vergleich zu fossilem Kerosin in Verbindung mit Emissionsabgaben führen. Die Hauptkosten für LH<sub>2</sub> werden durch die erneuerbare Energieversorgung, Wasserelektrolyse und H<sub>2</sub>-Verflüssigung verursacht. Das LH<sub>2</sub>-Betankungssystem macht nur 3-5% der Gesamtkosten aus.

Wenn zusätzlich technisch-wirtschaftliche Unsicherheiten reflektiert werden, ergibt sich eine Kostenspanne von 1,37–3,48 USD/kgLH<sub>2</sub> an verschiedenen Flughäfen mit günstigeren und teureren erneuerbaren Energiequellen. Bei letzteren Standorten können niedrigere Kosten nur durch H<sub>2</sub>-Importe aus größeren H<sub>2</sub>-Märkten erreicht werden.

Eine auf Europa ausgerichtete Fallstudie kombiniert die Optimierung der grünen Wasserstoffversorgung und des Flugzeugdesigns mit der Untersuchung operativer Strategien in einem bestimmten Luftverkehrsnetzwerk. Im Basisfallszenario für 2050 wird berechnet, dass LH<sub>2</sub> an Flughäfen in Europa etwa 2–3 USD/kgLH<sub>2</sub> kosten könnte. Damit wären die durchschnittlichen Gesamtbetriebskosten im betrachteten Netzwerk um 3% günstiger als beim Fliegen mit synthetischem Kerosin. Das "Tankering", eine betriebliche Strategie zur Senkung der

Treibstoffkosten, könnte nur in der frühen Einführungsphase von H<sub>2</sub>-betriebenen Flugzeugen eine Reduzierung der Betriebskosten ermöglichen, wenn H<sub>2</sub>-Importe noch nicht im größeren Maßstab verfügbar wären.

Außerdem ergibt sich, dass der Einsatz von LH<sub>2</sub> für den Flugzeugantrieb zu geringeren Ausbauanforderungen für erneuerbare Energiekapazitäten führen könnte im Vergleich zur Nutzung von synthetischem Kerosin. Dieser Aspekt der Ressourceneffizienz ist ein weiteres wichtiges Kriterium für die Wahl der zukünftigen Dekarbonisierungstechnologie im Luftverkehr, da grüner Strom in den nächsten Jahrzehnten höchstwahrscheinlich eine stark limitierte Ressource sein wird.

**Keywords:** Green Hydrogen, Liquid Hydrogen, Hydrogen-powered aviation, contains research data

**Schlagwörter:** Grüner Wasserstoff, Klimafreundlichere Luftfahrt, Wasserstoff-betriebene Luftfahrt, enthält Forschungsdaten

## Danksagung

Die vorliegende Arbeit entstand während meiner Tätigkeit als wissenschaftlicher Mitarbeiter am Institut für Elektrische Energiesysteme, Fachgruppe Elektrische Energiespeicher (IfES-EES) der Leibniz Universität Hannover. Die Untersuchungen wurden von der Deutschen Forschungsgemeinschaft (DFG) im Rahmen des Exzellenzclusters (EXC2163/1 – „Sustainable and Energy Efficient Aviation“, Projekt-ID 390881007) gefördert.

Mein besonderer Dank gilt meinem Doktorvater, Herrn Prof. Dr.-Ing. Richard Hanke-Rauschenbach, der ein sehr inspirierender Mentor für mich ist, der seit Tag eins an mein Vorhaben geglaubt hat und mit dem die Zusammenarbeit immer extrem bestärkend und vertrauensvoll ist.

Herrn Prof. Dr. Thomas S. Spengler und Prof. Dr.-Ing. Andreas Strohmayer danke ich vielmals für die Übernahme der Gutachten und für die guten Diskussionen im Rahmen der Prüfung. Ebenso gilt mein Dank Herrn Prof. Dr.-Ing. Lutz Hofmann für die Übernahme des Prüfungsvorsitzes.

Die Zeit am Institut hat vor allem wegen und mit den vielen aktiven sowie ehemaligen Kolleg:innen so viel Spaß gemacht, denen ich herzlich danken möchte. Um einige hervorzuheben, die mich auch immer mit Rat und Tat unterstützt haben, nenne ich an dieser Stelle Lukas Koenemann, Inga Beyers, Lukas Kistner, Finn Schenke, Clemens Lohr, Sven Wiegemann, Lena Böhre, Janis Woelke, Jonathan Brandt, Agate Martin, Waris Ziarkash und Levin Matz sowie vor allem Dr.-Ing. Astrid Bensmann und Dr.-Ing. Boris Bensmann als Betreuende während meiner Zeit am Institut. Auch meinen Studierenden möchte ich für die hilfreichen Diskussionen danken – vor allem Moritz Flohr, Nils-Eric Rahm, Nils Farid Kosfeld, Manuel Wilker, Timo Schelm und Erik Stabenow.

Zudem wäre der breite Themenschwerpunkt meiner Dissertation inklusive der Diskussion rund um das Flugzeugdesign nicht ohne Daniel Silberhorn und Thomas Zill vom Deutschen Luft- und Raumfahrtzentrum in Hamburg möglich gewesen. Danke für die lange und sehr inspirierende Zusammenarbeit.

Mein Dank gilt zudem auch der Stiftung der Deutschen Wirtschaft gGmbH, die meine Arbeit aus Mitteln der Promotionsförderung des Bundesministeriums für Bildung und Forschung gefördert hat.

Bei meinen Eltern, die mir das Studium und damit auch die Promotion ermöglicht haben, bedanke ich mich von ganzem Herzen. Ihr habt mir Kreativität und Forschergeist mitgegeben und mich immer auf meinem Weg mit allen Kräften unterstützt.

Zuletzt bin ich meiner Ehefrau und meiner Tochter zutiefst dankbar für die Unterstützung bei diesem zum Teil berufsbegleitenden „Projekt“. Trotz stressiger Zeiten habt ihr mich immer wieder aufgefangen und sichergestellt, dass es mir und uns als Familie gut ging.

**Contents**

<b>Abbreviations .....</b>	<b>IX</b>
<b>Nomenclature .....</b>	<b>X</b>
<b>Indices.....</b>	<b>XI</b>
<b>1 Introduction .....</b>	<b>1</b>
<b>2 State of research and research questions.....</b>	<b>4</b>
2.1 Role of green LH <sub>2</sub> infrastructure for aviation.....	4
2.2 Green LH <sub>2</sub> supply chains and components .....	10
2.2.1 Renewable electricity for green H <sub>2</sub> production .....	10
2.2.2 Gaseous hydrogen components.....	12
2.2.3 Liquid hydrogen components .....	15
2.3 Derived research questions and structure of the thesis.....	19
<b>3 Costs of flying and H<sub>2</sub>-powered aircraft design .....</b>	<b>22</b>
3.1 Direct operating cost method .....	22
3.2 H <sub>2</sub> -powered aircraft design and cost impacts .....	24
<b>4 Context for LH<sub>2</sub> aircraft refueling at airports .....</b>	<b>29</b>
4.1 LH <sub>2</sub> demand scenarios for aviation .....	29
4.2 Refueling routes and costs considerations.....	34
<b>5 Green LH<sub>2</sub> supply costs for airports .....</b>	<b>39</b>
5.1 Green LH <sub>2</sub> supply chain optimization .....	39
5.1.1 General design of study .....	39
5.1.2 Methodology and model equations.....	41
5.1.3 Scenario definitions.....	46
5.2 LH <sub>2</sub> on-site supply chains.....	50
5.2.1 LH <sub>2</sub> energy system design rules for fixed demand setting .....	51
5.2.2 Variation of annual LH <sub>2</sub> demands .....	57
5.2.3 Scenario analysis of on-site LH <sub>2</sub> setups .....	59
5.3 Off-site supply chains.....	61
5.3.1 LH <sub>2</sub> off-site setups .....	61
5.3.2 GH <sub>2</sub> off-site setups .....	64
5.3.3 Scenario analysis for import options.....	67
5.4 Implications for overall research objectives.....	70
<b>6 Green LH<sub>2</sub> supply in air traffic networks.....</b>	<b>71</b>
6.1 Reference air traffic network .....	71
6.1.1 Main characteristics of chosen air traffic network .....	71

---

6.1.2	Relevant airport categories.....	72
6.2	Optimized LH <sub>2</sub> supply costs at selected airports .....	73
6.2.1	Assumptions for LH <sub>2</sub> infrastructure optimization .....	73
6.2.2	LH <sub>2</sub> cost results in 2050 scenario .....	76
6.3	H <sub>2</sub> -powered aircraft fleets.....	79
6.3.1	Aircraft design results.....	79
6.3.2	Operation of H <sub>2</sub> -powered aircraft .....	82
6.4	Resulting operating costs for H <sub>2</sub> -powered aircraft .....	84
6.4.1	Comparison of decarbonized aircraft options in 2050 scenario.....	84
6.4.2	Re-evaluation of results in 2035-2040 (early adoption) scenario .....	87
6.4.3	Resource perspectives for the future of H <sub>2</sub> -powered aviation .....	87
<b>7</b>	<b>Conclusions.....</b>	<b>90</b>
7.1	Perspectives on research problem.....	90
7.2	Perspectives on methodology .....	95
7.3	Outlook.....	97
	<b>A Direct Operating Cost modelling .....</b>	<b>99</b>
	<b>B Aircraft design methodology .....</b>	<b>102</b>
	<b>C LH<sub>2</sub> demand projections.....</b>	<b>103</b>
	<b>D Modeling of LH<sub>2</sub> energy systems.....</b>	<b>109</b>
	<b>E Case study data and calculations.....</b>	<b>126</b>
	<b>F Publication contributor roles.....</b>	<b>132</b>
	<b>G Curriculum Vitae.....</b>	<b>133</b>
	<b>Figures.....</b>	<b>135</b>
	<b>Tables.....</b>	<b>137</b>
	<b>Bibliography .....</b>	<b>138</b>



**Abbreviations**

ASK	Available seat kilometer
BRE	Bremen Airport
CAPEX	Capital expenditures
DAC	Direct air capture
DOC	Direct operating costs
ELY	Electrolysis system
EIS	Entry-into-service
ES	Electric energy storage system
FRA	Frankfurt Airport
FT	Fischer-Tropsch-Synthesis
GH <sub>2</sub> Sto	GH <sub>2</sub> storage
GH <sub>2</sub> comp	GH <sub>2</sub> compressor
H <sub>2</sub> , GH <sub>2</sub> , LH <sub>2</sub>	Hydrogen, gaseous hydrogen, liquid hydrogen
HAM	Hamburg Airport
HYB	Tag for great hybrid RES location
IATA	International Air Transport Association
LCOE	Levelized costs of electricity
LFP	Liquefaction plant
MTOM	Maximum take-off mass
NH <sub>3</sub>	Ammonia
NM	Nautical miles
NO <sub>x</sub>	Nitrogen oxides
OEM	Operating empty mass
OPEX	Operating expenditures
PAX	Passengers
PV	Photovoltaics; tag for PV location
RES	Renewable energy source
SA	Single-aisle
SAF	Sustainable aviation fuels
SEC	Specific energy consumption
tpd	Tons per day
WEAK	Tag for weaker hybrid RES location
WOFF	Tag for wind off-shore location
WON	Tag for wind on-shore location

## Nomenclature

$a$	Annuity payment factor	1/a
$b$	Binary optimization variable	-
$C$	Cost	USD <sub>2020</sub>
$c$	Specific cost	USD <sub>2020</sub>
$d$	Distance	NM
$E$	Electric energy	kWh
$e$	Specific energy consumption	kWh
$f$	Factor (cost or availability)	-
$F$	Fill level of storage	%
$i$	Interest rate	%
$k$	Pipe roughness coefficient	m
$k_{BO}$	Self-discharging / boil-off loss factor for LH <sub>2</sub> storage	%/d
$K$	Compressibility	1/Pa
$\kappa$	Heat capacity ratio	-
$LR$	Learning rate	-
$m$	Mass	kg
$\dot{m}$	Mass flow	kg/s
$n$	Amount	-
$NRC$	Non recurring cost for aircraft manufacturing	USD <sub>2020</sub>
$\eta$	Efficiency	%
$P$	Electric power	kW
$p$	Pressure or price	Pa or USD <sub>2020</sub>
$PM$	Profit margin	%
$\rho$	Density	kg/m <sup>3</sup>
$r$	Cost reduction factor	-
$R$	Universal gas constant	J/(K mol)
$RC$	Recurring cost for aircraft manufacturing	USD <sub>2020</sub>
$S$	Market size	-
$T_{DP}$	Depreciation period	a
$T$	Temperature	K
$t$	Time	H
$v$	Speed	km/h
$\dot{v}$	Flow speed	m/s
$w$	Work	J

---

$x$	Design capacity	-
$Z$	State of a storage component	-
$Z_{H_2}$	Compressibility factor for hydrogen	-
$\lambda$	Friction factor	-

**Indices**

AC	Aircraft
ATC	Air traffic control
avail	Available
DOC	Direct operating cost
GH2Sto	GH <sub>2</sub> storage
GH2Comp	GH <sub>2</sub> compressor
HEX	Heat exchanger
$i$	Supply component $i$
ind	Indirect CAPEX
ins	Insurance
inst	Installation CAPEX
LH2sto	LH <sub>2</sub> storage
maint	Aircraft maintenance
misc	Miscellaneous (aircraft spare parts)
OM	Operation and maintenance
PL	Part-load
refri	Refrigerant
RV	Residual value
$t$	Time period/scenario
TAC	Total annual costs

## 1 Introduction

Time is running. Climate scientists are sharing alarming signals on climate change with new records-high surface temperatures and melting polar caps as well as catastrophic events like droughts, flooding, or wildfires [1,2]. The required 2.0- or even 1.5-degree targets, which must be achieved to prevent uncontrollable tipping points in the planet's climate and biodiversity, are approached faster and faster [3]. This is why, directives all over the world were introduced in the last years to reach carbon neutrality by 2050 over all sectors [4]. In Europe, this was done with the Green Deal of the European Commission [5].

The aviation sector also set itself the goal of decarbonization [6]. Even though only 2-3% of global carbon emissions stemmed from the sector in 2019 [7], this goal is especially hard to achieve due to five reasons.

First, air travel is one of the sectors with high growth projections over the next decades and hence, a strong increase in emissions is predicted [4]. This trend can be underlined by the fast recovery of the sector after the COVID health crisis, already reaching pre-COVID traffic volumes in 2023 instead of 2025 as predicted in several industry forecasts [8,9].

Second, the challenge is not only about CO<sub>2</sub> emissions but also about the total climate impact of aviation. There is still an ongoing scientific debate about whether the total climate impact of aviation is a factor two or even three as high as its CO<sub>2</sub> emissions alone, but there is high certainty on the importance of reducing these non-CO<sub>2</sub> emission effects [9–12]. The combustion of fossil fuels produces exhaust gas products such as nitrogen oxides (NO<sub>x</sub>), water vapor, and soot particles. While the former can cause the formation of climate-harming ozone, the latter two can lead to contrails and cirrus clouds with a high warming impact on the climate [11,12]. Furthermore, noise and local emissions around airports like particle matter – another product from fossil fuel combustion – are a threat to the health of local neighborhoods [13,14].

Third, the COVID health crisis and linked shutdowns led to significant financial instabilities for the aviation sector including the whole supply chain from aircraft manufacturers to airlines. Financial aid from governments was required. Even though some financial support schemes like in France were linked to the condition of developing more climate-friendly aircraft [15], the strained financial situation of the industry might still be a challenge for future billion-dollars-heavy technology innovation programs.

Fourth, the introduction of new aircraft underlies very long cycles of product development and then long times of fleet renewal [16]. Since the development cycles usually take around 15 years and more modern, efficient aircraft were introduced in the mid-2010s (e.g., Airbus A320neo, Boeing 737max), new products are expected to be on the market by the 2030s. If more climate-friendly aircraft technologies were developed by then, their impact on the climate would not be worth mentioning before the 2040s and hence, could still not lead to full climate impact reduction by 2050 [17–19].

Fifth, unlike in other sectors there is not one technology that will lead to climate neutrality for the whole sector while achieving competitive costs and best efficiency using constraint resources [18,20,21]. With a focus on commercial passenger transportation only (~85% of aviation's emissions), most emissions are caused by wide-body, then single-aisle, and only a small amount by regional and commuter aircraft segments [7]. Contrary to that, most efficient, climate-friendlier options such as battery-electric propulsion systems might only be eligible for the smaller aircraft segments. The larger the aircraft, flying longer distances, the more critical the gravimetric and volumetric densities of a future propulsion system get. Consequently, battery-electric flight with its low battery energy density might not help decarbonize the two major aircraft segments [22–25].

It becomes clear that several mitigation measures are required to overcome the climate impact challenge in the aviation sector. There are two approaches to achieve this: incremental improvements including different operations as well as new propulsion fuels and technologies.

In the first approach, efforts concentrate on further improving the propulsion and aerodynamic efficiency of aircraft. This includes even more advanced wing designs or new (fossil) propulsion concepts such as an open rotor engine concept [20]. However, these measures might only lead to 5-20% of further fuel burn reduction in the next decades [18]. Different operational procedures include more efficient air traffic control and routing in the air but also on the ground. Another operational lever is optimized routing to avoid forming of contrails and cirrus clouds. Their formation and hence, the global warming potential depends on the flight altitude and the atmospheric air conditions. So, re-routing flights to different altitudes or not flying through contrail-formation-likely regions, could lead to a significant reduction of non-CO<sub>2</sub> emission effects. Nevertheless, it still leads to an increase in CO<sub>2</sub> emissions when flying with fossil kerosene due to less efficient flight routes [26,27].

The second approach includes new propulsion technologies, e.g., battery-, hybrid-electric, or hydrogen (H<sub>2</sub>) approach, and alternative fuels, e.g., sustainable aviation fuels (SAF) [28]. Two main forms of SAF are considered here: biofuels from biomass or residual waste and electricity-derived synthetic fuels. Both are kerosene-like fuels that are in most cases compatible with existing aircraft without changes to the aircraft design. Biofuels can lead to a net CO<sub>2</sub> emission reduction of 94% [29], but in the long-term, their feedstock availability might be limited and comes with competition to other land use and/or potentially lead to other harmful climate impacts [30,31]. In contrast to that, electricity-derived synthetic fuels (synfuels, also called Ptl, power-to-liquids) require renewable energy for the production and synthesis of H<sub>2</sub> and CO<sub>2</sub> to derive a kerosene-like hydrocarbon. The latter is captured from industrial processes or directly from the air [32]. Depending on the source of CO<sub>2</sub> and the electricity, this can lead to carbon net neutrality using such synfuels. Nevertheless, hydrocarbons would still be combusted in flight and hence, the reduction potential of non-CO<sub>2</sub> emission effects is limited but also still highly uncertain [26,33].

Regarding new propulsion systems, these do not only require new fuel supply infrastructure setups such as SAF but also new aircraft designs. As mentioned, the future of battery-electric propulsion for larger commercial aviation is not given with current battery performance projections. This is also true for hybrid-electric propulsion which is scalable to much larger segments, but their climate impact reduction potential is very limited for larger aircraft than regional ones [34,35].

Only direct H<sub>2</sub> propulsion is currently discussed as a new technology applicable to larger aircraft and achieving true zero CO<sub>2</sub> emissions, if green H<sub>2</sub> is utilized [16,36]. H<sub>2</sub> can be either used via thermal conversion (e.g., jet engines) or through electrochemical conversion in fuel cells. Both require new aircraft designs to integrate the propulsion and the fuel system, i.e. H<sub>2</sub> storage on-board [37,38]. Since H<sub>2</sub> combustion engines have a higher power density than fuel cells, these are not only applicable to smaller single-aisle but also wide-body aircraft [29,39]. Both H<sub>2</sub> propulsion concepts do not cause any CO<sub>2</sub> emissions in flight. Moreover, NO<sub>x</sub> and soot emissions can be reduced significantly with the combustion approach and fully eliminated with fuel-cell-powered propulsion [40,41].

In addition, the first high-level estimates show that the fuel supply of H<sub>2</sub> might require fewer renewable energy sources (RES) compared to the requirements for synfuel production [16,42]. In a time where all sectors strive for decarbonization and most of them require green electricity, the latter might become a constraint resource, and hence, resource efficiency becomes crucial for successful decarbonization [43].

It has to be highlighted that most of the global H<sub>2</sub> production is not carbon-free and still relies heavily on fossil fuels today. However, strong momentum for the large-scale deployment

of green H<sub>2</sub> production capacities can be observed worldwide. There are more than 30 national H<sub>2</sub> strategies and more than USD 300 Bn investments for H<sub>2</sub> projects [44]. Thus, larger sector-overarching and even aviation-specific H<sub>2</sub> projects were announced in the last years: in 2020, Airbus announced their ZeroE aircraft program with H<sub>2</sub>-powered single-aisle aircraft [45], and the first commercial H<sub>2</sub>-powered test flights were conducted by ZeroAvia and Universal Hydrogen [46,47]. Furthermore, H<sub>2</sub> infrastructure developments have been started in the aviation sector. As an example, Airbus, Groupe ADP, AirFrance-KLM Group, Paris Region, and Choose Paris Region initiated an H<sub>2</sub> hub airport consortium that plans to work on supplying and handling H<sub>2</sub> at airports [48].

Overall, it is found that H<sub>2</sub>-powered aviation is a promising field of research aiming to reduce the climate impact of aviation. However, there are only limited financial resources in this sector available. Consequently, the transition to such a new technology must be as cost competitive as possible. Furthermore, time is also running out if H<sub>2</sub>-powered aircraft should become a reality. The final financial decisions on starting the commercialization of the next single-aisle aircraft programs for entry into service in the 2030s are due in less than 5 years according to Airbus [45]. So, all industry-relevant evaluations must be available in the next years to enable informed decisions on the future of flying.

This is why, this dissertation focuses on the future of H<sub>2</sub>-powered aircraft and its economic competitiveness. The main focus is set on the green H<sub>2</sub> supply and refueling setups for airports, since aircraft-focused studies already tackled the topic to a greater extent, but also because the economic uncertainties are specifically high when it comes to green H<sub>2</sub> supply. This is further elaborated in the next chapter. There, the main research questions and the dissertation's structural setup are derived based on the state of the literature and emerging research issues.

## 2 State of research and research questions

Existing literature on the topic of H<sub>2</sub>-powered aviation and H<sub>2</sub> infrastructure is screened to derive the main research gaps that this dissertation then builds on. This is done in two steps: scanning concrete studies on H<sub>2</sub> infrastructure for the aviation or mobility context and then, analyzing insights from studies on specific component groups to produce and deliver H<sub>2</sub> for use in aircraft.

This work focuses on commercial (passenger) air travel, which accounts for more than 85% of all CO<sub>2</sub> emissions in the aviation sector [7]. As described in the previous chapter, the main share of CO<sub>2</sub> emissions stems from larger commercial aircraft segments like the single-aisle and wide-body segments. This is why, the scope of this work is also set on these types of aircraft. Such larger aircraft would need onboard storage and hence, be refueled with liquefied, cryogenic hydrogen (LH<sub>2</sub>) to enable H<sub>2</sub> propulsion [37,49–51]. The reason for this is that LH<sub>2</sub> has a higher volumetric energy density compared to compressed gaseous hydrogen (GH<sub>2</sub>) and leads to smaller, lighter storages and thus, enables more efficient aircraft designs. Further insights into aircraft design will be shown in Chapter 3. Consequently, the literature review also targets research on LH<sub>2</sub> infrastructure.

**Disclosure:** The following section is in large parts based on the publication: J.Hoelzen, D. Silberhorn, T.Zill, B. Bensmann, R. Hanke-Rauschenbach, Hydrogen-powered aviation and its reliance on green hydrogen infrastructure – Review and research gaps, International Journal of Hydrogen Energy (2022) [52]. For a detailed description of the author's contributions see Appendix F.

### 2.1 Role of green LH<sub>2</sub> infrastructure for aviation

This section investigates previous research and the uncertainties behind all aspects of deploying a green LH<sub>2</sub> infrastructure for aviation including also a review of methodological approaches used in research so far. Thus, it leads to the first high-level assessment of cost uncertainties based on these previous studies.

#### Studies on H<sub>2</sub> for use in aviation

In the first step, detailed cost assessments in the literature are identified that fit the H<sub>2</sub> aviation context and focus on green H<sub>2</sub> supply. The relevant studies are summarized in Table 2.1. The literature is scanned for information on the different supply chain components, detailed cost assessments, LH<sub>2</sub> supply pathway analysis, and consideration of cost-reducing effects from a broader, global H<sub>2</sub> economy (columns of the table).

In general, only a few recent studies are found with a focus on an LH<sub>2</sub> fuel infrastructure for aviation use providing a detailed fuel cost assessment (Table 2.1). Most studies found investigated the technological feasibility of H<sub>2</sub> aircraft and only provide a short or qualitative overview of potential factors influencing H<sub>2</sub> fuel costs. These literature findings are clustered into older and more recent analyses as well as their thematic focus, describing H<sub>2</sub> infrastructure for aviation or related topics.

Older publications from the 1970s-1990s by Linde, NASA, Boeing, Lockheed, and other organizations as well as reports of the 2000s European Cryoplane project provided the first broader insights into LH<sub>2</sub> infrastructure for aviation.





Johnson [53], Brewer [54,55,58], Boeing [57], and Korycinski [56] developed comprehensive views on the technological feasibility for H<sub>2</sub>-powered aircraft and LH<sub>2</sub> infrastructure setups at airports including refueling systems and the design of the interface to the aircraft. However, their focus lay on grey H<sub>2</sub> sourcing and did not reflect a general uptake of a green H<sub>2</sub> economy. In 1983, Jones et al. [74] modeled cryogenic pipeline systems at airports to transport LH<sub>2</sub> from central storage facilities to the aircraft refueling stand, but without any economic evaluation or context to a broader setup of an LH<sub>2</sub> supply chain. In 1987, Alder and team [59] investigated the LH<sub>2</sub> supply costs for Zurich airport with a supply setup including electrolysis on-site at the airport fed by nuclear power. But their analysis considered a very small demand with 15-30 tons of LH<sub>2</sub> per day only and neglected other topologies making use of a global H<sub>2</sub> infrastructure. Other broader analyses including aircraft and infrastructure perspectives are from Contreras et al. [60] looking into the specific H<sub>2</sub> infrastructure at Chicago Airport. A similar overview is also provided by Armstrong et al. [75]. Schmidtchen et al. [61] qualitatively described the setup of LH<sub>2</sub> energy systems but with the main research goal to analyze the safety of H<sub>2</sub> handling at airports. A topic that was just recently brought up again in the ENABLEH2 project by Benson et al. [76].

Around the 2000s, Sefain [63] analyzed airport operations and the impact on the turnaround process for an LH<sub>2</sub>-fueled aircraft. In the Cryoplane project [62], detailed overviews can be found for H<sub>2</sub>-powered aircraft designs, fleet transition scenarios, supply of H<sub>2</sub>, and refueling options via truck and LH<sub>2</sub> pipelines. At that time, a certification standard for airport H<sub>2</sub> fueling facility operations (ISO/PAS 15594 [77]) was issued. It describes the requirements for a safe refueling setup at airports. However, it was withdrawn later. In the following years, further complementary, qualitative studies brought insights on H<sub>2</sub> aircraft design, H<sub>2</sub> fuel supply, and airport refueling implications, e.g., for a major airport in Sweden [64,65] or for other general overviews [37,78,79]. But in none of the mentioned studies, a detailed LH<sub>2</sub> cost analysis is conducted that reflects the developments of low-cost RES availability that have been observed in recent years [80].

Other investigations also target H<sub>2</sub> handling at airports but with a focus on other applications than aircraft propulsion. These studies consider H<sub>2</sub>-powered Ground Supply Equipment (GSE), taxiing systems, or Auxiliary Power Units (APUs) for aircraft – all with relatively low H<sub>2</sub> demand scales.

In a demonstration project at Munich Airport, the feasibility of GH<sub>2</sub> and LH<sub>2</sub> supply was tested for GSE [81,82]. In addition to that, Testa et al. [83] looked into the potential to reduce emissions at airports by switching the propulsion systems of GSE to H<sub>2</sub>. In 2010, Stiller and Schmidt [67] investigated H<sub>2</sub> infrastructure topologies to fuel APU systems. Stockford et al. [84] analyzed electric aircraft taxiing systems for an Airbus A320 powered by a fuel cell.

Furthermore, three studies are identified that research energy systems at airports. In the HYPOR project at Toulouse Airport [85], energy systems for the airport environment were modeled including H<sub>2</sub> applications. However, no clear focus on H<sub>2</sub> aircraft propulsion can be found, rather more highlights on other uses, e.g., ground transportation, general electrification, and building heat. Similar studies including H<sub>2</sub> use cases were also conducted by Robles [86] and Xiang [87].

Another group of analyses concentrates on the climate impact of H<sub>2</sub>-powered aviation with a focus on the production ways of H<sub>2</sub>. Victor [88], Janic [89,90], and Yilmaz et al. [91] determined emission overviews from LH<sub>2</sub> supply and propulsion in aviation based on different scenarios for H<sub>2</sub> aircraft deployment. Similar research can be found in [92] and [93].

Only recent studies on H<sub>2</sub>-powered aircraft investigate the economic competitiveness of green H<sub>2</sub> supply for aviation and include H<sub>2</sub> cost reduction effects of an industry-overarching global H<sub>2</sub> economy.

Stadler [69] conducted a techno-economic study of LH<sub>2</sub> supply for aviation based on thermochemical electrolysis. Results from that study were picked up in [68] and [94]. In the MA-HEPA project, Marksel et al. [70,71] looked into several infrastructure cost aspects for LH<sub>2</sub> for a regional airport, but without deriving or even optimizing total LH<sub>2</sub> supply costs. The Flying-V project at TU Delft [95] introduced a brief overview of LH<sub>2</sub> logistics aspects and LH<sub>2</sub> supply costs, but without providing any detailed insights.

In a case study for the Los Angeles Airport, Amy and Kunycky [72] assessed the costs for green H<sub>2</sub> on-site production and liquefaction. They included scaling factors for larger LH<sub>2</sub> demands and considered a growing H<sub>2</sub> economy that could lead to reduced CAPEX and optimized efficiencies. Nevertheless, the interconnection to off-site H<sub>2</sub> production capacities and demands as well as a pathway optimization were not investigated.

Fusaro et al. [73] provided an assessment of LH<sub>2</sub> supply costs for hypersonic H<sub>2</sub> transportation systems. The study shows supply costs for key components, but supply pathways including transport costs, or their optimization were not considered.

Only a recent study by the Clean Sky 2 JU and FCH 2 JU [42] provides more detail about supply topologies and their economics including on- and offsite H<sub>2</sub> supply. It also includes a roadmap for cost-efficient infrastructure deployment and scenarios on potential H<sub>2</sub> uptake.

From this first H<sub>2</sub> aviation-relevant literature survey it can already be summarized that there is a lack of research around LH<sub>2</sub> infrastructure optimization for aviation. Only a few recent studies touched on cost effects depending on the supply topology and the access to low-cost RES. This is why, also other studies with a related scope are considered in the following.

### **Studies on LH<sub>2</sub> energy system optimization**

Regarding the used methodologies behind H<sub>2</sub> energy system optimization approaches, most of the recent H<sub>2</sub>-powered aviation-linked studies use simpler techno-economic calculations (mostly in Microsoft Excel) [16,72,73]. While this might lead to good first overviews on the topic, statements on detailed interlinkages and design decisions of energy system components cannot be tested [96]. This is why, a short overview of other non-aviation studies with more detailed methodological approaches linked to LH<sub>2</sub> and H<sub>2</sub> energy system optimization is given in the following.

There are a large number of studies that apply more advanced methodologies to analyze H<sub>2</sub> energy systems [97–102]. Most of these optimize the general integration and design of renewable energy supply (RES) systems with GH<sub>2</sub> supply components. This often focuses on the general supply chain design, but can also concentrate on specific geographical contexts like global, national, or regional levels [103,104]. Due to the geographical complexity, linear modeling approaches with simplified techno-economic models are used to ensure reasonable computability [96]. Another related research field using the same linear optimization methodology is the investigation of distributed H<sub>2</sub> applications such as refueling stations or industrial applications [105–110]. Given the use of simplified component models and constant parameters, e.g., constant efficiency of conversion components, such analyses cannot and do not aim to fully reflect all techno-economic and design effects between components.

Only a recent study from Sens et al. [111] considers green LH<sub>2</sub> supply chains for LH<sub>2</sub>-powered heavy-duty vehicles using a comprehensive techno-economic study design. Nevertheless, the approach is also rooted in a linear modeling approach potentially neglecting dynamic

effects and change of efficiencies when operating RES and (L)H<sub>2</sub> component systems. Moreover, the study does not address significantly larger concentrated demands at one specific location (airport) which can lead to relevant economies of scale effects as expected for the LH<sub>2</sub> use in aviation [112].

### LH<sub>2</sub> supply chain costs derived from literature review

The first cost insights from the previous studies on green LH<sub>2</sub> supply systems that could be applied to the aviation context are briefly calculated. Based on the techno-economic assumptions and used methodologies in the respective studies, LH<sub>2</sub> costs are synthesized. For further information on the exact calculation method of the following results, please see the original published analysis in the paper [52].

A clear picture evolves when looking into three LH<sub>2</sub> fuel cost scenarios at the refueling dispenser compared to kerosene costs, see Figure 2.1. The scenarios can be distinguished by differently progressive techno-economic assumptions. For the comparison, average kerosene costs in 2019 of 0.6 USD per kg are converted into LH<sub>2</sub>-equivalent cost based on its gravimetric energy densities [29,52,113,114]. All costs in this thesis are shown in 2020-equivalent USD.

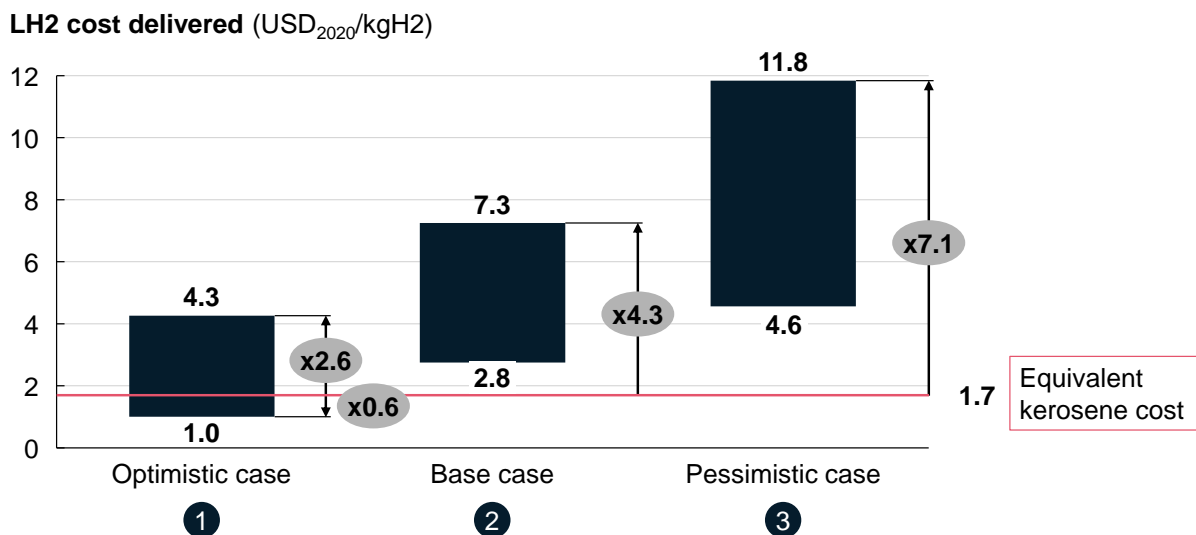


**Figure 2.1:** Cost ranges for LH<sub>2</sub> at the dispenser derived from literature review depending on three H<sub>2</sub> cost scenarios (from optimistic to pessimistic), see also [52]; comparison to kerosene costs translated into LH<sub>2</sub>-equivalent costs based on LHV of kerosene and LH<sub>2</sub> – not considering different aircraft efficiencies

The LH<sub>2</sub> cost analysis reveals that fuel costs for H<sub>2</sub>-powered aircraft could be competitive or even less expensive by a factor of 0.6 in an optimistic scenario only. Taking an average LH<sub>2</sub> cost in this scenario of 2.6 USD/kgLH<sub>2</sub>, this results in higher fuel DOC by a factor of 1.6. In a base case scenario, this cost premium factor would already be 3.0 for an average LH<sub>2</sub> cost of 5.0 USD/kgLH<sub>2</sub>. The uncertainty range for the cost premium is even broader for pessimistic scenarios, in which the difference in fuel costs could be up to a factor of 7.1 for LH<sub>2</sub> fuel.

In general, two trends are emphasized from this comparison and the cost calculations in the existing literature.

First, in optimistic scenarios, higher H<sub>2</sub> demands might lead to significantly lower LH<sub>2</sub> costs due to scaling and learning effects and only if access to low-cost RES is given.

Second, the cost assumptions from the aviation-specific studies mostly rely on such optimistic LH<sub>2</sub> cost assumptions, while the other non-aviation studies rather consider base and pessimistic case scenarios. This means that either the assumptions in studies investigating the use of LH<sub>2</sub> in aviation might have been too positive, or that reasonable aspects are supporting this. Latter could be that the H<sub>2</sub> demand for aircraft would trump the demand from other industries or that special, large-scale supply pathways could be enabled for the aviation use case. Both aspects will be further discussed in Chapters 4 and 5.

Moreover, the findings from Figure 2.1 underline the high volatility and uncertainty coming from the LH<sub>2</sub> fuel costs and hence, the setup of a large-scale, low-cost, and green H<sub>2</sub> infrastructure. While the aviation-specific studies count on more optimistic settings in the long term, transition scenarios might cause significantly higher fuel costs.

Nevertheless, it is also important to consider the uncertainty behind the development of kerosene costs over the next decades including potential emission taxes for fossil fuels.

### **Studies on a broader evaluation of H<sub>2</sub>-powered aircraft in future air traffic contexts**

In the last step and building on the first high-level LH<sub>2</sub> cost insights, a last review step is undertaken. Recent studies are identified that go beyond one specific aspect of H<sub>2</sub>-powered aviation (often either infrastructure or aircraft) but rather combine several topics in a broader picture.

There are three groups of literature with more holistic views on H<sub>2</sub>-powered aviation.

First, papers are considered that look into the integration of RES in an airport environment and combine this with an assessment of aircraft and airport requirements. Results of these studies are, e.g., scales of LH<sub>2</sub> demand for aircraft, the applicability of H<sub>2</sub> for other applications at the airport than aircraft, safety considerations, or qualitative LH<sub>2</sub> infrastructure deployment plans [16,112,115–119].

Second, there are some studies discussing the impacts of integrating H<sub>2</sub>-powered aircraft into specific air traffic networks on a qualitative basis [71,120–122]. In these, not only requirements for the installation of LH<sub>2</sub> supply chains are reflected, but also flight ranges and operational principles are included in the assessment. One report even brings together these first two groups of literature [21]. It calculates capital costs for LH<sub>2</sub> supply infrastructure at airports based on different supply and refueling pathways under consideration of several LH<sub>2</sub> demand scales. However, the report does not consider the aircraft itself and different design options.

Third, several publications focus on a more comprehensive view of novel aircraft's performance while using operating cost metrics including estimations on fuel supply costs [39,123–129]. Nevertheless, the LH<sub>2</sub> costs are often derived in a high-level estimate manner comparable to the assessment in Figure 2.1. Thus, impacts on the local supply infrastructure or their integration into specific air traffic networks are not addressed.

Only one report from the NAPKIN project [130] is found that tackles most of the above-mentioned areas of aircraft design, LH<sub>2</sub> supply cost assessments, and air traffic network effects. Based on a UK air traffic network, scales of LH<sub>2</sub> demands and two case studies for different aircraft sizes are evaluated including relevant cost metrics. However, this report does not optimize the broader context of different LH<sub>2</sub> supply pathways, nor discusses different operational strategies for H<sub>2</sub>-powered aircraft in the investigated air traffic network.

Consequently, besides the high uncertainty of future green LH<sub>2</sub> supply costs, there is a clear research gap in a holistic evaluation of the supply options, aircraft design choices, and the fit into air traffic networks based on proper cost metrics.

While this section derived the state of research on broader energy system levels including methodological approaches, also insights on investigations on a component level have to be considered. These are required for an informed decision on prioritizing the scope and depth of the energy system analyses for LH<sub>2</sub> infrastructure setups later in this thesis.

## 2.2 Green LH<sub>2</sub> supply chains and components

This section summarizes the relevant state of the research perspectives on the main components that are required to supply and refuel green LH<sub>2</sub>. The overview provides relevant background information on the complexity of designing and/or operating the components. Where necessary it also compares the status quo of technology readiness with expected future technology developments that should be of interest to this study. An overview of the relevant components is split into three groups, see Figure 2.2.

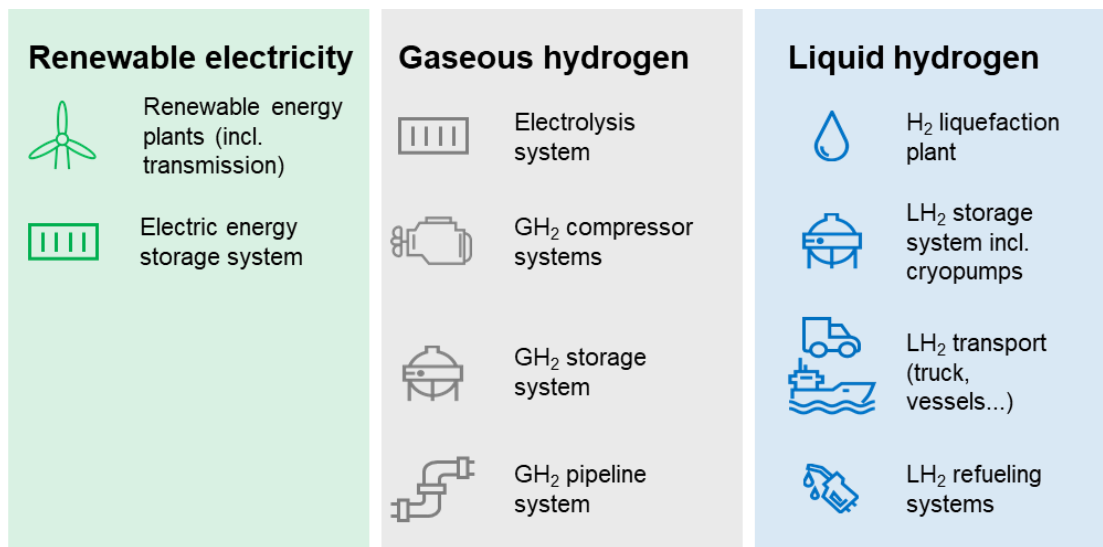


**Figure 2.2:** Overview of required components for green liquid hydrogen (LH<sub>2</sub>) supply

### 2.2.1 Renewable electricity for green H<sub>2</sub> production

As described in the introduction, renewable electricity sources (RES) are required to achieve the lowest carbon footprint when producing H<sub>2</sub> and hence, flying with it. In that case, the resulting H<sub>2</sub> is called green H<sub>2</sub> and has a significantly lower lifecycle emission than grey H<sub>2</sub> (current industry standard) but also blue H<sub>2</sub> [131]. Latter is produced like grey H<sub>2</sub> (e.g., coal, steam reforming), but the resulting carbon emissions are captured and stored.

Furthermore, recent European regulation made clear that an additionality criteria has to be fulfilled when labeling H<sub>2</sub> as green [132]. This means that purpose-built renewable electricity capacities for the production of H<sub>2</sub> are required. Thus, the production of green H<sub>2</sub> must have a temporal and geographical correlation with the RES. There are only a few exceptions to these conditions. In electricity markets with a share of >90% RES, green H<sub>2</sub> can also be produced with a grid connection. While the regulation is currently only valid for the European Union markets, further regulations for clear definitions of green H<sub>2</sub> production might also follow in other regions. This shows how important the availability of RES is for any green H<sub>2</sub> application such as aviation.

## Renewable electricity sources

There are several ways of renewable electricity generation available. Main RES production capacities are coming from solar photovoltaics (PV), wind on- and offshore turbines, and hydropower plants [133]. The installation of the latter is very restricted to the geography of a region and often potential sites are already exploited. This is why, only PV and wind turbines are considered in the following because their installation on large scales is still possible and ongoing.

Overall, more than 3,000 GW of RES was available in 2021 [134], which makes this component the most mature one in the present dissertation.

PV has experienced the largest growth and cost decline due to learning rates over the last decades. Solar PV panels can be installed across a wide range of scales, from rooftops to large-scale utility power plants which are considered here. When installed in such larger utility scales, a main design option for PV is to choose between fixed and 1-axis tracking systems. Here, the more flexible plants with 1-axis tracking are selected, because of higher and more consistent power generation with these modules vs. fixed ones. Even though this comes with slightly higher costs and space requirements, the higher power yields lead to faster amortization of the costs [135].

Wind onshore turbines are installed massively on a global scale. Thus, there is already an installation wave of repowering existing, older wind parks with more powerful and efficient turbines. Consequently, the main developments for this technology are high specific cost reductions, while building larger turbines achieving higher yields due to increased power ratings (>3 MW), hub heights (>100 m), and larger rotor diameters (>130 m) [136]. Moreover, turbines are used with lower specific power ratings that boost capacity factors at already lower wind speeds.

However, the main limitations for the future large-scale deployment of onshore wind parks are constraints on-land space availability, regulatory and permitting barriers, and social acceptance [137].

This is why, wind-offshore turbines are another RES that are currently deployed in gigawatt-scale projects, for which less space restrictions account today. Offshore wind projects often make use of higher and more consistent wind speeds throughout the day and the year. Furthermore, very large-scale projects and also large-size turbines are developed to drive down the high costs of installing wind turbines in offshore areas. Announced parks with installation in this decade use turbines with a power rating of up to 15 MW, hub heights of around 150 m, and rotor diameters of more than 200 m [138]. Nevertheless, the capital costs are still very high for offshore wind plants and underlie a larger uncertainty than the other two RES, since major the market is not yet as established [134]. Major gigawatt-scale projects will just start operation in the next years [138].

Best RES sites are not always at the location where the electricity is required to power an application. Consequently, short-distance electricity transmission is also considered in this thesis to enable competitive costs from RES at most sites, e.g., airports. Further details on transmission are provided in Chapter 5 and Appendix D2.1.

## Electric energy storages

Due to the volatility and seasonality of sun radiation and wind speeds, the availability of RES can differ significantly. This is why, grid-scale electric energy storages can be installed in com-

bination with renewable plants to buffer the energy yield for more constant feeding of any application thereafter. For H<sub>2</sub> production, this can also be of interest to increase the utilization of plants and hence, drive down total costs. However, this is only achieved, if the storage options are an economic choice [139].

There are several electric energy storage technologies available, but this study focuses on electrochemical ones such as lithium-ion energy storage. While there is no clear definition of the duration that such a system could provide/bridge electricity supply, most studies and also installations focus on charge and discharge durations of around 2 to 10 hours [140]. This means that RES variations throughout a day can be smoothed with such storages, but longer seasonal fluctuations most likely not.

The lithium-ion energy storage technology is already established in mobile applications, but also increasingly in grid-scale deployments. However, there are still two main challenges: its capital costs are still high and lifetimes are relatively short depending on the discharging cycles/usage [141]. While costs might further decline in the next decades and lifetimes might be improved, its future role in an H<sub>2</sub> production system has to be further investigated (see Chapter 5). Consequently, the use of such electric energy storage is included and optimized based on their techno-economics in this study.

### 2.2.2 Gaseous hydrogen components

Four main components are of importance in the class of GH<sub>2</sub> systems: the production of green H<sub>2</sub> through water electrolysis, the compression, storage, and transportation of GH<sub>2</sub>.

#### Water electrolysis

The most common method to produce green H<sub>2</sub> (the focus of this thesis) is water electrolysis (ELY). However, today most H<sub>2</sub> is produced via steam-reforming, grey (fossil) route and only <1% is green H<sub>2</sub> [142].

There are three main ELY technologies prominently discussed in H<sub>2</sub> energy systems: proton exchange membrane electrolysis (PEMEL), alkaline electrolysis (AEL), and solid oxide electrolysis (SOEL). In general, water electrolysis is a chemical process, in which electrons (electricity) are applied to split water into hydrogen and oxygen [143]. An electrolyte in the water facilitates the movement of ions between the electrodes. This is where the main differences between the three ELY technologies stem from: In the PEMEL, a solid polymer electrolyte membrane, e.g., Nafion, is used that conducts protons and blocks electrons. The electrolyte in the AEL is a liquid alkaline such as potassium or sodium hydroxide, which enhances the ion conductivity. Both AEL and PEMEL usually operate at temperatures below 100°C. In contrast to that, SOEL uses a high-temperature process and a solid ceramic electrolyte, e.g., based on zirconia which conducts oxygen ions at high temperatures. Even though the SOEL potentially offers the best efficiencies versus the other ELY processes, its location is not as flexible since it requires waste heat from other industrial processes and it is still on a lower TRL without commercialization status [144]. This is why, only the PEMEL and AEL are further in the scope of the analyses for optimizing RES-powered H<sub>2</sub> systems.

The balance of plant layout of the two ELY processes is briefly compared. A similarity is that both require feed water supply including potential desalination and other water purifying measures. Furthermore, they require power supply components and a dryer of the resulting GH<sub>2</sub>. While the GH<sub>2</sub> output of a PEMEL must condensate to separate water vapor from the GH<sub>2</sub>, the output of the AEL has to be purified to reach the required levels of purity.

As shown in Table 2.1, AEL and PEMEL performances are projected to be quite similar given future product developments. AEL plants are already more deployed today and hence, costs are lower. Nevertheless, with large-scale deployments of both technologies, costs, and system efficiency are forecasted to be similar in the next decades already [145]. For both AEL and PEMEL, economies of scale can reduce investment costs significantly – already today. This effect has already a large impact on system sizes above 10 MW [145–147].

**Table 2.2:** Comparison of main selected water electrolysis technologies based on [144,145,148]

Criteria	Alkaline electrolysis (AEL)	Proton exchange membrane electrolysis (PEMEL)
Capital costs for the system	~1,000 USD/kW today, but very similar cost projections vs. future PEMEL	~1,500–2,000 USD/kW today with significant cost reduction potential
System energy efficiency	Status quo: 50–55 kWh/kg, future: <50 kWh/kg	Status quo: 50–60 kWh/kg, future: <50 kWh/kg
Stack lifetime	~60,000 h, but in the future around ~100,000 h	~50–80,000 h, but in the future around ~100–120,000 h
Purity of hydrogen	99.9998%	99.9999%
Part-load operations	15–100%	5–120%
Rare materials required	Nickel	Iridium, Platinum, Titanium

Only two major differences are identified. First, PEMEL can be operated with more flexible loads as low as 5% of the nominal power rating (Table 2.1). This is beneficial when it is coupled with fluctuating RES. Second, the manufacturing of AEL requires less rare and potentially critical materials [149]. Nevertheless, mitigation levers are already developed to reduce the demand for such rare materials [145,150].

In general, research in the last 5–10 years ensured high data availability on the current and future performance of water electrolysis, even though today's share of green H<sub>2</sub> production is very small. In this dissertation, a more generic ELY technology is used, since projections of techno-economics show that both AEL and PEMEL might converge in the future to have similar performances [145].

### Compression of GH<sub>2</sub>

Hydrogen has a very low volumetric energy density in atmospheric conditions. For storage and transportation of H<sub>2</sub>, higher densities are required for better volumetric efficiency and hence, better economics (less space for storage and smaller diameters for a pipeline).

Several compressor technologies are available to achieve this – from smaller-scale diaphragm to piston engine/reciprocating, and centrifugal compressors. Their use and application depend on the H<sub>2</sub> volume flow rates and the required pressure ratios [151]. In this thesis, compression is used for relatively large H<sub>2</sub> volume flows and only medium pressure ranges (up to 200 bar). Larger pressure ratios are often required for applications that use high compressed GH<sub>2</sub> (350–850 bar), which is not the case for larger commercial aircraft with LH<sub>2</sub> storages on-board.

Today, reciprocating (piston) compressors are mostly used for high volume but low-medium pressure ratios applications. These are proven and reliable components known for affordable CAPEX and competitive efficiencies. Moreover, they are applicable for flexible loads – e.g., due to fluctuating ELY production profiles or varying demands [152].

While centrifugal compressors might offer better operational costs in the future with better efficiency and lower maintenance costs, there are main challenges to be overcome when used for GH<sub>2</sub> [153,154]. Due to the very low molecular weight of H<sub>2</sub> and its low viscosity, it is more



prone to leakages and exceptionally high rotational speeds. Improved sealing, optimized geometry/impellers, and pressure ratio designs are needed to enable such lower-cost compression. Furthermore, the creation of heat must be minimized in such compressors to ensure safety, which is critical because of hydrogen's low flammability and ignition energy range.

Other general challenges for all compressor types and components are H<sub>2</sub> leakages and material embrittlement – so, H<sub>2</sub> permeating and reacting with the material of the component leads to material degradation.

Since compressors are already commercialized (mostly used in grey H<sub>2</sub> supplies), data availability is given for the assessments in this dissertation – both on existing and projected compressor performances.

### **Storage of GH<sub>2</sub>**

Two forms of GH<sub>2</sub> storage are considered in this dissertation: containerized and geological formation storage – both enable relatively efficient storage volumes.

Starting with containerized storage, they are most often built in a cylindrical form and only require compressors for filling. Unloading is often done via a pressure differential between the storage vessel and a receiving part. These storages can also be constructed as long pipelines and installed underground to save on the visible footprint of such a storage system. The storage pressures of such containers vary. However, 200 bar is often the most economical for storage in locations without larger space constraints – higher pressures are only chosen for mobile storage, e.g., truck transportation [155,156].

Containerized GH<sub>2</sub> storage has relatively high installation costs, but offers geographic flexibility where to place it [157].

On the other side, geological formation storages have significantly lower costs due to very large available volumes. The formations can be salt or rock caverns, depleted gas reservoirs, or aquifers [158]. To operate these underground storages, compressors are required but also drying and purification units to ensure sufficient purity of H<sub>2</sub> when unloading.

A disadvantage of this storage type is that it highly depends on the geology pre-conditions and its operation cannot be performed as flexibly as for the containerized storage: when loading and unloading the underground storage, only limited variations are possible due to limitations in temperature changes inside the cavern or reservoirs. These flows create a pressure change and hence, a temperature increase which has to be limited for the stability of the geological formation.

There is very good data availability on underground storage – however, demonstrations are still limited and general deployment is still in the early phase. Also, implications of operating underground GH<sub>2</sub> storages in various geological settings, so different rock/material formations, are not fully investigated yet [159]. Furthermore, there are still no comprehensive views on the techno-economic feasibility of this storage form in all regions of the world. There are only indications in global mapping exercises such as shown in [158,160,161].

### **Transportation of GH<sub>2</sub>**

Transport is required to make use of central, sometimes off-site locations where the production of green GH<sub>2</sub> is more economical than at the site of usage. In this part, transportation in hydrogen's gaseous form is considered.

Due to the lower volumetric density of compressed GH<sub>2</sub>, it has been previously found that truck trailer transport with GH<sub>2</sub> containers is in most cases not favorable [105,162]. Consequently, another option is discussed in the literature: the use of pipelines.

Pipeline systems consist of pipes, compressors for increasing the pressure along the route and ensuring more constant flow speeds, safety valves, and measuring units [163,164]. Moreover, there are two options for deploying a GH<sub>2</sub> pipeline system. Either new pipes are built or existing decommissioned natural gas pipelines are retrofitted for the use of GH<sub>2</sub>. Challenges are the embrittlement of the materials used and hence, in retrofit cases, new coatings and also all other system components described above would need to be replaced [165]. In Europe, an international GH<sub>2</sub> pipeline system is currently planned, it is called the European Hydrogen Backbone (EHB) [166]. It should connect production and demand sites of H<sub>2</sub> in Europe and also neighboring regions building on existing, new, and even subsea pipelines.

When designing such a pipeline network, several optimization questions arise. Starting with the network design, also other aspects have to be considered such as flow speeds and pressure in- and outputs [167,168].

Also, different operational approaches can be modeled. So far, most publications concentrate on a balanced operational procedure. This means that all GH<sub>2</sub> which is fed into the pipeline is simultaneously also extracted at the end [163,165,168]. Nevertheless, other modeling approaches with more flexible load variations including a storage function of the overall pipeline system are currently discussed [165,169].

Even though larger GH<sub>2</sub> pipeline networks have not been realized yet, detailed publications and feasibility studies are available which are used for this dissertation.

### 2.2.3 Liquid hydrogen components

As described before, larger commercial H<sub>2</sub>-powered aircraft would most likely be refueled with LH<sub>2</sub>. This is why, all systems required to convert H<sub>2</sub> into LH<sub>2</sub> including storage and transportation are considered in the green LH<sub>2</sub> supply chain analysis.

The liquid state of hydrogen is reached at temperatures around 20 K in ambient pressures (1 atm). Compared to compressed GH<sub>2</sub> at 200 bar, which has a volumetric energy density of around 15 kg/m<sup>3</sup>, LH<sub>2</sub> is nearly five times more compact with ~71 kg/m<sup>3</sup> [170]. However, this advantage comes also with costs, e.g., for the conversion.

Additionally, there is a special characteristic of H<sub>2</sub> that is of importance when it is liquefied. The H<sub>2</sub> molecule has two so-called allotropes: ortho-H<sub>2</sub> and para-H<sub>2</sub>. They differ in the spin of the electron in each H<sub>2</sub> atom (ortho-H<sub>2</sub>: parallel nuclear spins; para-H<sub>2</sub>: anti-parallel nuclear spins). Equilibrium H<sub>2</sub> always contains a specific amount of para-H<sub>2</sub> depending on its temperature. At ambient conditions the para-H<sub>2</sub> content corresponds to 25% (normal-H<sub>2</sub>) while the para content of LH<sub>2</sub> is 99.8% [171], see Figure 2.3.

Ortho-H<sub>2</sub> has a lower energy state than para-H<sub>2</sub>. If no measures are taken, unconverted LH<sub>2</sub> at 1 bar releases heat which suffices for the H<sub>2</sub> to evaporate [172,173]. This spontaneous reaction leads to a so-called boil-off and has a half-life period of less than 5 days [174]. Therefore, it is necessary to dissipate as much heat as possible from the H<sub>2</sub> when liquefying to reach a para-H<sub>2</sub> content close to equilibrium conditions [175].

These characteristics of LH<sub>2</sub> are further discussed when introducing the most relevant LH<sub>2</sub> components in this dissertation in the following.

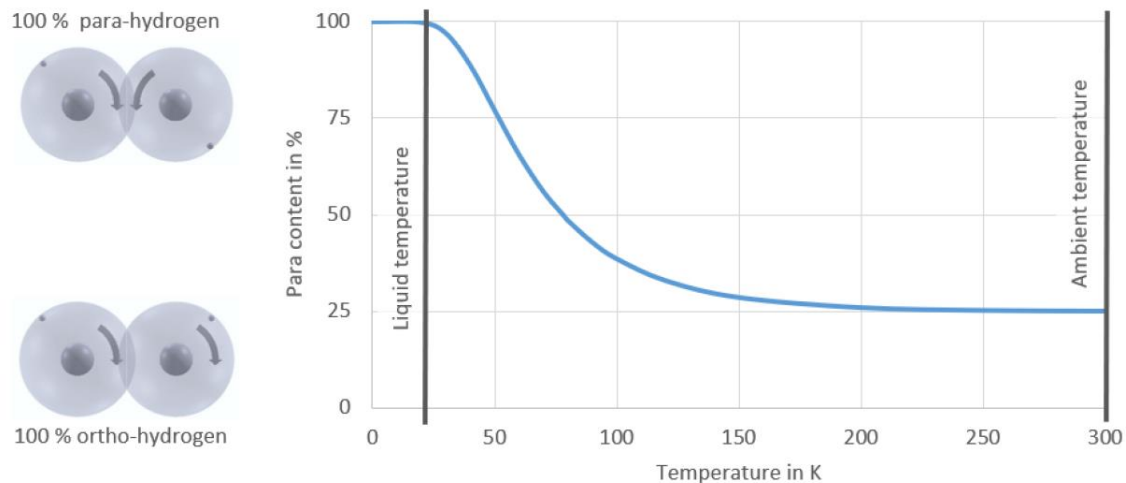


**Figure 2.3:** Para content of hydrogen as a function of temperature – adapted from [171]

### Liquefaction of hydrogen

An H<sub>2</sub> liquefaction plant (LFP) combines several process steps to cool down H<sub>2</sub>: (pre-)cooling, compression, and expansion [172,173,176–180].

The minimum work required to liquefy saturated H<sub>2</sub> depends on the feed pressure and its temperature [181,182], see also Appendix D2. In addition to that, energy is required for the ortho- to para-H<sub>2</sub> conversion as described before. Moreover, catalysts or magnetic fields are used in the liquefaction process to maintain a para-H<sub>2</sub> content close to equilibrium conditions and to prevent fast boil-off [153].

In total, the theoretical minimal physical work to reach LH<sub>2</sub> is 3.92 kWh/kgH<sub>2</sub> [183]. In reality, this cannot be achieved due to losses in the heat exchangers, pumps, compressors, expanders, air-coolers, separators, and mixers [184]. Moreover, the specific energy consumption (SEC) for liquefaction depends on the size of the plant and the used process design – economies of scale for efficiency can be reached with larger plants.

Different process designs are available for H<sub>2</sub> liquefaction – detailed process schemes can be found in [153,185]. In larger-scale industrial applications, the Claude Cycle process and helium Brayton Cycle are used in particular. Although the capital costs for the Claude Cycle process exceed those of the Brayton Cycle, the Claude Cycle process has a higher energy efficiency leading to lower operating costs. In practice, the Brayton and Claude Cycles are further developed to reduce energy consumption as much as possible. This is why, several expander stages and heat exchangers are used to optimize the mass flows and minimize temperature differences for minimal exergy losses [153]. In many cases, also cascade systems or dual pressure systems with high pressure and a medium pressure refrigerant stream are used. This often includes a pre-cooling cycle using, e.g., liquefied nitrogen. Hence, a co-location of an LFP to a source/production of liquefied nitrogen might be of benefit.

Today, all globally available LFP capacities are equal to around 600 tons per day (tpd) of liquefied H<sub>2</sub> only (see Appendix D1.1). The reason therefore is that only a few applications (e.g., spaceships) require LH<sub>2</sub> and most often it is rather used for transporting H<sub>2</sub> in larger quantities to save on transport costs. Nevertheless, future H<sub>2</sub> markets project a larger need for LFP capacities, if cost can be significantly reduced (see also Appendix D2). This can be achieved when using large-scale LFP concepts with optimized process steps [186].

Another aspect of LFP is its operation. Most sources state that it should always be highly utilized, but only one project, IDEALHY, derived changes in energy consumption and hence, operating costs when operating an LFP in part-load [187]. Furthermore, these operational aspects have never been modeled in energy system optimizations before.

It becomes clear that several studies and approaches are available to model the general performance of an LFP in energy systems. Furthermore, many studies are available on optimizing the process design for different scales of capacities [184,188,189]. However, most concepts have not yet been realized. Moreover, several aspects such as operational behaviors and limits were only investigated and published in the IDEALHY project. This means that several of these operational assumptions lead to some uncertainties when modeling an LFP.

### **Storage of LH<sub>2</sub>**

LH<sub>2</sub> storage is required either as a buffer of production or as a backup storage for supply reliability. While the former enables more flexible or even constant operation of the LFP especially for fluctuating LH<sub>2</sub> demand profiles, the latter is often a condition at airports to ensure fuel supply for at least three average days [16,190].

Two main shapes of LH<sub>2</sub> storage are normally used. Spherical or cylindrical shapes lead to optimized surface-to-volume ratios and hence, reduced heat input from the outside [55,70]. Moreover, vacuum-insulated double walls prevent heat transfer by convection [110,191]. Nevertheless, in passive storage concepts, H<sub>2</sub> losses cannot be fully prevented due to the spontaneous conversion of H<sub>2</sub> (ortho-to-para-conversion). In that case, the resulting vaporized H<sub>2</sub> might be vented off the storage to avoid overpressures. There are also active-cooling concepts that lead to zero boil-off [192,193]. However, these are still in the development stage.

Without an active (un-)loading mechanism the boil-off effect can be used. The pressure increases inside the tank due to the evaporated GH<sub>2</sub>, if the heat transfer is increased [194]. Given the resulting pressure differential, LH<sub>2</sub> can then be transferred to another vessel. However, this method leads to relatively high losses and might not be favorable in a large-scale green LH<sub>2</sub> supply chain.

As a solution, cryogenic pumps (cryopumps) can be used [195]. These require additional electricity but lead to minimized H<sub>2</sub> losses and fast fueling/transmission speeds. There are different types of cryopumps available, but most have not yet reached commercial maturity for large-scale applications. Further research is needed to achieve high flow rates that might be required in a large-scale supply context such as at airports [196,197].

In this dissertation, the use of LH<sub>2</sub> storage without active cooling mechanisms is targeted. Furthermore, it is assumed that also cryopumps will be available in the next decades for more efficient operation with storage.

### **Transport of LH<sub>2</sub>**

Several modes of transporting LH<sub>2</sub> would be required to enable more economic and efficient green LH<sub>2</sub> supply for aviation. Depending on the transport distance, trucks, rail, and even inland vessels are mostly discussed for shorter to medium on-land (river) trips. While trucks are commercially operated today, rail and inland vessels are still in a study phase [162,198]. For longer distances, larger LH<sub>2</sub> vessel transport is currently already being demonstrated [199].

Container-like trailers with LH<sub>2</sub> storage can be used flexibly with trucks, trains, or smaller vessels. Such LH<sub>2</sub> storages have capacities of around 4–5 tons of LH<sub>2</sub>, of which 90–95% of

the liquid can be used. The rest is called ullage and has to stay inside the tanks in normal day operation to keep the storage cool and losses low [162].

Studies including simulations and even one demonstration project provide data for larger LH<sub>2</sub> transport vessels [200–204], see Figure 2.4. These show that the main aspects to be considered transporting LH<sub>2</sub> on vessels are the synergistic integration of the storage into the vessel, use of boil-off gas for the propulsion, safety mechanisms like venting, but also loading and unloading procedures.

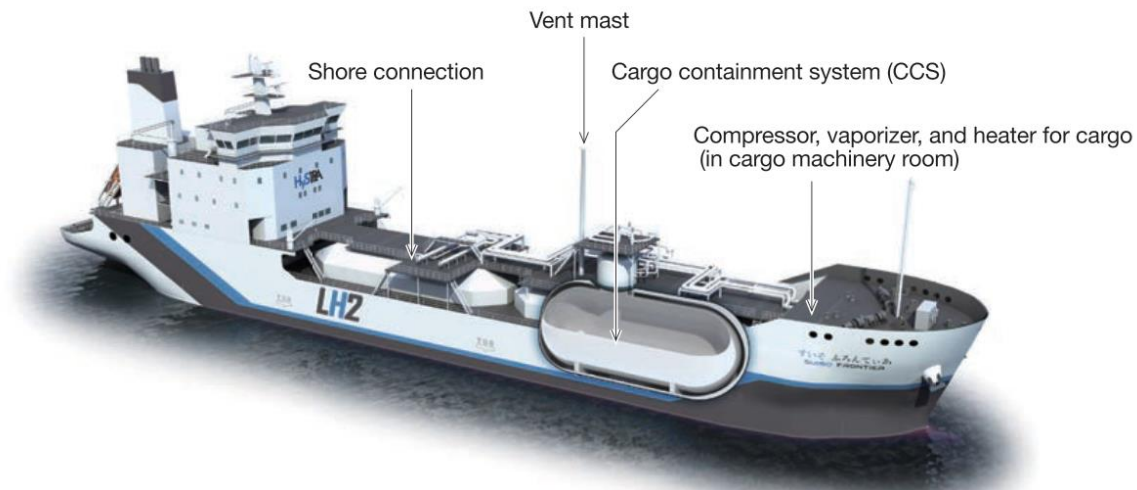


**Figure 2.4:** LH<sub>2</sub> vessel design from HySTRA demonstration project lead by Kawasaki – transport between Japan and Australia, picture taken from [200]

When shipping LH<sub>2</sub> with large-scale vessels, import and export terminals are needed to load and unload the vessels. Such a terminal consists of LH<sub>2</sub> storages, automatic loading arm systems with cryopumps, and boil-off gas back-feeding systems, see Figure 2.5.

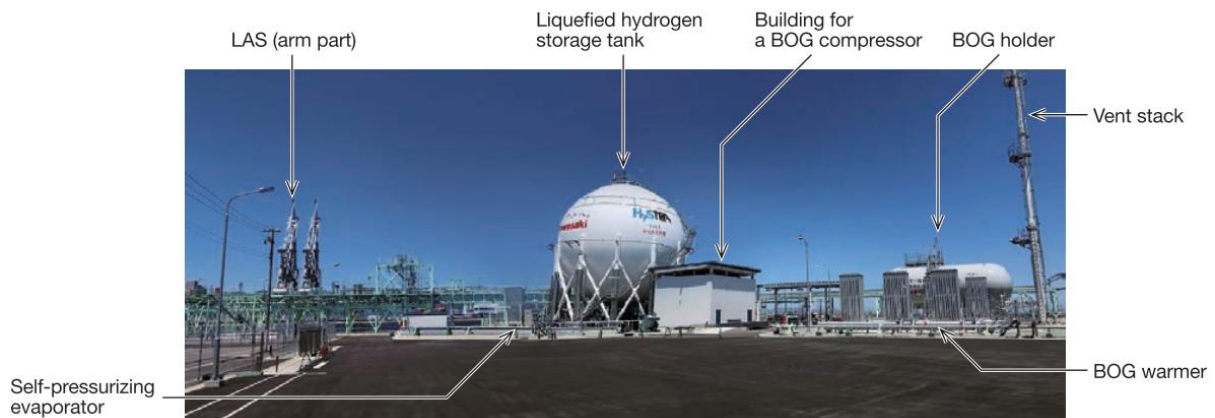


**Figure 2.5:** Import and export terminal design for shipping LH<sub>2</sub> via vessels, picture from HySTRA demonstration project lead by Kawasaki [200]

In this dissertation, the focus is set on truck and larger vessel transport of LH<sub>2</sub>, since data availability is best for both modes. However, there are still high uncertainties about the future performance of such systems including flash losses and other leakages – especially, when transport times are several days and not only a few hours.

### Refueling of aircraft with LH<sub>2</sub>

For a better understanding of the current status of refueling aircraft with LH<sub>2</sub>, the general process and two transport modes are briefly introduced.

The receiving (aircraft) LH<sub>2</sub> tank has to be prepared before it can be filled with new LH<sub>2</sub>. This can be either a warm and empty tank or a cold tank that only requires top-filling. Latter would be the preferred status in normal operation since it takes less time for refueling (no cooldown of tank required). This preparation can include purging of the tank if fuel hose couplings are used which might lead to small contaminations of LH<sub>2</sub> when connecting the refueling tank with the aircraft tank. However, the development of clean-break couplings is already ongoing which would not require purging and hence, save costs [115]. If these are not available in the next decades, helium as a purging gas would be used to clean the refueling system and receiving tanks from contaminations. The used helium evacuates the free space of oxygen and other gases to prevent damages potentially caused by frozen gases.

Furthermore, cryopumps and a sub-cooling unit for the LH<sub>2</sub> before refueling as described in [115] are required as part of the purging (also called dispensing) unit.

The transportation of LH<sub>2</sub> from the airport LH<sub>2</sub> storage to the aircraft stand can be done with trucks as described before or with cryogenic pipelines & hydrants. Latter, are double-walled vacuum-insulated pipelines with a minimum diameter of 254 mm to reduce friction inside the pipes for smaller diameters [54,74,205]. Further details on LH<sub>2</sub> flow rates can be found in [115]. Furthermore, the pipeline should be designed as a three-pipe system for reliable operation and to avoid two-phase flows of hydrogen in the pipeline [54,90]: a primary LH<sub>2</sub> supply loop, a spare loop for redundancy (supply reliability), and a collection loop for GH<sub>2</sub>. Thus, the pipeline would have a circular design to ensure a steady LH<sub>2</sub> flow and requires an inlet and outlet from the storage tank. This circulation, driven by cryopumps, prevents high heating at periods of low demands, so low flow rates [54].

Data availability is quite limited around LH<sub>2</sub> refueling systems. This leads to several uncertainties around the techno-economic assumptions for this dissertation discussed in Chapter 4.

### **Summarizing the state of research for components and processes**

The overview shows that research on the main component systems of an LH<sub>2</sub> energy system like RES, electrolysis, GH<sub>2</sub> transportation, and storages, LH<sub>2</sub> storages are already very advanced. Only limited insights are found for the LFP, cryopumps, LH<sub>2</sub> transportation, and refueling systems where aspects of general operational principles and technology development for large-scale applications have rarely been looked at. Additionally, projections of techno-economics over the next decades are very uncertain and rarely undertaken. This will be further discussed in Chapters 4 and 5.

### **2.3 Derived research questions and structure of the thesis**

While Section 2.1 emphasized a clear need for techno-economic analysis of green LH<sub>2</sub> supply for aircraft with a sound methodological approach, Section 2.2 revealed several supply components that were not fully addressed in depth by previous studies.

Based on this state of research and the resulting literature gaps the main objective of this dissertation is to answer the question: **Will liquid hydrogen play a major role as propulsion fuel in a future, decarbonized aviation sector?**

The main novelty of the present study is to bring together all aspects of the very broad question in one more holistic assessment. Therefore, all relevant methodologies required for the investigations are derived and techno-economic assumptions are harmonized. Moreover, a detailed projection of LH<sub>2</sub> demands, an optimization of the supply infrastructure based on non-linear

energy system modeling, and a design optimization of H<sub>2</sub>-powered aircraft while considering different operational strategies in an existing air traffic network are undertaken.

For a better overview of this approach, the overall objective is further split into five leading research questions.

1. Since there are several studies available on H<sub>2</sub>-powered aircraft design but with highly differing evaluation criteria, a main methodology for this thesis is derived along the questions:

**How to assess the operating costs flying with H<sub>2</sub>-powered aircraft and what is a first high-level estimate of the economic impact coming from green LH<sub>2</sub> supply?**

- 1.1. What is an established cost method that must be used to assess and benchmark the costs of flying with different fuels and/or propulsion technologies?
- 1.2. What would be the performance of a future kerosene-reference aircraft and how does this compare to a novel H<sub>2</sub>-powered aircraft?
- 1.3. Which are less relevant operating cost factors when introducing H<sub>2</sub>-powered aircraft?

2. Qualitative analyses on future airport design and technologies were undertaken in the last decades. However, only a few derive numbers on demand scales, and those who do differ greatly in the calculated magnitudes of scale. This leads to the questions:

**What is the impact on airport infrastructure when introducing H<sub>2</sub>-powered aircraft?**

- 2.1. How large would future LH<sub>2</sub> demands from aircraft be at one airport?
- 2.2. How does this compare to other H<sub>2</sub> demands from other sectors around an airport?
- 2.3. What are the refueling system options for LH<sub>2</sub> and when should which option be selected?

3. A large gap was identified around green LH<sub>2</sub> supply cost assessments in general but also for the aircraft use case. Few cost studies rather use high-level calculations without deeper insights into the availability/profiles of renewable energy generation or the operational specifics of the main energy system components. Even more detailed supply cost studies use linear modeling approaches. Consequently, this larger area of research potential is analyzed in detail along the following questions:

**What are the costs of supplying green LH<sub>2</sub> to airports?**

- 3.1. How do potential LH<sub>2</sub> supply pathways look like?
- 3.2. How to optimize the underlying energy systems given the different importance of modeling depths for each component?
- 3.3. What are the design rules that describe a general recipe on how to design an optimized green LH<sub>2</sub> supply system?
- 3.4. How do the cost results change due to the uncertainty of future techno-economic parameters in these systems?
- 3.5. If H<sub>2</sub> import options exist, what is their cost impact on future LH<sub>2</sub> supply?

4. Only a few recent studies approached the topic with a more holistic evaluation approach combining aircraft and/or supply infrastructure and/or air traffic network aspects. Most often, these studies still only concentrate on deriving detailed insights based on their assumptions for one of the topics. Then, the detailed insights are combined with inputs for the second analysis item from other studies that are not always aligned on the same scenario assumptions. Hence, a complete picture is often not achieved by comparing the same assumptions. This is why in this investigation detailed assumptions are derived for all aspects of the following research questions:

**How do green LH<sub>2</sub> supply options and H<sub>2</sub>-powered aircraft designs interlink in realistic airline operations?**

- 4.1. What are the LH<sub>2</sub> supply cost results in a case-study-based evaluation and a given air traffic network?
  - 4.2. How does the design of an aircraft family affect aircraft-related operational costs?
  - 4.3. What role do operational strategies with these aircraft play considering varying LH<sub>2</sub> supply costs at each airport?
5. Finally, the overarching objective and the insights of the previous four questions are synthesized and packed into a final broader analysis. There, the main economics and other decision criteria for choosing future decarbonization options in aviation are assessed along these questions:

**To inform industry and policy makers, what are the overall arguments for H<sub>2</sub>-powered aircraft compared to other decarbonization options?**

- 5.1. What are the main cost differences of flying with H<sub>2</sub>- compared to kerosene-powered aircraft?
- 5.2. How do the economics compare to other decarbonization options that might be available in the future?
- 5.3. What is the overall resource efficiency of these different decarbonization options compared to H<sub>2</sub>-powered aviation?

The dissertation is structured as follows. In Chapter 3, an operating cost model as the main evaluation methodology is introduced. Thus, reference aircraft designs and changes when switching to H<sub>2</sub> propulsion systems are highlighted.

Then, the airport context is derived including LH<sub>2</sub> demand projections and its role in a broader H<sub>2</sub> economy. Additionally, LH<sub>2</sub> refueling systems are discussed and their techno-economics are briefly evaluated.

In Chapter 5, the research field of green LH<sub>2</sub> supply costs and all related research questions are considered. At this stage, this is done for exemplary locations to focus on the underlying modeling methodology, design rules, and cost sensitivities when changing techno-economic parameters in a scenario analysis.

This is followed by a case-study-based evaluation of not only LH<sub>2</sub> supply costs but also operating cost analysis for single-aisle aircraft in a given flight network in Chapter 6.

Finally, all five research questions are answered and limitations as well as future fields of research are discussed in Chapter 7.

For better readability, detailed model descriptions, techno-economic assumptions, and cost optimization results are presented in the Appendix. Moreover, the underlying methodology approaches of this thesis' models are not introduced in a central chapter, but they are briefly described as a section of each relevant chapter. This should help the reader in better understanding the relevant part of the overall methodology for each chapter.



### 3 Costs of flying and H<sub>2</sub>-powered aircraft design

Instead of a central presentation of all methodology approaches used in this thesis, the first research question is addressed in this chapter.

Along this question, the overarching methodology for evaluating H<sub>2</sub>-powered aviation and other decarbonization options is introduced. This is done based on direct operating costs (DOC) for aircraft – a metric that is also applied in the chapters thereafter. Hence, the DOC introduction supports the reader in better understanding the underlying objectives of the analyses throughout the thesis.

In the second step, the reference designs of a kerosene- and H<sub>2</sub>-powered aircraft are optimized, which are required for the investigations in Chapter 4 and 6. Moreover, this optimization leads to a first result regarding the cost changes coming from re-designing the aircraft for H<sub>2</sub> propulsion systems. It also underlines which operating cost factors are less relevant when evaluating new propulsion concepts.

**Disclosure:** The following two sections are in large parts based on the publication: J. Hoelzen, D. Silberhorn, T. Zill, B. Bensmann, R. Hanke-Rauschenbach, Hydrogen-powered aviation and its reliance on green hydrogen infrastructure – Review and research gaps, International Journal of Hydrogen Energy (2022) [52]. For a detailed description of the author's contributions see Appendix F.

#### 3.1 Direct operating cost method

The analysis of DOC is chosen as an “industry-standard” framework to evaluate the economics when changing the existing aviation environment with technology innovation [206]. In contrast to the evaluation of other factors, e.g., energy efficiencies, climate impact, and macroeconomic factors such as the impact on employment, the DOC analysis reflects the costs and hence the economic viability for one of the main stakeholders, the operator [207].

Since the industry is highly cost-driven and operators are working on the edge of profitability, the change of economics related to introducing new technologies can be a major enabler or barrier for a potential uptake of new radical technology. Hence, these are investigated in the following.

DOC models can reflect all significant cost drivers. From aircraft manufacturing and vehicle performance, energy, and infrastructure cost as well as differences in aircraft operation and utilization:

$$C_{\text{DOC,total,yearly}} = C_{\text{DOC,CAPEX}} + C_{\text{DOC,maint}} + C_{\text{DOC,crew}} + C_{\text{DOC,fees,ATC}} + C_{\text{DOC,fees,airport}} + C_{\text{DOC,energy}} \quad \text{USD} \quad (3.1)$$

As seen in Equation 3.1, the total annual DOC  $C_{\text{DOC,total,yearly}}$  consists of capital  $C_{\text{DOC,CAPEX}}$ , maintenance  $C_{\text{DOC,maint}}$ , crew costs  $C_{\text{DOC,crew}}$ , fees for air traffic control (ATC)  $C_{\text{DOC,fees,ATC}}$  as well as for airport services  $C_{\text{DOC,fees,airport}}$  and energy costs  $C_{\text{DOC,energy}}$ . By referring the yearly DOC to the number of passengers as well as the distance traveled, the utilization in terms of available seat kilometers (ASK) per year is calculated. This is influenced by the vehicle's speed, turnaround time, and operational aspects as well as forced downtimes due to maintenance and night curfew. Further description of the DOC model is provided in Appendix A.

#### Changes to DOC from new technologies and fuels

To illustrate different cost effects on the DOC caused by new technologies or fuels, three concepts are discussed. Next to H<sub>2</sub> propulsion, which will be examined in detail hereafter, two

examples are now shortly analyzed on a qualitative level: the introduction of winglets and synfuels (first two levers of Table 3.1).

**Table 3.1:** High-level, qualitative impact on DOC factors by introducing new levers to reduce the climate impact of aviation

DOC factors	Exemplary levers to reduce the climate impact of aviation:		
	Winglets for improved aerodynamic design	New drop-in fuels such as synfuels	New propulsion technology based on hydrogen
<b>Aircraft CAPEX</b>	Slight change: costs depend on development, manufacturing / material cost for aircraft design change	No change	Change: costs increase for the propulsion system incl. LH <sub>2</sub> tank and aircraft system integration
<b>Aircraft Maintenance</b>	Slight change: airframe related maintenance could be affected by new designs	No change	Change: New propulsion system incl. LH <sub>2</sub> tank with different maintenance costs
<b>Crew</b>	No change		
<b>ATC fees</b>	No change		
<b>Airport fees</b>	No change	No change	Could change due to overall aircraft weight variation and more complex ground handling or other airport system costs affected by H <sub>2</sub> aircraft
<b>Fuel/energy</b>	Slight change: Same fuel, but lower total energy consumption	Change: Different fuel costs for synfuel production	Change: Liquid H <sub>2</sub> with different supply chains and supply costs
<b>Aircraft utilization</b>	No change	No change	Could change, if the refueling process increases the overall turnaround times or LH <sub>2</sub> tank maintenance causes higher yearly forced downtimes

First, the development of winglets as a lever of evolutionary improvements of box-size-limited aircraft design is described. The “shark-tail-like” looking ends of the wing tip are used to decrease lift-inducing vortex flows at the wing tips and increase aerodynamic efficiency and therefore reduce fuel burn [208].

Regarding the effects on DOC shown in Table 3.1 and Eq. 3.1, it is likely that the CAPEX might increase slightly due to development costs and potentially increased complexity in the manufacturing of the wing. Accordingly, also the airframe maintenance costs might increase. There are no changes in crew costs or air traffic control fees since they depend on the number of PAX onboard, cabin design, and distances flown – all factors are kept constant for all design changes including the introduction of new fuels or propulsion technologies.

Furthermore, the same airport fees are expected, given that the aircraft re-design has been compliant with airport size regulations. Since winglets reduce the fuel burn of aircraft, it leads to decreased fuel cost which is the main impact. The aircraft utilization is not affected at all.

The second column in Table 3.1 describes the cost impact of synthetic kerosene which has similar properties as jet fuel and could be directly used as drop-in fuel [29]. This means that although the process of fuel production strongly changes, which leads to different fuel costs, the aircraft is barely affected which allows using existing aircraft, supply, and refueling infrastructure.

In comparison to the presented levers of aerodynamic improvements and synfuels, introducing H<sub>2</sub> propulsion for aircraft affects nearly all DOC factors as shown in the rightmost column of Table 3.1. Starting from the top, aircraft CAPEX and maintenance will be examined in the next section.

### 3.2 H<sub>2</sub>-powered aircraft design and cost impacts

To evaluate the operational cost changes caused by re-designing the aircraft for integration of H<sub>2</sub> propulsion systems, first, the kerosene reference aircraft and then, the H<sub>2</sub>-powered version is optimized. For both designs a projection of future aircraft technology advancements is used to reflect regular evolutionary efficiency improvements between aircraft development cycles.

#### Reference conventional aircraft for comparison

In this work, single-aisle aircraft are designed and investigated that are normally operated on short-range flights. Since this aircraft segment is also targeted for H<sub>2</sub> propulsion by aircraft manufacturers like Airbus with their ZeroE aircraft concept and due to its large share of aviation's global emissions [7,45], it is a relevant choice for the following analyses.

The single-aisle aircraft is used as a reference to compare the effect of introducing H<sub>2</sub> propulsion for the segment itself. Interested readers can find further information about the modeling approaches for both the conventional aircraft design and the modifications for H<sub>2</sub> aircraft in Appendix B. In the original publication, smaller wide-body aircraft were also investigated, because this segment would also be eligible for disruption by H<sub>2</sub> propulsion technologies. Further information is provided in [52].

Table 3.2 shows the resulting specifications for the conventional single-aisle aircraft. It has been projected to be an Entry-Into-Service (EIS) year 2035 with increased performances and is designed for a maximum flight range of 1,500 NM and to transport 180 PAX. On an average mission of 800 NM, it consumes 166 GJ of kerosene. The flight cycles per year are calculated with forced downtimes of 2749 hours based on [209] and block time supplements of 1.5 hours per flight for the single-aisle/short-range concept.

**Table 3.2:** Conventional kerosene aircraft specifications – design criteria and outputs from modeling

Parameter	Unit	Single-aisle (short-range)
Design Entry-Into-Service	-	2035
Design Range	NM	1,500
Design PAX	-	180 (Single class layout)
Design Cruise Mach-Number	-	0.78
Calculated MTOM	t	65.6
Calculated OEM	t	39.7
Block-Energy for design mission	GJ	286
Block-Energy for typical mission (used for further evaluation)	GJ	166 (800 NM mission)
Calculated annual flight cycles	-	1,512 (800 NM mission)

The total DOC, see Fig. 3.1, is calculated by applying the DOC model described in Eq. 3.1 and Appendix A, which results in 5.14 USD per 100 available seat kilometer (ASK) for the single-aisle concept for 800 NM flights.

The resulting fuel/energy DOC value is calculated assuming the constant kerosene fuel costs of 0.6 USD/kg which were also used in Section 2.1. In this work, the kerosene price is kept constant due to the high uncertainty of price projections and the observed high price volatility in the last 10 years. No emission or other additional costs on top of the kerosene product costs are assumed in this first introduction of aircraft costs.

It can be seen that the kerosene fuel costs only account for 17% of the total DOC on an 800 NM trip. This is a typical cost characteristic for this aircraft segment. Since the flights are quite short, the time on the ground (passenger unloading, loading, and taxiing) takes a higher timeshare which is also reflected in higher cost shares coming from fixed fees like for the airport.

This characteristic becomes even more obvious when comparing this segment to wide-body aircraft as shown in [52], which fly on longer distances and hence, have higher energy cost shares.

## H<sub>2</sub> aircraft design and its influence on DOC

In the next step, the 2035-projected reference aircraft is now modified to an H<sub>2</sub>-powered aircraft.

Consequently, the DOC for aircraft CAPEX and maintenance change since H<sub>2</sub> propulsion technology comes with different costs and requires new aircraft design and different system integration. Additionally, the aircraft energy efficiency changes are mainly driven by the new energy carrier characteristics which have an impact on the fuel-related DOC.

Most reviews and detailed papers such as in [55,62] concentrate on H<sub>2</sub> propulsion technology and its implications on the aircraft design – with a clear focus on liquid hydrogen due to the lower total storage mass compared to solid or metal hydride and also volume requirements compared to GH<sub>2</sub>. However, there are many challenges concerning the passively insulated LH<sub>2</sub> tanks such as lifetime and thermodynamic cycle stability, maintenance, or the highly complex and multidisciplinary integration into the overall aircraft concept. The ground handling and operational flexibility in terms of the duration without vented GH<sub>2</sub> (dormancy time) highly influence the required insulation quality and hence, the tank mass and the aircraft performance. Achieving high LH<sub>2</sub> aircraft performances as well as a flexible ground operation is a major challenge and generates an important interface to the airport infrastructure.

In this work, the modeled H<sub>2</sub> aircraft concept is powered by H<sub>2</sub> turbofan engines. The two LH<sub>2</sub> tanks are integrated into the fuselage, both behind the cabin for the single-aisle concept. Further details can be found in Appendix B.

The resulting energy demand of the LH<sub>2</sub> short-range concept compared to the kerosene baseline increases from 166 GJ to 177 GJ (by 12%) for the 800 NM mission, see Table 3.3.

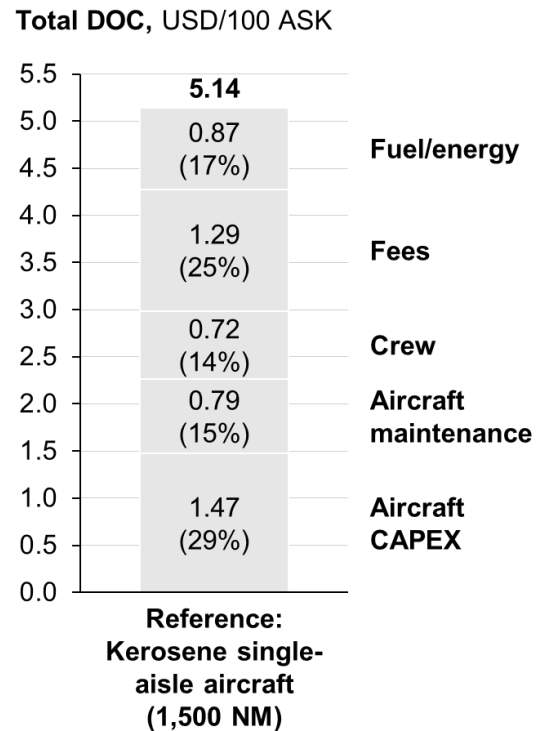


**Figure 3.1:** Total DOC evaluation of the reference kerosene-powered aircraft

**Table 3.3:** Hydrogen aircraft specifications – design criteria and outputs from modeling

Parameter	Unit	Short-range
Design Entry-Into-Service	-	2035
Design Range	NM	1,500
Design PAX	-	180 (Single class layout)
Design Cruise Mach-Number	-	0.78
Calculated MTOM	t	68.7
Calculated OEM	t	48.2
Block-Energy for design mission	GJ	303
Block-Energy for typical mission (used for further evaluation)	GJ	177 (800 NM mission)
Calculated annual flight cycles	-	1,514 (800 NM mission)

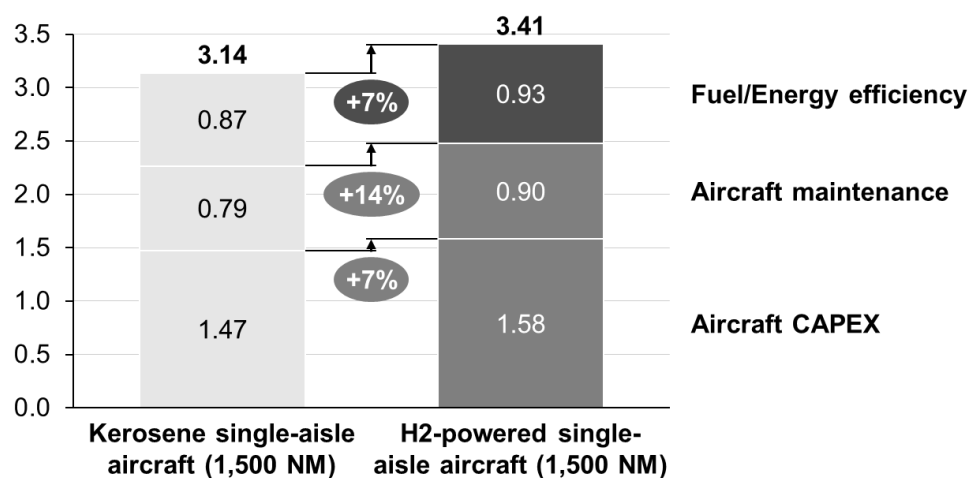
Roughly one-third of this drawback is caused by decreasing aerodynamic efficiencies due to the longer fuselage incorporating the relatively large volumes of the LH<sub>2</sub> tank. Two-thirds of this effect comes from the additional mass of the storage and structural snowball effects.

Since the cruise Mach number is the same for the kerosene and LH<sub>2</sub> concepts, the flight times and yearly cycles are similar. Small variations still exist due to slightly different flight paths, i.e. climb rates and cruise altitudes, and hence changed flight times. Additional factors which could decrease the utilization are the turnaround time as well as additional forced down-times due to LH<sub>2</sub> storage-related maintenance procedures. This topic is discussed later in this section.

As seen in Table 3.1, changing the energy carrier affects many DOC factors. To deal with these impacts, the conventional cost method has to be adapted (see details in Appendix A).

Based on the modeling and modified DOC evaluation, the costs increase by 7% for CAPEX and 14% for maintenance for 800 NM flights (Fig. 3.2).

If the different energy efficiencies of the kerosene- versus H<sub>2</sub>-powered aircraft are considered assuming the same energy costs as in the kerosene reference, the additional fuel costs for the H<sub>2</sub> aircraft are 7% for the single-aisle aircraft (Fig. 3.2). Concerning the total operating costs, all aircraft-related cost increases lead to a 5% increase of total DOC.

**Aircraft-related DOC, USD/100 ASK**

**Figure 3.2:** Change of selected DOC factors for the H<sub>2</sub>-powered single-aisle aircraft due to H<sub>2</sub> propulsion technology impacting aircraft CAPEX and maintenance costs as well as fuel costs through lower energy efficiency – bubbles show relative cost increase for each of these cost buckets

This and the cost uncertainties caused by different technology assumptions, especially around the LH<sub>2</sub> tank (further insights in Appendix B), underline that H<sub>2</sub> aircraft might come with higher DOC, which should be further targeted to be improved by research and development efforts.

### **H<sub>2</sub> airport infrastructural and operational impacts on DOC**

However, not only the aircraft CAPEX and maintenance costs but also the general fuel/energy costs and operational implications using H<sub>2</sub> must be investigated. This also influences the viability of the business case of introducing H<sub>2</sub> aircraft.

The DOC per flight depends on the aircraft utilization as already mentioned. This is determined by the turnaround time of the aircraft on the ground and the flight time, i.e. cruise speeds of the aircraft. This could change if LH<sub>2</sub> refueling times increase due to the more complex refueling procedures. Or if H<sub>2</sub> aircraft would be designed with slower cruise speeds to reduce power requirements for the fuel cell system [42].

Only a few studies are available concerning the refueling procedure of LH<sub>2</sub>-fueled aircraft. Most describe only high-level implications of the turnaround process without going into detail [37,42,63,94], see also Section 2.1. Boeing [57], Brewer [54,55], and ISO/PAS [77] describe the refueling process in more detail including flow rates and hose diameters. They indicate that similar energy flow rates and refueling times like for the kerosene reference are possible. Only one more conservative estimate was found in Brewer [54] who showed a 20% increase in turnaround time for a long-range LH<sub>2</sub> concept with no parallel fueling.

In the following, the same refueling rates and safety standards are assumed to be feasible for the chosen single-aisle aircraft segment. Insights on other factors influencing aircraft utilization, e.g., the use of additional and larger LH<sub>2</sub> refueling vehicles, are not found.

The supply of LH<sub>2</sub> does not only require green LH<sub>2</sub> production and logistic capacities but also new fuel and refueling infrastructure and operations at airports. Airport system costs implied by these changes mostly lead to costs for “into-plane” refueling players at airports that must be added to the LH<sub>2</sub> fuel costs at the dispenser. However, since H<sub>2</sub> aircraft can be designed in a way, that they fit the aerodrome regulations of the International Civil Aviation Organization for all segments, e.g., gate limits, potential further changes in ground handling and landing fees should be very low.

Also, no cost effects are expected from the safety aspects of H<sub>2</sub> aircraft handling at airports: many sources [57,66,115,210] state, that the safety measures of LH<sub>2</sub> refueling should not be higher than for kerosene ones. Even though there are studies from Brewer [54,55] considering changed – potentially more costly – ground operations due to an increased safety radius of 90ft around the fuel hoses, this does not seem to be a reasonable assumption. It would imply a secondary explosion protection standard which must ensure that no ignition sources exist in this perimeter. Due to the very low minimum explosion energy of hydrogen, this should not be an issue [61]. This leads to the primary explosion protection standard which implies that the system is designed in a way that avoids explosive atmosphere. Nevertheless, an exact safety radius for H<sub>2</sub> aircraft operation is not available yet and is identified as a research gap for future work when determining airport system costs.

Lastly, the largest uncertainty factor might be the LH<sub>2</sub> fuel cost: Since 17% of the total DOC is related to fuel costs for a conventional single-aisle (Fig. 3.1), the use of hydrogen as a direct fuel can have a significant impact. This will be analyzed in detail in the following chapters.

**Implications for overall research objectives**

As a brief summary of this chapter and the first research question (see 2.3), it is found that the DOC is a valid method to benchmark the economics of different decarbonization options including new fuels and/or new propulsion technologies. Furthermore, a first optimization of aircraft designs highlights that the H<sub>2</sub>-powered aircraft-related changes lead to a 5%-increase of total DOC. Thus, a main part (39%) of the total operating costs i.e. crew costs and other fees would not be affected by switching the aircraft propulsion system.

## 4 Context for LH<sub>2</sub> aircraft refueling at airports

Before the main cost uncertainty, supplying LH<sub>2</sub> to airports, can be investigated in detail, several aspects setting the context for the optimization tasks in Chapter 5 and 6 have to be analyzed. This is why the impact on airport infrastructure when introducing H<sub>2</sub>-powered aviation is determined in the following which also addresses the second research question (Section 2.3). Therefore, H<sub>2</sub> demand scenarios are derived for differently sized airports. Thus, these are compared to other potential H<sub>2</sub> applications at or around the airport to categorize its importance as future H<sub>2</sub> hubs. As a last step, the refueling system options for H<sub>2</sub>-powered aircraft and their costs are calculated which are an input value for the supply cost assessments in the chapters hereafter.

**Disclosure:** The following two sections are in large parts based on the publication: J. Hoelzen, M. Flohr, D. Silberhorn, J. Mangold, A. Bensmann, R. Hanke-Rauschenbach, H<sub>2</sub>-powered aviation at airports – Design and economics of LH<sub>2</sub> refueling systems, Energy Conversion and Management: X (2022) [112]. For a detailed description of the author's contributions see Appendix F.

### 4.1 LH<sub>2</sub> demand scenarios for aviation

For the sizing of LH<sub>2</sub> supply and refueling systems, it is necessary to know the approximate demand scales which have to be delivered to or at the airport. These LH<sub>2</sub> fuel demand scenarios are calculated within three steps in this section: scope, reference, and 2050 projections. Then, the resulting scenarios are used to categorize LH<sub>2</sub> demands for aircraft with general H<sub>2</sub> energy systems at and around airports.

#### Definition of scope for fuel demand calculations

This investigation focuses on all commercially used aircraft – so, regional, single-aisle, medium, and larger wide-body aircraft (see Table 4.1). In 2019, this group of airplanes accounted for approximately 99% of all commercial aircraft related CO<sub>2</sub> emissions worldwide [7,16]. General aviation – mostly smaller aircraft flown by private pilots or business aircraft – cargo and military aircraft are not considered in the following. Neither are smaller commercial aircraft included, so-called commuter aircraft with less than 20 PAX.

Since this work targets these larger commercial aircraft, only LH<sub>2</sub> demands for refueling aircraft are considered. The reasons for considering LH<sub>2</sub> and not GH<sub>2</sub> are shown in Chapters 2 and 3.

**Table 4.1:** Overview of commercial aircraft segments referenced in this study

Commercial aircraft category	Maximum take-off mass (MTOM) of aircraft, in tons	Typical capacity, in passengers (PAX)	Exemplary aircraft
Regional (jet and turbo-prop)	<50	20–100	ATR 42/72, DHC-8, Bae 146, CRJ-700, ERJ-135, E-175
Single-aisle	50–150	100–250	E-190, A220, A320 family, B737 family, B757
Medium wide-body	150–250	200–300	A330, B767, B787
Large wide-body	>250	>250	A340, A350, B777, B747, A380



### Reference fuel demands at three airport archetypes

Few other studies already investigated LH<sub>2</sub> demands at specific airports by translating historic kerosene demands into equivalent fuel amounts of LH<sub>2</sub>. In the 1970s, Korycinski [56] and Brewer [54] projected that annual demands for wide-body aircraft at each Chicago O'Hare Airport and San Francisco International Airport could be between 200 to 250 thousand tons (kt) of LH<sub>2</sub> in the year 2000. Looking at refueling all aircraft at Los Angeles Airport (LAX) with LH<sub>2</sub>, Amy and Kunycky [72] calculated that around 1,400 ktLH<sub>2</sub> would be required referenced on 2012 data.

Based on the large range of demand figures it becomes clear that an updated, more detailed overview of potential LH<sub>2</sub> demands at airports is required before designing LH<sub>2</sub> refueling and supply systems at airports. The demands determined in the following are not meant as market forecasts, but as assumption-based scenarios that provide general perspectives for the analyses undertaken in this study.

For a detailed understanding, three different airport archetypes are selected to determine potential LH<sub>2</sub> demands from the chosen aircraft segments: smaller national airports with less than 20,000, intercontinental hubs with more than 100,000 departing commercial flights per year, and major national airports in between. Thus, three exemplary airports in Germany are selected due to data availability. Bremen Airport (BRE) as a regional national airport, Hamburg Airport (HAM) as a major national airport, and Frankfurt-Main Airport (FRA) as an intercontinental hub are chosen. A detailed overview of the methodology, sources, and assumptions that are used for the LH<sub>2</sub> demand scenarios can be found in Appendix C and the Supplementary Material shown in [112].

In 2019, the calculated annual kerosene demand for commercial aircraft was 38, 366 and 4,661 kt of fossil kerosene at BRE, HAM, and FRA, respectively. At smaller and major national airports, flights with regional and single-aisle aircraft account for the majority of kerosene demand with 95% at BRE and 80% at HAM. Most flights with these aircraft connect national and intra-European airports. At intercontinental hub airports, the opposite is observed – for example, at FRA less than 20% of the kerosene demand comes from these aircraft segments. Since medium and larger wide-body aircraft carry more passengers, consume more energy per kilometer, and fly longer distances, these drive the high demand for fuel at the airport. At FRA around 3,000 kt of kerosene (64% of the total) are calculated to be refueled for larger wide-body aircraft only.

However, several studies state that true zero CO<sub>2</sub> emission propulsion systems like H<sub>2</sub> propulsion require larger technological breakthroughs to be an economic choice for such larger wide-body aircraft by the year 2050 [16,19,29,62]. Consequently, the following analysis does not consider this larger aircraft segment and assumes that such aircraft would rather be fueled with SAF to achieve net-zero carbon emissions. If these kerosene consumptions are subtracted from the 2019 figures, considered annual fossil fuel demands at these airports are 38, 322, and 1,686 kt of kerosene for BRE, HAM, and FRA, respectively (Figure 4.1A and second column Table 4.2).

Besides the total annual fuel demand, Figures 4.1B and 4.1C highlight another important design requirement for supply and refueling systems at airports. These show the variation of fuel demand over an average day and the months of a year for the example of Hamburg Airport in 2019 [211,212]. Like at most German airports a night curfew restricts aircraft operation which can be seen in Figure 4.1B. Furthermore, aircraft departures peak in the morning and evening times. Considering a whole year, April to October are busier months with around 10% higher

air traffic (departures) than in the colder months November to February with 15% less traffic compared to the annual average. Even though the exact distribution of air traffic will certainly differ for each airport depending on the type of airlines and flight destinations at the airport, similar phenomena are assumed for all airport types in this study.

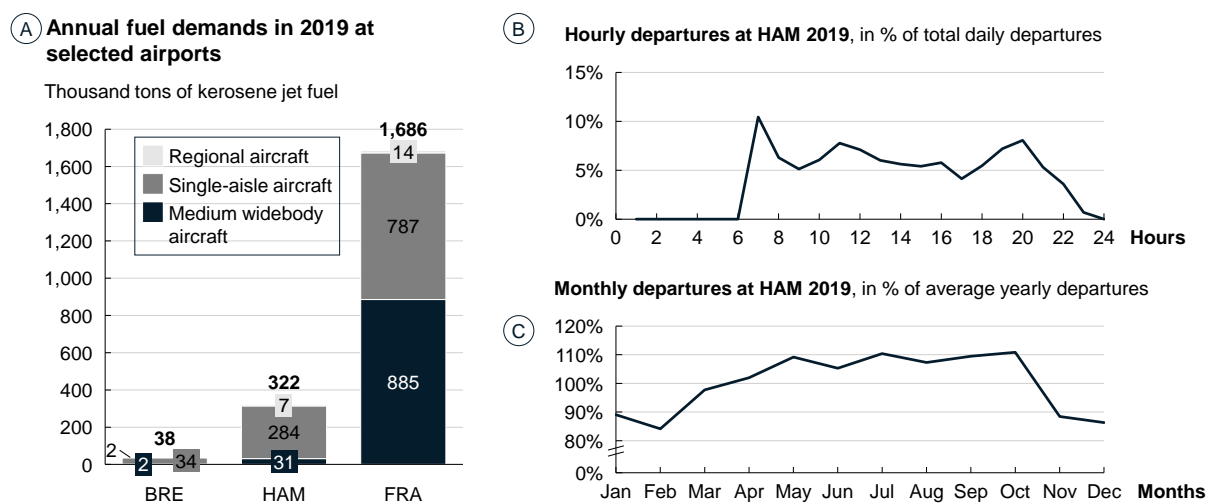


**Figure 4.1:** A) Considered annual fossil kerosene fuel demand in 2019 at three German airports without larger wide-body aircraft, B) average daily aircraft departures at HAM in 2019 [212], C) monthly aircraft departures at HAM in 2019 [211]

To enable aircraft refueling with LH<sub>2</sub> in seasonal but also daily peak times the design of a fuel system at an airport has to cover such fluctuations accordingly, further details will be briefly discussed in Section 4.2.

After the calculation of fossil kerosene demands in 2019, the figures are converted into LH<sub>2</sub>-equivalent fuel demands based on energy conversion factors also reflecting a change in specific energy consumption (SEC) per aircraft segment (see Appendix C). The results excluding larger wide-body aircraft are shown in the third column of Table 4.2. Based on these assumptions including the fuel demands and number of flights at the specific airports, flights with regional aircraft would consume on average 0.25 tLH<sub>2</sub>, with a single-aisle aircraft 1.8 tLH<sub>2</sub> and a medium wide-body aircraft 16 tLH<sub>2</sub>. Further detail can be found in the Supplementary Material of [112].

## 2050 fuel demand scenarios

In the next step, aircraft fuel demands are projected until 2050. Despite the temporally, drastic decrease in air traffic due to the COVID health crisis, strong growth is forecasted for the aviation sector over the next decades [8,213,214]. Airport-specific results are displayed in the column “Projected total fuel demand 2050” in Table 4.2. These reflect air traffic growth projections that lead to an overall increase in total fuel consumption as well as aviation efficiency improvements that decrease the specific energy demands per aircraft (see Appendix C).

Furthermore, two different deployment scenarios of H<sub>2</sub>-powered aircraft are used to project the demand for LH<sub>2</sub> for 2050. This is used to derive the demand context for LH<sub>2</sub> refueling setups at airports. Both scenarios consider a future in which H<sub>2</sub>-powered aircraft will be techno-economically feasible but with different progressive assumptions. In the base case scenario, deployment of H<sub>2</sub>-powered aircraft will start to scale between 2040 and 2050. In the ambitious

scenario, this deployment will already reach larger H<sub>2</sub> fleet delivery rates in the late 2030s (details provided in Appendix C).

The 2050 scenarios show clear differences between the magnitudes of LH<sub>2</sub> demands at airports depending on their size (fifth and sixth column of Table 4.2). This is now discussed and set into context with other H<sub>2</sub> applications.

**Table 4.2:** Calculated annual fuel demands for 2019 at selected airports and 2050 demand scenarios – all excluding large wide-body aircraft

Airport (Example)	Considering total fuel demand in 2019, in t of kerosene	Converted total fuel demand 2019, in t of LH <sub>2</sub> -equivalent	Projected total fuel demand 2050, in t of LH <sub>2</sub> -equivalent	Base case scenario: LH <sub>2</sub> demand 2050, in t per year	Ambitious case scenario: LH <sub>2</sub> demand 2050, in t per year
Smaller national airport (Bremen)	38,467	15,463	20,722	9,949	17,416
Major national airport (Hamburg)	321,722	130,235	175,505	80,600	142,390
Intercontinental hub (Frankfurt)	1,686,052	698,330	987,668	317,375	565,206

### LH<sub>2</sub> at airports and their role in an overarching H<sub>2</sub> energy system

At a smaller national airport like BRE, the 2050 projections indicate an annual LH<sub>2</sub> demand of 10 to 17 ktLH<sub>2</sub> (27 to 48 tLH<sub>2</sub> daily) depending on the base and ambitious case scenario assumptions.

This amount of LH<sub>2</sub> is in a similar order of magnitude such as projected demands for H<sub>2</sub>-powered road applications in regions with higher mobility demands. As highlighted by Ueckerdt et al. [215] and Staffell et al. [216], H<sub>2</sub>-powered heavy-duty vehicles might be an economically viable decarbonization option compared to other alternatives such as battery-electric vehicles. One H<sub>2</sub> refueling station (HRS) for such larger vehicles might have an average daily consumption of 2.5 tons of H<sub>2</sub> [217]. Hence, in a region with around 10 to 20 HRS, a similar H<sub>2</sub> consumption (10 to 20 ktH<sub>2</sub>) would result from aircraft at BRE in 2050 (Figure 4.2).

For H<sub>2</sub>-powered rail applications, H<sub>2</sub> demands at rail HRS are a similar size. At Bremervoerde, Germany, a HRS with a daily capacity of 1.6 tH<sub>2</sub> was already installed for trains [218]. However, the amount of required HRS in a specific region is significantly lower for rail applications [219]. Hence, regional H<sub>2</sub> demands from trains are assumed to be lower than for road applications.

The LH<sub>2</sub> demand scenarios for aircraft at major national airports such as HAM are calculated to be around 81 to 142 ktLH<sub>2</sub> in 2050. This equals 46 to 81% of a theoretically maximum LH<sub>2</sub> fuel consumption for aircraft in that year – similar to the results at BRE. The reason for this effect at BRE and HAM is that at both airports most flights are assumed to be operated with regional and single-aisle aircraft; both segments that are predestined for the potential deployment of H<sub>2</sub> propulsion [16].

For comparison, industrial applications are or might be operated with H<sub>2</sub>. Today, grey H<sub>2</sub> is used as a feedstock in fertilizer plants producing ammonia and in refineries for, e.g., hydrocracking. Furthermore, steel, iron, and cement plants are being discussed using green H<sub>2</sub> as a new feedstock for decarbonizing these heavy carbon-emitting sectors [44,220].

### Estimated H<sub>2</sub> demand ranges per sector in a specific region if fully converted to H<sub>2</sub>, in kt/year

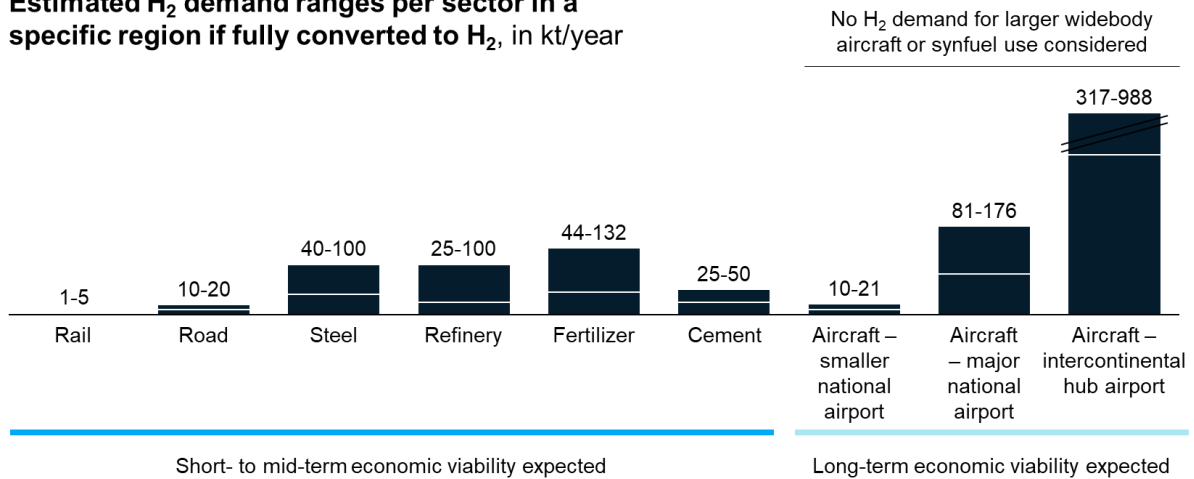


**Figure 4.2:** Annual H<sub>2</sub> demand ranges for different sectors at a specific region and their projected economic viability based on [44,220] – a specific region defined as a generic location (e.g., city, industry park) where these sectors are placed; due to economic uncertainty and highly varying demand sizes inputs from other sectors such as power services [142], building heating [215,216] or maritime [221,222] are not shown

In Germany, 40 million tons of steel were produced in 20 steel plants in 2019 [223]. Assuming a future green H<sub>2</sub> consumption for one ton of steel production of 20 to 50 kgH<sub>2</sub> [224–226], an average plant would require around 40 to 100 ktH<sub>2</sub> per year.

Similar H<sub>2</sub> consumption figures are calculated for refineries and ammonia production. Refineries with an annual capacity of 5 to 10 million tons of crude oil input would require 25 to 100 ktH<sub>2</sub>/a assuming a H<sub>2</sub> demand of 5 to 10 kg per ton of crude oil input [225]. A fertilizer plant with an output of 250 to 750 kt of ammonia (NH<sub>3</sub>) [227] and an H<sub>2</sub> consumption of 176 kgH<sub>2</sub> per ton of NH<sub>3</sub> [225] would also consume a similar demand with 44 to 132 ktH<sub>2</sub> per year.

These values show that potential LH<sub>2</sub> demands at major national airports could become as large as the H<sub>2</sub> demand of larger industrial plants operated with H<sub>2</sub>. In a specific region, such an airport could already take the role of an H<sub>2</sub> hub in a broader, surrounding H<sub>2</sub> energy system. In that case, the H<sub>2</sub> hub is the central and very large consumer of H<sub>2</sub> for which a dedicated H<sub>2</sub> supply could be designed. Other H<sub>2</sub> applications around such a hub might then benefit from potentially lower supply costs due to economies of scale.

At intercontinental hub airports such as FRA, the LH<sub>2</sub> demand scenarios result in 317 to 565 ktLH<sub>2</sub> in 2050. In this case, only 32 to 57% of the total equivalent fuel demand, excluding larger wide-body aircraft, would be substituted by H<sub>2</sub>-powered aircraft. Including the fuel demand of larger wide-body aircraft, this share decreases to 10 to 17% only.

While the LH<sub>2</sub> demand is rather low compared to the total fuel demand at FRA in 2050, it is already 2 to 4 times larger than the largest fertilizer plant assumed above (Figure 4.2). Moreover, this also shows significant potential for increasing demands in the decades thereafter, given that the fleet penetration of H<sub>2</sub> aircraft could increase further. Consequently, the role of such an intercontinental hub in a specific region might trump all other H<sub>2</sub> consumptions from other sectors around the airport. However, there are less than 100 such larger airports worldwide [228], as defined in this work, that might take such a special role in regional H<sub>2</sub> energy systems.

Next to the insight that LH<sub>2</sub> demands at airports could become dominant in some regions, two additional trends can be observed.

First, most other sectors might feed GH<sub>2</sub> and not LH<sub>2</sub> such as the aviation sector. So, cost synergies for LH<sub>2</sub> sub-systems might be limited. LH<sub>2</sub> is discussed in the heavy-duty road and

maritime sector or for general transportation of H<sub>2</sub> over longer distances only [216,229]. Consequently, the design of such LH<sub>2</sub> supply and refueling systems at airports could take a unique role in a future hydrogen economy.

Second, based on economic viability analyzed in [44] and [220] the introduction of the discussed other H<sub>2</sub> applications might happen until 2030 already (short- to mid-term horizon), while larger scale deployment might take longer than 2035 in the aviation sector [16,19]. This could mean that the installation of general H<sub>2</sub> fuel infrastructure might take place without considering the aviation use case.

## 4.2 Refueling routes and costs considerations

The choice of the LH<sub>2</sub> refueling systems poses its optimization challenges and is evaluated as a separate aspect from the overall supply systems. However, only a brief overview is presented on the potential LH<sub>2</sub> refueling setups and related costs in this airport context chapter, whereas the green LH<sub>2</sub> supply routes are discussed in detail in Chapter 5. Moreover, relevant safety aspects of handling LH<sub>2</sub> at airports are also shortly discussed in this section.

### LH<sub>2</sub> refueling routes

Given green LH<sub>2</sub> is supplied to the airport, the interface between the supply and the refueling infrastructure is the LH<sub>2</sub> storage farm at or near the airport (see Figure 4.3). These LH<sub>2</sub> storages are mainly required to buffer daily and seasonal fluctuations in fuel demands (see Figure 4.1b and 4.1c), but also to ensure LH<sub>2</sub> supply reliability over several days – in case, the supply chain is disrupted by other events. For safety reasons and since space at the terminals and gates is very limited, fuel farms are typically farther away from the terminals. They are often located as a central fuel farm with loading facilities for the refueling system. In some cases, these farms are even outside of the airport area but close by [230].

There are currently two major LH<sub>2</sub> refueling pathways discussed to distribute LH<sub>2</sub> from the LH<sub>2</sub> storages to the aircraft [16,190]: LH<sub>2</sub> refueling trucks (R1) or an LH<sub>2</sub> pipeline & hydrant system (R2), see Figure 4.3 and also Section 2.2.

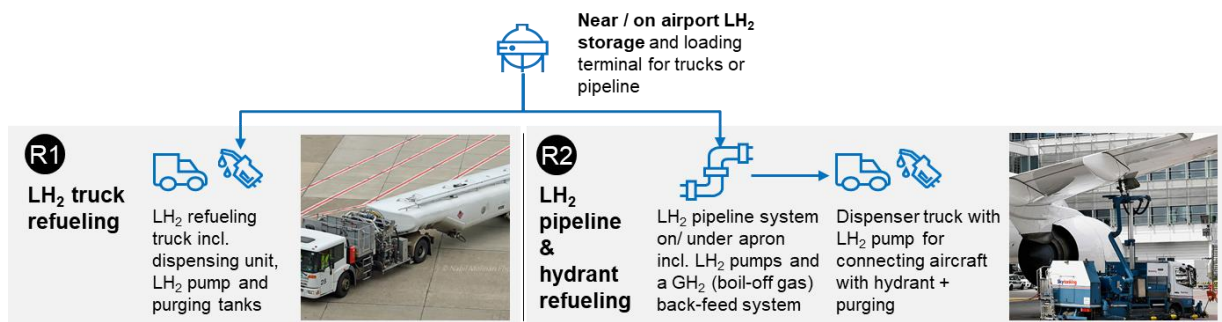


**Figure 4.3:** Topologies for LH<sub>2</sub> refueling setups at airports

The use of LH<sub>2</sub> refueling trucks enables a more flexible deployment option, but these would also contribute to increasing traffic on airport aprons. The investment per refueling truck is rather limited and the number of required trucks can be adjusted flexibly to the demand of LH<sub>2</sub> at airports. However, the LH<sub>2</sub> loading volume of one refueling truck is limited and space for a larger fleet of these could be rare at airports.

In addition to that, increased safety and potentially faster aircraft refueling and hence, faster turnaround times are the reasons why, LH<sub>2</sub> refueling pipelines & hydrant systems are seen as an alternative. These systems could be built underneath the airport apron and accessed

through a hydrant at each aircraft stand. In comparison to the deployment of refueling trucks, the installation of a pipeline & hydrant refueling system comes with high upfront expenses and a longer lifetime over several decades. Thus, the dimensioning of this system – and hence, its costs – are not as flexible to adjust as with refueling trucks. Similar considerations are also taken into account at airports for the design of current kerosene refueling systems [231,232].

For both refueling setups, a dispensing unit is required for the refueling procedure to connect the pipeline or the LH<sub>2</sub> tank on the refueling truck to the LH<sub>2</sub> storage onboard the aircraft [54,63]. Furthermore, such dispenser systems can function as purging units to “wash” out the LH<sub>2</sub> refueling hoses from other gases before refueling with cryogenic LH<sub>2</sub> (more details in [115]). This dispensing unit can be integrated onto the refueling truck. For pipelines a dispensing truck is operated between aircraft stands to connect the hydrant and the LH<sub>2</sub> aircraft tank.

### Optimized costs of LH<sub>2</sub> refueling systems

All techno-economic assumptions on modeling both LH<sub>2</sub> refueling setups including further airport layout aspects are presented in [112] with further technical details in [115]. The choice of the refueling system also impacts the supply route due to lower or higher H<sub>2</sub> losses at the airport. This is why the cost results for the choice of refueling systems are considered in a complete system setup in the following figures. However, in this first assessment, only linear modeling and simplified supply component models were used. The complete assessment can be found in [115]. In the present thesis, only the relevant results impacting the choice of the refueling system are briefly discussed, because the supply system effects are investigated in great depth in Chapter 5 and the following.

The calculated LH<sub>2</sub> costs at the dispenser including the simplified supply costs for a demand between 10,000 to 800,000 tLH<sub>2</sub> per annum in 2050 are presented in Figure 4.4 with a logarithmic scale.

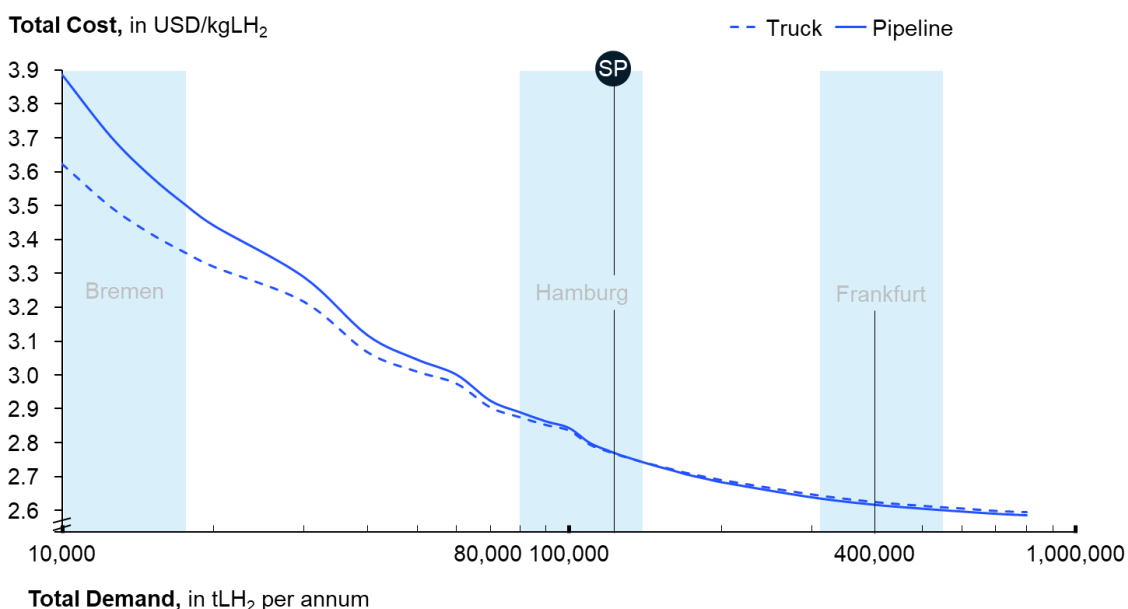


**Figure 4.4:** Total costs of LH<sub>2</sub> at the dispenser with a truck (dotted blue line) and pipeline & hydrant refueling (continuous blue line) in 2050; demand scenarios for exemplary German airports shown in light blue; point of interest highlighted: SP referring to the design switch point

In general, the results show that the LH<sub>2</sub> costs decrease with larger LH<sub>2</sub> demands both refueling setups from 3.6–3.9 to 2.6 USD/kgLH<sub>2</sub>. Nevertheless, the refueling system including the LH<sub>2</sub> fuel buffer storages at the airport only accounts for 0.09–0.11 USD/kgLH<sub>2</sub> for annual demands above 10 ktLH<sub>2</sub>. These costs increase significantly for very small demands: at a demand of 5 ktLH<sub>2</sub>/a or lower the refueling system costs reach levels above 0.15 USD/kgLH<sub>2</sub>.

Considering the optimization of the two different refueling systems, a design switch point (SP) for the given techno-economic assumptions can be identified. For an annual demand below 125,000 tLH<sub>2</sub>, the LH<sub>2</sub> truck refueling (15 trucks in use) is the more economical setup. Above that demand, pipeline & hydrant refueling is slightly less expensive by 0.01 to 0.02 USD/kgLH<sub>2</sub>. Consequently, the optimization for the refueling system's total annual costs follows the course of the lowest LH<sub>2</sub> costs as described.

### Sensitivity of optimized cost results for the refueling system

The assumptions made in these calculations for the year 2050 come with high uncertainties due to the very long-term projection period and since reliable data is not available. In addition to that, most of the components have never been built in large quantities or capacities before.

A sensitivity analysis (Figure 4.5) shows that the two main factors that influence the choice of the refueling setup most are the H<sub>2</sub> loss factor for truck refueling and the CAPEX for installing an LH<sub>2</sub> pipeline & hydrant system. The former occurs mostly when loading and unloading the refueling truck. The latter depends on the future development and research progress as well as larger production capacities (leading to economies of scale and learning rates) of cryogenic pipelines. Today most installed LH<sub>2</sub> pipelines are used in space or laboratory contexts [115]. Therefore, different properties and often less frequent usage lead to not fully comparable techno-economic parameters for this system, if applied to the aviation setup.

Figure 4.5 emphasizes the large range of resulting design switch points depending on the variation of these two factors. If the H<sub>2</sub> losses of realized refueling truck systems would increase, the annual demand for the design switch point decreases to around 55 ktLH<sub>2</sub>/a (SP1).

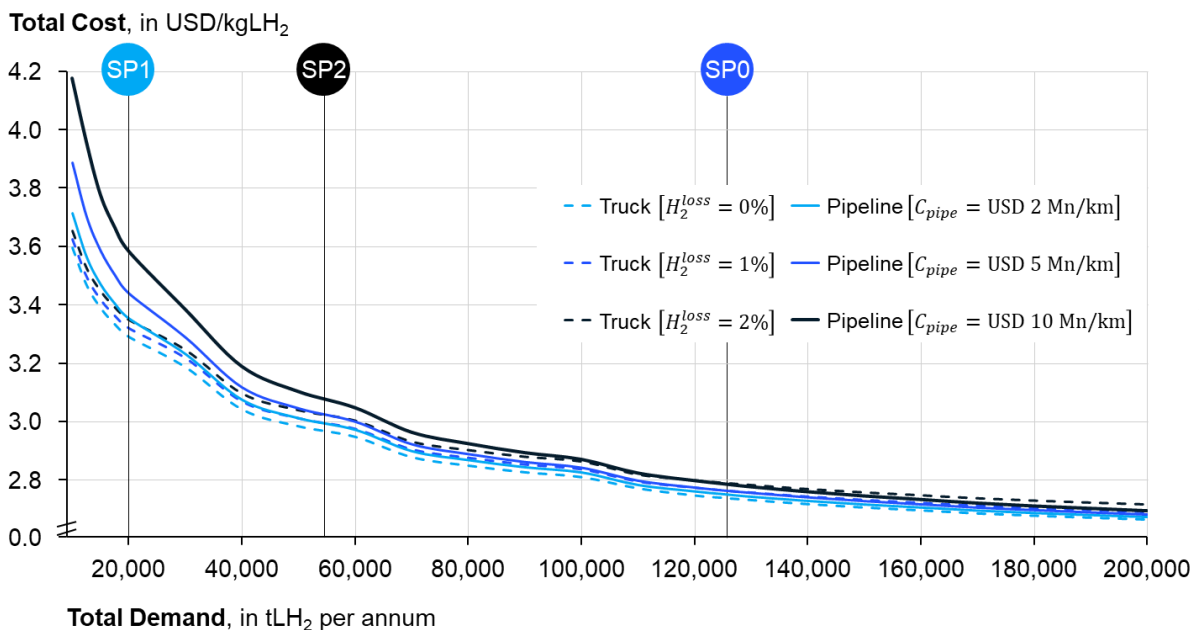


**Figure 4.5:** Variation of main techno-economic parameters for LH<sub>2</sub> truck and pipeline & hydrant refueling for annual LH<sub>2</sub> demands between 10 to 200 ktLH<sub>2</sub>



On top of this and assuming a most favorable case for the pipeline system with reduced CAPEX, the design switch point would even decrease to 20 ktLH<sub>2</sub>/a (SP2), see Figure 4.5. So, under certain conditions, a pipeline could already become the more economical choice even for smaller airports.

However, the technical challenges of constructing and operating such a LH<sub>2</sub> pipeline system should also be considered, which might outweigh the savings of 0.01–0.02 USD/kgLH<sub>2</sub> compared to the more flexible solution of using refueling trucks. In addition to that, the sensitivity analysis with these two selected factors also shows that a truck variant with no H<sub>2</sub> loss is always less costly than any of the pipeline systems considered – even for very large annual LH<sub>2</sub> demands.

Insights for another parameter, the transmission distance, are also briefly presented. It is found that a longer distance between the fuel farm and the aircraft gate favors the use of LH<sub>2</sub> trucks and leads to a shift of the design switch point to higher annual LH<sub>2</sub> demands. On the one side, trucks have a factor of 1.5 longer distances and therefore consume more time for driving between a fuel farm and a refueling stand. On the other side, the H<sub>2</sub> losses remain nearly stable for trucks, while the H<sub>2</sub> losses for pipelines depend on the length of the pipelines. Furthermore, CAPEX for refueling trucks has a lower relative increase than for pipeline systems.

### **Further aspects of choosing the LH<sub>2</sub> refueling system**

The design choice of LH<sub>2</sub> refueling systems for LH<sub>2</sub> pipeline & hydrant systems versus LH<sub>2</sub> refueling trucks might not fully depend on their economics. Even though the deployment of an LH<sub>2</sub> pipeline & hydrant transmission system might save 0.01–0.02 USD/kgLH<sub>2</sub> for airports with LH<sub>2</sub> demands significantly above a design switch point of 125 ktLH<sub>2</sub>/a, also other criteria play a role. Less traffic and reduced potential for human error (driving such trucks) could increase the safety of LH<sub>2</sub> handling at airports when using pipelines instead of refueling trucks. Especially for highly space constraint airports, the avoidance of further traffic on the apron might be more critical than enabling slightly more economic refueling pathways. Furthermore, it is shown in the sensitivity analysis that the economics for the switch point still depend on several techno-economic factors leading to a large variety of best economic scenarios. Therefore, the exact cost figures for the choice of the most competitive LH<sub>2</sub> refueling setup are still highly uncertain and will depend on the future development of each techno-economic factor.

Only for smaller airports like Bremen LH<sub>2</sub> refueling trucks will certainly be a more practical and economic choice for operation – expected demands were determined to be below 20 ktLH<sub>2</sub>/a in 2050.

In addition, three further aspects including safety have to be kept in mind when designing such LH<sub>2</sub> refueling systems:

First, the availability of space to place additional refueling systems at airports is often very limited, especially at larger airports [232]. Consequently, the design of LH<sub>2</sub> refueling systems has to reflect, if these can be placed at a specific space on the airport or on land nearby the airport.

Second, the responsible operator of refueling systems has to be determined to be able to allocate the costs for LH<sub>2</sub> refueling operations correctly. Most fuel infrastructures at airports are not operated by the airport managing company but by third parties such as oil & gas companies. This is often organized with concessions granted by the airport company for longer time periods (e.g., decades) [233]. Accordingly, refueling infrastructure and operating costs are often included in the fuel price paid by the aircraft operator and not as a separate fee or levy paid to the airport [231,234].



Third, airport infrastructure and the operation of aircraft are highly regulated to ensure safe operations [235]. That is why it is likely that the design of LH<sub>2</sub> supply and LH<sub>2</sub> refueling systems at airports will have to comply with high safety standards that are also applied to kerosene infrastructure. Several H<sub>2</sub> component-specific standards can already be found in the SEVESO [236], the ATEX directives [237], and the directive 2010/75/EU on industrial emissions [238]. These include general comments on plant safety, occupational safety, consumer protection, construction law, traffic law, environmental law, insurance law, and energy industry law, but nothing specifically applicable to an aviation context. Also, no safety zone radius and other distances are specified.

### **Implications for overall research objectives**

Addressing the second research question (see 2.3), it becomes clear that H<sub>2</sub>-powered aviation could have a significant impact on airport infrastructure and its role in a broader energy system. LH<sub>2</sub> demands from aircraft could reach large orders of scale by 2050. Nevertheless, for the design of the required supply and refueling systems, the whole context of H<sub>2</sub> infrastructure around airports has to be considered. Since other sectors might require an H<sub>2</sub> supply infrastructure already one decade earlier than needed for larger commercial aircraft, synergies or resource conflicts should always be investigated before deploying LH<sub>2</sub> systems at airports.

The two main refueling system setups for LH<sub>2</sub> are found to be truck and pipeline & hydrant refueling. Furthermore, it can be stated that a decision between these two setups can rarely be made on a purely economic basis. Rather safety aspects, space constraints, or existing know-how at the airports have to be considered for the design choice of LH<sub>2</sub> refueling systems.

All of the airport infrastructure deployments underlie a general uncertainty and economic risk. New refueling systems require new safety and certification standards. Thus, the sizing of the systems changes with different LH<sub>2</sub> demand scenarios which result from uncertainties of aircraft' EIS dates, manufacturing ramp-ups, and applicability to the different aircraft segments. In addition to that, such systems have not been demonstrated on larger scales which leads to further techno-economic uncertainties.

Finally, the results of optimizing LH<sub>2</sub> refueling systems are applied to the cost results in the following analyses on green LH<sub>2</sub> supply systems and will not be further explicitly discussed.

## 5 Green LH<sub>2</sub> supply costs for airports

This chapter addresses the third research question (see 2.3). Potential green LH<sub>2</sub> supply pathways are derived as well as the main insights on the supply costs to airports with the required methodological depth. Cost dynamics are shown based on the different LH<sub>2</sub> supply pathways and main energy system design choices (design rules) that lead to competitive costs. While the costs are determined for generic locations that are chosen to reflect highly differing production conditions, a scenario analysis investigates different assumptions for the main techno-economic parameters. Furthermore, this approach lays the foundations for further supply cost analyses in a realistic air traffic network in Chapter 6.

The chapter is structured as follows. First, the study design including the investigated supply pathways and the optimization methodology is introduced. Second, the supply costs for on-site LH<sub>2</sub> production are discussed and design rules are derived. Thus, varying LH<sub>2</sub> demand scales and scenarios with different techno-economic assumptions are considered. Third, the on-site cost results are compared to the main off-site supply setups, also investigating several techno-economic scenarios. In the last section, this chapter is concluded with a very brief summary.

**Disclosure:** The following section is based on the publication: J. Hoelzen, L. Koenemann, L. Kistner, F. Schenke, A. Bensmann, R. Hanke-Rauschenbach, H<sub>2</sub>-powered aviation – Design and economics of green LH<sub>2</sub> supply for airports, *Energy Conversion and Management: X* (2023) [239]. For a detailed description of the author's contributions see Appendix F.

### 5.1 Green LH<sub>2</sub> supply chain optimization

In this section, an overview is given of the study design, the optimization methodology, and generic scenario definitions. This enables a better understanding of the validity of results and underlying assumptions.

#### 5.1.1 General design of study

As a start, the study objectives, the main LH<sub>2</sub> supply chain setups that are relevant to the aviation use case, and brief component overviews are introduced.

#### Objectives

The general aim of this analysis in this chapter is to determine the most economically competitive, green LH<sub>2</sub> supply pathways for airports based on varying LH<sub>2</sub> demand sizes. Therefore, a dedicated deployment of renewable energy sources (RES) and LH<sub>2</sub> supply pathways to an airport is investigated.

It could be argued that larger LH<sub>2</sub> uptake from aviation is not expected before the years 2035 to 2040 [16], as also shown in Chapter 4, and hence, H<sub>2</sub> could then be bought from existing H<sub>2</sub> markets. However, it is assumed that there will be different accessibility to existing H<sub>2</sub> markets for airports in the future depending on the geography and the size of the airport. This justifies the analysis of dedicated LH<sub>2</sub> infrastructure installations. Consequently, this study's approach is relevant for larger airports, where the uptake of H<sub>2</sub> might dominate other close-by H<sub>2</sub> demand applications, see Section 4.1. There, a dedicated on-site or off-site infrastructure might lead to the lowest supply costs. It is also worth investigating dedicated infrastructure setups for smaller airports without any access to an existing H<sub>2</sub> market. On the other side, if smaller airports have access to an H<sub>2</sub> market i.e. through a GH<sub>2</sub> pipeline or a close-by

central production hub, dedicated infrastructure deployments might rather not be too relevant. Nevertheless, all resulting costs of dedicated LH<sub>2</sub> supply chains for aviation should always be compared to general H<sub>2</sub> market costs to decide on the best supply options.

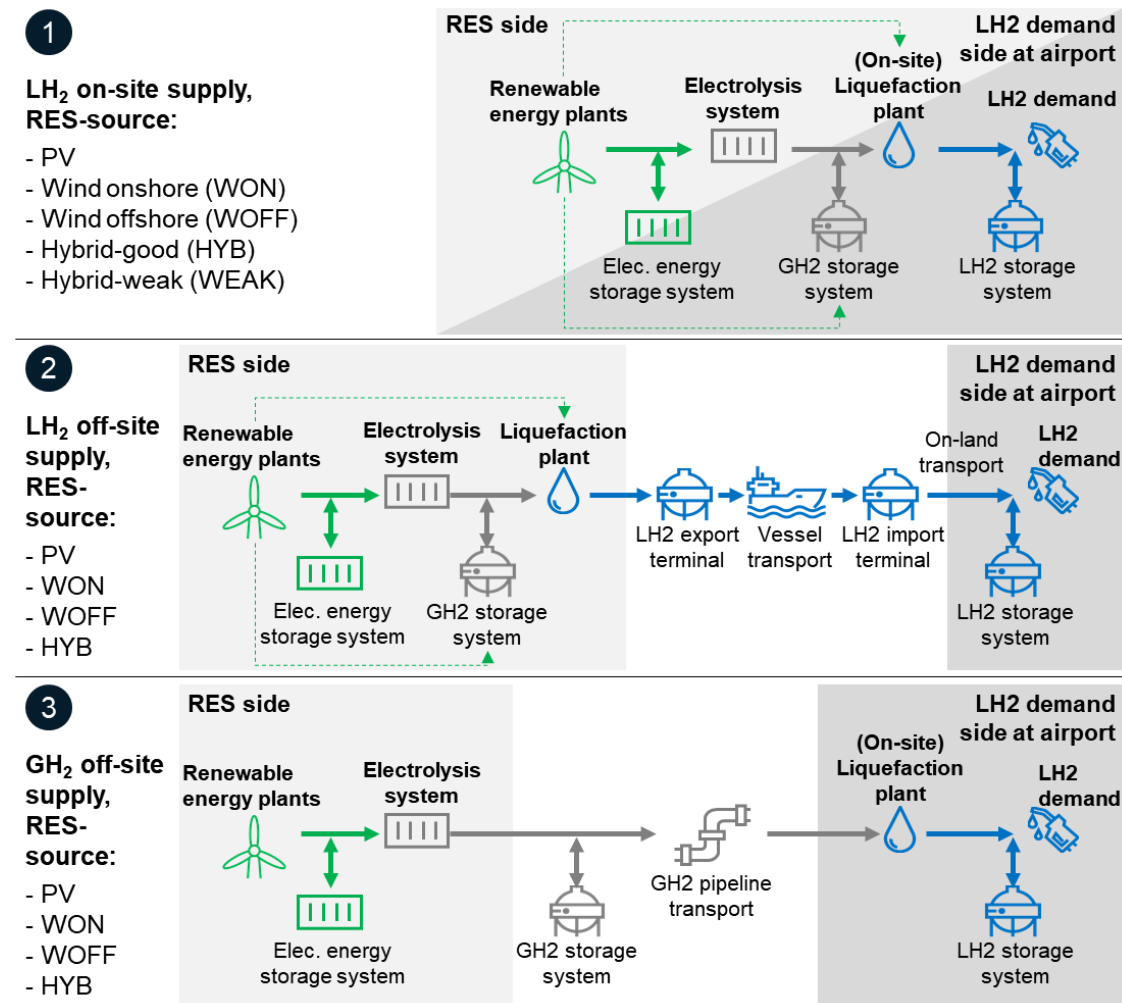


**Figure 5.1:** Considered LH<sub>2</sub> supply pathways to refuel LH<sub>2</sub>-powered aircraft in this study; naming of supply setups based on different renewable energy sources (RES): PV – photovoltaics, WON – wind onshore, WOFF – wind offshore, HYB – good hybrid, WEAK – weak hybrid location (see Section 5.1.3)

## LH<sub>2</sub> supply system: components and pathways

In general, the three component groups shown in Section 2.2 are relevant for LH<sub>2</sub> energy systems. Thus, three main supply setups are likely combining the component classes for an airport LH<sub>2</sub> supply chain [52,112,240,241]. In Figure 5.1, a LH<sub>2</sub> on-site, LH<sub>2</sub> off-site, and a GH<sub>2</sub> off-site supply are shown.

In a LH<sub>2</sub> on-site (LH<sub>2</sub>ON) supply scenario (case 1 in Figure 5.1) the RES, H<sub>2</sub> production and H<sub>2</sub> liquefaction are at or close to the airport and no longer-distance transport of H<sub>2</sub> is required.

In that setting, the following conversion components are required: green electricity is generated from RES which can be photovoltaics (PV), wind onshore (WON), or wind offshore (WOFF) plants. These power water electrolysis systems (ELY) convert water into GH<sub>2</sub> and oxygen. Such a system might also include a compressor to increase the pressure of the GH<sub>2</sub> output – depending on the electrolysis technology chosen and the system requirements behind

the ELY. Then, the GH<sub>2</sub> is cooled down to reach its liquid phase, LH<sub>2</sub>, at ~20 K in an H<sub>2</sub> liquefaction plant (LFP).

Alongside these conversion steps, storage systems can buffer and balance fluctuations in production versus demand. Electric energy storage systems (ES) can be combined with the RES, while GH<sub>2</sub> storage systems are placed behind the ELY. For the latter, either underground caverns or aboveground pressurized storage are considered. For both of these options, compressors are installed on the intake side. Given the H<sub>2</sub> output pressure of the ELY the GH<sub>2</sub> compressor increases the H<sub>2</sub> feed to the required nominal pressure of the storage (e.g., 180 bar for a cavern). The use of a constant pressure valve is assumed for unloading the GH<sub>2</sub> storages, so no further compressor power is needed. Lastly, an above-ground LH<sub>2</sub> storage system buffers the liquefied H<sub>2</sub>, before it enters the LH<sub>2</sub> refueling system at the airport. In this study, the LH<sub>2</sub> storage includes cryogenic H<sub>2</sub> pumps to fill and empty the storage most efficiently with the least H<sub>2</sub> losses [112,115]. Another option with high losses would be unloading making use of pressure differentials (see Section 2.2).

In this chapter, LH<sub>2</sub> refueling systems will not be considered in detail, since the main technoeconomics and design choices were already discussed in Section 4.2.

Compared to the on-site supply, the RES, ELY, and LFP are now at an exporting location in an LH<sub>2</sub> off-site (LH<sub>2</sub>OFF) scenario (case 2 in Figure 5.1). LH<sub>2</sub> is then transported via large overseas vessels and an on-land transport mode (can also be >100 km) to the airport. Export and import terminals are installed which consist mainly of LH<sub>2</sub> storages and cryopumps for loading and unloading of the LH<sub>2</sub> vessel. For on-land transportation, only LH<sub>2</sub> truck transport systems are considered in this study. However, this could also be done using inland vessels or train systems, e.g., to avoid road congestion. Such transport modes often come with higher costs for very short distances and only similar or lower costs for longer distances above 300 km [242].

In a GH<sub>2</sub> off-site (GH<sub>2</sub>OFF) scenario (case 3 in Figure 5.1), gaseous H<sub>2</sub> is generated at an export region but then transported via GH<sub>2</sub> pipeline systems to the receiving airport. In that case, the LFP is also placed at the airport which leads to a “disconnect” between the H<sub>2</sub> generation and the LH<sub>2</sub> energy system. The GH<sub>2</sub> pipelines can either be built “greenfield”, so installing new pipeline routes, or retrofitting existing natural gas pipelines that are currently or will not be operated anymore in the near- to mid-term future. Furthermore, GH<sub>2</sub> compressor and valve stations are required at a regular distance which depends on several parameters [105,163,168], see Appendix D2.4 and Section 5.3.2. In the retrofitting case, existing stations are replaced and H<sub>2</sub>-compatible coatings are applied to the pipes, see EHB in Section 2.2. Pipelines are assumed to only transport GH<sub>2</sub> and do not function as flexible storage in the energy system (static load operation). If H<sub>2</sub> is consumed at the importing location, the same amount has to be loaded into the pipeline at the origin/export location. Compared to current operating principles of larger natural gas pipelines this is a valid approach as shown in [163,165,168], see also Section 2.2.

### 5.1.2 Methodology and model equations

The optimization problem is defined by the objective function, optimization variables, main constraints, and operating principles.

### Optimization objective function

The overall objective is to minimize total costs for LH<sub>2</sub> supply at airports. Therefore, the total annual costs  $C_{TAC}$  per component  $i$  are calculated as shown in Eq. 5.1. The total annual costs are determined for a specific time period (scenario)  $t$  :

$$\min \sum_i \underbrace{C_{TAC,CAPEX,i,t} + C_{TAC,OPEX,i,t}}_{=C_{TAC,i,t}} \quad \text{USD} \quad (5.1)$$

The total annual costs are composed of capital expenditures (CAPEX)  $C_{TAC,CAPEX,i,t}$ , and operating expenditures (OPEX)  $C_{TAC,OPEX,i,t}$ . The CAPEX depends on the sizing  $x_i$  of each component (Eq. 5.2). Applying the annuity payment factor method (Eq. 5.2 & 5.5), the CAPEX is determined as follows:

$$C_{TAC,CAPEX,i,t}(x_i) = C_{CAPEX,total,i,t}(x_i) \cdot a_{i,t} \quad \text{USD} \quad (5.2)$$

$$\text{with} \quad C_{CAPEX,total,i,t}(x_i) = C_{CAPEX,direct,i,t}(x_i) \cdot f_{inst,i} \cdot f_{ind,i} \cdot \frac{1}{f_{avail,i}} \quad \text{USD} \quad (5.3)$$

$$\text{with} \quad C_{CAPEX,direct,i,t}(x_i) = r_{i,t} \cdot C_{CAPEX,direct,i,2020}(x_i) \quad \text{USD} \quad (5.4)$$

$$\text{with} \quad a_{i,t} = \frac{(1 + i_{i,t})^{T_{DP,i,t}} \cdot i_{i,t}}{(1 + i_{i,t})^{T_{DP,i,t}} - 1} \quad - \quad (5.5)$$

In Eq. 5.3, the total component CAPEX is calculated by multiplying the scenario-independent factors for installation costs  $f_{inst,i}$ , indirect project costs  $f_{ind,i}$ , and the availability of each component  $f_{avail,i}$  with the direct CAPEX ( $C_{CAPEX,direct,i,t}$ ) of the components. Latter is derived based on direct CAPEX reference curves in 2020 ( $C_{CAPEX,direct,i,2020}$ ) and a cost reduction factor  $r_{i,t}$ , see Eq. 5.4. The direct CAPEX functions are provided in Appendix D1. The cost reduction factors are used to translate costs into the specific time period (scenario) while reflecting learning effects (see Appendix D1.1). Lastly, the CAPEX calculation uses the annuity factor which is calculated with the interest rate  $i_{i,t}$  and the depreciation period  $T_{DP,i,t}$  (Eq. 5.5).

Total annual costs from OPEX (Eq. 5.6) are derived based on fixed operations and maintenance (OM) cost factors  $c_{OM,i,t}$  for most components. Only the ELY and transport modes have other OM costs  $C_{OM,other,i,t}$  which are described in Appendix D2.2 and D2.4.

$$C_{TAC,OPEX,i,t} = C_{CAPEX,total,i,t}(x_i) \cdot c_{OM,i,t} + C_{OM,other,i,t} + C_{H2O,i,t} + C_{refri,i,t} + C_{fuel,i,t} \quad \text{USD} \quad (5.6)$$

Furthermore, costs for water supply  $C_{H2O,i,t}$ , loss of refrigerant fluids  $C_{refri,i,t}$  and fuel  $C_{fuel,i,t}$  are relevant for the ELY, the LFP and transport modes, respectively.

Since the total energy system optimization already reflects the operational costs of drawing electricity by installing RES, electricity costs are accounted for separately and not for each component in this study. The same approach is used for accounting costs for H<sub>2</sub> losses, which are compensated by sizing all required system components bigger.

## Optimization variables and main constraints

In the following, technical aspects are highlighted of how these LH<sub>2</sub> supply pathways are optimized – starting with the optimization variables.

The optimization variables are shown in Table 5.1. The sizing of compressors and cryopumps are not treated as separate optimization variables and are always designed accordingly to the storage size and required charging/discharging mass flows. In addition to the design sizes, the decision of building a storage component or not is optimized using binary variables (row 8). Lastly, the pressure level of the GH<sub>2</sub> as the output of the ELY is also subject to optimization (row 9).

**Table 5.1:** Optimization variables considered in this study

Component or systems	Optimization variable
1 Renewable energy sources (PV, WON, WOFF) – maximum power rating	$P_{PV,max}, P_{WON,max}, P_{WOFF,max}$
2 Electrolysis system – max. power rating	$P_{ELY,max}$
3 Electric energy storage – max. electric energy stored	$E_{ES,max}$
4 GH <sub>2</sub> storage (Sto): cavern, above-ground (AG) – max. mass stored and the initial state of charge	$m_{GH_2Sto,cavern,max}, m_{GH_2Sto,AG,max}, F_{GH_2Sto,0}$
5 Liquefaction plant – max. capacity per day	$\dot{m}_{LFP,in,max}$
6 LH <sub>2</sub> storage (Sto) – max. mass stored and the initial state of charge	$m_{LH_2Sto,max}, F_{LH_2Sto,0}$
7 Transportation design – annual departures of LH <sub>2</sub> vessels	$n_{vessel,departures}$
8 Binary variables for storage systems $i$	$b_{built,i} (0,1)$
9 Pressure output of GH <sub>2</sub> from ELY and on the GH <sub>2</sub> bus	$p_{GH_2bus}$

Main constraints exist for each component system and are discussed in detail in Appendix D2. In general, constraints are that maximum power or mass flow settings as well as minimum and maximum fill levels of all storage systems must not be exceeded. Additionally, storage fill levels must be equal or larger at the end of the simulation compared to the initial state of charge.

Other modeling constraints result from the balance equations of the different components that are interconnected on electric power, GH<sub>2</sub> mass flow, and LH<sub>2</sub> mass flow level as shown in Figure 5.1.

First, the electric power balance is derived in Eq. 5.7a for the LH<sub>2</sub> on- and off-site supply pathway, for GH<sub>2</sub> off-site cases in Eq. 5.7b:

LH <sub>2</sub> -on- /off-site	$P_{RES} = P_{ELY} + P_{LFP} + P_{GH_2comp} + P_{ES}$	W	(5.7a)
GH <sub>2</sub> -off- site	$P_{RES} = P_{ELY} + P_{GH_2comp} + P_{ES}$	W	(5.7b)

In the LH<sub>2</sub> on-site scenario, the RES ( $P_{RES}$ ) powers all major components that draw electricity like the ELY (incl. compressors)  $P_{ELY}$ , the LFP  $P_{LFP}$ , the compressors of the GH<sub>2</sub> storage systems  $P_{GH_2comp}$  and the ES  $P_{ES}$ . For all storage components positive power or mass flow values are defined as charging (vs. negative for discharging). Only the cryopumps of the LH<sub>2</sub> storage system are not connected to the RES but to a local electricity grid as described for LH<sub>2</sub> refueling systems in [112]. This is important because it enables discharging the LH<sub>2</sub> storages to fulfill demands when no RES availability is given (no wind, no radiation).

For off-site LH<sub>2</sub> supply, the balance equation does not change, since the LFP is still placed at the exporting energy system site.

If off-site GH<sub>2</sub> supply (Eq. 5.7b) is analyzed, the LFP is placed at or close to the airport. Consequently, the electricity for the LFP is also sourced by grid electricity at the airport directly.

Second, the balance equation regarding GH<sub>2</sub> mass flows is defined in Eq. 5.8a-c:

LH <sub>2</sub> -on- /off-site	$\dot{m}_{ELY} = \dot{m}_{GH_2Sto} + \dot{m}_{LFP,in}$	kg/s	(5.8a)
GH <sub>2</sub> -off- site	$\dot{m}_{ELY} = \dot{m}_{GH_2Sto} + \dot{m}_{pipe,in}$ and $\dot{m}_{pipe,out} = \dot{m}_{LFP,in}$	kg/s	(5.8b,c)

The GH<sub>2</sub> mass flow output of the ELY  $\dot{m}_{ELY}$  feeds either the LFP directly  $\dot{m}_{LFP,in}$  or is stored in one of the two storage  $\dot{m}_{GH_2Sto}$  options (cavern or above-ground) in an LH<sub>2</sub> on- or off-site setup.

For off-site GH<sub>2</sub> supply, the pipeline system is added before the feed enters the LFP, leading to the separation of the balance equation in Eq. 5.8b. However, when realizing such a GH<sub>2</sub>-off-site system, the GH<sub>2</sub> storage could also be placed differently – at the airport side or even along the pipeline route.

Since different GH<sub>2</sub> pressure levels are required for filling the GH<sub>2</sub> storages (180–200 bar), the LFP (30–80 bar), or the pipeline system (intake at 70 bar), the pressure setting of the ELY output mass flow is a variable for optimization. With that not only the sizing of compressors can be optimized, but also the specific energy consumption of the LFP. As shown in Appendix D2.3, the minimal work required for liquefaction decreases slightly with higher input feed pressures. Further information on the pressure dependencies for the depicted components is presented in Appendix D2.2-4.

Third, the LH<sub>2</sub> mass flow balances are shown in Eq. 5.9a-d:

LH <sub>2</sub> -on- /GH <sub>2</sub> -off- site	$\dot{m}_{LFP,out} = \dot{m}_{LH_2Sto} + \dot{m}_{LH_2demand}$	kg/s	(5.9a)
LH <sub>2</sub> -off- site	$\dot{m}_{LFP,out} = \dot{m}_{LH_2,export} + \dot{m}_{LH_2vessel}$ and $\dot{m}_{LH_2vessel} = \dot{m}_{LH_2,import} + \dot{m}_{LH_2truck}$ and $\dot{m}_{LH_2truck} = \dot{m}_{LH_2Sto} + \dot{m}_{LH_2demand}$	kg/s	(5.9b-d)

In the LH<sub>2</sub> on-site and GH<sub>2</sub> off-site setups, the LFP mass flow output  $\dot{m}_{LFP,out}$  is directly linked with the LH<sub>2</sub> demand ( $\dot{m}_{LH_2demand}$ ) and the LH<sub>2</sub> buffer storages ( $\dot{m}_{LH_2Sto}$ ) at the airport. Only in the off-site LH<sub>2</sub> supply case, the LH<sub>2</sub> output of the LFP is decoupled with the airport side and first transported via vessels ( $\dot{m}_{LH_2vessel}$ ) and then with on-land transport modes (truck in this study,  $\dot{m}_{LH_2truck}$ ). On the export and import side, there are also storage terminals that can be used for buffering ( $\dot{m}_{LH_2,export}$ ,  $\dot{m}_{LH_2,import}$ ).

It has to be noted, that the chosen level of detail of the technical component model does not consider differing state variables such as temperatures or LH<sub>2</sub> pressures.

## Operation of components: energy management system and paradigms

To enable the optimization of the previously described systems, operating principles for each component have to be defined. Fixed operating rules are chosen to ensure the computability of the optimization even with non-linear models.

The main goal of the energy management system is to maximize the utilization of cost-dominating components, which in this study are the ELY and the LFP. In dependence on the RES availability  $P_{RES}$  and the LH<sub>2</sub> demand  $\dot{m}_{LH2demand}$  at the airport, these two components are steered to make maximum use of available RES while always fulfilling LH<sub>2</sub> demands for aircraft refueling. In addition to that, the given component constraints also apply.

If storage systems are installed, the state of charge / fill level influences the operation of the components, too. The state  $Z$  of the storage component  $i$  is defined as empty ("0"), full ("2"), and flexible ("1") when the storage can only be charged, discharged, or both, respectively.

In the LH<sub>2</sub> on-site supply pathway, the ELY is set ( $P_{ELY,set}$ ) for maximum usage of RES ( $P_{ELY,set,RES}$ ) or its output is limited, if no further GH<sub>2</sub> can be liquefied or stored ( $P_{ELY,set,GH2}$ ), see Eq. 5.10-12.

$$\begin{array}{l} \text{ELY set-} \\ \text{value} \end{array} \quad P_{ELY,set} = \min(P_{ELY,set,RES}, P_{ELY,set,GH2}) \quad (5.10)$$

$$\begin{array}{l} \text{with} \end{array} \quad P_{ELY,set,RES} = \begin{cases} P_{RES} - P_{LFP} - P_{GH2comp}, & Z_{ES} = 0 \\ P_{RES} + P_{ES,max} - P_{LFP} - P_{GH2comp}, & Z_{ES} \neq 0 \end{cases} \quad (5.11)$$

$$\begin{array}{l} \text{with} \end{array} \quad P_{ELY,set,GH2} = \begin{cases} P_{ELY}(\dot{m}_{LFP,in} + \dot{m}_{GH2Sto,max}), & Z_{GH2Sto} \neq 2 \\ P_{ELY}(\dot{m}_{LFP,in}), & Z_{GH2Sto} = 2 \end{cases} \quad (5.12)$$

The LFP operation  $\dot{m}_{LFP,in,set}$  is set similarly (Eq. 5.13-15). Here, also the GH<sub>2</sub> feed availability from ELY or GH<sub>2</sub> storages ( $\dot{m}_{LFP,in,set,GH2}$ ) or the offtake of LH<sub>2</sub> from aircraft or an LH<sub>2</sub> storage system ( $\dot{m}_{LFP,in,set,demand}$ ) can limit the maximum operation of the LFP:

$$\begin{array}{l} \text{LFP set-} \\ \text{value} \end{array} \quad \dot{m}_{LFP,in,set} = \min(\dot{m}_{LFP,in,set,GH2}, \dot{m}_{LFP,in,set,demand}) \quad (5.13)$$

$$\begin{array}{l} \text{with} \end{array} \quad \dot{m}_{LFP,in,set,GH2} = \begin{cases} \dot{m}_{ELY}, & Z_{GH2Sto} = 0 \\ \dot{m}_{ELY} + \dot{m}_{GH2Sto,max}, & Z_{GH2Sto} < 0 \end{cases} \quad (5.14)$$

$$\begin{array}{l} \text{with} \end{array} \quad \begin{array}{l} \dot{m}_{LFP,in,set,demand} \\ = \end{array} \begin{cases} \dot{m}_{LFP,in}(\dot{m}_{LH2demand} + \dot{m}_{LH2Sto,max}), & Z_{LH2Sto} \neq 2 \\ \dot{m}_{LFP,in}(\dot{m}_{LH2demand}), & Z_{LH2Sto} = 2 \end{cases} \quad (5.15)$$

The available RES should be used completely to reach maximum capacity factors and hence, minimized levelized costs of electricity (LCOE). However, when the settings of the ELY and LFP have to be reduced as described in Eq. 5.12 and 5.15, the renewable energy generation will also be capped.

The operating values for the storage systems are determined based on the ELY and LFP settings following the balance Eq. 5.7a/b, 5.8a-c, and 5.9a-d. It has to be noted that for the GH<sub>2</sub> storages, no re-allocation of GH<sub>2</sub> mass flows is considered between the two options (cavern and above-ground).



If the supply pathway is changed to an LH<sub>2</sub>OFF setup, the same operating rules apply for the energy system up to the point where LH<sub>2</sub> would be fed into the refueling system. The only difference is that a specific demand profile is used for the LH<sub>2</sub> export terminal (discussed in Section 5.1.3).

For GH<sub>2</sub>OFF supply pathways, the ELY and GH<sub>2</sub> storages are operated also in a similar manner as described above. Only the LFP is now steered more independently since it does not depend on the availability of RES at the export region but can draw electricity from a local grid at the airport flexibly. One limiting factor though is the availability of GH<sub>2</sub> from the ELY and GH<sub>2</sub> storages that are directly fed into the LFP via the pipeline system, which is operated statically as described in Section 5.1.1.

### 5.1.3 Scenario definitions

The given optimization problem is solved within the following scenarios. They are defined by main techno-economic parameters, RES locations, and airport settings.

#### Techno-economic parameters

Table 5.2 shows the main techno-economic parameters of the supply components used in this study. In total, three main scenarios are discussed based on 2020 cost reference values.

Since major LH<sub>2</sub> uptake from aviation is rather expected for 2050 and later [16,19,112,243], the main scenario is called the “2050 base case”. It reflects a great progress in the deployment of general green H<sub>2</sub> infrastructure for main use cases, e.g., chemicals, industry. With this, the cost reduction potential compared to today is already significant for GH<sub>2</sub> production, but also LH<sub>2</sub> components would be installed for hard-to-abate transport modes and for general transport/trade of H<sub>2</sub>. To be able to reflect sensitivities of the cost results from a 2050 base case scenario, two other scenarios are considered: a more conservative one, the “2035 base case” and a very progressive one, the “2050 progressive case”. Given these three scenarios, a valid range of resulting LH<sub>2</sub> supply costs in 2050 should result.

**Table 5.2:** Economic parameters for main components – further details are shown in Appendix D1 and D2. Note: resulting total specific CAPEX are shown incl. installation and indirect project costs, total cost equations are derived in D1

Component	Parameter	Unit	2020 reference	2035 base	2050 base	2050 progressive	Sources
<b>PV (1-axis tracking)</b>	Specific total CAPEX	USD/kW	650	600	400	300	[134,244–248]
	Depreciation period	Years	30	30	30	40	[134,244,245,248]
	O&M factor	%	2.5%	2.5%	2.5%	2.5%	[134,244,245]
<b>Wind on-shore</b>	Specific total CAPEX	USD/kW	1,300	1,100	900	675	[80,134,244,249,250]
	Deprec. period	Years	25	25	25	30	[245,249]
	O&M factor	%	3.6%	3.6%	2.8%	2.8%	[245,249]
<b>Wind off-shore</b>	Specific total CAPEX	USD/kW	2,900	2,500	2,250	1,687	[80,134,244,249,250]
	Deprec. period	Years	25	25	25	30	[245,248,249]
	O&M factor	%	3.2%	3.2%	3.3%	3.3%	[134,245,248,249]
	Specific total CAPEX	USD/kWh	350	200	150	112	[111,244,246,251]

<b>Electric energy storage</b>	Deprec. period	Years	15	15	15	15	[111,244]
	O&M factor	%	3.0%	3.0%	3.0%	3.0%	[111,244]
<b>Electrolysis system</b>	Specific total CAPEX	USD/kW	1,500	438	285	214	[44,145,220,252–254]
	Deprec. period	Years	30	30	30	30	[144,164,255–
	Stack lifetime <sup>a</sup>	Operating hours	<90k	90k	120k	120k	[144,145,254,256,257,260]
	O&M factor	%	3.0%	3.0%	3.0%	3.0%	[143,144,255,257,261,262]
<b>GH<sub>2</sub> compressor</b>	Specific total CAPEX <sup>b</sup>	USD/kW	1,636	1,489	1,243	1,243	[152,263–266]
	Deprec. period	Years	15	15	15	15	[152,198]
	O&M factor	%	2.0%	2.0%	2.0%	2.0%	[106,152,266–269]
<b>Liquefaction plant</b>	Specific total CAPEX <sup>b</sup>	Mn USD/tpd	1.33	1.13	0.84	0.63	[59,153,162,187,197,198,253,263,2
	Deprec. period	Years	20	20	20	25	[182,187]
	O&M factor	%	4.0%	4.0%	4.0%	4.0%	[182,254,272]
<b>GH<sub>2</sub> cavern storage</b>	Specific total CAPEX <sup>b</sup>	USD/kgGH <sub>2</sub>	18	18	18	18	[106,152,155–157,160,257,273,
	Deprec. period	Years	30	30	30	40	[155,157,160,274,
	O&M factor	%	2.0%	2.0%	2.0%	2.0%	[106,276]
<b>GH<sub>2</sub> above-ground storage</b>	Specific total CAPEX <sup>b</sup>	USD/kgGH <sub>2</sub>	581	529	442	442	[65,82,110,111,91,97,
	Deprec. period	Years	20	20	20	30	[111,152,269]
	O&M factor	%	1.5%	1.5%	1.5%	1.5%	[252,268,269,279]
<b>LH<sub>2</sub> storage</b>	Specific total CAPEX <sup>b</sup>	USD/kgGH <sub>2</sub>	41	35	26	26	[152,156,202]
	Deprec. period	Years	20	20	20	30	[106,269]
	O&M factor	%	2.0%	2.0%	2.0%	2.0%	[106]
<b>LH<sub>2</sub> cryopump</b>	Specific total CAPEX	USD per kg/h	416	354	264	264	[112,197,198]
	Deprec. period	Years	10	10	10	10	[112,198]
	O&M factor	%	3.0%	3.0%	3.0%	3.0%	[112,197,198]
<b>LH<sub>2</sub> truck</b>	Specific total CAPEX	Mn USD per truck	1.01	0.86	0.64	0.64	[106,111,152,162,254,263]
	Deprec. period	Years	12	12	12	12	[112]
	O&M factor <sup>c</sup>	%	3.0%	3.0%	3.0%	3.0%	[112]
<b>LH<sub>2</sub> vessel</b>	Specific total CAPEX <sup>b</sup>	Mn USD per vessel	n/a	342	274	274	[111,164,254,271,282–284]
	Deprec. period	Years	n/a	25	25	25	[111,271]
	O&M factor <sup>d</sup>	%	n/a	4.0%	4.0%	4.0%	[111,164,285]
<b>GH<sub>2</sub> pipeline</b>	Specific total CAPEX <sup>b</sup>	Mn USD/km	n/a	3.45	2.76	2.76	[111,164,198]
	Deprec. period	Years	n/a	40	40	40	[111,164]
	O&M factor	%	n/a	1.0%	1.0%	1.0%	[164]

a) stack replacement costs are assumed to be 20% of the total CAPEX (incl. installation and indirect costs) [164,255,259,262]

b) at largest design scaling – more detailed specific CAPEX curves for different component design sizes to be found in the Appendix D2

c) Further variable costs: driver salary of 35 USD/h and fuel costs of 3 USD/kgH<sub>2</sub> [112]

d) Further variable costs: annual other OPEX costs of 11.3 Mn USD and fuel costs of 2.5 USD/kgH<sub>2</sub> [164,286]

For better readability, not all cost and efficiency parameters are shown in Table 5.2. These as well as specific CAPEX functions and other factors (e.g., described in Eq. 5.3) are derived in Appendix D1 and D2.

Also, it is highlighted that all derived costs are transferred to 2020-USD like in the previous chapters and cost values from literature are corrected for the right currency as well as inflation effects. For the latter, the Chemical Engineering Plant Cost Index (CEPCI) is used [287].

Overarching energy or material costs are derived. Renewable electricity costs for the energy consumptions of LH<sub>2</sub> cryopumps and the LFP in the GH<sub>2</sub> off-site pathway are assumed to be 50 USD/MWh through a Power Purchase Agreement (PPA) [106,112].

Water for the electrolysis might come from the local supply or from desalination if only salt water is available. Costs for the latter are taken to have a rather conservative estimate on water costs given the potential scarcity of water in specific geographies. As shown by Caldera and Breyer (2019) [288] as well as other studies, desalinated water including transport costs could cost less than 2.24 USD/m<sup>3</sup> of water nearly everywhere, which is used as a cost assumption in this study.

For the application of the annuity payment factor method, a fixed interest rate (cost of capital) is derived. In this study, RES incl. ES – technologies with an established market with less financing risks – come with a 4% interest rate which is in line with [134,249,289]. H<sub>2</sub> generation, conversion, and storage components are assumed to have an interest rate of 6% to reflect slightly larger risk or higher return expectations in H<sub>2</sub> business plans [112,198]. It has to be noted that the interest rate highly depends on the country where the project is planned and executed [165,289]. Since the analyses in this chapter focus on more generic techno-economics, no further sensitivities from differing interest rates are considered. This is considered in Chapter 6.

### **RES locations and settings**

The chosen modeling approach is based on a time resolution of 8760 hours per year. Therefore, input profiles of RES availability and the LH<sub>2</sub> demand at the airport are derived accordingly. In this part, the choice of RES locations and their conditions are explained.

It is one of the main goals in this chapter to derive general design rules for LH<sub>2</sub> energy systems as well as best versus worst potential supply costs. Consequently, five more generic locations are investigated that stand for specific, “archetypical” RES (weather) conditions:

- PV: strong PV (e.g., Saudi-Arabia),
- WON: strong wind onshore (e.g., Scotland [290,291]),
- WOFF: strong wind offshore (e.g., Denmark / Baltic Sea [292,293]),
- HYB: hybrid location with great wind onshore and PV conditions (e.g., Morocco) and a
- WEAK: hybrid location with weaker conditions for wind onshore and PV (e.g., Central Germany, Frankfurt).

The solar yield and wind speed weather data for the reference year 2019 is obtained from the open-science platform “Renewable.ninja” described in [294,295] – further assumptions are presented in Appendix D2.1. Additionally, projections of future wind power performances in the form of power curves are used for wind on- and offshore plants. These are also open-source and published by the U.S. National Renewable Energy Laboratory (NREL) and the International Energy Agency (IEA) [296–298].

The resulting capacity factors of the RES are shown in Figure 5.2. For the wind on- and offshore locations (WON and WOFF) very high capacity factors can be achieved. Compared to

previous work like in [103] the full load hours are higher here and might be more accurate since they reflect future wind turbine performance. Many previous energy system studies use existing (older) wind turbine power curves that might not reflect the technological improvement of larger wind turbines (Section 2.2). Great capacity factors at wind locations are followed by the hybrid wind onshore location. PV capacity factors are in general lower due to day-night cycles, but similarly good for the great PV and the good hybrid (HYB) location. At the weaker (WEAK) hybrid location, both capacity factors are significantly lower.

In addition to that, it is assumed that the RES might be placed in a radius of <100 km around the airport to make use of the best local RES sites. This is why costs for very short electricity transmission distances are also reflected, explained in Appendix D2.1.

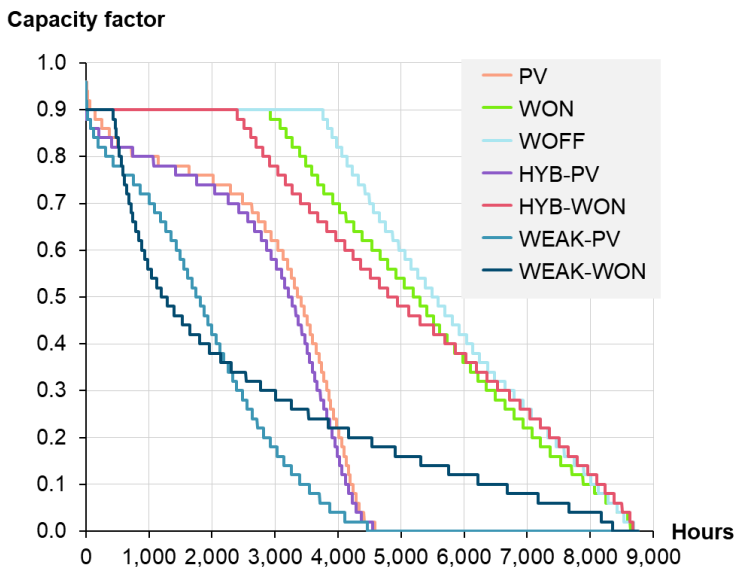


**Figure 5.2:** Capacity factors of RES at chosen locations for the year 2019 (8760 hours) incl. array losses for wind parks (see Appendix D.2.1)

There is no grid connection modeled for the ELY and the LFP for two reasons. First, this is in compliance with recent regulation presented by the European Commission [132]: For green H<sub>2</sub> supply, it will be required to have purpose-built renewable energy generation (additionality criteria) that has a temporal and geographical correlation to the H<sub>2</sub> production, see Section 2.2.1. Second, drawing electricity from a grid in times of no wind or solar radiation availability, an LH<sub>2</sub> production system designed for constant (grid) operation might lead to unacceptable loads in such a local grid. Especially at medium and larger airports where LH<sub>2</sub> production would require significant power capacity in that region [112]. In that case, grid supply might be prioritized for all basic energy consumption applications (private, commercial, and main industry sectors) and not for the use of aviation fuel. Nevertheless, the chosen dedicated infrastructure setup without a major grid connection can be seen as a “worst case” cost scenario, since no synergistic integration with local renewable energy systems is included in this analysis.

### Airport settings

Lastly, the airport setting with the resulting LH<sub>2</sub> demands is briefly characterized for the following analyses. A more detailed derivation of demands, safety, and operational aspects of H<sub>2</sub>-powered aviation is already presented in Chapter 4.

Future LH<sub>2</sub> demand projections at airports highly depend on the size of the airport and air travel routes from that airport (short vs. long-range flights) as shown in Chapter 4. While it is calculated that these demands could reach levels of >80k and >300k tLH<sub>2</sub> per annum (p.a.) at medium and larger airports in a 2050 base case scenario, demands at smaller, national airports could be below 10–20k tLH<sub>2</sub>/a.

In addition to the total size of demands, the monthly and daily demands differ by season and day time, see Figure 5.3 (built based on input Figure 4.1). Many European airports have a night curfew from 10/11 pm to 5/6 am, but there are also some without such a restriction. Seasonality of air travel demand with peaks in summer and autumn and lows in the winter season is also considered for the profile here, see Section 4.1.

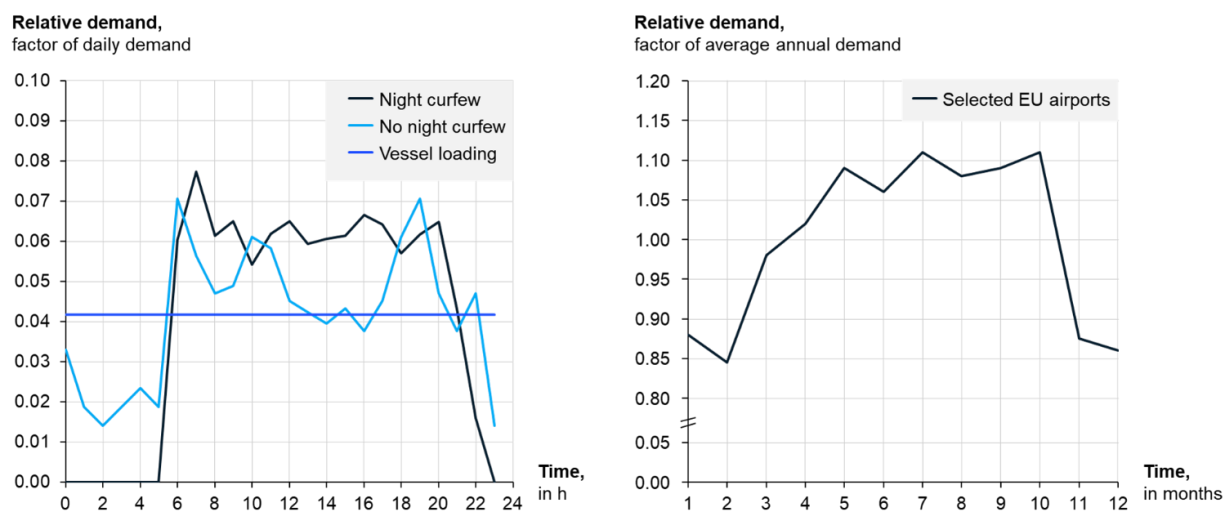


**Figure 5.3:** LH<sub>2</sub> demand profiles – left: daily profile for airports with night curfew, no night curfew, or export regions (vessel loading); right: annual demand variation for an “average” EU airport

For the following analysis of LH<sub>2</sub> off-site pathways, the demand curve at an export terminal (loading the LH<sub>2</sub> vessels) is also shown for reference. The vessel is loaded with a constant mass flow over 48 hours. The variation of total LH<sub>2</sub> demand in a month is also applied in this off-site setup.

## 5.2 LH<sub>2</sub> on-site supply chains

The techno-economics of LH<sub>2</sub> on-site supply chains are now investigated. The purpose of this analysis is to derive design rules for the on-site energy systems based on different geographic conditions and annual LH<sub>2</sub> demand sizes at airports. Furthermore, the lowest versus highest costs for supply chains should be identified to answer the overarching question of the general economic implications for H<sub>2</sub>-powered aviation.

The section is structured into three sections. First, the LH<sub>2</sub> costs are computed and general design rules are explained in detail for one specific LH<sub>2</sub> demand point in the 2050 base case scenario. Second, the techno-economic effects of varying LH<sub>2</sub> demands are highlighted. Third, the sensitivities of the resulting designs and LH<sub>2</sub> costs are tested based on scenarios with different techno-economic parameter assumptions.

### 5.2.1 LH<sub>2</sub> energy system design rules for fixed demand setting

This section showcases the optimization results for the on-site supply chains for a fixed annual demand point of 100k tLH<sub>2</sub>/a. The demand point represents a medium to larger sized airport, see Section 4.1. Furthermore, most economy-of-scale effects apply to such larger demands and make this point more relevant for deriving general design rules or generic design “recipes” for LH<sub>2</sub> energy systems.

The resulting total LH<sub>2</sub> supply costs at the dispenser (incl. refueling costs) are shown in Figure 5.4. Great hybrid RES locations provide the best techno-economic conditions for LH<sub>2</sub> supply chains – costs range from 2.04 USD/kgLH<sub>2</sub> (HYB) to 2.25–2.27 USD/kgLH<sub>2</sub> (WON, PV) and between 3.04–3.63 USD/kgLH<sub>2</sub> at WEAK and WOFF, respectively.

**LH<sub>2</sub> costs at dispenser for 100k tLH<sub>2</sub>/a demand (2050 base), in USD/kgLH<sub>2</sub>**

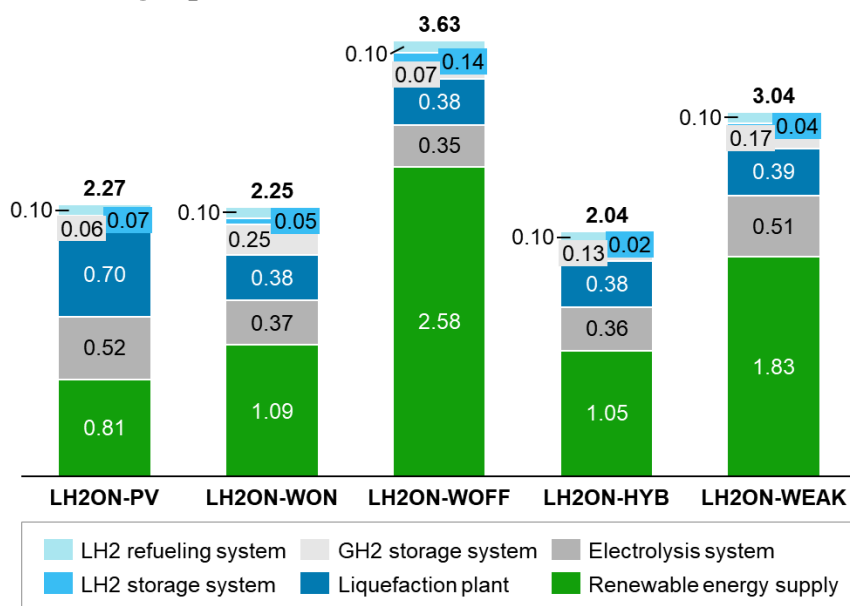


**Figure 5.4:** LH<sub>2</sub> supply costs at the dispenser for on-site setups at five locations: PV, wind onshore (WON), wind offshore (WOFF), great hybrid conditions (HYB), weaker hybrid conditions (WEAK); 2050 base case scenario with 100k tLH<sub>2</sub>/a demand

At all locations, the RES (electricity) takes the main share of total costs (36–71%). The costs for RES also lead to the main economic difference in supply at the five locations. Looking into the LCOE of renewable energy generation this is emphasized: at PV, WON, HYB, WEAK, and WOFF electricity is generated at levelized costs of 14, 18, 18, 31, and 44 USD/MWh, respectively. While the high RES costs at WEAK locations are caused by low capacity factors, the comparably very high CAPEX of wind offshore turbines leads to the highest LCOE in a 2050 base case scenario at WOFF. Vice versa, the very low CAPEX for PV installations enables the lowest LCOE at PV regions even though its worse capacity factor compared to the wind regions.

Similar trends are observed analyzing the total investment costs of the on-site energy systems. These range from 1.9 Billion (HYB), 2.0 Bn (WON & PV), 2.9 Bn (WEAK), and 3.5 Bn USD (WOFF) with main investments required for RES, followed by the LFP and similar magnitudes for the ELY. CAPEX for the refueling system incl. all (on-site) LH<sub>2</sub> storage systems make up for only a 2-5% share of total investments.

### Analysis of optimization results and derivation of design rules based on 100k tLH<sub>2</sub>/a demand point

For a better understanding of the results presented in Fig. 5.4, the optimization data will be analyzed in more detail and seven design rules for LH<sub>2</sub> energy systems (for aviation) are derived.

- I. Component selection: Electric energy storage as well as aboveground GH<sub>2</sub> storage capacities are not installed in the 2050 base case scenario (see corresponding columns in Table 5.3).

Both storage systems have too high CAPEX per energy stored (150 USD/kWh<sub>el</sub> for ES, 12-15 USD/kWh<sub>H<sub>2</sub></sub> for GH<sub>2</sub> above-ground storage) compared to GH<sub>2</sub> caverns and LH<sub>2</sub> storages (both <1 USD/kWh<sub>H<sub>2</sub></sub>). Even though the installation of an ES gives flexibility on the electricity balance and hence, would enable higher utilization of the ELY, it leads to very high supply costs.

**Table 5.3:** Optimal design for five locations, 2050 base case scenario with 100k tLH<sub>2</sub>/a demand

LH <sub>2</sub> setup / location	Component	Ely-system	LFP	Electric energy storage	Cavern storage	Above-ground storage	LH <sub>2</sub> storage	GH <sub>2</sub> pressure behind Ely-system $p_{GH_2bus}$
		$P_{ELY,max}$	$\dot{m}_{LFP,in,max}$	$E_{ES,max}$	$M_{GH_2Sto,cavern}$	$M_{GH_2Sto,AG}$	$M_{LH_2Sto}$	
	Unit	MW	tons per day (tpd)	MWh	tons GH <sub>2</sub>	tons GH <sub>2</sub>	tons LH <sub>2</sub>	bar
<b>LH2ON-PV</b>		1,439	642	-	1,498	-	2,066	30
<b>LH2ON-WON</b>		957	316	-	9,740	-	1,329	61
<b>LH2ON-WOFF</b>		923	331	-	2,084	-	4,701	44
<b>LH2ON-HYB</b>		946	304	-	4,091	-	384	73
<b>LH2ON-WEAK</b>		1,364	314	-	5,672	-	1,018	77

- II. RES: Smallest RES capacity installations are required at great wind on- and offshore and largest for weaker RES locations (see  $P_{RES}$  in Figure 5.5).

Great PV conditions still lead to more than a factor of 2 higher capacity requirements vs. the wind setups, because H<sub>2</sub> can only be produced at day times when solar radiation is available. For great hybrid locations, RES installations are 1.5 factor higher than at strong wind regions, making use of both high PV and wind onshore power yields. This factor increases to 3 for WEAK setups due to the low capacity factors, which are also shown as utilization factors in Figure 5.6A. In the hybrid setups, no strong preference for PV or wind onshore plant installations is observed (Figure 5.5).

**LH<sub>2</sub> on-site design for 100k tLH<sub>2</sub>/a demand (2050 base),**  
in MW max. power rating

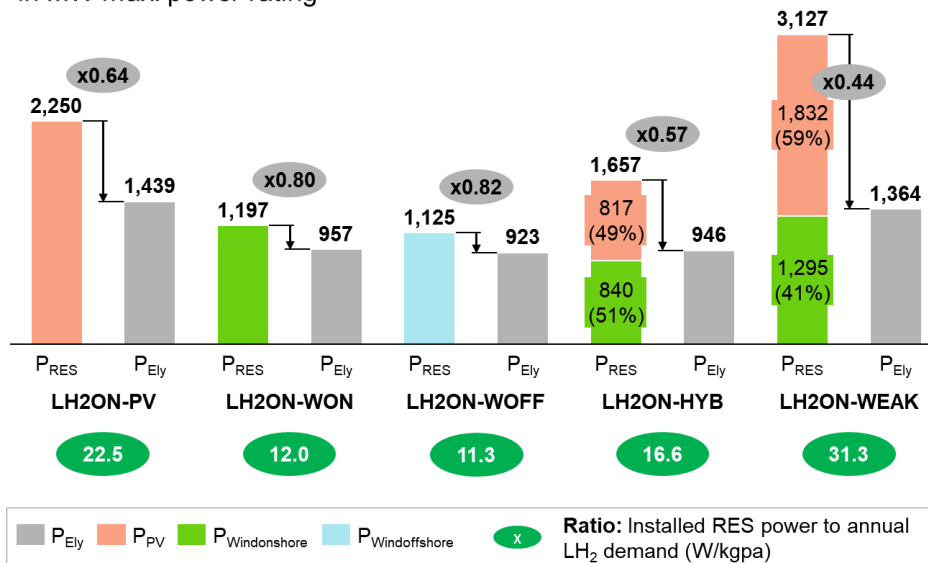


**Figure 5.5:** Design of RES and eLy-system for five locations, 2050 base case scenario with 100k tLH<sub>2</sub>/a demand

Figure 5.6A also reveals that the renewable energy generation has to be capped in all regions for some time periods, leading to lower realized capacity factors (RES used) than available (RES total). The reason for this is that no ES is installed to buffer the electricity when the ELY operates at maximum power.

Besides the costs and installation requirements, also the land use of the different RES has to be considered. If a land use of 20 MW/km<sup>2</sup> [299] and 100 MW/km<sup>2</sup> [134,300] is assumed for large-scale future wind onshore turbines and 1-axis tracking PV systems, respectively, the land needs become huge – comparable to the area of ~1,500–6,000 soccer fields. In the 100k tLH<sub>2</sub>/a demand setup, 23–83 km<sup>2</sup> of land would need to be available for RES. Such high land uses would justify the existence of wind offshore supply setups with significantly fewer turbines for regions with high land constraints despite higher supply costs.

**Utilization of main components for 100k tLH<sub>2</sub>/a demand (2050 base, LH<sub>2</sub> on-site), in % of full year (8760h)**

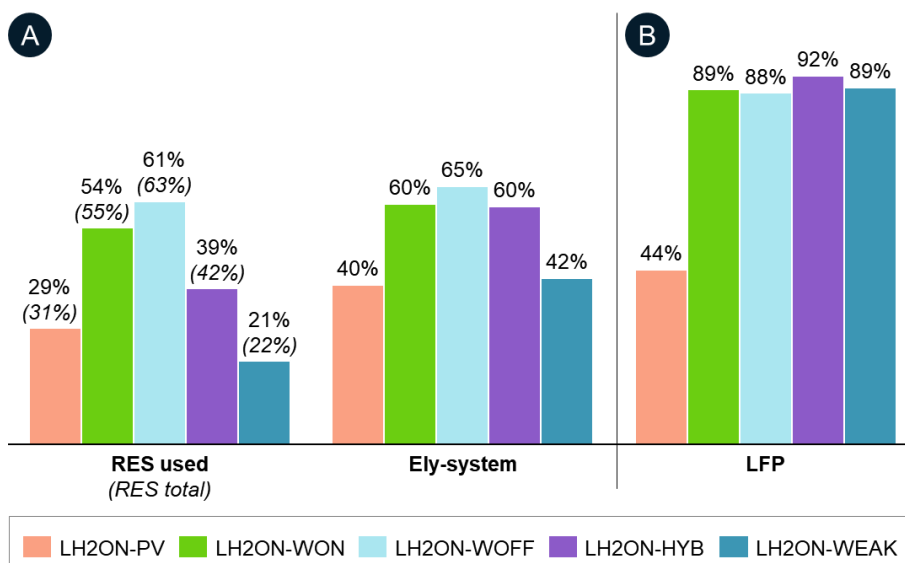


**Figure 5.6:** Annual utilization of main components for five locations, 2050 base case scenario with 100k tLH<sub>2</sub>/a demand – left side, A) RES, eLy-system; right side, B) LFP



- III. ELY: Ely-system capacities are designed the smallest for locations with the least fluctuating RES profiles throughout the day (see Figure 5.5, Table 5.3).

Since no electric energy storage is installed, the ELY has to be operated flexibly in accordance with the availability of RES. Consequently, the smallest ELY capacities are installed at WON, WOFF, and HYB regions, where RES availability is relatively constant throughout the day.

So, the ELY is also designed smaller at the WEAK compared to the PV location due to a more evenly distributed RES availability (no large day and night difference). The resulting utilization of the ELY underlines this design rule, see Figure 5.6A and the relative ELY size in relation to average daily LH<sub>2</sub> demands in Figure 5.7.

- IV. LFP: Its design is optimized for the smallest capacity and hence, maximum utilization due to high costs (mostly CAPEX) and significantly higher specific electricity consumption in part-load operation in all cases (see Table 5.3).

The annual utilization reaches 88–92% (see Figure 5.6B) – minor utilization “losses” are caused by time periods with part-load operation. In the case of the ELY (rule III), this is not an issue leading to significantly higher costs, since the ELY’s specific energy demand even decreases in part-load operation (see also Figure 5.7 for comparison of sizes between LFP and ELY).

Only at the great PV location, no electricity is available at nights. This is why, plus given that there is no ES installed, the LFP cannot be designed for the highest utilization (44% only). Thus, the LFP is shut off at nights (~12 hours). The costs for installing ES to enable maximum utilization of the LFP are higher than having a more flexible operation of the LFP and the penalty of higher electricity consumption. It has to be noted that there is no information available on the energy consumption or general feasibility of such an operation of the LFP. Hence, only cost penalties for part-load operations but not for “half day on” / “half day off” operations are considered in this study.

**Component sizes for 100k tLH<sub>2</sub>/a demand (2050 base, LH<sub>2</sub> on-site), in kg capacity per kgH<sub>2</sub>demand/day**

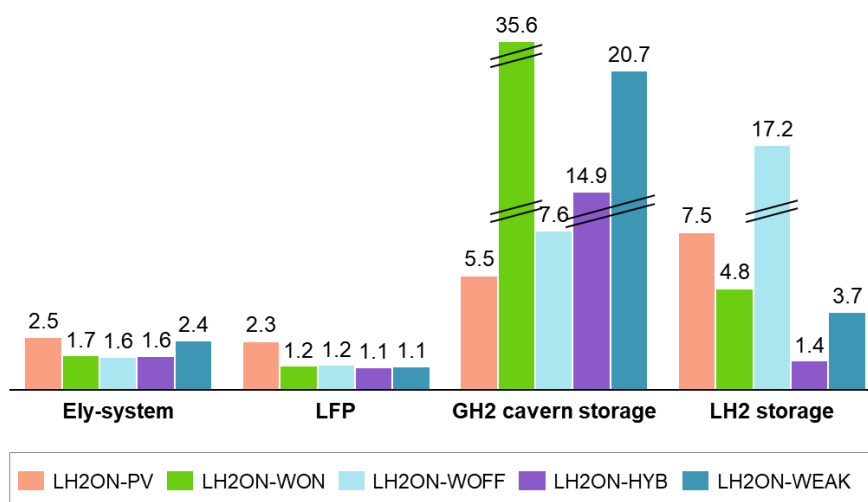


**Figure 5.7:** Relative component design sizes compared to the average daily LH<sub>2</sub> demand (274 tLH<sub>2</sub>/d) for five locations, 2050 base case scenario with 100k tLH<sub>2</sub>/a demand – ely-system in kgH<sub>2</sub>/d output, LFP in kgH<sub>2</sub>/d intake and storages in kgH<sub>2</sub>stored capacity

- V. Storages: Designs highly depend on RES fluctuations (daily and seasonal). In most cases, building larger GH<sub>2</sub> cavern storages should be preferred versus LH<sub>2</sub> storages (see Table 5.3 and Figure 5.7).

Even though the CAPEX of larger GH<sub>2</sub> cavern and LH<sub>2</sub> storage systems do not differ too much, the main benefit of having a large GH<sub>2</sub> storage is a more constant feeding of the LFP and hence, enabling its maximum utilization (rule IV).

When adding GH<sub>2</sub> and LH<sub>2</sub> storage sizes, total storage capacities are lowest for the PV location where seasonal RES fluctuations are not too distinctive. There, the LH<sub>2</sub> storage is used for the daily mass flow buffering when the sun is not shining, but air traffic is requiring LH<sub>2</sub> as a fuel. Then, the hybrid (HYB, WEAK) locations follow with very small sizing requirements for daily buffering storage in the LH<sub>2</sub> tanks. Wind turbines can supply the energy system also at times without sunlight. However, the seasonal storage in the form of the GH<sub>2</sub> cavern storage has to be sized significantly larger (factor ~3 vs. PV) to compensate for larger seasonal fluctuations in RES availability. At WON, both larger seasonal GH<sub>2</sub> and larger daily LH<sub>2</sub> buffer storages are installed to enable the high utilization of the LFP (rule IV).

Only in the WOFF location, a larger LH<sub>2</sub> storage is built than the GH<sub>2</sub> cavern storage. It can be explained by the annual wind power curve which shows not a large seasonal variation of availability over several months in a year, but higher, recurrent fluctuations in each month with very low wind power yields over several days mixed with very high wind power yields on other days. This profile requires a more flexible storage system with high mass flow rates per hour. Since the filling and discharging mass flow rates of the GH<sub>2</sub> cavern storage are more limited due to maximum allowed pressure changes (see details in Appendix D2.2) than for LH<sub>2</sub> storages, only the latter can be used for this specific requirement in the WOFF setup.

It has to be noted that the resulting GH<sub>2</sub> cavern sizes in this demand setting are already very large. They equal or even exceed cavern deployments that are discussed in Europe with capacities of 2,000–4,000 tGH<sub>2</sub> [301]. Hence, such a large cavern might not always be available due to other H<sub>2</sub> users, even if geological conditions are given. Further discussion on this aspect follows in a remarks section.

- VI. GH<sub>2</sub> pressure: Higher ELY (GH<sub>2</sub>) output pressures of >60 bar should be chosen for slightly better economics, if larger GH<sub>2</sub> storage systems are installed (see Table 5.3 – right column).

This leads to synergies in less compression work when filling GH<sub>2</sub> storages and lower energy consumption for the LFP, because less liquefaction work is required for intake feeds with higher pressure (Appendix D2.3). At WON, WOFF, HYB, and WEAK, this is the case. In the PV setup, smaller cavern storages and lower utilization of the LFP lead to no additional compression at the output of the ELY (30 bar).

Overall, the cost effects of this choice of GH<sub>2</sub> pressure are limited. Optimizations with fixed pressures show that the resulting costs of designs with not optimized pressures lead to small cost increases of around 0.02–0.04 USD/kgLH<sub>2</sub>.

- VII. Part-load dynamics & H<sub>2</sub> losses: Non-linear (part-load) effects have to be considered when designing LH<sub>2</sub> energy systems (Figure 5.8). These lead to a 15–20% higher average energy consumption of LFP than in its design point (~6 kWh/kgH<sub>2</sub>). H<sub>2</sub> losses do not significantly influence the optimized design in a 2050 base case on-site supply scenario.

**Energy consumption by component for 100k tLH<sub>2</sub>/a demand (2050 base, LH<sub>2</sub> on-site), in GWh**

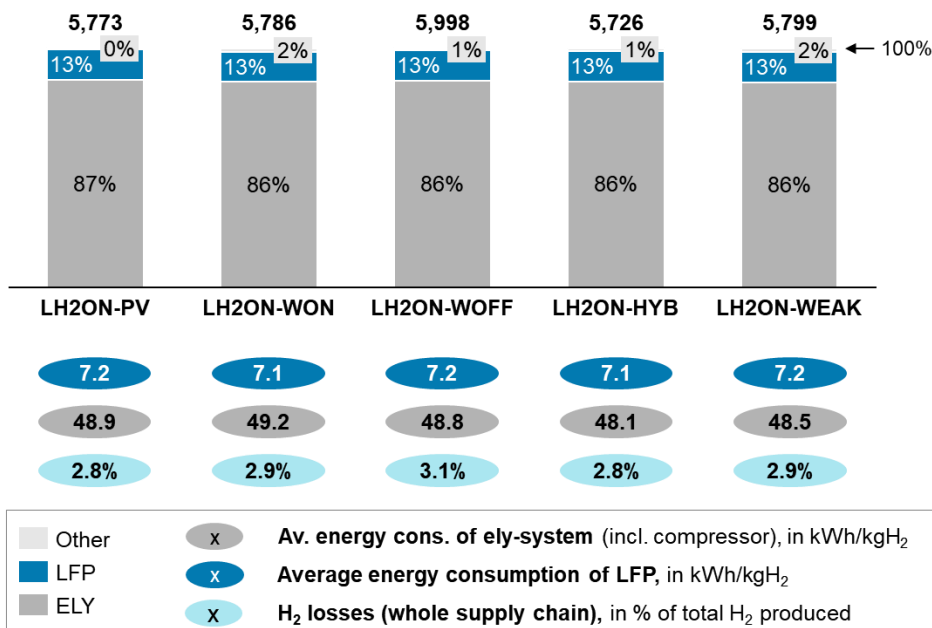


**Figure 5.8:** Total and average energy consumptions as well as total H<sub>2</sub> losses along the supply chain for five locations, 2050 base case scenario with 100k tLH<sub>2</sub>/a demand – category “other” describes compressors and cry-opumps

In general, the total energy consumption is similar for all locations with 5.7–6.0 GWh per year which equals 57–60 kWh of electricity required for the supply of 1 kgLH<sub>2</sub>. This means that the total energy efficiency on the infrastructure side is 56–58% (based on the LHV of H<sub>2</sub> and for on-site pathways). Also, the relative share of ELY vs. LFP consumption is similar with 86–87% to 13% for all analyzed regions.

However, the average energy consumptions of the ELY and the LFP differ depending on the location. This regional variation is smaller for the LFP with slightly higher consumption for WOFF (see design rule V explanation), for PV and WEAK (see design rule IV). But the average energy consumption of the ELY ranges from 48.1–49.2 kWh/kgH<sub>2</sub>. The ELY’s specific energy consumption decreases in part-load operation, which leads to lower average energy demand for HYB and WEAK setups with more flexible ELY operation (rules III & IV). Only in the WON, WOFF, and PV setups, the ELY is operated more continuously in its design point over the day (shut off at night at the PV location) which leads to a slightly higher average energy demand.

Most H<sub>2</sub> losses along the supply chain stem from the refueling system (~1/3) and the LFP (~1/3) and are very similar for all on-site regions (2.8–3.1% of total supplied LH<sub>2</sub>). The remaining losses occur at the compressors and storages – both amounts depending on the designs of the components described in the previous design rules. This is why in the WOFF supply the H<sub>2</sub> mass losses are slightly higher vs. the other regions due to boil-off losses in the LH<sub>2</sub> storage (largest LH<sub>2</sub> storage installed, Figure 5.7).

The total LH<sub>2</sub> supply costs shown in Figure 5.4 were explained along seven design rules. Main techno-economic factors were derived for on-site supply pathways at a demand of 100k tLH<sub>2</sub>/a that led to economically competitive LH<sub>2</sub> supply costs for H<sub>2</sub>-powered aviation. In the next sections, these are further tested and challenged for different demand points and techno-economic scenarios.

## Remarks on dependencies of the study design

Small changes in the main study design could affect the discussed results. Therefore, in the following, three main aspects of the scenario definition (in Section 5.1.3) are briefly reevaluated: (1) the geological availability of GH<sub>2</sub> cavern storage, (2) a differing LH<sub>2</sub> demand profile to an airport without any night flying restrictions (more constant operation, Figure 5.3) and (3) different weather data from other years than the reference year 2019. Detailed information on the optimization results can be found in the Supplementary Material (SM) Figures S1-3 of [239].

First, the unavailability of GH<sub>2</sub> caverns does not have a larger impact on the LH<sub>2</sub> supply costs at PV, WOFF, and HYB regions. However, cost increases are observed for the WEAK setup with a 9% total cost increase – at WON it is more moderate with 5% higher costs.

In all cases, rule I is still valid and no ES or GH<sub>2</sub> aboveground storages are installed but larger LH<sub>2</sub> storages. This leads to minor changes in design rules III and IV, since the utilization of the LFP cannot be realized without a constant GH<sub>2</sub> feed anymore (no GH<sub>2</sub> storage). The utilization decreases from ~90% to 70% and less. Only in the PV location, that change in utilization is only moderate, since it was already very low (rule IV). Furthermore, the ELY is sized slightly smaller and better utilized as fluctuations in RES availability are compensated by the larger LFP and the LH<sub>2</sub> buffer storage. In the WEAK region, the oversizing of the LFP leads not only to higher CAPEX and energy costs (part-load operation) for the LFP, but also to a 14% cost increase for RES to enable the flexible operation of the LFP.

Second, a study design without a night curfew at the LH<sub>2</sub> demanding airport affects the costs insignificantly at all five locations. The supply costs only change by 0.01 to 0.03 USD/kgLH<sub>2</sub>. As described in rule III, the ELY is best sized when demand or RES availability is least fluctuating throughout the day, ELY costs slightly decrease with more constant demand profiles. Only in the PV setup, where no RES is available at night, this leads to minor cost increases.

Third, different weather years have a high cost impact at the stronger wind (WON, WOFF, HYB) locations. There the costs change by -1% to +10% in the WON, +5 to +11% in the WOFF, and +4 to +6% in the HYB setup, if weather data is taken from 2017 or 2018. In regions with only or primarily reliance on PV electricity generation, the costs only differ by 1–2%. The main reason for the cost changes are the differences in RES fluctuations and seasonality which cause both changes in design as well as costs for the RES and storages. However, all design rules hold true for all locations and reference weather years.

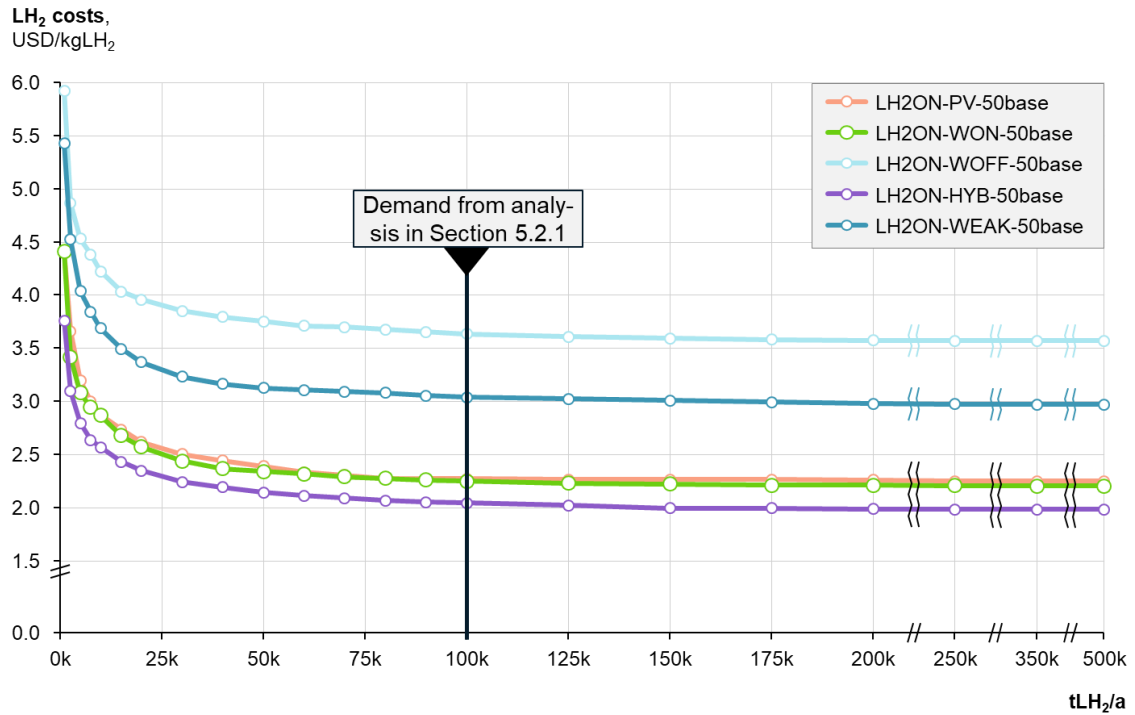
### 5.2.2 Variation of annual LH<sub>2</sub> demands

As a next step, the LH<sub>2</sub> demand sizes are varied for the five locations to analyze scaling effects, see Figure 5.9A.

Only limited cost reduction effects for larger demand settings are observed versus the 100k tLH<sub>2</sub>/a demand. Further cost reductions of 0.05–0.07 USD/kgLH<sub>2</sub> are gained in the WON, WOFF, HYB, and WEAK setups. At the best location, HYB, costs decrease to 1.98 USD/kgLH<sub>2</sub>. The reason for this trend in these four regions is a further specific cost reduction for the LFP. In this study, it is assumed that the LFP reaches all economies of scale effects at a capacity rating of 500 tLH<sub>2</sub> per day (tpd). Consequently, less cost decreases are achieved for larger demands in the PV location with 0.02 USD/kgLH<sub>2</sub>, because the LFP is already designed larger than 500 tpd in the 100k tLH<sub>2</sub>/a demand setting. Only a few further improvements in specific CAPEX for storage are reached. In all these setups, no changes in design rules are observed.

For smaller demand settings than 100k tLH<sub>2</sub>/a, cost effects are significant and lead to nearly doubling of figures for very low annual demands. Lowering the demand from 100k to 20k tLH<sub>2</sub>/a, supply costs increase by 15%, 14%, 9%, 15%, and 11% for PV, WON, WOFF, HYB, and WEAK locations, respectively. From 20k to 5k tLH<sub>2</sub>/a demands (an average of ~14 tLH<sub>2</sub> demand per day), the cost increase is reaching levels of 25–41% compared to the 100k tLH<sub>2</sub>/a demand setting.

**A LH<sub>2</sub> costs at dispenser for selected locations (2050 base scenario)**



**B LH<sub>2</sub> costs at dispenser for best (2050 progressive) and worst scenario (2035 base)**

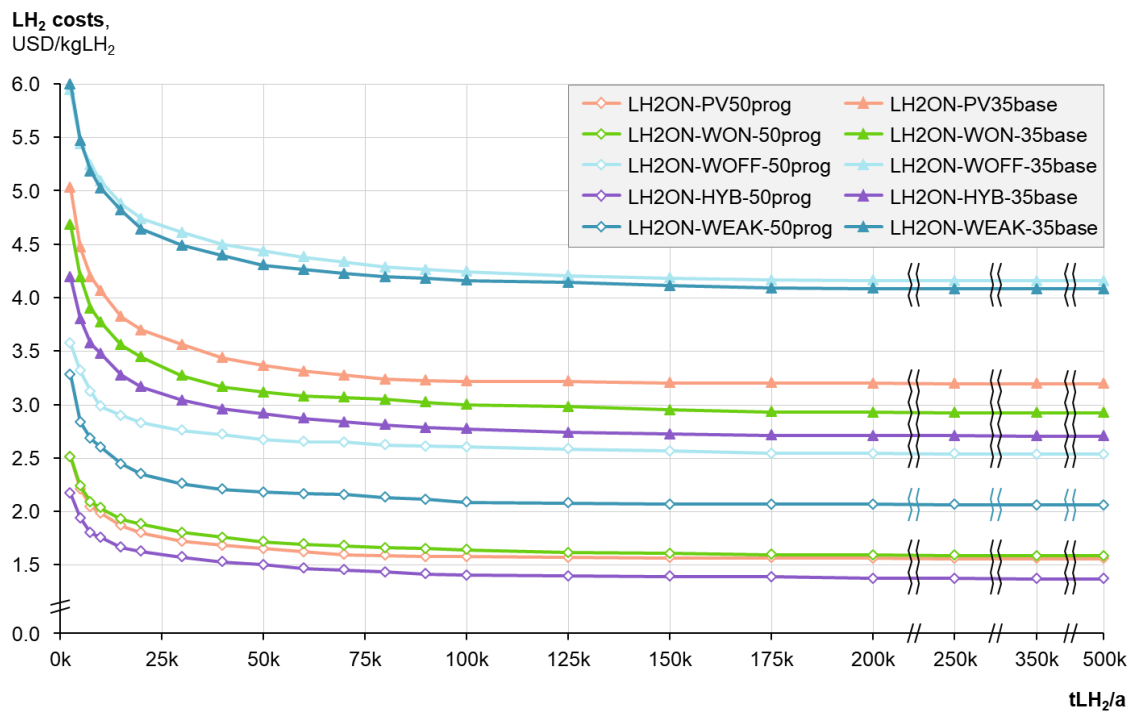


**Figure 5.9:** LH<sub>2</sub> supply costs at the dispenser for on-site setups at five locations for variable annual LH<sub>2</sub> demands at the airport – A) 2050 base case scenario, B) 2035 base, and 2050 progressive case scenarios

The underlying effects are explained along two main design effects that apply especially below 20k tLH<sub>2</sub>/a settings. Design aspects depicted for the 5k tLH<sub>2</sub>/a settings are shown in the Supplementary Material (Figures S4-8 and Table S1) of [239].

First, since specific CAPEX for GH<sub>2</sub> cavern storages increases significantly more for smaller capacities compared to LH<sub>2</sub> storages (Appendix D2.2 and D2.3), only LH<sub>2</sub> storages are installed in these energy systems. So, even in smaller demand settings, a design without ES or GH<sub>2</sub> above-ground storages is more economical (design rule I). Only for the WEAK location the flexibility of having a cavern buffer storage in the GH<sub>2</sub> balance between ELY and LFP, is still slightly less expensive than oversizing the LFP and other systems.

This is why the utilization of the LFP decreases again from ~90% to ~70% and hence, the oversizing of RES and LFP increases for the regions without a GH<sub>2</sub> storage installation – as already described in the remarks aspect in Section 5.2.1 (rules II, IV). In addition to that, the ELY output pressure is designed to be the default setting (30 bar), not requiring a compressor in the ELY which is in line with design rule VI.

Second, for all regions, the LFP is designed below a 100 tpd capacity except for PV where this effect applies for demands at and below 10k tLH<sub>2</sub>/a. In this smaller sizing, the CAPEX increase significantly as well as the specific energy consumption from an average of ~7 kWh/kgH<sub>2</sub> to 10–12 kWh/kgH<sub>2</sub> for 2.5–10k tLH<sub>2</sub>/a and even 13–15 kWh/kgH<sub>2</sub> for 1k tLH<sub>2</sub>/a demand. In the latter setting, a very small LFP with less than 10 tLH<sub>2</sub>pd capacity is installed. Consequently, the part-load dynamics of the LFP are even stronger in such settings, as described in design rule VII. See also Appendix D2.3 for detailed cost and efficiency characteristics of the LFP.

### 5.2.3 Scenario analysis of on-site LH<sub>2</sub> setups

As described in Section 5.1.3, there is a high uncertainty for the techno-economic parameter assumptions for the year 2050. In the present model setup, the number of uncertain techno-economic parameters is too large for a comprehensive sensitivity analysis. This is why, the impact is analyzed based on two additional scenarios – one worse (2035 base) and the other very optimistic (2050 progressive) than the parameter set of the 2050 base case scenario previously discussed, see results in Figure 5.9B. It has to be noted that in this work only the techno-economic assumptions for each component are varied. An important other cost aspect in the annuity payment factor method is the interest rate/cost of capital. This parameter often differs by country and the project which has to be financed [165]. The analysis of the LH<sub>2</sub> cost impact from changing the interest rate will be the subject of future work.

The resulting cost bands for each location around the 2050 base case range from 1.56–3.22 (-31%/+42%), 1.59–3.00 (-28%/+33%), 2.53–4.25 (-29%/+17%), 1.37–2.77 (-31%/+36%), 2.06–4.16 USD/kgLH<sub>2</sub> (-31%/+37%) for demands of 100k tLH<sub>2</sub>/a or more at PV, WON, WOFF, HYB, and WEAK, respectively. This shows that at the best sites (WON, HYB) costs are always below 3 USD/kgLH<sub>2</sub> and could even reach levels of 1.40–1.60 USD/kgLH<sub>2</sub> in a very optimistic scenario.

The cost bands are significantly larger for very small demands at 5k tLH<sub>2</sub>/a with 2.21–4.47, 2.24–4.20, 3.32–5.44, 1.94–3.80, 2.84–5.47 USD/kgLH<sub>2</sub> for the PV, WON, WOFF, HYB, and WEAK sites, respectively. At WOFF sites, the high CAPEX assumptions of wind turbines in all scenarios compared to the other setups still cause the highest LH<sub>2</sub> costs. Even with more optimistic wind offshore CAPEX in the 2050 progressive case, LH<sub>2</sub> supply costs at WOFF are more expensive than from PV, WON, or HYB locations in the 2050 base case.

The future supply costs at WEAK also represent a large uncertainty for the economics of H<sub>2</sub>-powered aviation with cost levels above 4 USD/kgLH<sub>2</sub> for larger and more than 5 USD/kgLH<sub>2</sub> for very small demands.

In any of the scenarios and sites, design rule I is not changing, and no electric energy and GH<sub>2</sub> above-ground storages are installed even if they become less costly. Further design and cost effects are discussed for both scenarios separately.

### **Scenario: 2035 base case**

This scenario depicts more conservative techno-economic assumptions, mostly for the CAPEX projections of all components including the RES plants. This is why the total LH<sub>2</sub> supply costs increase to 2.77–4.25 USD/kgLH<sub>2</sub>. The main factor behind this is higher costs for electricity supply with LCOEs of 20, 24, 24, 43, and 47 USD/MWh for the PV, WON, HYB, WEAK, and WOFF locations, respectively. Relative CAPEX reductions between the 2035 and the 2050 base case scenarios are lowest for wind offshore parks and highest for PV installations. Consequently, total investment needs increase less at WOFF by 13% and more drastically at the other sites by 28–44% compared to the 2050 base case. All information on costs and design of the resulting LH<sub>2</sub> energy systems are presented in the Supplementary Material Figures S9-13 and Table S2 of [239].

PV locations show the largest increase in total costs compared to other locations, e.g., 42% for the 100k tLH<sub>2</sub>/a setting. In the base case 2050, already high cost penalties apply at PV sites for oversizing the LFP and ELY. For the 2035 base scenario with higher specific CAPEX for both components, it is leading to the highest supply cost increase, proving that design rules III and IV are still valid. In addition to that, the costs for RES are 44% higher and hence, cause more expensive LH<sub>2</sub> supply (design rule II).

The contrary is applying to the WOFF location with the smallest total cost increase (17%). Since RES costs increase only moderately and the LFP has a high utilization again, the more conservative techno-economic assumptions do not lead to drastically higher LH<sub>2</sub> costs for WOFF regions.

The energy efficiencies of the ELY and LFP do not change compared to the reference case (2050 base). Hence, installed capacities, the RES designs, utilizations, and resulting average energy consumptions are very similar to the 2050 base case (design rules III, IV, VII).

Regarding storages, design rule V proves to be still valid. Larger GH<sub>2</sub> storages are installed for the PV setting since both higher RES and LFP costs make it more economical to buffer more GH<sub>2</sub> and hence, enable a slightly higher utilization of the LFP (design rule IV). At WOFF now also larger GH<sub>2</sub> cavern storages are installed, since the specific CAPEX does not increase, but for the LH<sub>2</sub> storages, they do. However, larger LH<sub>2</sub> buffer storages are still required to compensate for seasonal and daily fluctuations in both strong wind locations.

### **Scenario: 2050 progressive case**

In this scenario, all CAPEX of RES and H<sub>2</sub> components are reduced due to larger learning effects in a larger H<sub>2</sub> market. Thus, more optimistic efficiencies, operation cost factors, and depreciation periods are assumed for selected components. This leads to a further decrease in total supply costs (Figure 5.9B), mostly driven by lower RES costs with LCOEs of 10, 12, 14, 22, and 34 USD/MWh for the PV, HYB, WON, WEAK, and WOFF locations, respectively. Total investments decrease by -23–30%, see all details in Supplementary Material Figures S14-S18 and Table S3 of [239].

At nearly all sites, the RES and ELY capacity is designed smaller due to an increase of energy efficiency of the ELY by 11% (design rules II and III are still valid). This can also be seen in the new average energy consumption of 43–44 kWh/kgH<sub>2</sub> due to part-load operation (design rule VII).

Since specific CAPEX for LFP is lower, it is generally a bit oversized for more flexible operation compared to the 2050 base case, also leading to decreased storage demands and costs. This is why, storages in total are sized slightly smaller (0–27%) – the effect is largest for WOFF and WON locations with larger seasonal fluctuations in RES availability. Furthermore, LH<sub>2</sub> storage systems are sized larger than in the base case scenario and larger than the GH<sub>2</sub> cavern capacities at WON/WOFF. This strengthens the findings from design rule V for WOFF, but also WON. One main reason for the preference of LH<sub>2</sub> storages is that only for them a further cost reductions are assumed (longer lifetimes) and not for installations of GH<sub>2</sub> cavern storages in the 2050 progressive scenario.

### Intermediate summary

In this section, seven design rules were derived for five locations of which the HYB followed by the PV and WON regions are best suited for lowest cost on-site LH<sub>2</sub> production for H<sub>2</sub>-powered aviation. The WOFF location has great RES potential for efficient and not oversized LH<sub>2</sub> energy system designs. However, due to the very high specific CAPEX of offshore wind turbines, its economic LH<sub>2</sub> supply potential might only be given, if space constraints for other RES (e.g., wind onshore) are too high or other supply options are not available.

Contrary to that, the weaker hybrid location does not offer highly efficient and potentially low-cost designs of LH<sub>2</sub> energy systems. Consequently, larger RES capacity installations by a factor of 3 would be required to realize such a WEAK setup which might lead to infeasibility due to limited land availability. As a result, LH<sub>2</sub> off-site (import) options that could leverage more economic LH<sub>2</sub> supply costs at airports within WEAK regions are considered in the next section.

## 5.3 Off-site supply chains

In the following, off-site (import) options are investigated for an airport located in the WEAK region, which might enable lower costs than with an on-site LH<sub>2</sub> supply pathway (see previous section).

First, LH<sub>2</sub> import pathways are analyzed. Then, GH<sub>2</sub> import pathways are derived and compared to the LH<sub>2</sub> import options. In a brief comparison, the effects on the LH<sub>2</sub> energy system design by adding transport options are also explained. As a last step, again a scenario analysis is performed for the supply options for WEAK.

This chapter focuses on dedicated infrastructure development for LH<sub>2</sub> in aviation. Consequently, a greenfield approach is chosen for the importing supply chain like in the on-site setups. Potentially existing infrastructure like an international GH<sub>2</sub> pipeline system (European Hydrogen Backbone [163]), LH<sub>2</sub>, or ammonia vessel transport networks [199,227,302] is not reflected in the following analysis. As discussed in Section 4.1, H<sub>2</sub>-powered aviation might create new magnitudes of scale for H<sub>2</sub> demands at selected regions around the airport and therefore lead to further cost reduction effects. Furthermore, the transport of hydrogen as ammonia is in most cases costlier than shipping LH<sub>2</sub>, if it is the final aggregate of H<sub>2</sub> required at the end consumer (airport) [111]. The conversion process of GH<sub>2</sub> to ammonia and vice versa adds costly and energy-inefficient process steps to LH<sub>2</sub> supply chains.

### 5.3.1 LH<sub>2</sub> off-site setups

In this section, the chosen LH<sub>2</sub> off-site setup is described, transport costs are calculated as well as resulting total LH<sub>2</sub> supply costs are discussed.



### Setup of LH<sub>2</sub> off-site supply chain

As described in Section 5.1.1, LH<sub>2</sub> could be transported via larger oversea vessels on longer distances. In that case, import and export terminals are required as well as on-land truck transport from the importing port to the targeted airport. Thus, it is assumed that the LH<sub>2</sub> production is close to a port where the LH<sub>2</sub> vessel would be loaded in the three exporting regions (PV, WON, HYB).

Since the transport costs depend on the utilization of the export terminal, the LH<sub>2</sub> transport capacity per vessel is optimized as a main aspect of the transport network design (see optimization variable in Table 5.1 and Appendix D2.4). Hence, for low demands and short distances, there can be setups with only one vessel arriving at the export site per week vs. a continuous arrival of vessels, once the previous vessel has been loaded (48h). The LH<sub>2</sub> truck on-land transport is calculated based on the optimization of the transport network.

While the energy system setup at the export location does not differ significantly from the on-site production case (see Section 5.1.1), the need for the LH<sub>2</sub> storage system changes slightly. In on-site setups, it is mostly used as a buffer between the daily liquefaction of H<sub>2</sub> and the direct use of LH<sub>2</sub> at the airport. For the LH<sub>2</sub> export system, the LH<sub>2</sub> storages are required to buffer LH<sub>2</sub> until the next vessel arrives. So, depending on the number of vessels in the transport network, this LH<sub>2</sub> export terminal buffer can be significantly larger.

For a better overview of data, the focus is set on three different trip lengths: short (1,000 km), medium (3,000 km), and long (7,500 km). Exemplary trips could be from Southern Europe to the next northern countries (short distance), from Northern African countries to Central Europe (medium distance), or from the Middle East to Central Europe (longer distance).

In addition, the on-land transport is assumed to be on average 300 km long, because this study looks at generic supply pathways. This length is also used in other studies, e.g., in [44].

### LH<sub>2</sub> transport costs

Cost results for the optimized system are shown in Figure 5.10 for the three distances using an LH<sub>2</sub> demand mass variation (x-axis). As described above, the costs for the LH<sub>2</sub> export terminal (storage and cryopumps) are considered part of the main LH<sub>2</sub> energy system and are not shown in the LH<sub>2</sub> transport costs.

For an annual demand of 500k tLH<sub>2</sub>, the transport costs over 1,000 and 3,000 km stem from 41% for vessels, 19% for the import terminal (storage and cryopumps), and 40% for the trucks. In the 7,500 km distance, the cost share of LH<sub>2</sub> vessels increases to 58% (import terminal with 13% and truck with 29%). In that demand case, required investments would already range from 1.4 Bn USD (696 Mn USD for vessels, 413 Mn USD for import terminal, and 292 Mn USD for LH<sub>2</sub> trucks) for 1,000 km to 2.1 Bn USD for 7,500 km for the transport network only.

In general, the transport costs decrease significantly with larger LH<sub>2</sub> demands from more than 2.5 USD/kgLH<sub>2</sub> for <100k tLH<sub>2</sub>/a to around 0.5–0.7 USD/kgLH<sub>2</sub> for >1,000k tLH<sub>2</sub>/a. Costs for short and medium transport distances differ only by less than 0.01 USD/kgLH<sub>2</sub>, because in both cases a minimum number of two vessels is required to utilize the transport network (see Appendix D2.4).

H<sub>2</sub> losses also cause costs in the total energy system, but are not represented in Figure 5.10. They occur in the form of flash losses while loading the vessel and the LH<sub>2</sub> truck. For all transport distances, boil-off losses on the vessel trip are nearly sufficient to power the vessels' propulsion system. On the truck transport part, nearly no boil-off losses are observed on such shorter distances and fast turnarounds. Hence, the trucks require extra fuel which is accounted for in this study.

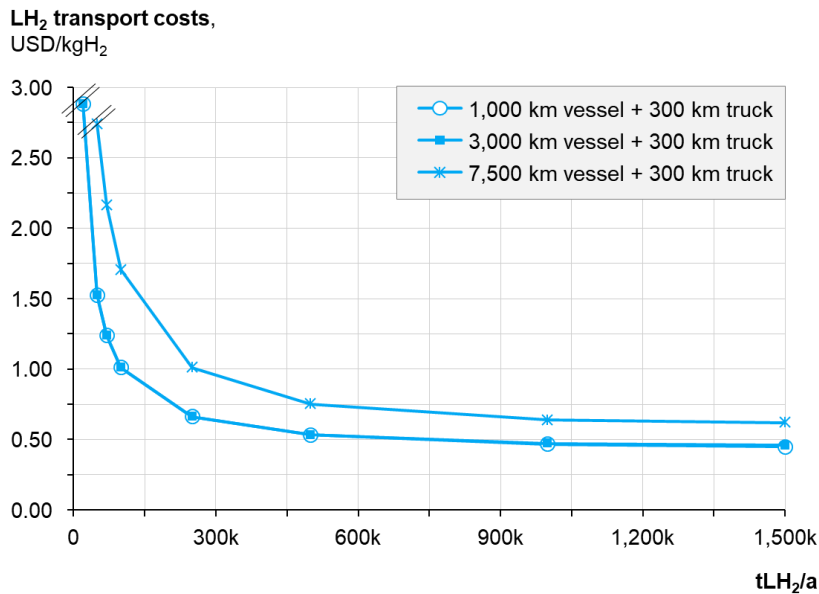


**Figure 5.10:** Transport costs in the 2050 base case scenario for three distances (short: 1,000 km, medium: 3,000 km, long: 7,500 km) with LH<sub>2</sub> overseas vessels and a fixed 300 km truck transport on land from the importing port to the destination airport – costs for importing LH<sub>2</sub> terminal included, export terminal costs excluded and part of “LH<sub>2</sub> energy system”

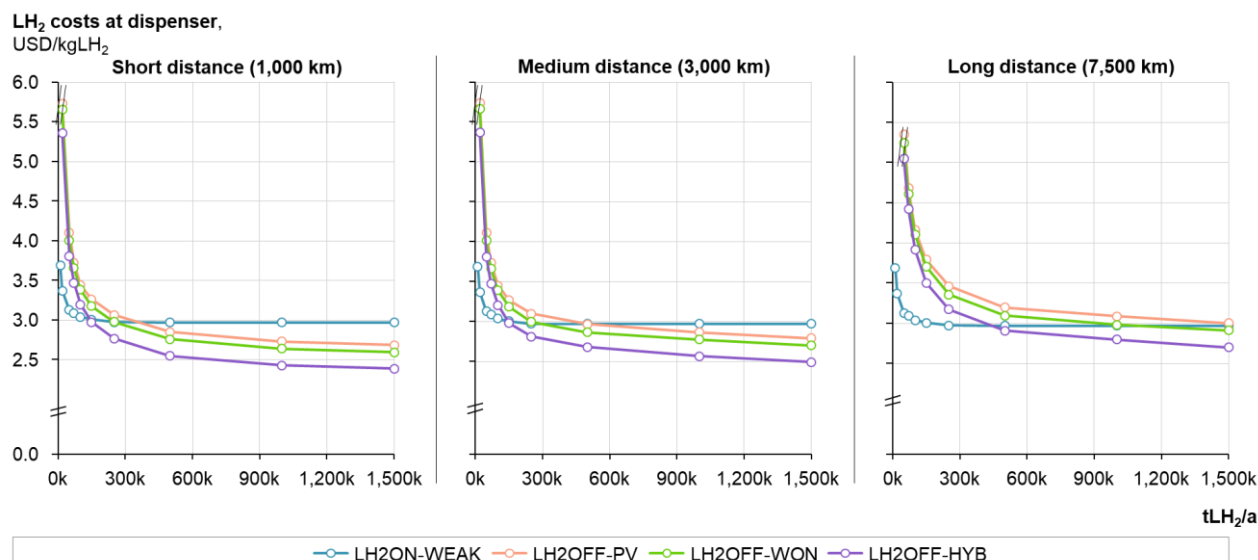
### Total LH<sub>2</sub> import costs

Figure 5.11 shows the resulting total LH<sub>2</sub> import costs at the dispenser for an airport at a WEAK location and the 2050 base case scenario. In total, LH<sub>2</sub> costs at the WEAK location can be reduced by up to 0.5–0.6 USD/kgLH<sub>2</sub> with LH<sub>2</sub> off-site supply, if a vessel transport over 1,000 km or 3,000 km from HYB locations at very high annual demands is available.

Generally, LH<sub>2</sub> import from HYB is always more competitive than from WON and PV locations – same as in Section 5.2 for on-site production. In addition to that finding, the LH<sub>2</sub> import option is less economically competitive compared to on-site supply at WEAK airports for smaller annual demands with increasing transport distances. For the short and medium distances, LH<sub>2</sub> import from an HYB region is the economically best option for demands larger than 150k tLH<sub>2</sub>/a. In the long-distance setup, the break-even demands increase to larger than 400k tLH<sub>2</sub>/a.

More detailed energy system design effects are explained at the end of Section 5.3.2.

The total cost curves for LH<sub>2</sub> import already show that if very large annual demands are reached, more competitive delivery costs would result vs. the dedicated on-site LH<sub>2</sub> production at the WEAK location (100k tLH<sub>2</sub>/a) with 3.04 USD/kgLH<sub>2</sub>. To reach such demand levels, an accumulation of demands might be required from several airports or even other H<sub>2</sub>-demanding applications in one broader region. It has to be noted that such a deployment highly depends on transport distances between export and import regions and the proximity of the receiving airports to the importing port.



**Figure 5.11:** Costs at the dispenser for receiving airport at WEAK location with LH<sub>2</sub> import (off-site) pathway over three distances compared to costs of on-site LH<sub>2</sub> production, 2050 base case scenario

Several studies project H<sub>2</sub> market costs for importing H<sub>2</sub> in several forms (GH<sub>2</sub>, NH<sub>3</sub>, etc.). However, these do not create a homogenous picture of future H<sub>2</sub> market costs, e.g., in Central Europe, but rather a broad range of future cost projections. Consequently, a comparison of the results of this dissertation with such a range would not lead to a clear picture of whether dedicated LH<sub>2</sub> import scenarios for H<sub>2</sub>-powered aviation might be less or more expensive than another H<sub>2</sub> market. Nevertheless, these “greenfield” calculations show the lowest costs of dedicated LH<sub>2</sub> supply (on-site and off-site) infrastructure that has to be underbid by a general H<sub>2</sub> market (plus costs for liquefying GH<sub>2</sub>) to be a more economically competitive option.

### 5.3.2 GH<sub>2</sub> off-site setups

This section follows the same structure as the previous one. Additionally, a brief overview is given of changes in the energy system design setups for both off-site pathways.

#### Setup of GH<sub>2</sub> off-site supply chain

The main characteristic of this supply chain setup is the placing of the LFP at the receiving airport and not the exporting H<sub>2</sub> production center. As described in Chapter 5.1.1, a grid connection (renewable electricity PPA) is used to power the LFP at the airport in this case.

Gaseous H<sub>2</sub> from the export region is then transported through pipeline systems that are either newly built or retrofitted and recommissioned natural gas pipelines (see Section 5.1.1). For the latter, new coatings, valves, and compressor stations suitable for H<sub>2</sub> usage have to be installed. The need for compressor stations depends on the chosen input and output pressure, the length of the pipeline, its diameter, and the design flow speed of GH<sub>2</sub> – which is an optimization variable. The equations describing the dependencies of these parameters that are required for the optimization of the transport network can be found in Appendix D2.4.

In this chapter, only on-land pipeline systems and no routing factors are considered – otherwise, the specific CAPEX factor for newly built pipelines would further increase for undersea pipeline installations. Furthermore, the pipeline is modeled without any storage functionality which is in line with current natural gas operating principles (see Sections 2.2 and 5.1.1).

## GH<sub>2</sub> transport costs

The optimized transport costs for the pipelines differ significantly between a new built and a retrofitted system, see Figure 5.12. Additionally, a very large cost increase by a factor of 3–4 and 8–11 results from longer pipeline lengths over 3,000 and 7,500 km compared to 1,000 km. A similar effect can be observed for smaller annual H<sub>2</sub> demands – higher specific CAPEX per installed pipeline diameter per kilometer lead to very high transport costs.

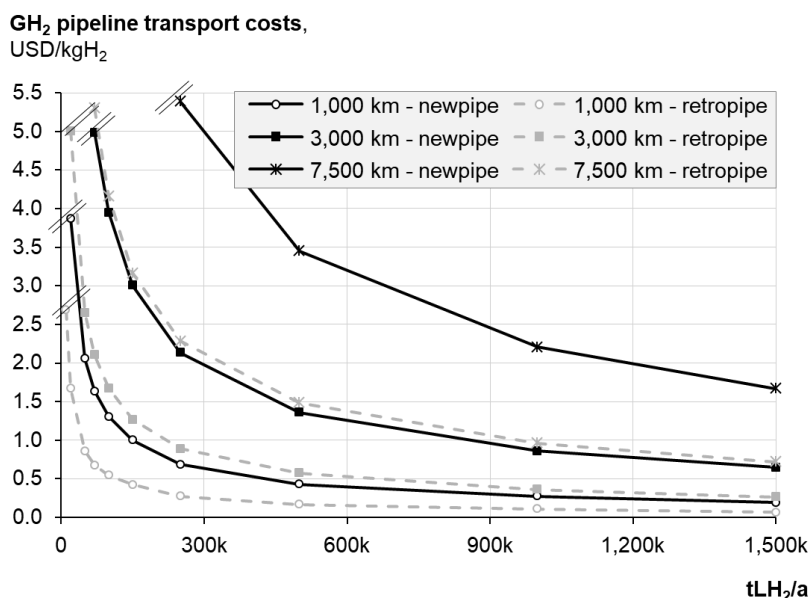


**Figure 5.12:** Transport costs in the 2050 base case scenario for three distances (short: 1,000 km, medium: 3,000 km, long: 7,500 km) with GH<sub>2</sub> pipelines on land (new and retrofitted pipelines) from the importing site to the destination airport – costs for compressor systems included

## Total GH<sub>2</sub> import costs

The resulting total costs for the optimized GH<sub>2</sub> off-site supply are shown in Figure 5.13. In total, costs at the WEAK location can be reduced by up to 0.70 USD/kgLH<sub>2</sub> with GH<sub>2</sub> off-site supply when retrofitted pipelines are available over 1,000 km in a 2050 base case scenario from HYB at very high annual demands.

As expected, the GH<sub>2</sub> import costs are lower for retrofitted pipeline setups versus new built ones, if this option is available. If retrofitted systems for short distances can be used, GH<sub>2</sub> import underbids LH<sub>2</sub> on-site supply costs at WEAK already for demands of 70k tLH<sub>2</sub>/a or larger. With medium distances this is the case for demands of ~400k tLH<sub>2</sub>/a, while for longer distances cost parity with the on-site production is never achieved.

In new built setups, GH<sub>2</sub> import only becomes an economically more attractive option for very large annual LH<sub>2</sub> demands. For short and medium distances from HYB, PV, or WON export regions, LH<sub>2</sub> supply costs at WEAK could be reduced by up to 0.58 USD/kgLH<sub>2</sub> for very large demands. In long-distance import cases, new built pipelines also never lead to better LH<sub>2</sub> costs than the on-site supply (see right graphs Figure 5.13).

Contrary to the LH<sub>2</sub> off-site scenarios, import costs from WON locations are more expensive than from PV locations in the GH<sub>2</sub> off-site supply. The cause will be explained in the following.

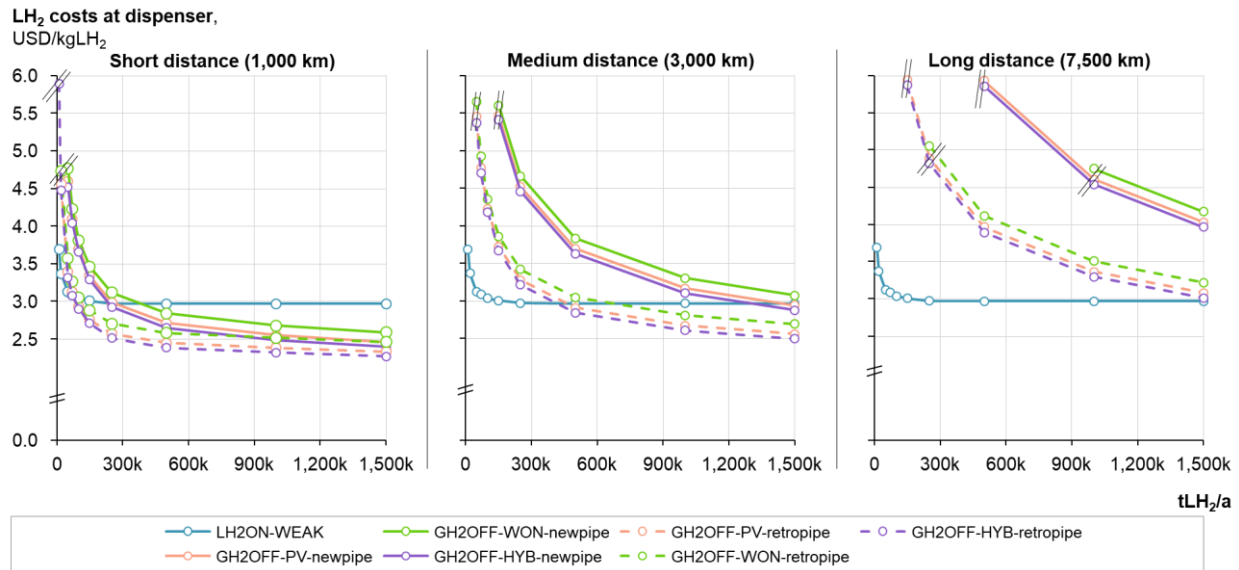


**Figure 5.13:** Costs at the dispenser for receiving airport at WEAK location with GH<sub>2</sub> import (off-site) pathway over three distances compared to costs of on-site LH<sub>2</sub> production; two options with new built and retrofitted pipelines; 2050 base case scenario

### Remarks on energy system designs for LH<sub>2</sub> and GH<sub>2</sub> off-site pathways

This chapter does not aim to answer the economics of LH<sub>2</sub> supply at five generic locations only, but also to investigate design aspects and main factors leading to less costly supply. The energy system design effects for off-site supply differ from on-site pathways and are analyzed in the following for the 100k tLH<sub>2</sub>/a reference base case scenario (see Figure 5.14).

First, LH<sub>2</sub> import requires larger export buffer storages as part of the LH<sub>2</sub> production site, costs for LH<sub>2</sub> storages increase by 0.07–0.15 USD/kgLH<sub>2</sub>. As mentioned earlier, only two vessels would be required to establish such a transport network and these would only be loaded once per week at the export region. Hence, the produced LH<sub>2</sub> has to be stored at the export terminal for five days until the next vessel arrives and is loaded (48 hours). This even leads to a change in design rule V (storages), because in the HYB location the preference switches to the installation of LH<sub>2</sub> storages only (see also Supplementary Material Figures S19-23 and Table S4 of [239]). Since LH<sub>2</sub> storages are required for buffering for export, it becomes slightly less expensive to operate the LFP more flexibly with a lower utilization than installing also a GH<sub>2</sub> cavern storage – whose specific CAPEX increase significantly for smaller installation sizes. Other design rules are not affected in the LH<sub>2</sub> off-site setups.

Second, both import setups have higher total H<sub>2</sub> losses along the supply chain, especially in LH<sub>2</sub> off-site cases over longer distances. These are caused by flash losses while filling LH<sub>2</sub> from the terminal to a vessel and to a truck as well as boil-off losses in LH<sub>2</sub> storages and GH<sub>2</sub> losses in pipeline compressor stations. Hence, the LH<sub>2</sub> energy system is sized larger to compensate for these losses. These additional H<sub>2</sub> losses lead to an extra cost increase of 0.06 USD/kgLH<sub>2</sub> (Figure 5.14) for LH<sub>2</sub> import and 0.03–0.04 USD/kgLH<sub>2</sub> for GH<sub>2</sub> pipeline import.

Third, GH<sub>2</sub> off-site setups come with higher total electricity costs, since the LFP at the airport is sourced with a green PPA at fixed costs of 50 USD/MWh. If a deployment of dedicated RES at the airport would be the only solution to power the LFP, total electricity costs would increase even more. Only for the GH<sub>2</sub> off-site supply pathways from PV locations, this effect is not as strong. As explained in Section 5.2.1, the LFP is oversized for on-site PV setups, since no RES is available at night (design rule IV). Hence, the LFP can only be operated during the day which requires nearly doubling of design capacities. In the GH<sub>2</sub> off-site supply, the LFP capacity at

the WEAK airport can be sized smallest with constant electricity availability from a local grid. This is why, the LFP utilization increases to 90% also for the PV GH<sub>2</sub> off-site pathway and smaller LH<sub>2</sub> buffer storages are built (design rule V), see also Supplementary Material Figures S24-28 and Table S5 of [239]. Consequently, the GH<sub>2</sub> import from stronger PV regions becomes more competitive than from WON.

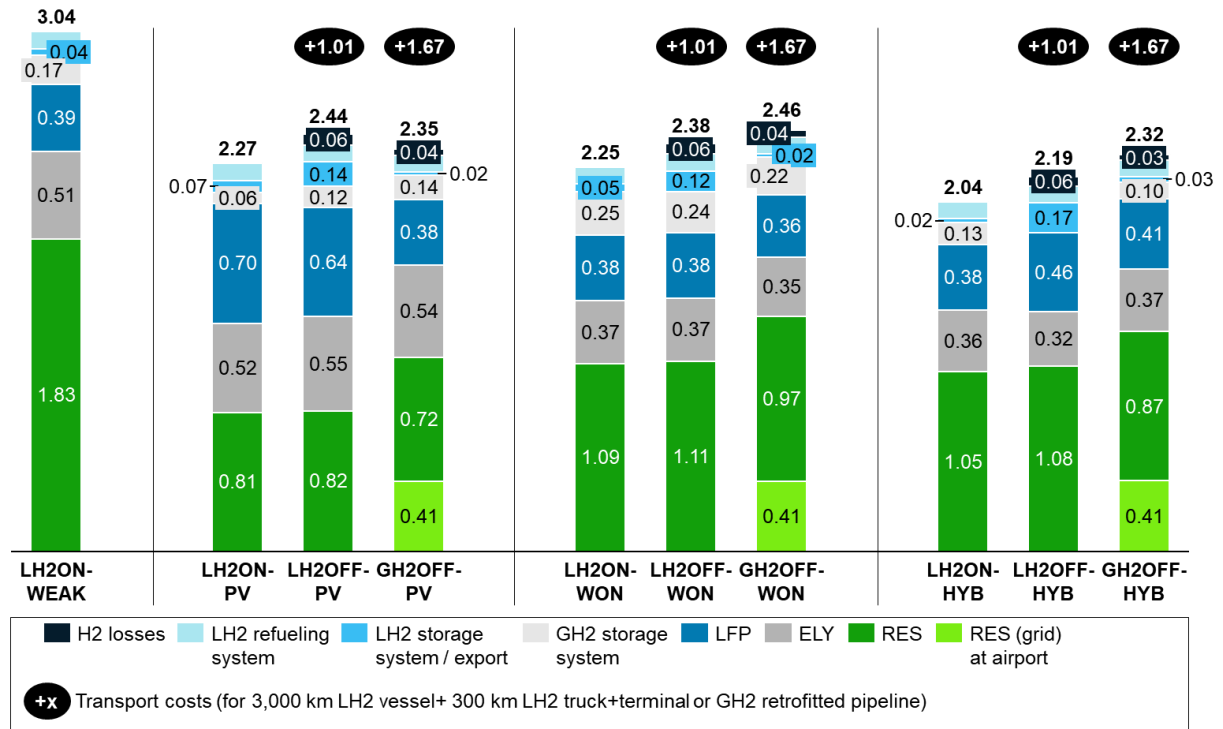


**Figure 5.14:** LH<sub>2</sub> energy system costs (transport & import terminal costs shown in bubbles separately, have to be added), 2050 base case scenario with 100k tLH<sub>2</sub>/a demand – comparing energy system designs: reference LH<sub>2</sub> on-site system at WEAK location (left) and comparison of LH<sub>2</sub>ON, LH<sub>2</sub>OFF and GH<sub>2</sub>OFF systems at PV, WON and HYB location; tag for the 0.1 USD/kgLH<sub>2</sub> refueling costs not shown, because the refueling costs are not subject for change for all setups

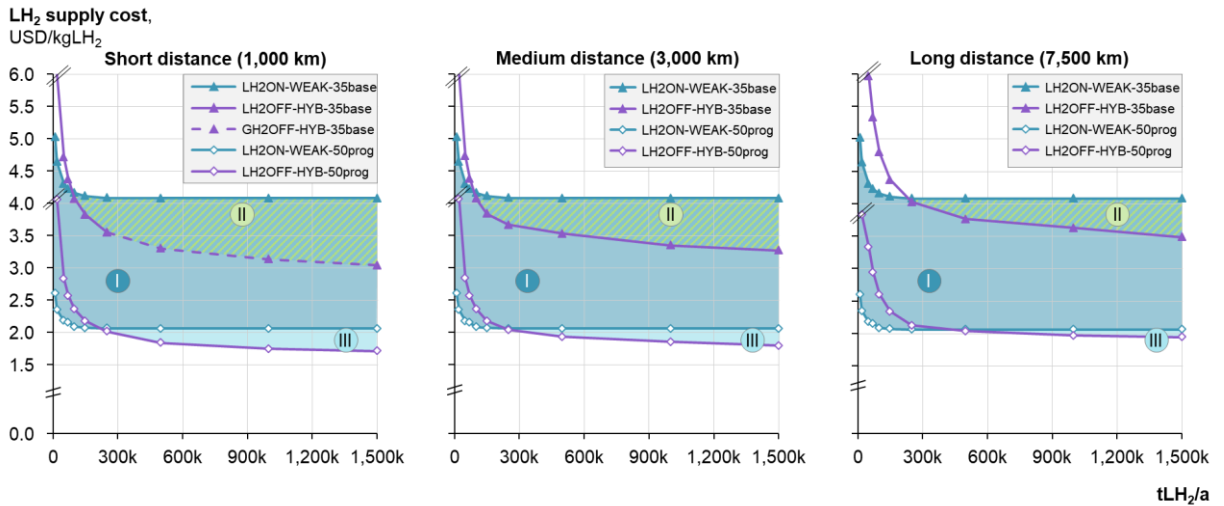
### 5.3.3 Scenario analysis for import options

In the next step, like in Section 5.2.3, not only the 2050 base but also the 2035 base and the 2050 progressive case scenarios are considered for supply options to or at the WEAK location. Combining all scenarios and all supply pathway options enables a comprehensive evaluation of the future LH<sub>2</sub> cost ranges at an airport with weaker RES conditions and hence, the techno-economic potential for H<sub>2</sub>-powered aviation from an LH<sub>2</sub> fuel perspective.

In Figure 5.15A and 5.15B, the costs of the LH<sub>2</sub> on-site WEAK setups are compared to the best off-site supply for all three scenarios, three transport distances and given that only new pipeline installations (A) or also retrofitted pipeline options (B) are available, respectively. All detailed results can be found in the Supplementary Material Figures S.29-32 of [239].

For the sake of clarity, only the best off-site results – the location and supply pathway – are shown for each scenario.

**A New pipeline**



**B Retrofitted pipeline available**

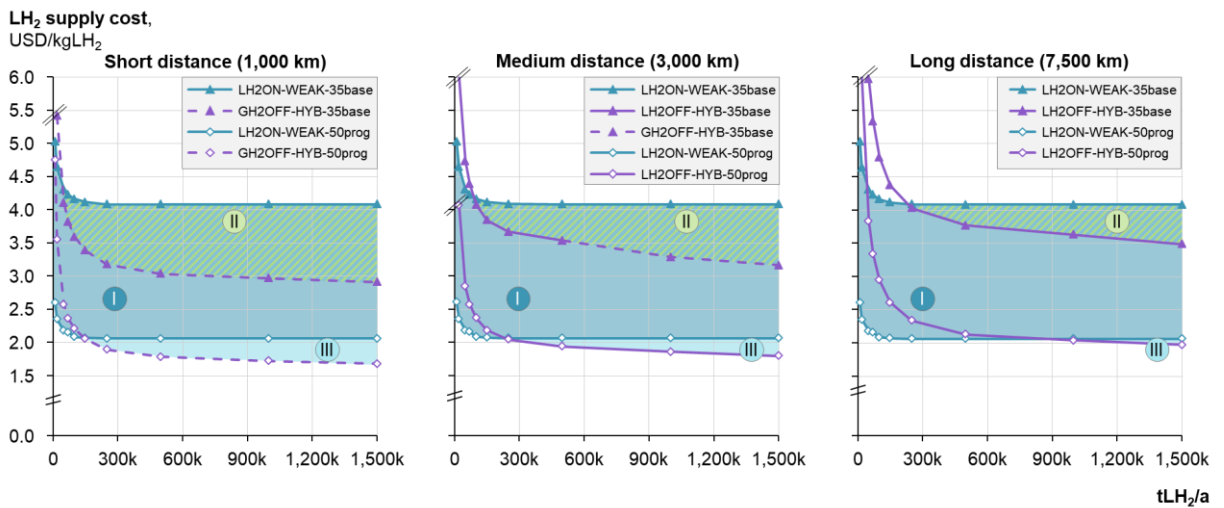


**Figure 5.15:** Total LH<sub>2</sub> supply costs at the dispenser for three transport distances considering only a GH<sub>2</sub> off-site supply pathway with A) new pipeline system installations (top) or B) with retrofitted pipeline systems (bottom); in each graph, only the best off-site (LH<sub>2</sub>/GH<sub>2</sub>) supply cost curve to WEAK for each scenario (2035 base, 2050 base, 2050 progressive) is shown and compared to the LH<sub>2</sub> on-site cost curve at the WEAK location; three cost bands highlighted in each sub-figure (“I” for the cost range of the LH<sub>2</sub>ON-WEAK setups, “II” for reduced costs in the 2035 base scenario due to import options, “III” for the cost range in which import pathways underbid the 2050 progressive LH<sub>2</sub>ON-WEAK scenario)

**Best off-site supply pathways without availability of retrofitted pipelines**

If new pipelines need to be installed, then only an LH<sub>2</sub> import setup is the most economical choice for all demands and all distances. Only for short distances the GH<sub>2</sub> import is the best option for demands of 250k tLH<sub>2</sub>/a or larger in a 2035 base scenario (see the purple line in the top left graph of Figure 5.15A that changes from a solid to a dotted line).

The figure can be characterized by three cost bands that create one final cost interval for future LH<sub>2</sub> costs at WEAK airports. Cost band “I” (includes also improved upper-cost band “II”) shows the on-site LH<sub>2</sub> cost range at the WEAK airport location when no import options would be available, explained in Section 5.2.3.

On the upper end of the cost band “I”, LH<sub>2</sub> off-site supply could reduce the costs at WEAK by up to 1.04 USD/kgLH<sub>2</sub> for very large demands and short distances in the 2035 base case scenario. For medium and long distances this improvement potential is 0.81 USD/kgLH<sub>2</sub> and



0.59 USD/kgLH<sub>2</sub>, respectively. In addition, the HYB location always offers the best export costs in the 2035 base but also the 2050 progressive scenario.

On the other side, with optimistic cost assumptions (2050 progressive), LH<sub>2</sub> off-site supply costs are decreased only slightly (lower cost band “III”). While in a short-distance setup, the costs can be reduced by 0.35 USD/kgLH<sub>2</sub>, cost reductions are lower for long-distance import supply with 0.09 USD/kgLH<sub>2</sub>.

In total and for demand scenarios of 100k tLH<sub>2</sub>/a, the best resulting supply costs at the airport in a weak RES region would be 2.09 USD/kgLH<sub>2</sub> for all distances as a result of on-site supply deployment and 2050 progressive techno-economic assumptions. Furthermore, the highest cost range in a 2035 base case can be decreased from 4.16 USD/kgLH<sub>2</sub> (on-site) to 4.07 and 4.08 USD/kgLH<sub>2</sub> for short and medium import transport distances and LH<sub>2</sub> import, respectively.

If large demands of 1,500k tLH<sub>2</sub>/a or import for a broader H<sub>2</sub> market are considered, off-site scenarios always lead to the best costs. Then, for short distances, the cost range at WEAK airports decreases to 1.71–3.04 USD/kgLH<sub>2</sub> with LH<sub>2</sub> off-site in the progressive and with GH<sub>2</sub> off-site supply (new pipeline) in the more conservative scenario. For medium and long distances, LH<sub>2</sub> off-site supply always leads to best cost ranges of 1.79–3.27 and 1.97–3.48 USD/kgLH<sub>2</sub>, respectively.

### **Best off-site supply pathways including retrofitted pipelines**

If a retrofit pipeline option exists, GH<sub>2</sub> off-site supply chains become more economical than LH<sub>2</sub> off-site setups in all short and partially also in medium-distance scenarios (Figure 5.15B).

Even though the costs for the GH<sub>2</sub> off-site energy system increases (Section 5.3.2, Figure 5.14), the total LH<sub>2</sub> supply costs decrease in combination with the significantly lower transport costs for retrofitted pipelines compared to LH<sub>2</sub> vessel imports. Only for longer distances the LH<sub>2</sub> off-site supply chain is still the best option in all scenarios. This result is also in alignment with other studies considering H<sub>2</sub> transport options, e.g., in [44,303,304].

For medium distances, both LH<sub>2</sub> and GH<sub>2</sub> import can play a leading role. In the 2035 base case scenario, import via retrofitted pipelines is more economical for larger demands above 500k tLH<sub>2</sub>/a due to two reasons. First, the specific CAPEX for the retrofitted pipeline deployment decreases significantly for larger installed diameters. With these reduced CAPEX, the pipeline becomes the optimal transport option compared to the LH<sub>2</sub> vessels. Second, the specific costs for LH<sub>2</sub> storage are significantly higher than for GH<sub>2</sub> storage systems in the 2035 base case scenario only. In the LH<sub>2</sub> off-site setups, these storages are required with high capacities for the export and import terminals. On the contrary, only smaller LH<sub>2</sub> storages are installed in the GH<sub>2</sub> off-site scenario at the airport, which is sized comparably small as expressed in costs (see Figure 5.14 or Table S5 in the Supplementary Material of [239]).

For demand scenarios of 100k tLH<sub>2</sub>/a, on-site supply is still the most economical choice in a 2050 progressive case. However, the upper cost range can be further decreased with retrofitted pipeline import options for short distances to 3.59 USD/kgLH<sub>2</sub>. For the very large demand setting of 1,500k tLH<sub>2</sub>/a, costs can be reduced with GH<sub>2</sub> import setups to 1.68 USD/kgLH<sub>2</sub> in the best case for short distances.

So, total cost uncertainties can be reduced to a maximum of 2.91 or 3.16 USD/kgLH<sub>2</sub> in a region with a large H<sub>2</sub> market (1,500k tLH<sub>2</sub>/a) where retrofitted pipelines are available in short and medium distances.



#### 5.4 Implications for overall research objectives

Addressing the third research question (see 2.3), three general green LH<sub>2</sub> supply pathways are identified in this chapter. These can be differentiated by the position of the liquefaction plant and the electrolysis system (off-site vs. on-site).

Furthermore, a non-linear optimization approach is developed to reflect dynamic characteristics of the main conversion components. It reveals that, e.g., average energy consumptions of the electrolysis and liquefaction deviate by ~10-20% from the nominal values.

To better understand the resulting energy systems, seven rules are derived that explain the optimized system designs. The seven recipes are also tested and evaluated for different geographic conditions and techno-economic sensitivities.

If these sensitivities are considered, a broad LH<sub>2</sub> supply cost range can be found for on-site green LH<sub>2</sub> production. Then, the costs differ between ~1.40 USD/kgLH<sub>2</sub> and 6.00 USD/kgLH<sub>2</sub>, in a more conservative techno-economic scenario with very small LH<sub>2</sub> demands. Building on that, three overarching aspects are highlighted for the economic future of H<sub>2</sub>-powered aviation from this first in-depth, generic, green LH<sub>2</sub> cost optimization.

First, if import options are available, LH<sub>2</sub> cost uncertainties can be significantly reduced even at airports with weaker weather conditions for renewable energy generation and hence, H<sub>2</sub> production. Also, LH<sub>2</sub> costs at the dispenser are most likely below 4 USD/kgLH<sub>2</sub> in a more conservative scenario, lower import demands (100k tLH<sub>2</sub>/a), and when dedicated infrastructure deployment is required (no retrofit available). If larger LH<sub>2</sub> import markets can be created (1,500k tLH<sub>2</sub>/a), then the highest cost mark might be even reduced to below 3.05 or 3.30 USD/kgLH<sub>2</sub> due to import options via short and medium distances, respectively.

Second, in regions with main air travel markets like Central Europe, “worst case” LH<sub>2</sub> supply costs could even be lower than in other regions where no retrofitting option would be available. In Europe, such plans exist to retrofit large parts of existing natural gas pipeline networks for H<sub>2</sub> use with the European Hydrogen Backbone.

Third, also smaller airports (e.g., with a demand of <100k tLH<sub>2</sub>/a) might profit from potentially lower H<sub>2</sub> market prices through large-scale import compared to the costs with a dedicated infrastructure deployment approach discussed earlier. Therefore, aggregation of larger H<sub>2</sub> demands would be required in a broader region driving the previously shown economies of scale for H<sub>2</sub> import scenarios (>500k tLH<sub>2</sub>/a). This might especially be the case for GH<sub>2</sub> markets with pipeline transport via retrofitted systems like the EHB. However, if only LH<sub>2</sub> import supply would be available in a region (e.g., for islands or no existing pipelines), LH<sub>2</sub> market assumptions are more critical. Since most other large-scale H<sub>2</sub> applications do not require LH<sub>2</sub> for end use, other forms (aggregates) for H<sub>2</sub> import like ammonia shipping might already be implemented which would then hinder achieving beneficial LH<sub>2</sub> market masses for LH<sub>2</sub> import deployments in such regions.

## 6 Green LH<sub>2</sub> supply in air traffic networks

In this last chapter of results, the fourth and fifth overarching research questions are addressed in one larger case study. For that, all approaches from the previous chapters are brought together: the DOC evaluation as well as the aircraft, the airport infrastructure, and the green LH<sub>2</sub> supply optimization methodology. Hence, the following assessments combine three main aspects in one holistic evaluation: green LH<sub>2</sub> infrastructure at airports, H<sub>2</sub>-powered aircraft, and an exemplified air traffic network.

Based on representative input data, the impact of H<sub>2</sub>-powered aviation on airline operation and profitability is investigated (research question 4). Furthermore, the analyses also target the general industry and policy perspective in research question 5 (rephrased): Should H<sub>2</sub>-powered single-aisle aircraft or other decarbonization options be prioritized in the sector to fulfill its 2050 net-zero objective?

While the airline-related lens focuses more on the possible integration of H<sub>2</sub>-powered aircraft in air traffic networks, the broader sector lens requires a general comparison of the H<sub>2</sub>-powered aviation options to other net-zero pathways. This does not only include economic but also other sector-relevant criteria that are introduced at the end of the chapter.

Consequently, the chapter is structured as follows. The reference air traffic network is introduced in Section 6.1. Then, green LH<sub>2</sub> supply pathways and best costs are calculated for the airports of the air traffic network. In Section 6.3, more specific H<sub>2</sub>-powered aircraft characteristics are derived and different operational strategies are discussed. In Section 6.4, both aspects are combined and total DOC are calculated for the given network to compare H<sub>2</sub>-powered aircraft to different fuel options.

**Disclosure:** The following section is based on the publication: J. Hoelzen, D. Silberhorn, F. Schenke, E. Stabenow, A. Bensmann, T. Zill, R. Hanke-Rauschenbach, H<sub>2</sub>-powered aviation – Optimized aircraft designs and green LH<sub>2</sub> supply chains in air transport networks, In publication process (2023) [305]. For a detailed description of the author's contributions see Appendix F.

### 6.1 Reference air traffic network

In this section, the reference air traffic network is introduced which determines the chosen airports for the LH<sub>2</sub> supply infrastructure analysis and the distribution of trip lengths for the operation of H<sub>2</sub>-powered aircraft.

#### 6.1.1 Main characteristics of chosen air traffic network

There are two main forms of airline operation characterizing the resulting air traffic network. In a hub-and-spoke operation, the airline has a central hub, from which all flights start followed by a return flight to that hub. Contrary to that, airlines with a point-to-point operation fly from one destination to another based on optimized networks, but without a repeating main airport [306]. For the present analysis, a hub-and-spoke air traffic network offers more options to test different operational strategies such as central refueling at the main hub, which is further explained in Section 6.3.

Here, Lufthansa is chosen as an exemplary airline that operates with a classic hub-and-spoke network and is in the top five most-flown airlines in Europe [307]. Their largest hub is Frankfurt, which is selected for the analysis. Flight data was collected for one representative week, September 5<sup>th</sup>-11<sup>th</sup> 2022 from Flightradar24 [308]. In total, 108 larger single-aisle aircraft were tracked: 19 Airbus A319, 42 A320, and 47 A321. These aircraft flew from Frankfurt to

103 additional airports, which therefore present the main airports of this study. Of these airports, ten destinations lay outside Europe in the MENA region – a list of all airports can be found in Appendix Table E1.1. Figure 6.1 gives an overview of all flights in the chosen network and the cumulative frequency distribution of these flights sorted by different performance indicators. It shows that a single-aisle aircraft with a design range of 1,500 NM could cover already 97% of all departures, which translates into 89% of all CO<sub>2</sub> emissions of the chosen network.

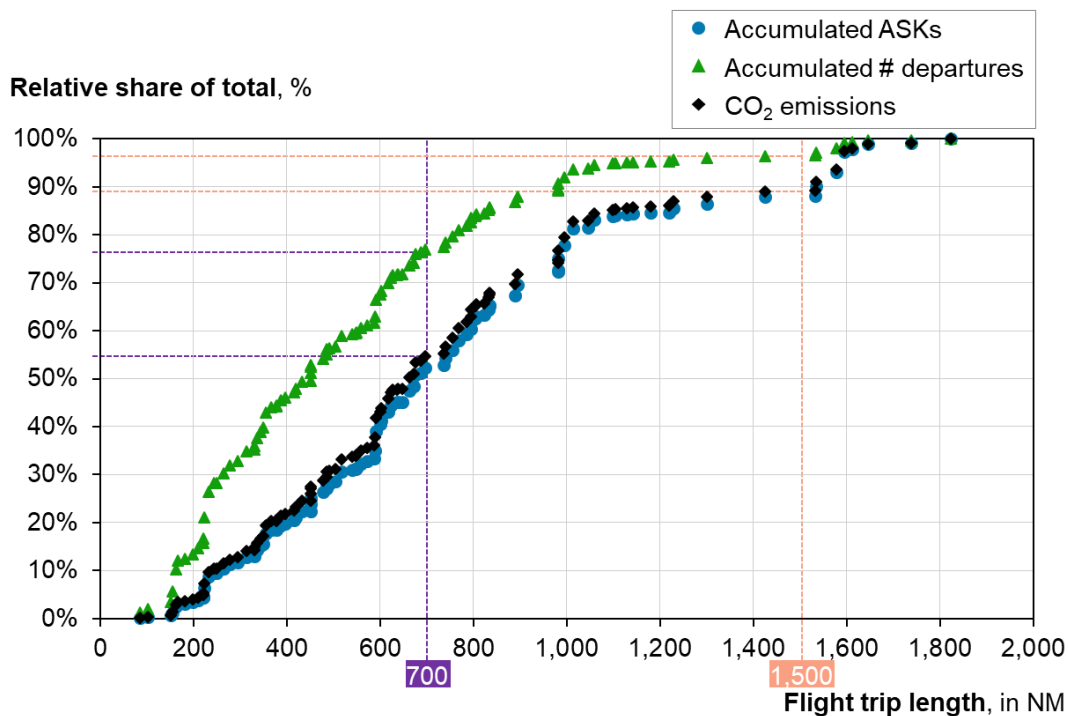


**Figure 6.1:** Characteristics of selected air traffic network considering Lufthansa flights from Frankfurt-Main in the week of September 5<sup>th</sup>-11<sup>th</sup> 2022 and only flights of larger single-aisle aircraft (Airbus A320 family aircraft: all versions of A319, A320, A321 aircraft), based on data from [308]

This study investigates H<sub>2</sub>-powered aircraft which are especially discussed for smaller up to larger single-aisle aircraft [18]. Such aircraft caused around 85 Mt CO<sub>2</sub> emissions in Europe only [228]. This accounts for ~9% of the global air travel emissions from passenger transport (785 Mt CO<sub>2</sub> emissions) and 77% of all intra-European commercial air traffic [7]. Of the 85 Mt CO<sub>2</sub> emissions, 68% were emitted by single-aisle and smaller aircraft departing at the 104 airports in the reference network. If also neighboring airports are included, e.g., London Gatwick, Stansted, and others next to London Heathrow Airport, the share increases to 80%.

### 6.1.2 Relevant airport categories

The 104 considered airports are categorized by their size and potential future LH<sub>2</sub> demands which serve as main inputs for the cost optimization of the fuel supply. As found in Chapter 5, larger annual LH<sub>2</sub> demands have significant supply cost impacts due to economies of scale. Hence, the categorization for the case study differs slightly from the airport archetypes defined in Chapter 4. In this analysis, total annual passenger handling statistics are used as a reference to distinguish between airport sizes, see Table 6.1. This enables a more sensitive cost optimization also distinguishing potential demands at smaller airports more precisely. Hence, five categories are introduced to calculate realistic supply costs at each of the airports. Nevertheless, the same LH<sub>2</sub> demand projection methodology from Chapter 4 is used.

The first projection refers to the years 2035-2040, see also Section 4.1. These mark the planned potential entry-into-service for larger single-aisle aircraft, while regional H<sub>2</sub>-powered aircraft could already be in use by then [16]. However, very low demands would be expected in these first years [17,18]. Only at very large airports/airline hubs several flights per day could already take off in this “early” timeframe. This is different for the reference time frame around the year 2050. After 15 years of manufacturing ramp-up and fleet renewing, larger H<sub>2</sub>-powered fleets and hence, larger LH<sub>2</sub> demands are expected.

**Table 6.1:** Overview of commercial airport categories used for LH<sub>2</sub> demand calculations in this study

Commercial airport category (# of airports)	Total annual passenger (PAX), Mn	LH <sub>2</sub> demand range in 2035/40, tLH <sub>2</sub> /a	LH <sub>2</sub> demand range in 2050, tLH <sub>2</sub> /a	Exemplary airports
Very large (25)	>10	5,000–10,000	100,000–300,000	London Heathrow Airport, Frankfurt Airport
Large (21)	5-10	1,000–5,000	50,000–100,000	Hamburg Airport, Birmingham Airport
Medium (28)	2.5-5	1,000–5,000	20,000–50,000	Valencia Airport, Gothenburg Airport
Small (19)	1-2.5	1,000–5,000	10,000–20,000	Bremen Airport, Madeira Airport
Regional (11)	<1	1,000–5,000	5,000–10,000	Graz Airport, Mykonos Airport

It has to be noted that the total PAX size for the very large airport category is set relatively low. However, no further cost scaling effects can be achieved for demands above 100k–200k tLH<sub>2</sub>/a as shown in Section 5.2.2. In total, LH<sub>2</sub> demands at the 104 airports in 2050 would sum up to a range between 4.4 to 11.5 MtLH<sub>2</sub>/a.

## 6.2 Optimized LH<sub>2</sub> supply costs at selected airports

In the first part of the analysis in this chapter, the optimal LH<sub>2</sub> supply costs at the 104 airports are investigated. Therefore, the methodology from Chapter 5 is re-defined with case-specific techno-economic assumptions. Then, the optimization results are presented.

### 6.2.1 Assumptions for LH<sub>2</sub> infrastructure optimization

This section introduces the study’s scope of LH<sub>2</sub> supply and refueling setups for the given case study and the relevant techno-economic assumptions. The optimization approach for the LH<sub>2</sub> supply chains is kept the same as described in detail in Section 5.1.

#### Possible LH<sub>2</sub> supply chains and refueling setups

To the three supply pathways introduced in Section 5.1 (LH<sub>2</sub>ON, LH<sub>2</sub>OFF, GH<sub>2</sub>OFF) one additional supply option is added: LH<sub>2</sub> off-site supply over shorter distances via truck if the export hub is close to the receiving airport or is even a neighboring airport (2b-LH<sub>2</sub>OFF-A in Fig 6.1). Consequently, the known pathway LH<sub>2</sub>OFF from Chapter 5 with longer distance vessel supply

is called LH<sub>2</sub>OFF-V in the following (see 2a in Fig. 6.2). All options including 1-LH<sub>2</sub>ON and 3-GH<sub>2</sub>OFF are shown for two exemplarily displayed airports A and B in Figure 6.2.

Such as in Chapter 5, the two options for designing the LH<sub>2</sub> refueling system are also taken for the following analyses: a hydrant & pipeline system or a truck refueling system with all parameters from Section 4.1 (and [112]).

### Optimization of LH<sub>2</sub> supply chains

The optimization approach to select the optimal supply chain for a specific airport and the related dimension of all supply components is taken from Section 5.1. Here, only the main aspects are presented that are relevant for the specific investigations in this case study.

The chosen methodology to reflect interest rate (see also Eq. 5.5) is often called weighted average cost of capital (WACC). In Chapter 5, the interest rate is considered constant for all generic locations. In the present Chapter, specific input is available on the capital costs in each country, especially for RES projects. Consequently, the financial costs considered for the interest rate for each country in the given network are derived, see Table E1.1 in the Appendix.

Based on the modeling, the three main supply chain setups (LH<sub>2</sub>ON, LH<sub>2</sub>OFF-V, GH<sub>2</sub>OFF) and the underlying energy systems are optimized for each of the 104 airports independently. In the second step, the LH<sub>2</sub>OFF-A option is tested for all airports taking the previous LH<sub>2</sub>ON results and adding costs for the LH<sub>2</sub> truck to the neighboring airport calculated with the road distances between the different airports.

### Study-specific techno-economic assumptions

The chosen optimization approach is built on three levels of techno-economic assumptions.

General parameters for the techno-economics of each component are location-independent but vary with different time-dependent scenarios, see Chapter 5. In the present analysis, the base case 2050 scenario assumptions are chosen for the main analysis and will be compared to the 2035 base case scenario.

The next level focuses on LH<sub>2</sub> on-site relevant assumptions, see Table E1.1 in the Appendix. The RES site is selected based on the best weather conditions in no larger distance than 100 km to the airport and given space availability – as possible to detect this based on satellite



**Figure 6.2:** Exemplary LH<sub>2</sub> supply pathways shown for an Airport A; 1 – LH<sub>2</sub> on-site supply at/close to the airport, 2a- LH<sub>2</sub> off-site import via vessels, 2b – LH<sub>2</sub> off-site import via road from a neighboring Airport B, 3 – GH<sub>2</sub> off-site import via pipelines and a LFP at the receiving Airport A; export hub perspective shown on bottom of map

image research and not considering local regulations. Therefore, weather data is required to calculate the hourly resolved availability of RES. Here, data is taken from [294,295] for the reference year 2019, which is based on the MERRA-2 database. For an analysis of the uncertainties using one specific weather year for the chosen optimization approach, see Section 5.2. At some sites only very limited land is available for RES, these airports are highlighted in Table E1.1. At two airports, Bergen and Tromsø in Norway, no possibility is seen to install wind or PV plants locally. Current legislation shows that H<sub>2</sub> production could also be labeled as green when produced from electricity in a grid where more than 90% of electricity stems from RES (mostly hydropower), see also Section 2.2.1. So, at airports like these two without any space for RES but a grid qualifying for green H<sub>2</sub> generation, the grid option is also considered [132,309]. For Norway, which already fulfills these regulatory criteria today [310], the grid supply option is feasible and is used for the two airports with an assumed future electricity price of 50 USD/MWh [311]. RES generation from wind offshore turbines is not considered in this chapter, since it is often more expensive than RES from hybrid wind onshore and PV plants as shown in Section 5.2.

Besides the RES side, again hourly-resolved demand profiles for LH<sub>2</sub> at the airports are inputs for the modeling. These are already shown in Sections 4.2 and 5.1 and are not further individualized for each airport. Furthermore, as found in Chapter 5, the availability of large-scale GH<sub>2</sub> underground storage can lead to significant cost reductions of the LH<sub>2</sub> supply costs, especially at weaker RES sites. Their assumed availability is also mapped for each airport in Table E1.1.

The last level of assumptions concerns off-site production and transport. Seven locations are chosen as potential export hubs: Scotland, Ireland, Portugal, Spain, Morocco, Saudi, and Australia. It is expected that these countries will have a surplus of green electricity to generate H<sub>2</sub> compared to their green electricity consumption in 2050 [312]. While the chosen sites in Scotland and Ireland qualify for a pure wind onshore RES setup, the other sites have a hybrid setup with wind onshore and PV plants. In addition to that, all hubs except Ireland should have geological preconditions to exploit the potential of integrating local GH<sub>2</sub> underground storages. For more information on the characteristics of all hubs see Table E1.2.

On the transport side, the distances between airports, ports, and the hubs for LH<sub>2</sub> vessel import are shown in the Supplementary Material Table S1.1 of [305]. Costs for the LH<sub>2</sub> vessel and truck transports are based on [239] and a cost range results from varying future market sizes of 0.5–1.5 MtH<sub>2</sub> for such transport networks [304].

For GH<sub>2</sub> pipeline transport, all transport distances are given in Supplementary Material Table S1.2 of [305]. These are based on the 2040 picture of the planned European Hydrogen Backbone (EHB) pipeline network [166]. As the market size, a 1.5 MtH<sub>2</sub> GH<sub>2</sub> pipeline system is considered for transmission routes using the pipeline cost function from [239] and a share of 40% new and 60% retrofitted pipelines [164]. For the distribution pipeline connecting the airport with the EHB, on average a 0.15 MtH<sub>2</sub> pipeline and a 0.05 MtH<sub>2</sub> pipeline are considered to supply very large and large airports and all other airports, respectively. For the subsea transmission sections, an additional cost factor of 1.7 is used vs. land pipelines [164].

Assumptions on the interest rates were selected individually for the component systems in the off-site pathways. All annual capital costs for the systems at the export hub are determined by the local interest rates. The GH<sub>2</sub> and LH<sub>2</sub> transport systems are seen as “international” encounters and hence, a central European interest rate of 6% for H<sub>2</sub> systems is taken [239]. The truck transport in the receiving country, as well as the refueling systems (incl. airport storage) at the airports, are calculated using the local interest rates, see Table E1.1.

## 6.2.2 LH<sub>2</sub> cost results in 2050 scenario

Based on the considerations made in Chapter 5, the LH<sub>2</sub> cost optimization results are shown for the selected airports. This is done for the 2050 base scenario as it represents a time frame of already established H<sub>2</sub>-powered aviation. As a start, the overall results and then, the results for three selected airports are explained.

### Optimized supply pathways

Figure 6.3 shows the optimized LH<sub>2</sub> supply costs at the dispenser at each airport. In the following, average values of the optimized supply cost ranges are discussed for simpler comparability. The cost ranges result from low and high demand assumptions at the airport (Table 6.1) as well as from smaller or larger import market sizes as discussed above.

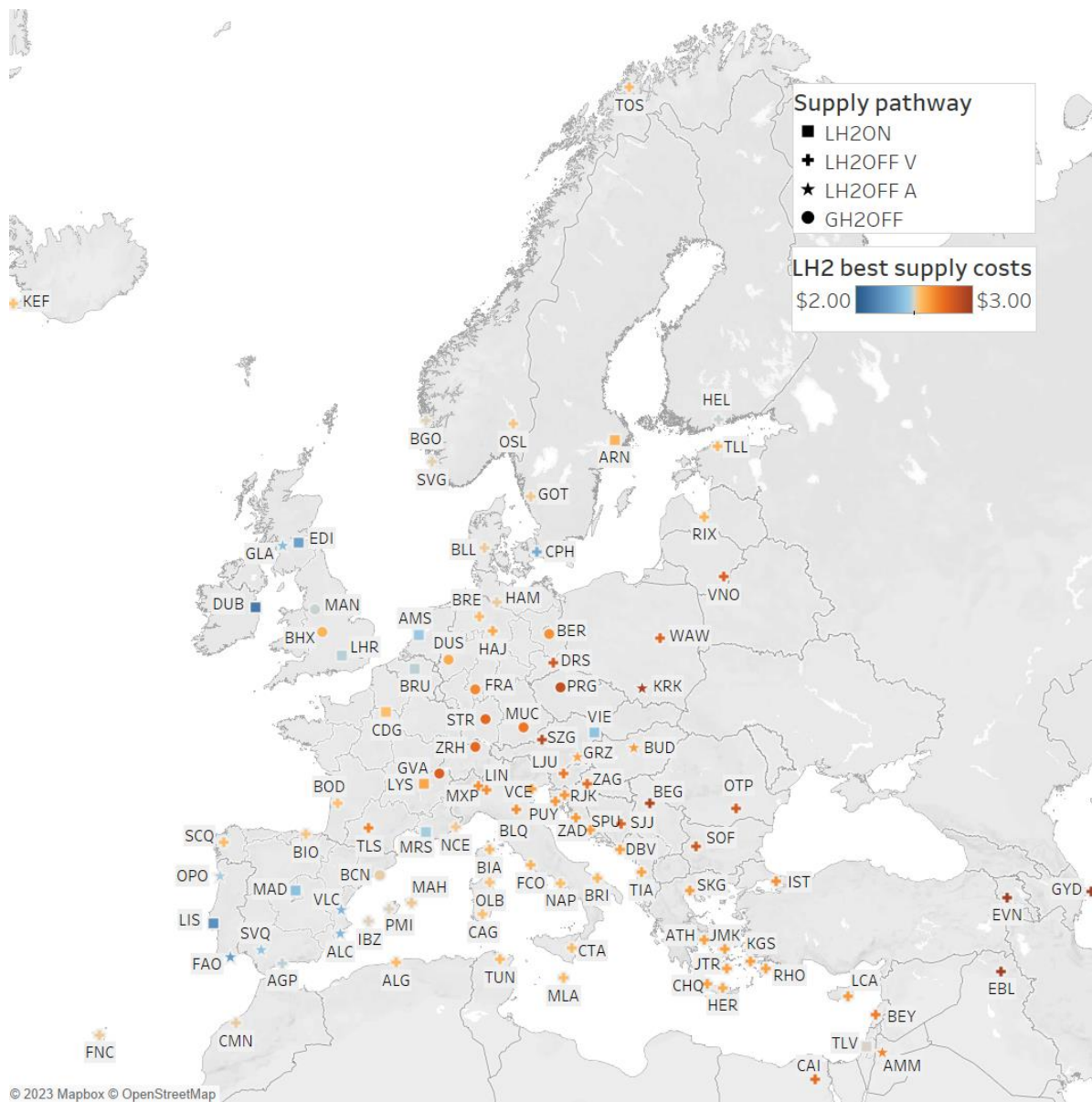


**Figure 6.3:** Optimized LH<sub>2</sub> supply costs at all selected 104 airports and 6 hubs – Australian hub not shown, costs at the dispenser (incl. LH<sub>2</sub> refueling system) in USD/kgLH<sub>2</sub>, LH<sub>2</sub>ON – LH<sub>2</sub> on-site supply at/close to the airport, LH<sub>2</sub>OFF V - LH<sub>2</sub> off-site supply from central hubs via vessel transport, LH<sub>2</sub>OFF A – LH<sub>2</sub> off-site supply from a neighboring airport/export hub via LH<sub>2</sub> trucks, GH<sub>2</sub>OFF – GH<sub>2</sub> off-site supply via pipelines



Based on the optimization results, on-site production (LH<sub>2</sub>ON) is the most economical supply pathway at 14 airports. These are mostly larger airports with high LH<sub>2</sub> demands leading to economies of scale for the CAPEX and efficiencies of main components like the LFP. The airports are either located close to export sites or in Northern-West European regions with good RES conditions. Some of these very large airports would also function as a broader H<sub>2</sub> hub for neighboring airports or other use cases, e.g., Edinburgh, Lisbon, Vienna, and Tel-Aviv airport. At the smaller neighboring airports, LH<sub>2</sub> on-site supply would also be a competitive option. However, due to smaller demand scales driving up costs, especially for the LFP, it is less costly to import from the next very large airport with similar RES conditions. In total, 10 airports are supplied by this “neighboring” option with 6 airports sourcing from a larger airport and 4 airports from a closely located hub (Portugal, Spain). Due to the very short distances to these hubs, it would be less costly to transport LH<sub>2</sub> via trucks to the smaller airports (LH<sub>2</sub>OFF-A) than using larger-scale off-site supply setups (pipelines or vessels).

In general, the chosen hubs reach the best economies of scale due to the very large demand scales above 0.5 MtH<sub>2</sub>/a. Plus, they will most likely function as main exporters for all H<sub>2</sub> markets and not only aviation. Australia, Portugal, and Scotland are the most competitive hubs with exporting costs of 2.06–2.13 USD/kgLH<sub>2</sub> before losses, the transport and refueling system costs. However, the results indicate that no airport would be supplied from Australia given the very long LH<sub>2</sub> transport distances. At the sites in Saudi Arabia and Morocco, supply costs could also be slightly higher due to interest rates of 6% and 9% for RES projects, respectively. This leads to exporting costs of 2.34 and 2.65 USD/kgLH<sub>2</sub>. In the Morocco example, which was also investigated in Chapter 5 (HYB location), the cost increased by 24% due to higher costs of financing. Hence, it remains uncertain whether countries with currently higher costs of financing like Morocco will play an important exporting role in a global H<sub>2</sub> economy in the next 10–30 years. If these financing risks decrease in the future as indicated by [313,314], then imports from such countries could become superior to the other European options.

From such central hubs, 69 airports would be supplied via LH<sub>2</sub> vessels (LH<sub>2</sub>OFF-V), most of them being located in more coastal areas or also being inland airports that might have very low LH<sub>2</sub> demands. 17 airports would import from Scotland and 52 from the Portugal hub. As an extreme, results from the Iraqi airport EBL and Azerbaijan airport GYD indicate that even though distances from the import harbor to the airport are nearly 1,000 km, it might be less costly to import via LH<sub>2</sub> vessels and then trucks than having dedicated infrastructure due to weaker local RES and also high interest rates. For larger coastal sites such as Barcelona Airport, there is an exception to the rule, since it is closely located to the Spanish H<sub>2</sub> hub and it is cheaper to connect via the GH<sub>2</sub> pipeline system than importing LH<sub>2</sub>.

GH<sub>2</sub> off-site supply (GH<sub>2</sub>OFF) is the best option for 11 airports, which are located farther inland and have higher LH<sub>2</sub> demands. Consequently, scaling effects for the LFP and storage at the airport are driving down costs as already explained previously.

This trend can be emphasized when investigating similarly located airports but with smaller demands like Dresden Airport. While surrounding airports like Berlin and Prague would be supplied by the GH<sub>2</sub> pipeline, the on-site LFP in Dresden would be very small, and hence, specific CAPEX and energy consumption are significantly higher. With higher energy requirements and more expensive grid electricity costs for the LFP, this trend is even more significant. This is why, longer LH<sub>2</sub> truck transport from a central LH<sub>2</sub> import terminal is still the more economical choice for such smaller inland airports.



### Comparison of costs with LH<sub>2</sub> on-site supply only

To provide a perspective on the importance of such import supply options, the previous results are compared to a 2050 LH<sub>2</sub> fuel network where only on-site supply (LH<sub>2</sub>ON) would be available, see Figure 6.4.

The cumulative frequency distribution of optimal results shows that if import options are available, only for 2% of airports or less than 0.5% of LH<sub>2</sub> amounts the supply costs would be above 3 USD/kgLH<sub>2</sub> (blue markers in Figure 6.4). On the contrary, for on-site supply only LH<sub>2</sub> costs in the network would increase significantly. In that case, 50% of airports would have higher supply costs at the dispenser than 3 USD/kgLH<sub>2</sub>. Considering the amount of delivered LH<sub>2</sub> this would be 26% (see orange markers). All on-site cost results are shown in Table S1.3 and a comparison between all supply options for each airport is in Figures S1.2-S1.10 in the Supplementary Material of [305].

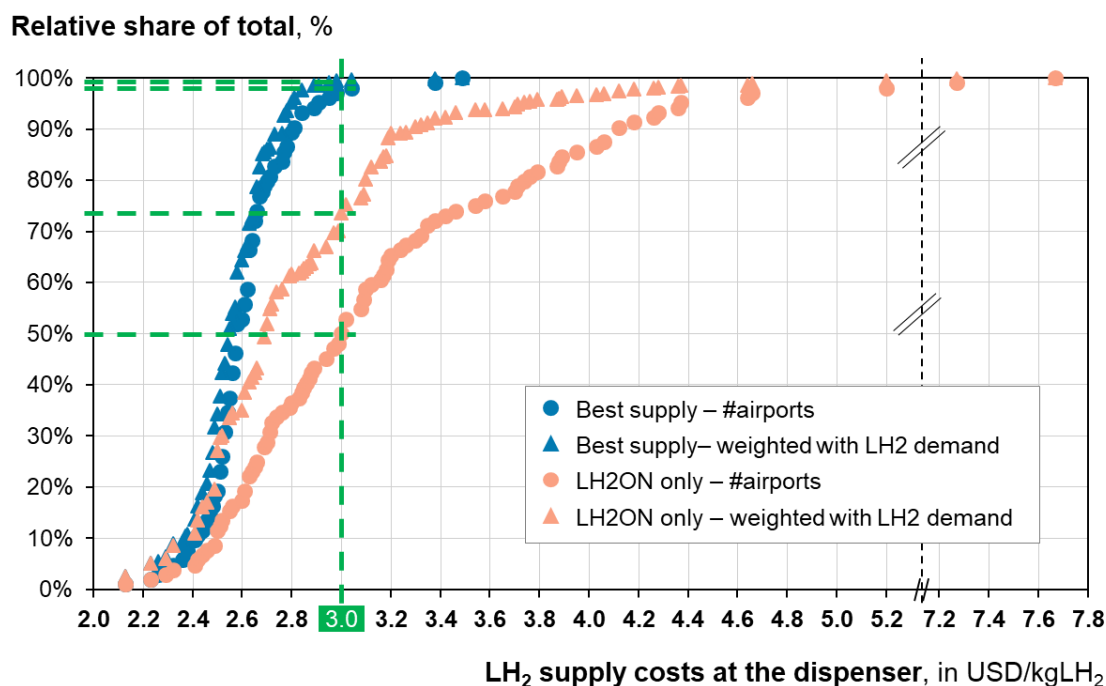


**Figure 6.4:** Cumulative frequency distribution of cost results for the best-supply-cost-pathways and LH<sub>2</sub>ON only supply, either weighted by the LH<sub>2</sub> demand scale of each airport or only by the number of airports

Besides the higher costs in the on-site-only network, also the required resources like RES capacities differ. Since RES would be installed at even weaker weather sites, 44% larger on-shore wind and PV capacities would then have to be installed. However, since fewer H<sub>2</sub> losses occur in on-site setups (no longer distance transport), the total energy efficiency per fuel delivered increases slightly.

### Three airport case studies

To give an impression of the cost breakdown of different supply pathways and effects at different locations, the results are briefly discussed for three exemplarily selected airports, see Figure 6.5.

At Vienna Airport, LH<sub>2</sub> on-site production achieves the lowest costs due to very good RES conditions and the availability of space in a 100-km radius around the airport. Otherwise, if RES availability would be limited, GH<sub>2</sub> off-site supply is the second best option like at Munich

Airport. Due to the long distances to the next importing harbor, LH<sub>2</sub> off-site supply is the costliest.

Graz Airport has a smaller LH<sub>2</sub> demand scale (5–10k t/a vs. VIE with 100–300k t/a) which would lead to high costs for the LFP in the GH<sub>2</sub> pipeline setup. Even though LH<sub>2</sub> vessel import routes would be cheaper, the best option would be to transport LH<sub>2</sub> with trucks from Vienna to Graz (ca. 200 km distance). Then, Graz Airport could also profit from economies of scale at the central Vienna hub.

As the last site, Ibiza as an island airport without a potential connection to a GH<sub>2</sub> grid is presented. On-site production costs are comparably low because the levelized costs of electricity (LCOE) are already competitive and the medium-sized demand category leads to the before-mentioned cost scaling effects. However, large-scale LH<sub>2</sub> import via vessels would enable the lowest supply costs for Ibiza where the truck distance for the “last mile transport” is also very short (<10 km from potential import terminal to airport). An overview of the LCOE at or nearby all airports is shown in Figure S1.1 in the Supplementary Material of [305].

LH<sub>2</sub> costs at dispenser in 2050 base, in USD/kgLH<sub>2</sub>

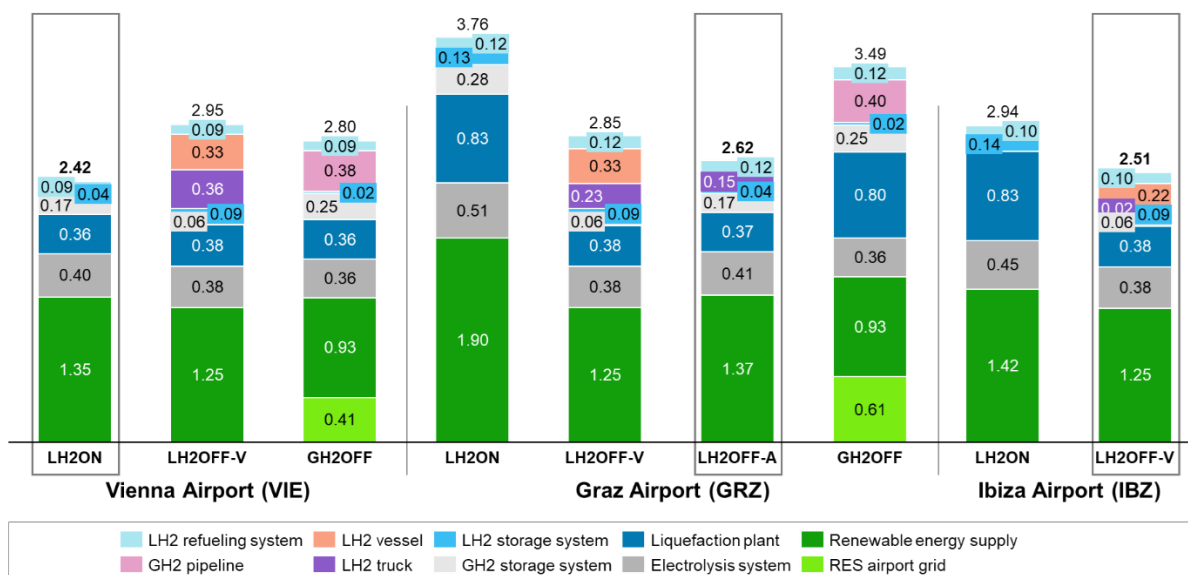


**Figure 6.5:** LH<sub>2</sub> costs at dispenser for three selected airports, LH2OFF-V import for all cases from Portugal for best costs, GH2OFF import from Scotland but not available for Ibiza (island); Graz Airport with LH2OFF-A supply from neighboring airport VIE; RES airport grid means that LFP at the airport in GH2OFF setups is supplied with green grid electricity, see [239]

### 6.3 H<sub>2</sub>-powered aircraft fleets

In the second step, the aircraft-related cost aspects are considered. As a start, the underlying aircraft design methodology is briefly introduced. Then, the resulting H<sub>2</sub>-powered aircraft designs and potential operational strategies with these are investigated to evaluate the operational cost impact of green LH<sub>2</sub> supply for aviation.

#### 6.3.1 Aircraft design results

As shown in Section 3.1, calculating direct operating costs (DOC) is a common approach to evaluating new aircraft technologies and designs. DOC consists of five cost categories: (1) fees for air traffic control and airport services, (2) crew, (3) aircraft CAPEX, (4) aircraft mainte-

nance, and (5) energy costs. While fees and crew costs are not affected by changing the aircraft propulsion from kerosene- to, e.g., H<sub>2</sub>-powered, the impacts on the latter three categories are investigated in this study.

Existing airlines' single-aisle fleets are often built on one aircraft type with slightly different performances for specified use in the airline's network, e.g., different flight lengths. In the reference case study, the airline's fleet consists of Airbus A320-family-aircraft (A319, A320, A321). To reflect a similar family-aircraft approach, three additional single-aisle aircraft with differing design ranges but constant payload (PAX) capabilities are analyzed with both propulsion options, i.e. kerosene/synfuel and H<sub>2</sub> direct combustion. This is done in addition to the H<sub>2</sub>-powered aircraft presented in Chapter 3 and using the same aircraft design optimization methodology. As part of this, general fuel efficiency improvements are accounted for all propulsion types, because a new technology should be compared to a similarly advanced kerosene-powered aircraft with entry-into-service in 2035, see Section 3.1.

Flight trips in the reference air traffic network are below 2,000 NM, shown in Section 6.1. However, the four chosen aircraft designs differ in their design ranges from 1,500 NM to even 3,000 NM. The reason is that there is an operational strategy, called tankering, which might make use of these different design ranges. Tankering means that instead of refueling the aircraft for the return trip at the destination airport, it is already loaded with enough fuel at the origin airport for both flights. Such a strategy is used today already when the fuel costs between the origin and destination airport differ greatly. To enable longer flight trips with a tankering strategy, aircraft with longer design ranges are needed.

First analyses showed that this strategy might be of interest when operating H<sub>2</sub>-powered aircraft in a network with highly differing LH<sub>2</sub> fuel costs at airports [21,121,122,129,130]. The underlying logic is that H<sub>2</sub>-powered aircraft require a heavy LH<sub>2</sub> tank onboard while the mass of the LH<sub>2</sub> itself takes only a small portion of the total weight when the aircraft is fully fueled. Consequently, the increase in fuel consumption for longer distances vs. shorter distances due to the fuel weight is relatively low. This is different for kerosene-powered aircraft. First, kerosene is stored in the wings of the aircraft and does not require an extra heavy tank. Second, the kerosene weight is roughly three times higher for the same energy content vs. LH<sub>2</sub>, because of its lower gravimetric energy density. This is why for kerosene-powered aircraft the fuel consumption for the outbound trip can increase significantly due to the higher take-off weight when a tankering strategy is applied [315].

Therefore, in the present study, designs with longer single trip lengths (>2,000 NM) are modeled enabling tankering over distances up to 1,425/1,430 NM.

All resulting aircraft designs and their performances are presented in Table 6.2. For the four kerosene-powered aircraft, no significant change in the block energy demand can be observed for a fixed trip length (here 800 NM). This is because the kerosene is stored in the wings and thus, the maximum take-off mass does not increase too much between a 1,500 NM and a 3,000 NM design. However, for the H<sub>2</sub>-powered aircraft, this effect is stronger. Due to the heavy and volume-consuming LH<sub>2</sub> tank integration, the fuselage has to be extended and total efficiencies decrease. Further aircraft design parameters are shown in Appendix Table E2.

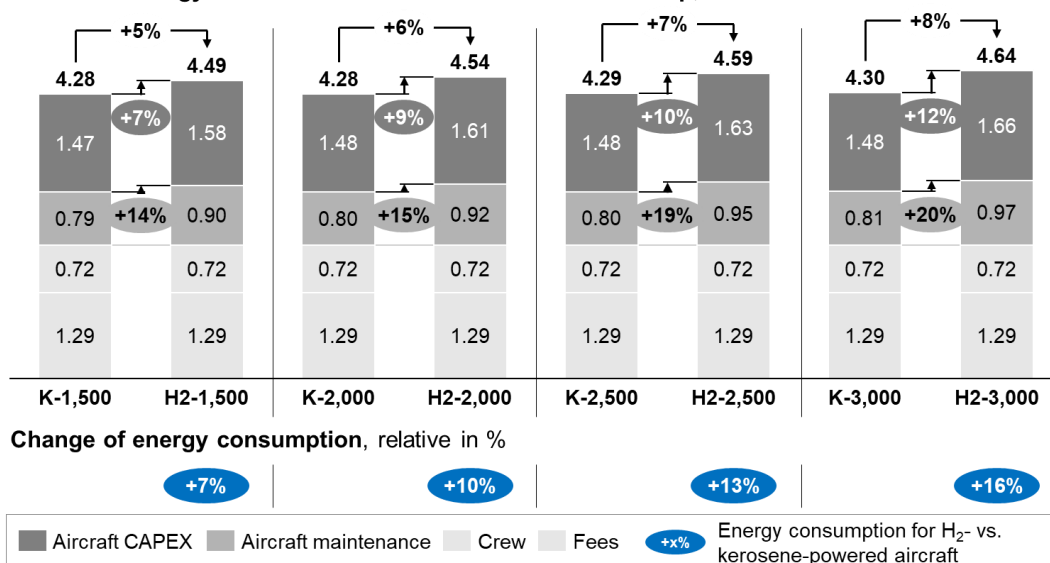
Figure 6.6 shows the resulting DOC for the four aircraft designs at a fixed trip length of 800 NM. It underlines the same trend – no big changes for kerosene- but for H<sub>2</sub>-powered aircraft – for the DOC from aircraft CAPEX and maintenance when comparing both fuel technologies. Due to the larger LH<sub>2</sub> tanks, and increasing aircraft size and mass, these two DOC factors become costlier. Crew costs and fees stay constant for all designs.

**Table 6.2:** Future kerosene vs. H<sub>2</sub>-powered aircraft specifications for the four single-aisle (SA) designs; MTOM: maximum take-off mass, OEM: operating empty mass (no payload, no fuel on board the aircraft)

	Unit	SA-1,500 NM	SA-2,000 NM	SA-2,500 NM	SA-3,000 NM
<b>Input parameters valid for both aircraft technologies</b>					
Design Entry-Into-Service	-	2035	2035	2035	2035
Design PAX (Single class layout)	-	180	180	180	180
Design Cruise Mach-Number	-	0.78	0.78	0.78	0.78
Design Range <sup>a</sup>	NM	1,500	2,000	2,500	3,000
<b>Results for kerosene-powered reference aircraft</b>					
Calculated MTOM	t	65.6	68.1	70.6	73.2
Calculated OEM	t	39.7	40.0	40.3	40.6
Block-Energy for design mission	GJ	286	376	470	567
Block-Energy for typical 800 NM mission	GJ	166	167	167	168
Calculated annual flight cycles (800 NM)	-	1,512	1,512	1,512	1,512
Max. trip length for tankering <sup>b</sup>	NM	670	920	1,170	1,425
<b>Results for H<sub>2</sub>-powered reference aircraft</b>					
Calculated MTOM	t	68.7	71.6	74.7	77.7
Calculated OEM	t	48.2	50.5	52.3	54.3
Block-Energy for design mission	GJ	303	408	522	641
Block-Energy for typical 800 NM mission	GJ	177	183	190	196
Calculated annual flight cycles (800 NM)	-	1,514	1,515	1,516	1,516
Max. trip length for tankering <sup>b</sup>	NM	675	925	1,175	1,430

a) Considering 200 NM, 30 minutes loiter, and 3% contingency reserves that are on top of the shown design range

b) Assuming no additional losses at the intermediate airport

**DOC excl. energy costs for selected aircraft for a 800 NM trip, USD/100ASK****Figure 6.6:** Change of selected DOC factors excluding energy costs and energy consumption for kerosene- (K-XXXX) vs. H<sub>2</sub>-powered aircraft (H2-XXXX), XXXX representing the design range of the aircraft – grey bubbles show relative cost increase for the aircraft DOC levers

### 6.3.2 Operation of H<sub>2</sub>-powered aircraft

Next, the impacts of the operational strategy, tankering, are investigated for the previously derived four aircraft designs. While tankering could lead to better fuel costs with H<sub>2</sub>-powered aircraft, the changes in the aircraft's performance and operating costs have to be investigated.

In Figure 6.7A, the four individual H<sub>2</sub>-powered aircraft cost curves (DOC excluding energy costs) are shown concerning the kerosene reference. Two general trends can be observed. First, the cost increase is lower for each aircraft when flying longer distances. The underlying cause is that the cost increase of aircraft CAPEX and maintenance for H<sub>2</sub>-powered versions weighs more on very short trips. With shorter trips, the ground time of the aircraft increases, and fewer annual flight cycles can be flown. Hence, the costs per available seat kilometer (ASK) increase. Second, the longer the aircraft's design ranges the higher the cost change vs. kerosene. This is also due to the heavy LH<sub>2</sub> tank weight and related enlargement of the aircraft design explained in the previous section.

Evaluating the results on a fleet level, this study assumes that always the smallest aircraft is used to fly the specific trip distance, see the resulting blue line in Figure 6.7A. It has to be noted that this assumption is required as a simplification for the total DOC calculations in Section 6.4. However, in reality, this rule is not fully realizable when optimizing flexibilities in the fleet portfolio and the network routes.

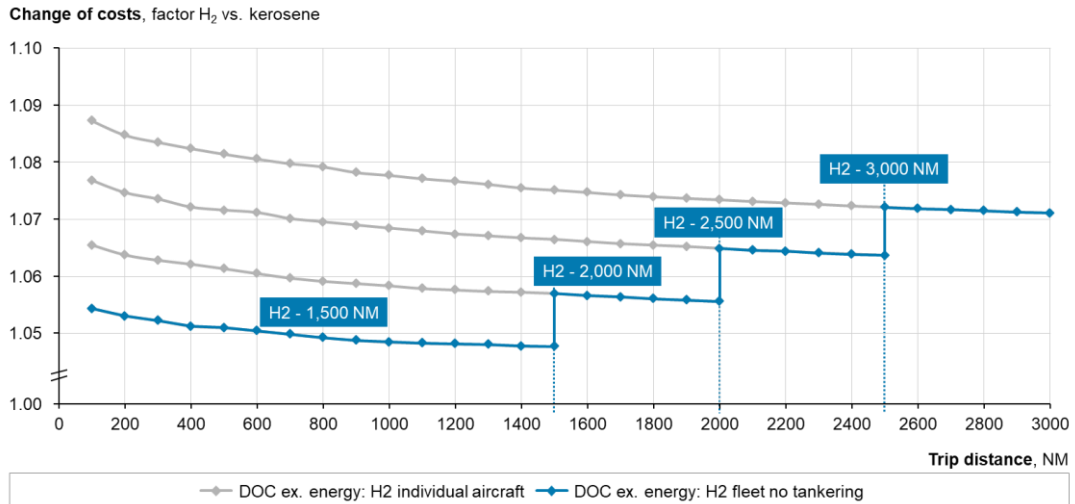
In the next step (Figure 6.7B), the tankering option is compared to the normal single-trip operation on the fleet level. So, the DOC for tankering is always mapped against the DOC of the smallest required aircraft operated on single trips without tankering. Since the maximum flight distance between the origin and destination airport can be 675 NM with the SA-1,500 aircraft, a drastic increase in the DOC result from longer flight trips with tankering using larger, more expensive aircraft (see orange line). So, the benefit of lower energy costs must be even greater for such trips to compensate for the higher aircraft-related operating costs.

Similar effects are found when comparing the specific energy consumption (SEC) as a function of the trip distance in Figure 6.7C. Here, the SEC change vs. kerosene increases for the larger H<sub>2</sub>-powered aircraft. Furthermore, the tankering option up to 675 NM leads to slight increases in SEC and very high increases for tankering flights (up to 8% increase in SEC).

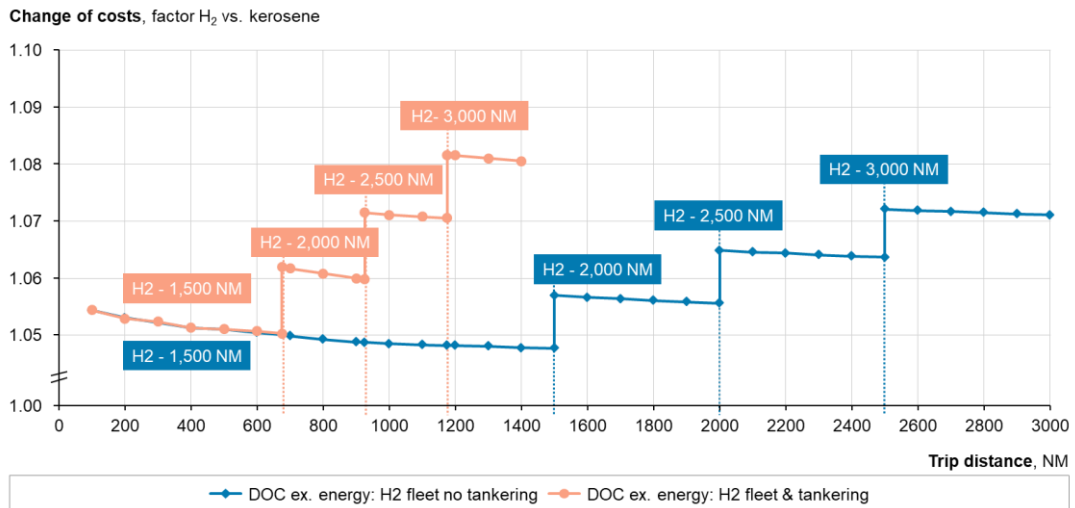
In general, the SEC with the tankering strategy increases by 4% for a kerosene- vs. less than 1.5% for an H<sub>2</sub>-powered aircraft compared to the non-tankering flight on a 1,430 NM trip with the SA-3,000 NM designs. This explains why tankering is not too often considered with kerosene-powered aircraft but might be a valid option when introducing H<sub>2</sub> propulsion in aviation. Additional data on the aircraft design optimization are given in Supplementary Material Table S2 and Figures S2.1-S2.2 of [305].

As a brief intermediate conclusion, it can be emphasized that the aircraft-related cost increase of flying with H<sub>2</sub> is lowest for aircraft with the shortest design ranges. Furthermore, tankering strategies could lead to significant cost penalties for flights above 675 NM – requiring high benefits in saving LH<sub>2</sub> fuel costs at a destination airport to compensate for the additional aircraft costs. Consequently, the supply and aircraft cost perspectives have to be evaluated together.

**A Annual DOC excluding energy costs for four different H<sub>2</sub>-powered aircraft**



**B Annual DOC excluding energy costs on a fleet level with and without tankering**



**C Resulting in specific energy (fuel) consumption per trip for H<sub>2</sub>-powered aircraft**

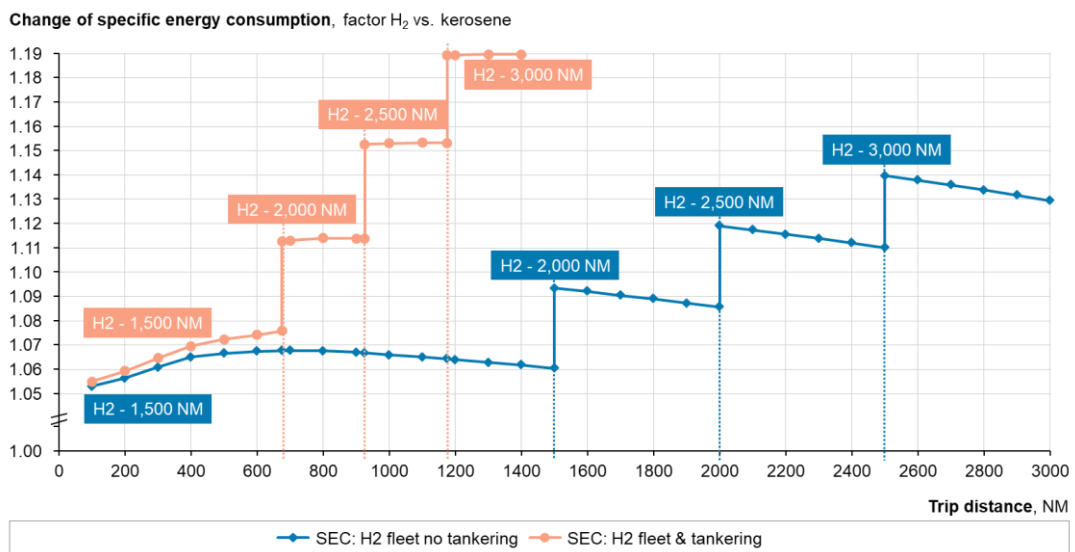


**Figure 6.7:** H<sub>2</sub>-powered aircraft results (design ranges indicated by boxes) compared to kerosene equivalent designs – A) DOC excl. energy costs comparison, B) DOC excl. energy costs comparison against best kerosene aircraft option, C) SEC comparison against best kerosene aircraft option

## 6.4 Resulting operating costs for H<sub>2</sub>-powered aircraft

In this final step, the costs for the LH<sub>2</sub> supply infrastructure at the selected airports and the H<sub>2</sub>-powered aircraft are combined. This is done with the calculation of total DOC for all flights in the given network, which are discussed in comparison with kerosene and synfuel cost benchmarks. This should enable a more holistic answer on the competitiveness of H<sub>2</sub>-powered single-aisle aircraft based on the 2050 scenario assumptions. Then, the analyses are repeated for a different scenario representing an early phase (2035-2040) of the introduction of H<sub>2</sub> in aviation to also evaluate economics in such a scenario. Lastly, resource efficiency aspects are investigated for conclusions on the future of single-aisle H<sub>2</sub>-powered aircraft.

### 6.4.1 Comparison of decarbonized aircraft options in 2050 scenario

The direct operating costs are calculated based on the flight data of the reference air traffic network for the one exemplary week (see Section 6.1). Then, the sum of all flights' costs is divided by the total flown available seat kilometers to derive an average DOC value. Moreover, the tankering strategy is analyzed reflecting the change in aircraft-related DOC and higher energy consumption per flight.

For the technology comparison, the energy cost benchmarks are derived for the calculation of the total DOC in the given network for also kerosene- and synfuel-powered aircraft.

#### Energy cost benchmarks for kerosene and synfuels

While the oil price is highly volatile and hence, the future cost development of kerosene is very uncertain, costs of 0.60 USD/kg kerosene at the dispenser are assumed, see Sections 2.1 and 3.1. Additionally, European commercial aviation is increasingly becoming a subject for regulating CO<sub>2</sub> emissions with the European Trading Scheme (ETS) in the future [316]. In this study, three mid- to long-term ETS cost scenarios are assumed – 50, 100, and 200 USD/tCO<sub>2</sub> – which are in line with investigations in [317]. The CO<sub>2</sub> emissions for kerosene-powered aircraft can be calculated using a factor of 3.16 kgCO<sub>2</sub>/kg kerosene consumption [16]. This mechanism and calculation does however not consider any non-CO<sub>2</sub> emission effects caused by conventional aircraft.

Synfuel costs are calculated based on the same energy system assumptions discussed in Section 6.2. Since synfuel production also requires green H<sub>2</sub> and a well-utilized fuel conversion afterward – which has a comparable power/energy consumption share like the LFP – energy system design and cost assumptions are taken from the LH<sub>2</sub> calculations. In [239] it was shown that utilization of the LFP of ~90% is achievable with RES and GH<sub>2</sub> storages. The conversion of hydrogen to its liquid form is comparable to the fuel conversion in the synfuel process. Hence, the same utilization is taken for the synfuel processes behind the electrolysis. The calculation method and techno-economic assumptions are shown in Appendix E3 including the costs for direct air capture, the Fischer-Tropsch synthesis, fuel transportation, and refueling.

The resulting costs for the 2050 base case assumptions [239] range from 1.25–1.43 USD per kg synfuel at central production hubs like Scotland, Portugal, Saudi Arabia, or Australia. This includes transport and refueling to the 104 selected airports. Based on that an average synfuel cost of 1.31 USD/kg synfuel is assumed in the following.

### Cost of aircraft operation in the 2050 scenario

Both synfuel- and H<sub>2</sub>-powered single-aisle aircraft would be costlier to operate in this air traffic network compared to a future kerosene-powered aircraft, if the costs for CO<sub>2</sub> emissions are 100 USD/tCO<sub>2</sub> or lower, see Figure 6.8A. In a scenario with 200 USD/tCO<sub>2</sub> costs in the EU, synfuel-powered aircraft would still be slightly (2%) more expensive while LH<sub>2</sub>-fueled aircraft would be 1% less expensive. In all cases, the energy costs for kerosene plus ETS, synfuel, or LH<sub>2</sub> have a major share of the total DOC. For LH<sub>2</sub> fuel costs, the main lever to achieve competitive energy costs is the availability of import supply pathways with 0.17 USD/100ASK cost reduction potential. Then energy DOC costs with H<sub>2</sub> propulsion would be 24% lower than with synfuels including the change in aircraft efficiency. Nevertheless, the switch to novel aircraft with H<sub>2</sub> propulsion causes a cost increase of 0.28 USD/100ASK in the DOC aircraft categories compared to the kerosene and synfuel versions. Combining both fuel cost and aircraft perspectives, the H<sub>2</sub> aircraft would be 3% less expensive to operate than a synfuel alternative.

In total, the energy costs still account for only 22% of the operating costs with H<sub>2</sub>- and 28% with synfuel-powered aircraft. This is a typical characteristic when considering DOC for single-aisle aircraft operated on shorter routes where fixed costs for crew or each landing plus passenger handling are the main cost drivers.

The DOC dependency on the trip length is also emphasized in Figure 6.8B. While the costs for synfuel-powered flying do not change drastically with longer trip distances (slight increase only; also highlighted in Section 6.3), this is different for H<sub>2</sub>-powered operation. Three effects explain this: first, the share of energy costs for total DOC is decreasing for short vs. longer trips as explained before. The LH<sub>2</sub> costs account for 19% of the total DOC for all flights below 675 NM, but for 27% for flight lengths between 1,000–1,500 NM, see also Figure S3.1 in the Supplementary Material of [305]. Since the H<sub>2</sub> aircraft has significantly lower energy costs vs. synfuel alternatives, this advantage only leads to greater cost-saving potentials for longer distances. Second, the cost increase for H<sub>2</sub> aircraft CAPEX and maintenance is higher for shorter distances as shown in Figure 6.7A. Next to the fuel costs, this also increases total DOC for shorter flights. Moreover, the DOC further increases when switching to the next larger aircraft with a design range >1,500 NM (Fig. 6.8B). Third, the variation of total DOC for H<sub>2</sub>-powered aircraft can be explained by the highly differing LH<sub>2</sub> supply costs whereas synfuel costs are assumed to be constant at all airports. Another effect explaining higher energy costs for the three airport pairs above 1,600 NM is that these non-EU destination airports come with significantly higher LH<sub>2</sub> fuel costs (Fig. 6.3: EBL, EVN, GYD).

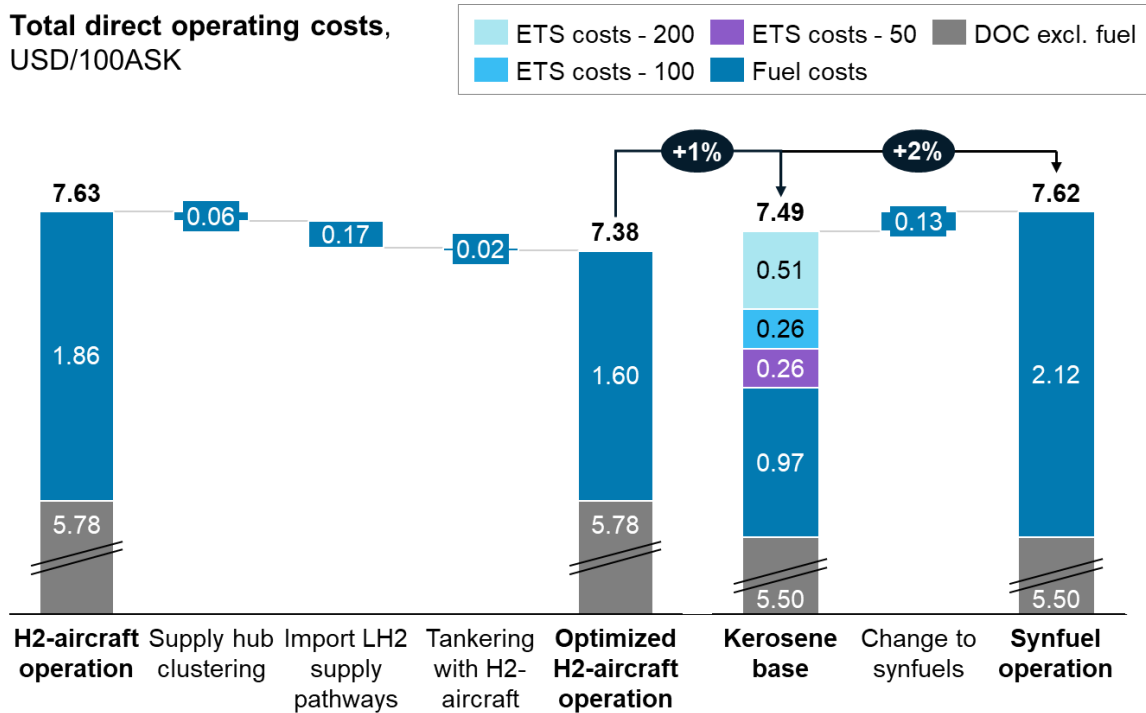
Overall, this means that H<sub>2</sub>-powered single-aisle aircraft is an economic choice for air traffic networks which do not only consist of very short trip lengths.

In the 2050 scenario, the role of tankering is found to be minor in reducing total DOC (0.02 USD/100ASK in Fig. 6.8A), if all supply pathways including the import options are available. In this case, tankering would be economically eligible only on shorter trips below 700 NM and on 59 routes with minor energy cost savings, see also Figure S3.2 in the Supplementary Material of [305]. On 14 of the 59 routes aircraft would be refueled at the hub in Frankfurt, not requiring LH<sub>2</sub> fuel supply at the destination airports. Otherwise (45 routes), the aircraft would be refueled at the destination airports and not in Frankfurt. The tankering trips could still be flown with the smallest and most economical H<sub>2</sub>-powered aircraft (1,500 NM) design with only minor cost penalties coming from a slightly higher SEC. Consequently, the aircraft design ranges in the optimized fleet are identical for kerosene-/synfuel-powered aircraft and the H<sub>2</sub> versions.



**A Total average DOC for all flights in the given network**

Total direct operating costs, USD/100ASK



**B Comparison of total DOC for each flight pair in the given network**

Cost change factor vs. reference

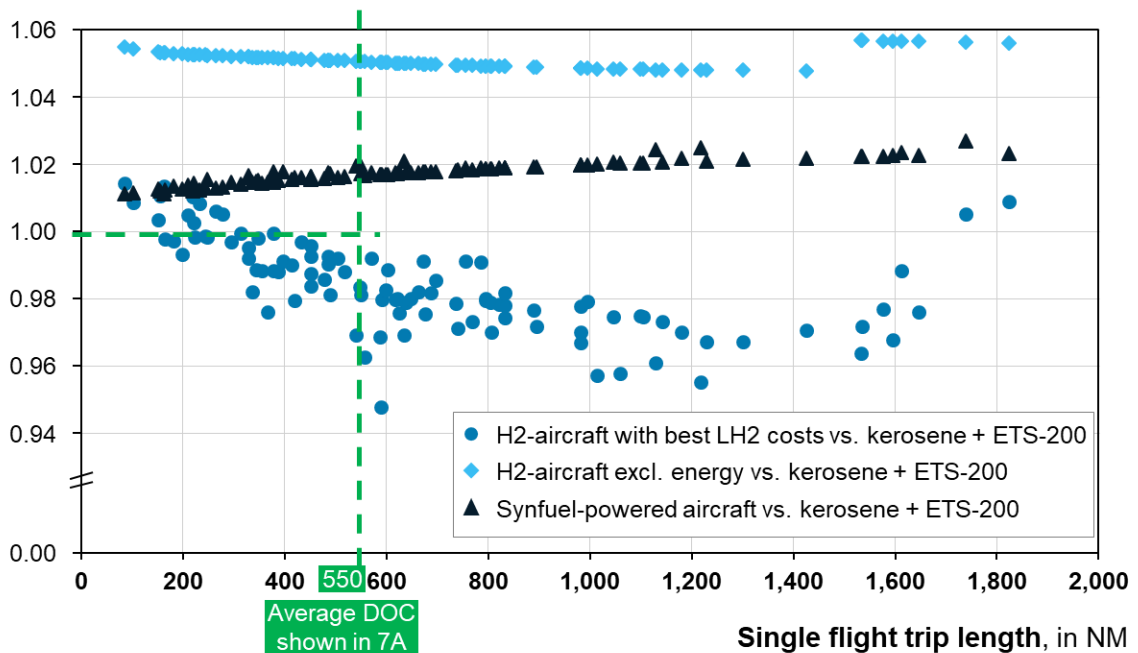


**Figure 6.8:** A) Average total DOC of kerosene-powered aircraft in a given air traffic network including different ETS-CO<sub>2</sub>-cost scenarios in USD/tCO<sub>2</sub> compared to synfuel- and H<sub>2</sub>-powered aircraft operation; B) Total DOC for H<sub>2</sub>- and synfuel-powered aircraft for each flight pair concerning kerosene-powered aircraft operation incl. 200 USD/tCO<sub>2</sub> costs

However, if no import supply options would be available, tankering becomes more relevant. Then, tankering from Frankfurt could be applied to 28 destination airports not requiring a fuel supply over single-trip lengths up to ~925 NM. This leads to an average DOC for H<sub>2</sub>-powered aircraft of 7.49 USD/100ASK and a DOC fuel cost reduction due to tankering of

0.08 USD/100ASK. Further information on tankering routes and DOC cost-saving potentials are presented in the Supplementary Material.

#### 6.4.2 Re-evaluation of results in 2035-2040 (early adoption) scenario

In an early deployment phase, the DOC for H<sub>2</sub> aircraft CAPEX and maintenance do not change while techno-economic assumptions for green LH<sub>2</sub> infrastructure would be more conservative. Also, the LH<sub>2</sub> demands at airports, as shown in Table 6.1, are significantly lower, since it would be the beginning of fleet renewal with the first H<sub>2</sub>-powered aircraft entering into service. This is why, the analyses from Sections 6.2 and 6.4.1 are repeated for the 2035 base case described in [239] to re-evaluate the economics of H<sub>2</sub>-powered aviation versus the other options in that time frame. All results are shown in Table S1.4, Figures S1.11-S.1.12, and Figures S3.4-S3.6 in the Supplementary Material of [305]. Here, only the main findings are briefly described.

LH<sub>2</sub> supply costs increase significantly above 3 to even 5 USD/kgLH<sub>2</sub>. The main driver for these results is not only the higher costs for each component. It is also the smaller installation sizes at an airport and hence, only LH<sub>2</sub> off-site supply pathways would be an economic choice – if available in this early adoption phase. Then, LH<sub>2</sub> would be supplied via vessels from Scotland, Portugal (97 airports) or via truck around the European hubs (7 airports). In an on-site and GH<sub>2</sub> off-site supply setup, limited to no economies of scale could be achieved for on-site components (e.g., the LFP). The average LH<sub>2</sub> costs would then increase by 53% compared to the import supply to beyond 5 USD/kgLH<sub>2</sub>.

The total DOC (analogous to Figure 6.8) for flying with H<sub>2</sub> increased by 8% due to higher fuel costs in 2035-2040. Despite the higher costs, the comparison with synfuels shows even greater advantages in that case for H<sub>2</sub>-powered aircraft. Taking the same techno-economic assumptions for synfuels with the best production setups in this earlier scenario, synfuel would cost on average 2.14 USD/kg. This leads to an 11% decrease in total DOC with H<sub>2</sub>- compared to synfuel-powered aircraft.

Similarly to the 2050 picture, tankering is only a relevant cost improvement option for H<sub>2</sub>-powered aircraft, when no LH<sub>2</sub> import options would be available. That might be more likely in such an early adoption phase with not too many other large LH<sub>2</sub> markets. In that case, tankering reduces energy DOC by 0.37 USD/100ASK – with the availability of LH<sub>2</sub> import supply it would be 0.97 USD/100ASK though.

#### 6.4.3 Resource perspectives for the future of H<sub>2</sub>-powered aviation

Lastly, the implications of deploying green LH<sub>2</sub> vs. synfuel supply are discussed from a resource efficiency perspective. Besides the cost results, this is another important aspect since resources like RES capacities will always be a constraint [16,318].

Comparing both decarbonization options based on the fuel supply perspective (well-to-tank) and the same 2050 scenario assumptions, the energy efficiency is significantly higher with green LH<sub>2</sub> vs. synfuel supply, see Table 6.3. This already includes all H<sub>2</sub> losses like boil-off and flash losses when transporting LH<sub>2</sub> over longer distances – on average 4.3% in the total supply network. Furthermore, in the given optimization, 40% less renewable energy generation is required for the LH<sub>2</sub> supply setup including import described in Section 6.2 compared to the synfuel option. In that comparison, synfuels would be produced for best costs purely at central sites like Portugal, Scotland, Saudi, and Australia and distributed via ship like most of the fossil kerosene/oil products are traded today. The same trend can also be observed for the needed

electrolysis capacity installation for synfuel vs. the LH<sub>2</sub> supply network for the 104 airports, see Table 6.3. As a side fact, the LH<sub>2</sub> supply network for the 104 airports would then require the installation of liquefaction plants with a capacity of approximately 26,000 tpd in 2050.

Resulting from the lower capacity deployments, also the required capital expenditures are lower for green LH<sub>2</sub> fuel supply. The CAPEX required for the synfuel production is 73% higher than for green LH<sub>2</sub> supply, not including the extra-CAPEX for the H<sub>2</sub>-powered aircraft development vs. a 2035-updated aircraft design as well as the transport and refueling system CAPEX for both fuels.

From a fleet-level perspective, which includes the slightly lower efficiencies of the H<sub>2</sub>-powered aircraft, the differences between green LH<sub>2</sub> and synfuels are slightly reduced but still significant. On average (considering all trips flown in the network), 11% more fuel energy is required for 100 ASK when flying with hydrogen. However, still, 34% less renewable electricity is required for the H<sub>2</sub>-powered aircraft fleet when all losses are considered (fuel and flight efficiencies).

**Table 6.3:** Comparison of fuel technologies for decarbonizing the existing air traffic network, so LH<sub>2</sub> demands at all 104 airports – for all techno-economic assumptions on green LH<sub>2</sub> supply, see [239]; for synfuel supply, see Appendix E3

Decarbonization option for single-aisle aircraft	Impact on average DOC vs. kerosene (ETS-200) – Fig. 7A	Fuel supply perspective (well-to-tank)				Fleet perspective (well-to-thrust)	
		Well-to-tank av. energy efficiency, before aircraft propulsion	RES capacity requirement per annual MWh output of fuel <sup>a</sup>	ELY capacity requirement per annual MWh output of fuel <sup>a</sup>	Total capital costs <sup>b</sup> per annual MWh output of fuel <sup>a</sup>	Fuel requirements for aircraft fleet per 100ASK	RES energy for aircraft fleet (well-to-thrust) per 100 ASK
H <sub>2</sub> -powered aircraft – best supply setups	-1%	56%	52 kW	31 kW	602 USD	21 kWh	37 kWh
Synfuel supply	+1%	35%	87 kW	51 kW	1,041 USD	19 kWh	56 kWh

a) using the lower heating value of each fuel

b) excluding CAPEX for transportation and refueling systems for both fuels

### Implications for overall research objectives

All in all, the present case study of this chapter addressed both final research questions (4 and 5 from Section 2.3).

From an airline operations perspective, it is shown that the introduction of H<sub>2</sub>-powered aircraft leads to slightly higher direct operating costs compared to conventional kerosene operations in case of lower CO<sub>2</sub> taxation. If costs for CO<sub>2</sub> emissions increase to around 200 USD/tCO<sub>2</sub>, H<sub>2</sub>-powered will become the most economic choice.

Furthermore, a family aircraft concept is required for most economic operation and to enable all flights in the given airline network. These different H<sub>2</sub>-powered aircraft could also be used for tankering operation, but in a 2050 LH<sub>2</sub> supply network projection, the economic advantages would be limited. The tankering operation only achieves more significant cost savings when an early infrastructure setup around the years 2035-2040 is considered.

Regarding the broader sector research question, the analyses showed that the total DOC picture and also resource efficiency could be more positive for H<sub>2</sub>-powered aircraft in the single-aisle segment than for synfuel. However, this is not an argumentation against synfuels or SAF in general. Since decarbonization of air travel is needed as soon as possible and the entry-into-service of H<sub>2</sub>-powered aircraft and a meaningful renewal of existing fleets will take longer than until the year 2050, SAF is also required to power these “smaller” commercial aircraft – at least in the intermediate time period. Also, there is still no holistic, clear perspective on DOC and resource efficiency for wide-body aircraft. In such larger segments, SAF including synfuels will most likely be the main decarbonization choice.

## 7 Conclusions

The present thesis investigates the future role of H<sub>2</sub>-powered aviation as part of the sector's journey to a future with decarbonized, potentially climate-neutral, air travel. This is done along five main research questions (see 2.3). The corresponding results are summarized in the following section. Furthermore, Section 7.2 provides a perspective on the methodology used in this thesis and its limitations. Then, Section 7.3 closes this work with an outlook and list of recommendations for industry players and policy makers.

### 7.1 Perspectives on research problem

This study investigates H<sub>2</sub>-powered propulsion as decarbonization option for commercial aircraft which caused ~85% of all aviation CO<sub>2</sub> emissions worldwide in 2019 [7]. Moreover, the focus of analysis is set on (larger) single-aisle aircraft which account for 50% of the above-mentioned global CO<sub>2</sub> emissions. Such aircraft require a liquid H<sub>2</sub> fuel system due to the highly constraint volume and weight onboard the aircraft (see Chapter 3).

Consequently, liquid H<sub>2</sub> is needed as a new fuel for these aircraft. In this thesis, the focus is set on green hydrogen production, because of its low carbon lifecycle emissions compared to other production methods of H<sub>2</sub>. In contrast to the aircraft analyses, the LH<sub>2</sub> fuel cost assessments are independent of the chosen aircraft segment and apply to all airport sizes.

In the following, the five overarching research questions from Section 2.3 are addressed.

#### 1. How to assess the operating costs flying with H<sub>2</sub>-powered aircraft and what is a first high-level estimate of the economic impact coming from green LH<sub>2</sub> supply?

A frequently used economic benchmarking methodology is the calculation of total direct operating costs of aircraft. This method distinguishes between five cost categories and is adjusted and applied to H<sub>2</sub>-powered aircraft in this thesis.

In general, three of the five cost factors would change when introducing H<sub>2</sub>-powered aircraft, since both aircraft-related costs and the costs for energy and airport supply infrastructure are affected significantly.

However, it is found that single-aisle aircraft are often operated on relatively short trips, e.g., 800 NM, that come with relatively low energy demands. Hence and as a first high-level estimate, only 17% of the total direct operating costs are caused by the fuel demand for a conventional kerosene reference aircraft. This cost share would be affected when switching the aircraft' propulsion system to hydrogen. For further comparison, the reference kerosene cost assumption can be translated into 1.70 USD/kg LH<sub>2</sub>-energy-equivalent fuel costs. A literature review in Chapter 2 then clarified that only few studies project such low costs for green LH<sub>2</sub> in the long-term. Future LH<sub>2</sub> costs could be even several factors larger than that. Consequently, the cost effect from changing the fuel for single-aisle aircraft could be significant with hydrogen and should not be neglected.

On the opposite, 44% of the total direct operating costs come from aircraft-related aspects such as aircraft CAPEX and maintenance. This distribution of shares with lower importance of fuel/energy costs is typical for the aircraft segment compared to the next larger segments of aircraft (see [52] for more information on wide-body H<sub>2</sub>-powered aircraft).

Regarding the other two cost factors (39% of total direct costs for kerosene reference), no effects are found for crew costs and fees (for air traffic control and airport handling), if H<sub>2</sub>-

powered single-aisle aircraft can be operated with the same turnaround times as the conventional one. Then, the aircraft utilization does not change due to similar amounts of annual flight cycles which otherwise would affect the direct operating costs.

## **2. What is the impact on airport infrastructure when introducing H<sub>2</sub>-powered aircraft?**

Overall, LH<sub>2</sub> demands at airports could become significant by 2050. The scenario analysis derived demands at intercontinental hubs and major national airports with 300–600 ktLH<sub>2</sub> p.a. and 80–150 ktLH<sub>2</sub> p.a., respectively. Such airports could qualify to form central H<sub>2</sub> distribution hubs for other H<sub>2</sub> applications around the airport in a specific region. Given the projections that a future H<sub>2</sub>-powered aircraft fleet would further increase after 2050, the scales of demand could even play a more important role in local H<sub>2</sub> hubs. However, LH<sub>2</sub> supply chains for aviation might be the latest realized application when compared to other H<sub>2</sub> use cases. Consequently, the future role of airports as H<sub>2</sub> hubs in the 2050s must actively be anticipated early on, while other H<sub>2</sub> applications are already commercialized and scaled in the next decade.

It is also found that refueling including the LH<sub>2</sub> storages for supply reliability might only account for a very minor share of the total green LH<sub>2</sub> energy costs delivered to an aircraft. In a base case 2050 scenario, this section of the fuel supply chain causes a 3–5% cost share only, around 0.09–0.12 USD/kgLH<sub>2</sub> at most airport size categories. In contrast to that, the costs for H<sub>2</sub> production and liquefaction dominate the economics of green LH<sub>2</sub> supply.

Two refueling systems are identified as most relevant for H<sub>2</sub>-powered aircraft: truck and pipeline & hydrant refueling. The right choice of one of the systems depends on the airport and hence, the LH<sub>2</sub> demand sizes and can save 0.01–0.02 USD/kgLH<sub>2</sub>. Thus, a design switch point from truck to pipeline & hydrant refueling is identified around 125 ktLH<sub>2</sub>/a at an exemplary airport. Nevertheless, it is found that other criteria such as operational practicability, economic risk, and safety might influence choice of the refueling system more. While a pipeline & hydrant system could reduce apron traffic and human errors when driving, it requires high up-front capital costs and gives less flexibility in scaling LH<sub>2</sub> demands. Only for smaller national airports the preferred refueling system choice is more certain with a clear recommendation for LH<sub>2</sub> truck refueling.

Lastly, a sensitivity analysis highlighted the techno-economic uncertainties when designing LH<sub>2</sub> refueling systems. These are not only driven by heterogeneous CAPEX projections for LH<sub>2</sub> pipelines but also by highly uncertain H<sub>2</sub> loss rates for both refueling setups. Hence, this part of the LH<sub>2</sub> costs at the dispenser will depend on future developments and demonstrations in this field.

## **3. What are the costs of supplying green LH<sub>2</sub> to airports?**

Three main green LH<sub>2</sub> supply pathways are identified: LH<sub>2</sub> on-site, LH<sub>2</sub> off-site, and GH<sub>2</sub> off-site supply. While the H<sub>2</sub> production and also liquefaction plants are all centered at one site (airport or export site), the H<sub>2</sub> liquefaction plant is separated from the electrolysis system in the GH<sub>2</sub> off-site pathway. Additionally, GH<sub>2</sub> pipeline systems are then required, whereas transport of LH<sub>2</sub> would be done via roads, rail, or oceans/rivers.

The major share of LH<sub>2</sub> supply costs is caused by the renewable electricity supply, which results from costs for renewable energy plants and their capacity factor depending on the weather at the generation site. Given very good renewable energy conditions, on-site LH<sub>2</sub> production could become as economical as possible with final costs of 2.04 USD/kgLH<sub>2</sub> at a major national airport in a 2050 base case scenario. In that case, LH<sub>2</sub> costs would still be 21% more

expensive than the equivalent kerosene costs presented above. In a future world with carbon or even climate impact taxes for kerosene usage, the cost difference might disappear: given constant kerosene costs (0.60 USD/kg kerosene), cost parity between LH<sub>2</sub> and kerosene fuel is achieved with a carbon tax of 111 USD/tCO<sub>2</sub>.

Seven design rules are derived from the optimization results. These show that a hybrid renewable energy system setup, PV and onshore wind turbines, leads to the lowest supply costs due to the best-utilized liquefaction plants and relatively small GH<sub>2</sub> and LH<sub>2</sub> storages. Compared to the liquefaction plant, the electrolysis system is operated relatively flexibly in most setups though. Moreover, all optimization results emphasize that neither electric energy nor above-ground, containerized GH<sub>2</sub> storage would be built. These are costlier than other storage, even if no underground storage option is available. Thus, the results show that LH<sub>2</sub> supply from wind offshore sites is rather not competitive despite high, constant wind speeds that enable a very high utilization of all energy system components. The main reason for that is the high CAPEX for the offshore wind park.

The non-linear modeling approach also clarified that some dynamic effects should not be neglected when designing LH<sub>2</sub> energy systems. It revealed that especially part-load characteristics of the electrolysis system and liquefaction plant influence the techno-economics significantly. On the one side, this approach proves better average energy efficiencies for the electrolysis system and hence, lower renewable energy requirements. On the other side, the average renewable energy consumption increases for the liquefaction plant by 10–20%, because part-load operation cannot be prevented in some periods with highly fluctuating renewable energy availability and demand profiles.

A scenario analysis of the supply costs derives uncertainties due to different techno-economic assumptions. The supply cost ranges are mostly impacted by the CAPEX of the renewable energy plants – in total, LH<sub>2</sub> costs range from 1.37–4.19 USD/kgLH<sub>2</sub> at best LH<sub>2</sub> on-site production spots in a more conservative vs. a more optimistic scenario. In addition to the techno-economic uncertainties, weather records from different years also influences cost uncertainties by up to 11% of the supply costs. Thus, the demand profiles at airports and the availability of GH<sub>2</sub> cavern storages do not have a larger design and cost impact. Only at weaker renewable energy locations, LH<sub>2</sub> costs increase clearly by 9% if no cavern storage is available.

A main lever to reduce the relatively high cost uncertainties is the import of LH<sub>2</sub> with the described off-site supply pathways. This is of special importance for locations with weaker renewable energy conditions. If import options are available from regions with great renewable energy conditions within short or medium transport distances, supply costs might be reduced to less than 3.30 (LH<sub>2</sub> import) or 3.20 USD/kgLH<sub>2</sub> (retrofitted GH<sub>2</sub> pipeline import). However, these costs can only be achieved for large exporting demands as high as 0.5 or even 1.5 Mt of GH<sub>2</sub> or LH<sub>2</sub>. This implies that demands from several airports or other H<sub>2</sub> markets might need to be aggregated to reach such demand scales and the related cost benefits. Then, also smaller national airports with lower LH<sub>2</sub> demands could profit from such a market, if accessible.

Besides the economics, another reason for importing GH<sub>2</sub> or LH<sub>2</sub> is potentially constrained space availabilities for renewable energy systems or cavern storages. Since required renewable energy capacity installations at weaker renewable energy locations are factor three larger than at the other generic locations, resulting space requirements could become a significant constraint.

#### 4. How do green LH<sub>2</sub> supply options and H<sub>2</sub>-powered aircraft designs interlink in realistic airline operations?

An airline case study with a focus on one central air traffic market, Europe, is chosen in this thesis. Based on that the individual assessments of evaluating H<sub>2</sub>-powered aircraft, the airport context, and LH<sub>2</sub> supply infrastructure are brought together. However, it is important to highlight that there are many more air traffic markets with different characteristics than the selected region. Hence, the transferability of the following results might only be limited to other case studies.

The study is based on the single-aisle aircraft network from Lufthansa with their base at Frankfurt-Main Airport. In total, 104 airports and all supply setups to these airports are considered.

As a result, it is found that LH<sub>2</sub> fuel costs might be between 2–3 USD/kgLH<sub>2</sub> in that air traffic network if the airports have access to larger H<sub>2</sub> import markets or great renewable energy conditions for on-site fuel production. Moreover, it is calculated that it could be less expensive for smaller airports to import H<sub>2</sub> via the LH<sub>2</sub> off-site pathway than produce it on-site despite great local renewable energy conditions. This is due to high economies of scale effects for the export production site which cannot be reached at smaller airports for their production. Another insight is that availability of GH<sub>2</sub> import is less important for such smaller airports. Only at larger airports, this is a viable option because there the larger sizing of the on-site liquefaction plant reaches scales with significant economies of scale. At medium or smaller airports, higher specific CAPEX and energy consumption for smaller liquefaction plant capacities cause higher LH<sub>2</sub> costs than importing LH<sub>2</sub> directly, e.g., via vessels and trucks.

Regarding the single-aisle aircraft designs, four versions of the single-aisle aircraft are optimized with the same passenger capability but different design ranges. This enables airlines to operate longer-distance trips with such aircraft. Of course, it also comes with increasing costs. On an 800-NM-long reference mission, the total H<sub>2</sub>-powered aircraft-related direct operating costs increase by 8% with the 3,000 NM design range instead of 5% with the 1,500 NM version compared to a respective kerosene-fueled aircraft. This effect is even stronger for the specific energy consumption which increases compared to the kerosene aircraft by 16% versus 7% for the H<sub>2</sub>-powered aircraft with 3,000 NM vs. 1,500 NM design range, respectively.

As a main operational strategy for airlines, tankering is identified as an option to reduce infrastructure deployment needs. Nevertheless, the increase in the aircraft's fuel consumption and aircraft-related direct operating costs can only be outbalanced, if the LH<sub>2</sub> fuel cost savings are large enough. This is not too significant for destinations within a 700 NM distance from the main airport hub. On longer distances, the larger aircraft designs are required to enable tankering strategies, which leads to an even greater cost penalty compared to a single-trip-fueling operation with a reference aircraft.

Consequently, the total cost perspective revealed no larger economic leverage for tankering strategies in the given air traffic network with LH<sub>2</sub> supply costs as low as presented above for 2050. However, this conclusion changes in an early adoption time frame (2035-2040), if no LH<sub>2</sub> import options would be available. In that case, tankering could reduce the energy direct operating costs by 12% on trips with distances below 1,000 NM which would lead to a competitive advantage for H<sub>2</sub>-powered aircraft.



## 5. To inform industry and policy makers, what are the overall arguments for H<sub>2</sub>-powered aircraft compared to other decarbonization options?

The average total direct operating costs for the single-aisle fleets is calculated for H<sub>2</sub>-, and the reference kerosene-powered aircraft based on the flight distribution in the given air traffic network. Furthermore, this holistic evaluation method is also applied to the main other decarbonization option for this larger commercial aircraft segment: synfuels. These have the best net carbon footprint of all sustainable aviation fuels and are also the most scalable such as LH<sub>2</sub>. Therefore, and for comparability, synfuel costs are determined based on the same techno-economic inputs and optimization results for the energy system design as for green LH<sub>2</sub> supply systems. The resulting costs range between 1.25–1.43 USD per kg synfuel at central production hubs like Scotland, Portugal, Saudi Arabia, or Australia in the 2050 base case scenario.

The analysis revealed a potential average cost benefit over all flights of 3% for H<sub>2</sub>- versus synfuel-powered aircraft. The main underlying factor for this is the 24%-lower direct operating costs for energy with LH<sub>2</sub> compared to synfuel supply. In an early adoption phase (2035 base case scenario), the total direct operating cost benefit vs. synfuels even increases from 3% to 11%. In both cases, the energy cost difference outweighs the higher aircraft-related costs for the H<sub>2</sub> version while these do not change for a synfuel- compared to a kerosene-powered aircraft.

In comparison with the latter, the H<sub>2</sub>-powered aircraft fleet could lead to a 1%-decrease in total direct operating costs, if a carbon or climate impact tax of 200 USD/tCO<sub>2</sub> is added to the kerosene fuel costs. Synfuel would still be 2% more expensive given the same carbon tax assumption.

From a resource perspective, the case study emphasized the advantage of using LH<sub>2</sub> versus synfuel as fuel for this aircraft segment. The H<sub>2</sub>-powered aircraft fleet would require 34% less renewable energy per 100 available seat kilometers flown than the synfuel-powered fleet. This is mostly driven by the higher fuel production and delivery efficiency (well-to-tank) which is 56% for all airports with on- and off-site LH<sub>2</sub> supply compared to only 35% for the central off-site synfuel production. Hence, also less renewable energy and electrolysis capacities would need to be installed and capital costs would be 42% lower per MWh of fuel produced when using H<sub>2</sub>-powered single-aisle aircraft.

### Final remarks

Beyond the above results, the consequences of the sector's journey to decarbonize by 2050 are briefly discussed.

Even though the results of this dissertation emphasize the potentially more economic and resource-efficient role of H<sub>2</sub>-powered aircraft in the single-aisle aircraft segment, this comes with a caveat: The LH<sub>2</sub> demand projections (Chapter 4) revealed that a larger fleet penetration of H<sub>2</sub>-powered single-aisle aircraft is only achievable in ambitious scenarios by 2050. The reason for this are the long development cycles and fleet penetration times. As a consequence, other main climate impact mitigations are also required to be implemented as mitigation measures already in the next years.

Sustainable aviation fuels such as synfuels will be needed in most aircraft segments as net-zero CO<sub>2</sub> options – either for the transition period or even as a long-term solution. However, this creates a significant challenge, since the resource efficiency debate might be very central, especially in the next decades. Then, most sectors are likely to demand as many renewable electricity capacities as possible for each sector's decarbonization roadmaps while renewable energy capacity expansions would still be ongoing. So, renewable energy sources would be a

very precious resource. This is why, all further incremental aircraft, operations, and fuel supply efficiency improvements must be targeted to reduce the resource requirements. Moreover, measures such as re-routing to avoid contrails will be needed to reduce the full climate impact of aviation in the mid- and long-term.

Nevertheless, the development of H<sub>2</sub>-powered aviation might lead to positive long-term effects (even beyond 2050) for the socio-/macro-economics of most countries with a strong aviation market/industry. As indicated in [240,241], fossil kerosene and most likely also synfuels are and would be imported from a few exporting countries. This leads to high political dependence on these countries and only minor value creation including employment potential for the importing countries. This could change with more distributed, decentralized, and local LH<sub>2</sub> supply infrastructures – further studies are required to investigate such effects.

Overall, the time is now for starting the development and commercialization of H<sub>2</sub>-powered aircraft that might contribute significantly to a lower climate impact from aviation in 2050 – but also later on, because it must not be neglected that achieving long-term climate goals after 2050 should be equally important due to the projected growth in air travel for the next decades.

## 7.2 Perspectives on methodology

In this section, the relevant research progress achieved by this dissertation for the general academic landscape is highlighted. Thus, limitations are derived here which lead to an outlook in Section 7.3.

### Scientific novelty of this thesis

The novelty of this thesis is not only the holistically evaluated economics and efficiencies of H<sub>2</sub> propulsion and supply for aviation but also six developed methodologies that could be used in future research:

1. **Evaluation of direct operating costs:** In this dissertation, the direct operating cost methodology is adjusted to evaluate not only conventional but also H<sub>2</sub>-powered aircraft which could be applied in future studies. Cost effects caused by the H<sub>2</sub> aircraft development with new propulsion systems and different maintenance aspects as well as different fuel costs are included.
2. **H<sub>2</sub>-powered aircraft design optimization:** While the exact aircraft design methodology is out of scope of the present thesis and handled by the colleagues of the German Aerospace Center (see CRediT's statement in Appendix F), the approach for modeling H<sub>2</sub>-powered aircraft is derived. Furthermore, all relevant insights and data on these aircraft are presented that could be used by others for further analyses.
3. **LH<sub>2</sub> demand modeling for aviation:** A process is presented on forecasting future air traffic demand and translating it to LH<sub>2</sub> demands. For this, adjustable assumptions for the development of H<sub>2</sub>-powered aircraft, e.g., entry-into-service years, are given. This enables researchers to study broader H<sub>2</sub> forecasts or hub-forming approaches including aviation as a potential application for H<sub>2</sub>.
4. **Techno-economic optimization of LH<sub>2</sub> refueling systems:** An optimization approach is presented to minimize the costs of future LH<sub>2</sub> refueling systems at airports. It combines a first-of-its-kind techno-economic data collection with an outlook on the optimization choices to select the most suitable refueling setup for any airport. This methodology is a solid start to be further advanced by other researchers. These could further elaborate, e.g., on the detailed thermodynamic efficiency effects of refueling.

5. **Green LH<sub>2</sub> supply optimization:** This thesis combines a detailed techno-economic assessment of three different green LH<sub>2</sub> supply chains with energy system optimization. To the best of the author's knowledge, it is the first attempt to not only evaluate green LH<sub>2</sub> supply costs end-to-end, but also to reflect the operational dynamics of the required components. Furthermore, a manual on design rules for such systems is derived. The targeted application is aviation, but the methodology and design rules could also be useful for research on other applications requiring LH<sub>2</sub>.
6. **Holistic evaluation of aircraft decarbonization options in realistic case studies:** An approach is shown that can be used to benchmark the economics and resource efficiency of H<sub>2</sub>-powered aircraft compared to other fuel technologies. Based on three steps – optimization of supply costs, aircraft designs, and integration into existing air traffic networks – the direct operating costs and operational strategies are determined. The approach might be used and modified for further investigations with slightly adjusted research scopes (see “outlook” part below).

## Limitations

There are three fields of limitations of the presented analyses and methodologies.

In the first field, the high uncertainties behind the future techno-economics and operational procedures of the investigated supply components are highlighted.

The development of the components' CAPEX, OPEX, and efficiencies for the next decades is highly dependent on the technology development, material costs, and large-scale deployment of H<sub>2</sub> infrastructure. As shown in Chapter 5, the cost results further depend on the renewable energy costs which are largely influenced by the reliability of the weather data taken into account.

Moreover, the analyses evaluate costs but not prices for green LH<sub>2</sub>. Due to the lack of data on the profit margins of relevant energy companies or H<sub>2</sub> component manufacturers, this is not considered in this thesis.

Furthermore, the technological feasibility of economic transportation for LH<sub>2</sub> with efficient loading and unloading processes is still a scientific debate. Inefficiencies along the whole supply chain must be minimized, but the size of the potential and its costs of reducing or reusing the H<sub>2</sub> losses has still not been characterized for most components yet.

Additionally, operational procedures, e.g., for the liquefaction plant or the GH<sub>2</sub> pipeline systems, have only been simulated but actual data from realized plants are not publically available. Thus, most simulation efforts for the liquefaction plant stem from one research consortium of the IDEALHY project [187] with Linde Kryotechnik [186] and SINTEF [201]. Hence, the assumed inefficiencies in operating an H<sub>2</sub> liquefier in part-load (see design options with less LFP utilization in Chapter 5) or even shutting it down for the night (at PV-only locations, Section 5.2) must be further validated.

This field of limitations highlights the clear need for technology demonstration and development for the components/processes that are not developed on a technology readiness level (TRL) 9 or not offered with the required large-scale capacities. Only then, new studies with more realistic techno-economic parameters, price perspectives, and operational procedures can be conducted. Such demonstrations will also support the certification of LH<sub>2</sub> infrastructure systems at airports to ensure safe operations.

The second field centers around the geospatial aspects of green LH<sub>2</sub> supply networks. While the analyses in Chapter 6 consider routing distances for GH<sub>2</sub> and LH<sub>2</sub> transport, the placement of components such as the liquefaction plant is not kept flexible for optimization. This means

that e.g., in a GH<sub>2</sub> off-site setup, the liquefaction plant is only located either at the production or the consumption (airport) site. A central placement in between or causing a detour is not considered, even though it might enable optimized transport costs from that central place to several airports. This would require an optimization approach that ensures computability with detailed techno-economic considerations and geographic information. Most often this would be done using linear models [225]. Then, existing H<sub>2</sub> production and renewable energy plants as well as future H<sub>2</sub> markets could also be reflected. Thus, the transport modes such as rail or inland vessels, which are not in the scope of this thesis, might be modeled, too.

The third field focuses on transition-optimized modeling. The thesis investigates cost benchmarks at a specific point in time/scenarios, e.g., 2035 or 2050. This is a valid approach to comparing the economics of different technologies. However, for the calculation of business cases and investment decisions, the deployment must be evaluated over a longer relevant period of time. This includes the transition years where large investments are required, but the LH<sub>2</sub> demand is ramping up slowly. In that case, computability with non-linear modeling is often not given, and linear models are needed [96]. Nevertheless, the insights from the design rules (Chapter 5) can be used as an informed decision for more realistic linear assumptions.

### 7.3 Outlook

Building on the limitations, this work is concluded with an outlook on future research topics as well as industry and policy recommendations derived from the previously shown methodology and results.

#### Research agenda

Three research fields could be addressed based on this thesis to further increase the scope of investigation or the depth of the techno-economic analyses.

First, a more holistic evaluation of the economics of decarbonizing other aircraft segments with hydrogen should be of interest. For example, the investigation of LH<sub>2</sub> supply chains for smaller airports and operating costs for regional-sized aircraft (i.e. below 100 passengers) would give a perspective of the business cases for regional H<sub>2</sub>-powered aviation before 2035.

Second, the case study approach of Chapter 6 might be used for other relevant regions with their specific techno-economic assumptions or air traffic network characteristics. Since other major air traffic markets, e.g., Northern America or Asia, also cause high climate impacts, evaluating the future of single-aisle H<sub>2</sub>-powered aircraft in that markets would be very relevant for the sector's journey to net zero.

Third, modeling the access to existing renewable electricity markets or even H<sub>2</sub> markets, including also blue hydrogen, might positively influence the resulting LH<sub>2</sub> supply costs. Then, H<sub>2</sub> might be procured from such markets in times of low renewable energy production to avoid over-designing such plants. Next to local H<sub>2</sub> markets, also international trade schemes could be included in the analysis. As an example, an auction-based platform (H2GLOBAL) is currently being discussed to reduce H<sub>2</sub> import costs in Germany [319].

#### Recommendations

This thesis contributes to more informed decision-making for main stakeholders in the aviation sector and their actions for decarbonizing air travel. The main insights and recommendations for seven relevant stakeholders are briefly summarized.

For airlines, it is derived that green LH<sub>2</sub> might be a more economical fuel choice for decarbonizing single-aisle and smaller aircraft compared to synfuels. This holds also in comparison with fossil kerosene if carbon/climate impact taxes are applied. Furthermore, this insight means to aircraft manufacturers that the development of H<sub>2</sub>-powered aircraft might be an interesting business opportunity given the technological and economic feasibility of aircraft manufacturing. Since medium to larger airports could then become hydrogen hubs, LH<sub>2</sub> for aviation and designing supply networks around these airports might be growth markets for energy providers and H<sub>2</sub> component manufacturers. But also airport operators and refueling companies should prepare and acquire relevant knowledge on the topic and design potential business cases that enable LH<sub>2</sub> handling at airports.

For governments, this study derives that clear regulation or incentives are required to get past fossil-fueled aviation, e.g., carbon or climate impact taxes. Also, strategies for import or export roles for each country are needed as soon as possible to secure economic supply already when H<sub>2</sub>-powered aircraft would enter the market.

Research institutions also play an important role in enabling the development of H<sub>2</sub>-powered aviation. As derived above, there is still a lot of research required to go into more details of the LH<sub>2</sub> supply chain designs and economics including the investigation of synergies with other H<sub>2</sub> markets/applications.

For end consumers, the thesis shows that climate-friendlier aviation with H<sub>2</sub> propulsion might be possible in 10–20 years, but that ticket costs compared to today might increase – e.g., by at least 14% on average in the selected flight network.

Overall, this thesis shows that H<sub>2</sub>-powered single-aisle aircraft could be a key option to decarbonize the segment while saving costs and resources compared to a synfuel option. Therefore, clear regulations, cost mechanisms, or incentives are needed now to steer industry action accordingly. Since processes for large-scale deployment of new fuels might take 5–10 years, investment decisions have to be taken by the main stakeholders as soon as possible.

## Appendix

### A Direct Operating Cost modelling

The Direct Operating Cost (DOC) model was taken from Thorbeck [209] and modified to ensure the proper comparison between kerosene- and hydrogen-powered aircraft. The main aspects considered are already described in Eq. 3.1 (Chapter 3). The different DOC shares are laid out in the following. Thus, modifications for measuring DOC for H<sub>2</sub>-powered aircraft are highlighted.

In comparison to DOC, COC (cash operating cost) – DOC without capital expenditures (CAPEX) for aircraft manufacturing – are often used to compare rather conventional technologies or aircraft concepts. However, if more radical changes such as new energy carriers are applied, the capital costs should be included since they have a major influence.

#### DOC energy

The only difference to the method from Thorbeck [209] is that instead of mass specific costs, energy specific costs are implemented. The energy DOC are affected by both the vehicle's performance and the energy specific costs. The interface is the refueling dispenser or fueling adapter. Every losses and efforts before are accounted within the energy price.

#### DOC fees

The strong dependency on maximum take-off mass of air traffic control and airport landing fees is correct for conventional aircraft powered with kerosene since it roughly correlates with the profitability of the vehicle. However, if new energy carriers are applied, this correlation is not given, and new cost structures are likely to be implemented. To cope with this, the same fees are assumed for the kerosene baseline and the H<sub>2</sub> concepts. However, this must be seen carefully since today's "conventional" airport fee structures highly depend on the maximum take-off mass.

#### DOC crew

There is no reason to expect differences in crew DOC from a methodology standpoint. This is why the method from Thorbeck [209] is applied in this work. Since the cruise speed and ground times are assumed to be similar as for conventional kerosene-powered aircraft, there is no effect at crew DOC.

#### DOC maintenance

Due to the absence of literature dealing with aviation-specific LH<sub>2</sub> tank maintenance processes and costs, the same mass related approach for the averaged airframe, including systems, is applied for the LH<sub>2</sub> tanks, see [209]. In other words, the LH<sub>2</sub> tank and fuel system have the same maintenance expenditures per mass as the rest of the airframe.

The combustion of H<sub>2</sub> instead of kerosene also causes different engine maintenance costs especially because of changing turbine inlet temperatures. Since these changes are considered as rather small and due to the lack of literature, the same approach is applied.

## DOC CAPEX

As shown in Eq. A1, CAPEX consist of the depreciation (annuity factor  $a$ ) and the insurance ( $f_{ins}$ ) of the aircraft's delivery price ( $p_{AC}$ ) which again assembles of Recurring Costs (RC) and Non-Recurring Costs (NRC) multiplied by the miscellaneous factor ( $f_{misc}$ ) which includes additional costs such as spare parts, see Eq. A2. In addition, an absolute Profit Margin ( $PM_{AC,absolute}$ ) is added – instead of a relative calculated profit margin, which penalizes more expensive aircraft.

$$DOC_{CAPEX} = p_{AC} \cdot (a + f_{ins}) \quad (A1)$$

$$p_{AC} = \left( RC + \frac{NRC}{n_{AC}} \right) \cdot (1 + f_{misc}) + PM_{AC,absolute} \quad (A2)$$

$$RC_{kerosene} = \sum C_i + C_{load\&handling} + C_{finalAssembly\&delivery} + n_{engine} \cdot p_{engine} \quad (A3)$$

The share of the NRC per aircraft produced ( $n_{AC}$ ) which mainly consists of development, flight testing and prototype expenditures, is rather small for successful commercial aircraft families. The RC, shown in Eq. A3, represent the major part of the aircraft price and consist of the production related costs. They are calculated by applying the RC method from Beltramo et al. [320]. It consists of the sum of each individual component and system costs ( $C_i$ ) as well as additional terms for loading and handling ( $C_{load\&handling}$ ) and final assembly ( $C_{finalAssembly\&delivery}$ ). The equations for each component can be found in [320]. Since the engine is a purchased part, the price per engine ( $p_{engine}$ ) is added and multiplied by the number of engines ( $n_{engine}$ ). This approach allows an aircraft component wise evaluation and is especially important for the manufacturer's competitiveness.

Even if there are many unknowns in estimating the aircraft delivery price, which often strongly differs from list prices, the described approach provides much more realistic capital cost sensitivities than the operating empty mass (OEM) related approach, described in [209,321]. If more radical changes in propulsion technology or energy carrier are compared with conventional aircraft, the described approach is mandatory.

$$RC_{LH2} = RC_{kerosene} + n_{LH2tank} \cdot p_{LH2tank} \quad (A4)$$

$$\text{with } p_{LH2tank} = E_{stored,max} \cdot k_{LH2tank} \quad (A5)$$

For the LH2 application, the RCs described in Eq. A3 are extended by the LH<sub>2</sub> tank price ( $p_{LH2tank}$ ) multiplied by the number of tanks ( $n_{LH2tank}$ ), see Eq. A4. It is approximated by the maximum energy stored in the tank ( $E_{stored,max}$ ) multiplied by the factor  $k_{LH2tank}$  in USD per kWh LH<sub>2</sub>, see Eq. A5. An averaged factor of  $k_{LH2tank} = 650$  USD/kWh<sub>LH2</sub> from [322] is used. Differences between the kerosene and the hydrogen concepts in terms of additional non-recurring factors like development expenditures are not considered.

## DOC related uncertainties

If the costs for fuel are excluded, key uncertainties for the economic evaluation of H<sub>2</sub>-powered aircraft arise from the main assumptions around the LH<sub>2</sub> tank in two ways. First, aircraft CAPEX and maintenance costs depend on different cost assumption for the LH<sub>2</sub> tank. Considering the most conservative and optimistic tank CAPEX factors from [322], the uncertainty in total CAPEX are  $\pm 6\%$  for the single-aisle concept. Based on the total DOC, this results in a variation of around  $\pm 1\%$ . However, if the LH<sub>2</sub> tanks need to be removed and replaced during the lifespan

of the aircraft due to cycle limitations, much higher costs arise. The uncertainties for the maintenance costs cannot be properly predicted yet due to the missing research in this field.

Second, the LH<sub>2</sub> tank mass also influences the performance of the single-aisle H<sub>2</sub> aircraft. By varying the LH<sub>2</sub> tank mass assumptions between very optimistic and pessimistic scenarios, the design block energy consumption increases between increases by 5% in a best and 25% in a worst case compared to the kerosene baseline. This indicates the importance of detailed aviation-specific LH<sub>2</sub> tank research.



## B Aircraft design methodology

The aircraft design has been conducted with a multidisciplinary sizing loop build in RCE (Remote Component Environment) [323] including the conceptual design tool openAD [324]. Additionally, higher fidelity methods comprising aerodynamics, engine performance, mission performance as well as liquid hydrogen (LH<sub>2</sub>) tank thermodynamics and structural sizing are implemented. To assure a seamless communication within the sizing process, the data scheme CPACS [325] is applied.

The single-aisle design is based on a recalculated Airbus A320neo. This aircraft has been projected to the Entry-Into-Service year 2035 by applying new conventional technologies such as Carbon Fiber Reinforced Polymer (CFRP) wing and new high-bypass ratio geared turbofan engines. Furthermore, the cabin layouts are applied for the design case and the cost evaluation case. The single-aisle concept is equipped with a 180 PAX single class standard layout with a seat pitch of 28/29 inch which is described in [326].

For H<sub>2</sub>-powered aircraft, the propulsion system can be either fuel cell systems paired with electric motors creating thrust through fans or propellers, direct hydrogen combustion in a combustion engine or turbine, or a hybrid system of both fuel cells and H<sub>2</sub> combustion [42].

In general, it can be stated that the lower the power class of the air-vehicle, the higher the potentials for fuel-cell propulsion since the core efficiency of gas turbines highly depend on the overall maximum power rating whereas fuel-cells hardly show sensitivities to scaling. However, the contrary behavior of efficiency versus throttle settings offers new hybrid potentials: Whereas high throttle settings result in high efficiencies and vice versa for gas turbines, the opposite is true for fuel cells [327].

The LH<sub>2</sub> tank sizing is conducted with conceptual tank structural and thermodynamic design methodologies [49,328].

Characteristic mid. cruise parameters as well as total LH<sub>2</sub> tank volumes and gravimetric indexes are listed in Table B1. The gravimetric index is defined as LH<sub>2</sub> mass divided by total tank structural and maximum LH<sub>2</sub> mass, including the fuel delivery and subsystems mass.

**Table B1:** Hydrogen aircraft specifications – Performance characteristics

Parameter	Unit	Single-aisle (1,500 NM)
Lift to Drag (mid. cruise)	-	17.5
TSFC (mid. cruise)	kg/s/N	4.90e-06
Total propulsion efficiency (mid. cruise)	-	39.2%
Total LH <sub>2</sub> tank volume	m <sup>3</sup>	59
LH <sub>2</sub> tank gravimetric index	-	42%

## C LH<sub>2</sub> demand projections

In this part, the approach, sources and assumptions for projecting LH<sub>2</sub> demands for aircraft propulsion at airports in 2050 are explained. All calculations and detailed results can be found in the supplementary material.

Four steps are taken to derive the LH<sub>2</sub> demand scenarios for four different aircraft size segments presented in Chapter 4:

The kerosene demand for aircraft propulsion is calculated for the reference year 2019 at three exemplary airports. These airports are meant to be archetypes for intercontinental hubs, major national and smaller national airports.

Based on the results, traffic growth projections reflecting the impact of the COVID health crisis are used to determine potential fuel demands at these airports from 2019 to 2050.

The development of aircraft fleet from 2019 to 2050 is projected in a next step. This enables the calculation of the share H<sub>2</sub>-powered aircraft might have of all flights at the selected airports in 2050. Two different introduction scenarios for the introduction of H<sub>2</sub>-powered aircraft are used to reflect more and less progressive assumptions.

Finally, LH<sub>2</sub> demand projections at these airports are calculated based on the kerosene forecast, the share of H<sub>2</sub>-powered aircraft in each aircraft category and energy conversion factors.

The underlying methodology and assumptions are detailed out in the following.

### Kerosene baseline 2019

In this step, historic air traffic data is used to derive the kerosene demand at three selected airports that represent intercontinental hubs, major national and smaller national airport archetypes. As reference year 2019 is selected to have an undistorted view of traffic data without any influences of the COVID health crisis.

The German Airports Association (ADV) publishes monthly and annual air traffic reports including number of passengers and movements at German airports [211]. Since this data is not reported by the defined aircraft segments used in this study but by length of the flights (national, international), these are translated accordingly. Therefore, it is assumed that national flights are flown with regional and single-aisle, international-European flights with single-aisle and medium wide-body and international-non-European flights with medium and large wide-body aircraft. Thus, the assumptions for the relative splits of the aircraft segments in each flight category are derived from company reports such as from Frankfurt Airport [329] and flight profiles from Flightradar24 [308]. These splits can be very specific for the region that is focused on in this work. In countries with very high air traffic demand on short routes (e.g., China) also wide-body aircraft could be used for national, short-range flights [7].

Based on average passenger (PAX) capacities per aircraft segment from [16] and load factors (here load factors reported for flights departing or arriving in Europe are used) from [330] the number of passengers are translated into aircraft departures per each segment.

Then, average flight distances that are assumed to be specific to the size of airport are determined from ICCT average traffic data [7] and reported flight profiles [308].

In a final calculation step, the total flight kilometers flown per aircraft segment are multiplied by reported average kerosene consumption data (kg kerosene per aircraft km) from the European Environment Agency [331] to derive total kerosene demands in 2019 at the selected airports – shown in Chapter 4.

### **Kerosene forecast 2050**

Since the projection of future LH<sub>2</sub> demands in 2050 is targeted in this work, air traffic growth projections are used to calculate a kerosene demand forecast as a reference.

As part of the WeCare project of the German Aerospace Center air traffic growth forecasts were developed [27]. In a recent publication from Grewe et al. [9] these were used to model climate impact from aviation over the next 30 years. Their publication including all relevant data sets is used in this work to forecast air traffic growth in terms of global revenue passenger kilometers (RPK) and the annual improvement of aircraft efficiency over the global fleet. In addition to that, a recent market forecast from the International Air Transport Association (IATA) is incorporated to reflect the different growth perspectives between domestic and international aviation [8]. It is assumed that domestic air traffic growth affects regional and single-aisle aircraft segments and international air traffic growth the wide-body segments. Thus, the IATA report also provides insights on the effects of the COVID health crisis on air traffic demand, which are built into this forecast by assuming no air traffic growth between 2020 to 2023. Compared to an average annual growth rate of air traffic between 2020 to 2050 of 3.7% without the COVID-“shock”, the calculated average growth rate in this work is 3.0% per annum. So, the used air traffic projections for the next 10 to 30 years are 16% lower than a projection without a COVID-“shock”, which might be a more conservative estimation but is in line with a forecast by Embraer [332].

Last, the kerosene demand from 2019 to 2050 is projected for the three different airports taking the kerosene baseline for 2019 and applying the air traffic growth rates and efficiency changes discussed. Results are shown in Table 4.2 and the Supplementary Material of [112].

### **Aircraft fleet forecast and H<sub>2</sub>-powered aircraft scenarios**

Next, a forecast is determined for the selected commercial aircraft fleets from 2019 to 2050 for each aircraft segment. This is required to calculate potential penetration scenarios of H<sub>2</sub>-powered aircraft in relation to the total fleet and new aircraft deliveries.

As a starting point the global existing fleet of active and temporary parked aircraft in the four segments is determined using data available on the open source data base Airfleets.net [333]. The fleet numbers are cross-checked with the Commercial Aircraft Market Analysis from Aviation Week Intelligence Network (AWIN) [334] and used as a reference for 2019.

The development of the commercial aircraft fleet and aircraft deliveries is taken from market forecasts published by Boeing [213], Airbus [335] and Embraer [332]. Since Boeing's and Embraer's market analysis already mention COVID effects, their projected annual fleet growth from 2019 to 2029 and 2039 as well as total aircraft delivery units are used for this modeling. Furthermore, the growth rates were extrapolated to 2050, since no contradictory indicators or forecasts are available for that time period.

To account for less deliveries and more retirements of aircraft due to COVID effects the fleet projection from 2019 to 2024 is adjusted to fit reported market data from AWIN for 2020 and 2021 [334].

In a second part, two different scenarios for the market introduction of H<sub>2</sub>-powered aircraft are derived and the resulting penetration in relation of the total aircraft fleet is calculated. Therefore, assumptions for three main parameters are determined for each aircraft segment: the entry-into-service (EIS) year, the time for full manufacturing ramp-up – when an aircraft manufacturer would be able to fully utilize their production with H<sub>2</sub>-powered aircraft – and the take-rate. The latter describes the quota of H<sub>2</sub> aircraft that are sold to airlines or lessors compared to all aircraft deliveries including non-H<sub>2</sub> aircraft.

As a base case it is assumed that H<sub>2</sub>-powered regional aircraft will be available from 2030 on. Manufacturers would reach full production capacity of regional aircraft by 2034 and 80% of these new delivered aircraft would be equipped with H<sub>2</sub> propulsion. Assumptions for all segments are shown in Table C1. In general, these reflect a scenario which already counts on the introduction of H<sub>2</sub>-powered aircraft and that major technological and economic barriers can be overcome. While regional and single-aisle aircraft would be a viable purchase option for operators, H<sub>2</sub>-powered medium-range aircraft do not play a larger role in the total aircraft fleet by 2050 mainly due to late EIS and long manufacturing ramp-up times. Here, other decarbonized options such as synthetic fuels would be a main option for such aircraft operators in this scenario at least until 2050 as also highlighted by [16,19].

**Table C1:** Assumptions for fleet projection of H<sub>2</sub>-powered aircraft – base case

Aircraft segment	Entry-into-service (EIS) year	Time for full manufacturing ramp-up, in years	Take-rate of H <sub>2</sub> aircraft vs. all aircraft deliveries in segment
Regional (jet and turboprop)	2030	4	80%
Single-aisle	2035	5	67%
Medium wide-body	2040	6	50%
Large wide-body	>2050	n/a	n/a

In a significantly more progressive scenario, called ambitious case, a radical transition to true zero emission aircraft concepts is assumed. This could be caused by regulation limiting emissions and emission-related climate effects or by the introduction of very high emission taxes. Furthermore, this scenario reflects that H<sub>2</sub> propulsion could be the dominant true zero propulsion option for regional and single-aisle aircraft – only commuter aircraft with less than 20 PAX, which are not considered in this study, might be powered by battery-electric propulsion. In such a scenario, a LH<sub>2</sub> supply and refueling infrastructure would be available at all airports and also medium wide-body aircraft would be available for purchase in the late 2030s to early 2040s. All assumptions are summarized in Table C2.

**Table C2:** Assumptions for fleet projection of H<sub>2</sub>-powered aircraft – ambitious case

Aircraft segment	Entry-into-service (EIS) year	Time for full manufacturing ramp-up, in years	Take-rate of H <sub>2</sub> aircraft vs. all aircraft deliveries in segment
Regional (jet and turboprop)	2028	2	100%
Single-aisle	2033	3	100%
Medium wide-body	2038	4	67%
Large wide-body	>2050	n/a	n/a

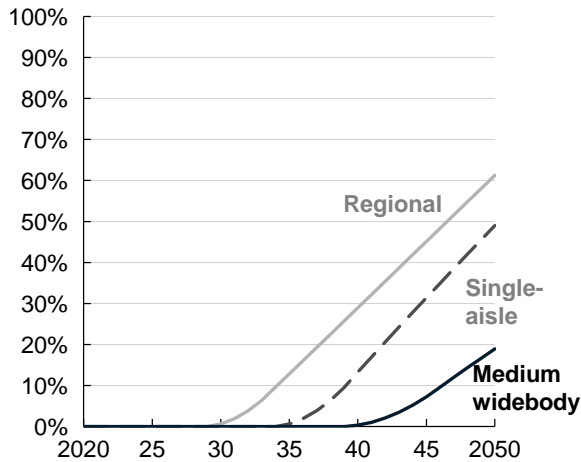
As shown in both tables and explained in Chapter 4, an EIS of a large wide-body aircraft powered by H<sub>2</sub> propulsion is not assumed to happen before 2050.

The resulting H<sub>2</sub> aircraft fleet penetrations are displayed in Figure C1A for the base case and Figure C1B for the ambitious case scenario. These clearly show that the share of H<sub>2</sub> aircraft is relatively low in a base case scenario in 2050. Only in the regional and single-aisle

segments, fleet shares of 50% or more would be achieved. Since larger wide-body aircraft that account for a major share of emissions from commercial aviation would not be powered by H<sub>2</sub> propulsion, H<sub>2</sub> aircraft would be still a “minority” compared to other aircraft at larger airports. This is also in accordance with a statement from Airbus saying that traditional aircraft concepts will be dominating until 2050 [17].

**(A) H<sub>2</sub> aircraft fleet penetration in a base case scenario**

H<sub>2</sub> aircraft %-share of total aircraft fleet



**(B) H<sub>2</sub> aircraft fleet penetration in an ambitious case scenario**

H<sub>2</sub> aircraft %-share of total aircraft fleet

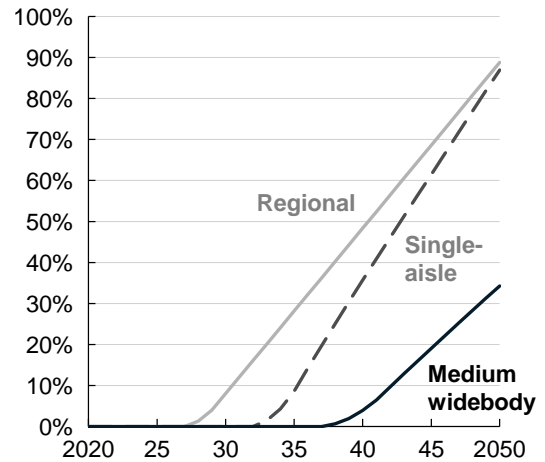


**Figure C1:** Assumption-based H<sub>2</sub> aircraft fleet penetration until 2050 in A) a base case and B) an ambitious case scenario

It is important to highlight that more conservative scenarios with lower adoption rates of H<sub>2</sub> aircraft could also be likely. However, these were not further considered for this energy system design study. Nevertheless, readers could derive their own scenarios with the help of the Supplementary Material of [112] and see resulting LH<sub>2</sub> refueling costs in Chapter 4 where a broad range of LH<sub>2</sub> demands are investigated.

### LH<sub>2</sub> demand projections

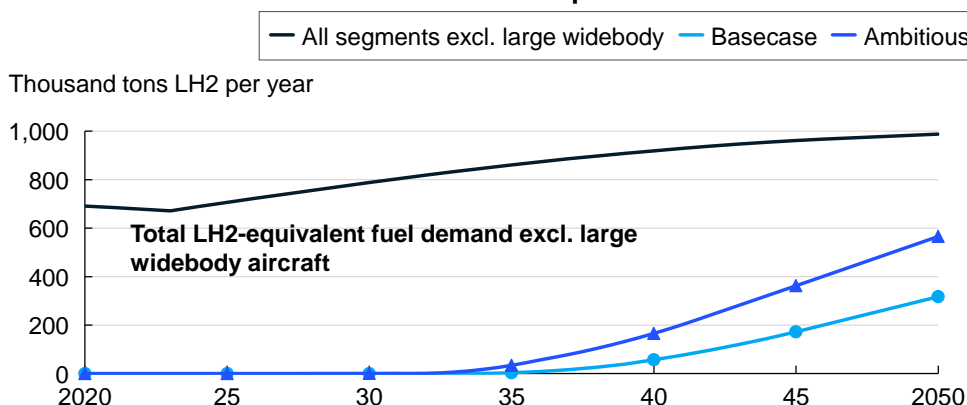
Based on the kerosene demand projections 2019-2050 and the fleet penetration scenarios of H<sub>2</sub>-powered aircraft the resulting LH<sub>2</sub> demands at the selected airports are calculated. Therefore, the equivalent energy demand of H<sub>2</sub>-powered aircraft compared to kerosene powered aircraft is determined for each aircraft segment. Based on relative changes of the specific energy consumptions (SEC) of H<sub>2</sub> aircraft and the different gravimetric energy densities of the fuels (H<sub>2</sub> with 33.3 kWh/kg, kerosene with 12 kWh/kg lower heating values) LH<sub>2</sub> fuel substitution factors are derived, see Table C3. Changes of aircraft efficiencies for single-aisle and medium wide-body aircraft are taken from [52] – for large wide-body aircraft from [16]. Since the regional aircraft segment comprises of jet and turboprop aircraft, a synthesis is taken from [16] with an decrease of SEC for turboprop and from [336] with an increase of SEC for jet variants.

**Table C3:** Efficiency factors for novel H<sub>2</sub>-powered compared to kerosene-powered aircraft used to calculate LH<sub>2</sub> demand scenarios

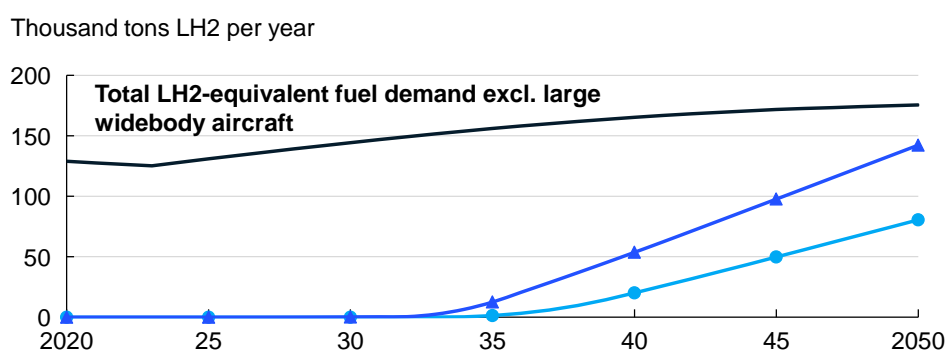
Commercial aircraft category	Relative change of specific energy consumption for H <sub>2</sub> -powered aircraft vs. kerosene reference	Resulting calculation factor for substitution, kg LH <sub>2</sub> per substituted kg kerosene	Sources
Regional (jet and turboprop)	~0%	0.36	Seeckt and Scholz [336] and Clean Sky JU and FCH JU [16]
Single-aisle	+12%	0.40	Hoelzen et al. [52]
Medium wide-body	+18%	0.42	Hoelzen et al. [52]
Large wide-body	+42%	0.51	Clean Sky JU and FCH JU [16]

The resulting LH<sub>2</sub> demands at the three selected airports are shown in Figure C2A-C. Since large wide-body aircraft are not assumed to be powered by H<sub>2</sub> propulsion in 2050, the total LH<sub>2</sub>-equivalent fuel demand at the airports does not consider this segment.

**(A) LH<sub>2</sub> fuel demand scenarios at Frankfurt airport**



**(B) LH<sub>2</sub> fuel demand scenarios at Hamburg airport**



© LH2 fuel demand scenarios at Bremen airport

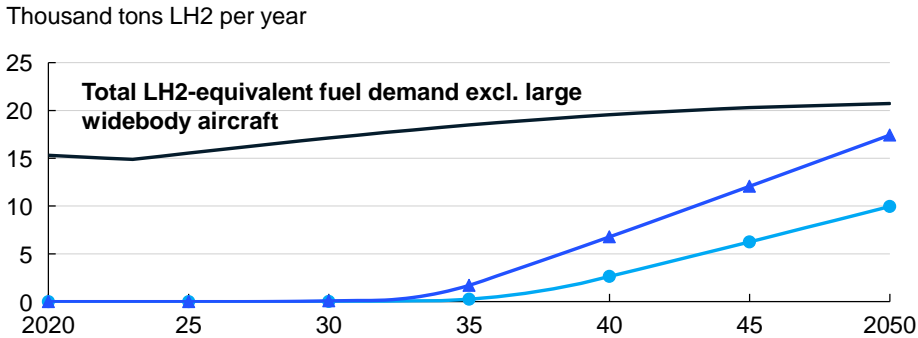


Figure C2: Calculated annual LH<sub>2</sub> fuel demand scenarios at A) Frankfurt airport (FRA), B) Hamburg airport (HAM), C) Bremen airport (BRE)

## D Modeling of LH2 energy systems

### D1 Overview

The modeling appendix is divided into two parts. First, further information is given on the methodology to derive CAPEX and future cost projections. Second, detailed techno-economics are derived for each component group described in Chapter 2 and Section 5.1.

#### D1.1 Direct CAPEX incl. scaling approach and concept of learning rates

The learning rate concept is a standard approach to project future costs in energy technologies and is frequently done in research, e.g., [337–341]. For a 2050 cost forecast, the direct CAPEX for the reference year 2020 are calculated and then translated into 2050-CAPEX based on specific learning rates. It is important to highlight that the learning rate approach does not reflect any inflation or interest rate effects. In Eq. 5.4 (Chapter 5), they are represented by the cost reduction factor  $r_{i,t}$  for each component  $i$ .

#### Reference 2020 direct CAPEX

Direct CAPEX  $C_{\text{CAPEX,direct},i,2020}(x_i)$  are derived in detail for each component in Appendix D2. As a summary, the 2020 direct CAPEX cost functions are based on the following Eq. D1 and D2:

$$C_{\text{CAPEX,direct},i,2020}(x_i) = c_{i,2020}(x_i) * x_i \quad (\text{D1})$$

with 
$$c_{i,2020}(x_i) = f_{a,i} * x_i^{-f_{b,i}} \quad (\text{D2})$$

The specific cost factor  $c_{i,2020}(x_i)$  for each component depends on the scaling factors  $f_{a,i}$  and  $f_{b,i}$ , both shown in Table D1.1 for all relevant components. While this scaling approach is used for most H<sub>2</sub> components, it is assumed that the RES plants and the electrolysis will not scale with larger design capacities. Reasoning is that these components are built modularly and hence, only learning rate effects apply.

**Table D1.1:** Specific direct CAPEX functions in 2020 for selected components from regressions shown in Appendix D2

Component $i$	Cost scaling factor $f_{a,i}$ for $c_{i,2020}$	Cost scaling factor $f_{b,i}$ for $c_{i,2020}$	Cost function defined for $x_i \leq$	Fixed cost value $c_{i,2020}$ for $x_i >$ (see left)
GH <sub>2</sub> compressor	16.3 USD <sub>2020</sub> /W <sub>el</sub>	0.163	16 MW <sub>el</sub> power	1.1 USD <sub>2020</sub> /W <sub>el</sub>
GH <sub>2</sub> salt cavern	3,239 USD <sub>2020</sub> /kg <sub>GH2</sub>	0.355	4,000 t <sub>GH2</sub> stored	15 USD <sub>2020</sub> /kg <sub>GH2</sub>
GH <sub>2</sub> above-ground storage	776.9 USD <sub>2020</sub> /kg <sub>GH2</sub>	0.053	500 t <sub>GH2</sub> stored	385 USD <sub>2020</sub> /kg <sub>GH2</sub>
H <sub>2</sub> liquefaction plant (LFP)	7,389,583 USD <sub>2020</sub> /tpd <sub>LH2</sub>	0.276	500 tpd <sub>LH2</sub>	1,330,000 USD <sub>2020</sub> /tpd <sub>LH2</sub>
LH <sub>2</sub> storage	126 USD <sub>2020</sub> /kg <sub>LH2</sub>	0.125	400tLH2 stored	25 USD <sub>2020</sub> /kg <sub>LH2</sub>



Furthermore, the CAPEX functions do not apply for very large design sizes, but a fixed cost value is used, see Table D1.1. Otherwise, the cost functions would lead to further decrease of costs, which might not be realistic and such large plants might never be realized. The GH<sub>2</sub> compressor size is limited to 16 MW<sub>el</sub> which is a maximum size found in the report of the H2A Delivery Model [197]. Cost effects for salt and rock cavern are kept fixed above 4 Mn kgGH<sub>2</sub> as shown by [156]. For GH<sub>2</sub> aboveground storages, no larger facilities were found in literature. Largest size of a planned LFP is around 300 tpd, so a limit of 500 tpd is chosen. Above that design, it is more likely to see a modularization of LFP plants, since cost savings might be limited and modular plants could allow a more flexible operation. For LH<sub>2</sub> storages, the largest installed projects are at the NASA site with around 300 tLH<sub>2</sub> stored [193].

### Cost reduction factors due to learning rate concept

Projection of CAPEX functions (Eq. 5.4, Chapter 5) for a scenario or future point in time  $t$  are calculated with cost reduction factors, the learning rate  $LR_{i,t}$  and the relevant market sizes  $S_{i,t}$  (see Table D1.2):

$$r_{i,t} = \left( \frac{S_{i,t}}{S_{i,2020}} \right)^{b_{i,t}} \quad (D3)$$

with

$$b_{i,t} = \frac{\log(1 - LR_{i,t})}{\log(2)} \quad (D4)$$

**Table D1.2:** Overview of this study's assumptions for learning rate effects behind all components and underlying sources; mean values of market sizes are calculated based on the values found in indicated studies

Component $i$	Relevant market size today $S_{i,2020}$	Forecasted market size in 2035 $S_{i,2035}$	Forecasted market size in 2050 $S_{i,2050}$	Learning rate until 2035 $LR_{i,2035}$	Learning rate 2035-2050 base $LR_{i,2050}$	Resulting cost reduction in 2035 base vs. 2020 costs (1- $r_{i,2035}$ )	Resulting cost reduction in 2050 base vs. 2020 costs (1- $r_{i,2050}$ )
ELY	0.29 GW ELY cap. installed [258]	230 GW [220,258,260,342]	3,800 GW [220,258,260,342]	12%	10%	71%	81%
GH <sub>2</sub> compressor	90 Mn tGH <sub>2</sub> p. a. [258]	150 Mn tGH <sub>2</sub> p. a. [220,258,260,303,342]	500 Mn tGH <sub>2</sub> p. a. [220,258,260,303,342]	12%	10%	9%	24%
GH <sub>2</sub> AG storage	Same market assumptions as for GH <sub>2</sub> compressor			12%	10%	9%	24%
LFP	0.2 Mn tLH <sub>2</sub> p. a. [304]	2 Mn tLH <sub>2</sub> p. a.	105 Mn tLH <sub>2</sub> p. a.	5%	10%	15%	54%
LH <sub>2</sub> storage	Same market assumptions as for LFP			5%	10%	15%	54%

For the ELY, installed capacities of water electrolysis systems are considered – excluding grey GH<sub>2</sub> production. Learning rates for such systems vary largely [44,142,145,258], here 12% is assumed for the main growth period until 2035 and 10% later on.

GH<sub>2</sub> compressor and GH<sub>2</sub> aboveground storages are already in use today for the current H<sub>2</sub> production capacities and distribution equipment. Consequently, the total H<sub>2</sub> market is taken to calculate cost reduction factors. Since, GH<sub>2</sub> cavern storages are highly individual for each project, no learning rates based on market sizes are used.

For LH<sub>2</sub> components, no specific market reports are found. The market size is derived as follows. In 2015, the global H<sub>2</sub> liquefaction capacity was around 350 tpd capacity [202] with another 250 tpd announced until 2020 [304]. If it is assumed that 600 tpd LFP capacity were operated on 365 days, this results in an annual LH<sub>2</sub> production amount of around 0.2 Mn tLH<sub>2</sub> for 2020. As a next step, H<sub>2</sub> market forecasts are screened for demands that might require LH<sub>2</sub> and not compressed GH<sub>2</sub> in the future. Next to aviation, this could be heavy-duty trucking and the maritime sector. It is assumed that 20% of these applications could be either fueled by LH<sub>2</sub> or the supply to refueling stations would be via the LH<sub>2</sub> route. With an average demand of 10 Mn tH<sub>2</sub> p.a. [258,303,342] the LH<sub>2</sub> share would be 2 Mn tLH<sub>2</sub> in 2035.

In 2050, this study includes further LH<sub>2</sub> demands from H<sub>2</sub>-powered aircraft. An average value of 70 Mn tLH<sub>2</sub> p.a. is taken from two studies [16,128] predicting demand values of 20–130 Mn tLH<sub>2</sub> for H<sub>2</sub> in aviation in 2050. Thus, again 20% of the average market size of H<sub>2</sub>-powered trucks and maritime applications (about 170 Mn tH<sub>2</sub> p.a.) are added – a total resulting LH<sub>2</sub> market size of around 105 Mn tLH<sub>2</sub>.

Since relevant LH<sub>2</sub> markets are not expected to grow significantly before the 2030s, but rather between 2035 and 2050, the learning rates are estimated to be higher for the second period than for the first. Consequently, a learning rate of 5% is assumed for the time period between 2020-2035 and 10% for 2035-2050. Such an approach of different learning rates distinguishing between an early, intermediate and mature market phase is also used in previous studies, e.g., by CSIRO [343].

All resulting cost reduction factors are well in line with other reports like from ANL [263] or the Hydrogen Council [44]. For the 2050 progressive scenario, the CAPEX are further reduced by 25% in all relevant cases compared to the 2050 base case (see Table 2, Section 2.3).

## D1.2 Installation, indirect CAPEX and other economic parameters

Direct CAPEX only consider the equipment costs. However, the supply components need to be installed and the project also includes further costs like for engineering design, project contingencies and owner's costs, e.g., for financing the project. These costs are reflected by the cost factors  $f_{inst,i}$  and  $f_{ind,i}$  for each component, see Table D1.3 and Eq. 5.3 in Chapter 5.

Several literature sources are found on installation and indirect CAPEX cost factors. In most cases, installation CAPEX factors vary between 1.1–1.3 [253,259,262,277,344]. In this study, factor 1.2 is taken for all GH<sub>2</sub> and 1.3 for more (thermodynamically) complex LH<sub>2</sub> components. The RES, ES and LFP CAPEX functions already describe total CAPEX.

Indirect CAPEX factor assumptions mostly range from 1.2–1.3 for different applications [253,259,262]. Consequently, an average value of 1.25 is chosen for all components.

On the availability factor, only a limited amount of sources is available. In general, it is assumed that storage components have a slightly higher availability than conversion components. Latter often require shorter maintenance intervals. An availability factor of 98% for conversion components is taken in [259] for the ELY, in [197] also for the LFP and in [345] for the

RES components. Hence, the availability of storages is assumed to be around 99% which is in accordance with [259].

**Table D1.3:** Further economic assumptions for selected supply chain component – parameters not changing over considered time periods

Component $i$	Installation CAPEX factor $f_{inst,i}$	Indirect CAPEX factor $f_{ind,i}$ (incl. engineering & design, project contingency etc.)	Availability rate $f_{avail,i}$
Electrolysis system	1.2	1.25	98%
GH <sub>2</sub> compressor	1.2	1.25	98%
GH <sub>2</sub> cavern storage	Already included in CAPEX function	1.25	99%
GH <sub>2</sub> aboveground storage	1.2	1.25	99%
H <sub>2</sub> liquefaction plant (LFP)	Already included in CAPEX function		98%
LH <sub>2</sub> storage & cryopumps	1.3	1.25	99% for storage and 98% for cryopumps

## D2 Component specific assumptions and models

In this part, all relevant techno-economic parameters and models are derived along the three energy balances of electricity, GH<sub>2</sub> and LH<sub>2</sub>. All techno-economic parameters that are not explicitly discussed in the following are shown in Section 5.1.3 Table 5.2.

### D2.1 Renewable energy supply, transmission and electric energy storage

Renewable electricity is generated via utility/large-scale PV, onshore and offshore wind parks. For all three options, an availability curve for a specific location is generated with data from the open-source platform “Renewable.ninjas” [294,295]. Furthermore, AC electricity transmission is assumed for the short distances between best locations for the RES and the H<sub>2</sub> energy system. Thus, an ES can increase flexibility of operating electricity sourced components.

#### Photovoltaics (PV)

In this study, one-axis azimuth tracking PV systems with 5% system losses are used, since they offer the best cost to output value at the chosen locations. While the azimuth value is fixed at 180 degrees, the tilt value differs for each site. Coordinates for the weather data profiles (solar yield) are shown in Table D2.1.

#### Wind on- and offshore

In general, land use of wind turbines is a limiting factor for new installations [346]. Therefore, a trade-off between larger power ratings of the turbines and its performance must be made for wind onshore plants. Hence, a 7 MW turbine is selected as suggested in [249] for the 2050 technology projection (today the average is around 4 MW). This turbine is characterized by a 150 m hub height, 200 m rotor diameter and a resulting specific power around 225 W/m<sup>2</sup> are selected in accordance with [245,249,298].

**Table D2.1:** Coordinates for weather data sourcing via open-source tool “Renewable.ninja” [294,295]

Location	Coordinates for solar yield data	Coordinates for wind speed data
PV	28.1759, 36.0174	-
Wind onshore (WON)	-	57.4890, -2.2560
Wind offshore (WOFF)	-	55.9211, 7.5256
Great hybrid (HYB)	27.9459, -10.4636	28.3574, -11.2906
Weak hybrid (WEAK)	50.2205, 8.7154	50.2205, 8.7154

For offshore wind parks, the IEA/NREL reference offshore turbine for 2050 is taken [296], which has a power rating of 15 MW with a 150 m hub height, 240 m rotor diameter and a specific power of 330 W/m<sup>2</sup>.

The locations for the wind power plants are also shown in Table D2.1. Scotland is chosen for WON due to its great potential and space availabilities compared to other countries like Denmark and Germany (<5–10 GW). For offshore wind parks there is still great potential at many sites, here, a space in the Northern Sea is selected [292,293].

The LH<sub>2</sub> energy systems considered in this study require the installation of several wind turbines already for very small annual LH<sub>2</sub> demands. Previous studies highlight that forming such wind parks at sites with limited availability of space can cause significant aerodynamic losses for all wind turbines (on average) in that park. Such array losses are highly dependent on several park parameters (number, placing, height or rotor diameters of turbines) and the specific geography that is investigated [347]. In this study, an representative average energy loss for on- and offshore wind parks of 10% is chosen for all sites, a mean value based on [348–355].

### Electricity transmission

Since space availability for RES is not always directly at the airport or not both PV and wind sites are directly co-located, electricity transmission over 50 to 100 km is assumed on average.

On short distances, high voltage AC (HVAC) transmission is less expensive than HVDC due to costly converter stations [356–359]. Based on values from [358] and [359] costs for HVAC cables are 0.3 USD/kW/km which is also in line with [360,361]. Furthermore, substations incl. transformers are needed which cost 7.8 USD/kW [358]. This results in total transmission costs of 30 USD/kW for 75 km distances. Since this technology is state-of-the-art, no cost differences are assumed for the different techno-economic scenarios.

For the depreciation period, a lifetime of 40 years is assumed with 100% availability [358,362]. Electricity losses for the 75 km due to the cables and the substations are 2.5% [358,363].

### Electric energy storages

There are several electric energy storage technologies available. Here, a Lithium-Ion based grid storage with a 4-hours-durability is chosen. It is modelled via an energy balance. The efficiency is assumed to be 95% for charging and discharging (~90% total efficiency) [111,244].

## D2.2 Gaseous hydrogen equipment

Techno-economics of the ELY, compressors and GH<sub>2</sub> storages are explained in this section.

## Electrolysis systems

Several water electrolysis technologies are available, but only two low-temperature ELY are currently discussed for H<sub>2</sub> generation in combination with RES and without making use of any heat sources: polymer electrolyte membrane (PEMEL) and alkaline electrolysis (AEL). Long-term projections of both technologies' performances are quite similar, which is why generic techno-economic assumptions are derived in the following.

In Figure D2.1, the system efficiency of low-temperature water electrolysis and the relative GH<sub>2</sub> mass output are shown for rated power and part-load operations. The system describes the electrolysis stacks, cooling, purification, drying and control, but not compression of GH<sub>2</sub>. The curve characteristics are derived based on a realized Siemens PEMEL (excluding compressors) [364]. The absolute energy consumption for the stack and system energy consumption (around 50 kWh/kgH<sub>2</sub> at rated power) are in line with values found in several sources [144,148,155,220,256,259,260,365]. The chosen consumption also represents the degradation of the stacks leading to 3-5% less performance on average over the whole ELY lifetime [143]. More progressive assumptions (green graph) leading to a system energy consumption of 45 kWh/kg are based on values from [145,258,262].

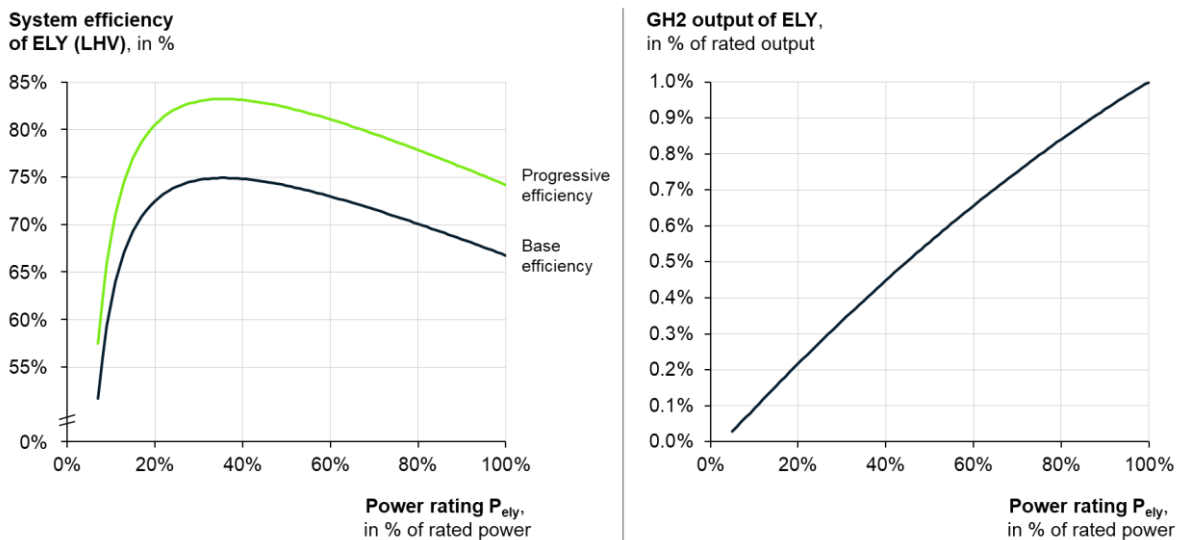


**Figure D2.1:** Electric energy efficiency of chosen electrolysis system in dependence of the relative system power rating – left: system efficiency (LHV) with base efficiency of 50 kWh/kgH<sub>2</sub> on a system level for 2035 base, 2050 base case scenarios and progressive efficiency of 45 kWh/kgH<sub>2</sub> for 2050 progressive case scenario; right: relative GH<sub>2</sub> mass flow rate in dependence of power setting

The default pressure output behind the electrolysis stacks and before a potentially installed ELY-compressor is 30 bar. The freshwater consumption of 13 liters per kg H<sub>2</sub> generated is taken from [111,366].

Regarding the economics of the ELY, CAPEX scaling factors are limited, if plant sizes are larger than 5–10 MW [145–147,220,256,258]. Hence, fixed direct CAPEX are considered – 1,000 USD/kW<sub>el</sub> in the reference year (2020). Based on the learning rates, these decrease to 292, 190 and 143 USD/kW<sub>el</sub> in the 2035 base, 2050 base and 2050 progressive cases, respectively.

The operating cost factor  $c_{OM,ELY,t}$  (Eq.5.6) for the ELY is calculated based on a fixed operations & maintenance (OM) factor  $c_{OM,ELY,fixe,d,t}$  and a lifetime depending OM factor  $c_{OM,ELY,stack,t}$ , see Eq. D5. The latter accounts for replacement costs of ELY stacks, when their end of lifetime is reached. Therefore, the cost factor for replacing the stacks  $c_{ELY,stack}$  depends

on the total CAPEX, the operating hours in the specific year of investigation  $t_{\text{on}}$  and lifetime of the ELY stacks  $t_{\text{ELY,stack,life}}$  (Eq. D6):

$$c_{\text{OM,ELY},t} = c_{\text{OM,ELY,fixed},t} + c_{\text{OM,ELY,stack},t} \quad (\text{D5})$$

$$\text{with} \quad c_{\text{OM,ELY,stack},t} = c_{\text{ELY,stack}} * \frac{t_{\text{on}}}{t_{\text{ELY,stack,life}}} \quad (\text{D6})$$

Main parameters are shown in Table 5.2 (Chapter 5).

### Gaseous hydrogen compressors

Compressors are installed as part of the electrolysis system to increase the pressure of the  $\text{GH}_2$  mass flow and as part of the  $\text{GH}_2$  storages or the  $\text{GH}_2$  pipeline for loading them at the right input pressure. For larger mass flows, which are required in this study, reciprocating compressors are often used. The required electric power rating of the compressor  $P_{\text{GH}_2\text{comp}}$  is calculated as shown in Eq. D7 and D8:

$$P_{\text{GH}_2\text{comp}} = \frac{1}{\eta} \cdot \frac{\kappa}{\kappa - 1} \cdot \frac{R \cdot Z_{\text{H}_2} \cdot T_{\text{in}}}{n_{\text{H}_2}} \cdot \left( \left( \frac{p_{\text{out}}}{p_{\text{in}}} \right)^{\left(1 - \frac{1}{\kappa}\right)} - 1 \right) \cdot \dot{m}_{\text{GH}_2\text{comp,in}} \quad (\text{D7})$$

$$\text{with} \quad \eta = \eta_{\text{isen}} \cdot \eta_{\text{ele}} \cdot \eta_{\text{motor}} \quad (\text{D8})$$

Inputs are the universal gas constant  $R$  (8.314 J/(mol\*K)) and the temperature of the  $\text{GH}_2$  feed  $T_{\text{in}}$  which is assumed to be equal to an average ambient temperature of 288.15 K. Multi-stage compressors and cooling of these compressors stages should lead to constant temperatures for  $\text{GH}_2$  compression. The compressibility factor  $Z_{\text{H}_2}$  (1.0059) is relatively constant in a  $\text{GH}_2$  pressure range of 30-200 bar [170]. Further constants are  $\kappa$  (1.4), the molar mass of  $\text{H}_2$   $n_{\text{H}_2}$  (2.01588 g/mol), the isentropic efficiency  $\eta_{\text{isen}}$  (85%) [197,266], the electric efficiency  $\eta_{\text{ele}}$  (95%) [197] and the motor efficiency  $\eta_{\text{motor}}$  (91%) [197].

The input pressure  $p_{\text{in}}$  for the incoming  $\text{GH}_2$  feed is an optimization variable. The resulting output pressure  $p_{\text{out}}$  behind the compressor is given by the operating pressure of the storages or the pipeline.

Furthermore,  $\text{H}_2$  losses occur at every compressor station with 0.5% per kg $\text{GH}_2$  feed [106,111], which is reduced to 0.4% in the 2050 progressive scenario [152].

Direct CAPEX are derived from sources that focus on lower-pressure compressors (120-200 bar target pressures), shown in Figure D2.2.

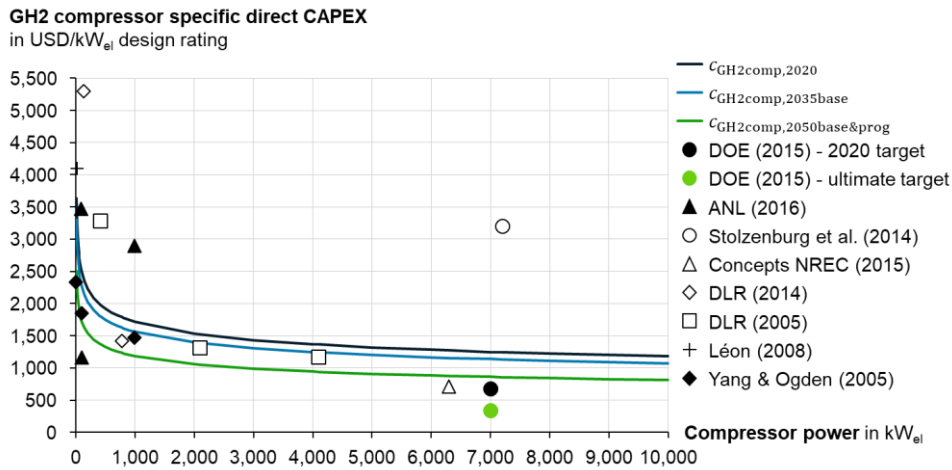


**Figure D2.2:** Direct CAPEX functions for GH<sub>2</sub> compressor systems based on DOE [152], Argonne National Laboratory [263], Stolzenburg et al. [257], Concepts NREC report [154], DLR [264,275], Léon [265], Yang & Ogden [266]

### Gaseous hydrogen storage

GH<sub>2</sub> is stored in underground caverns or aboveground pressure tanks that store H<sub>2</sub> at maximum pressures of 180 bar and 200 bar, respectively. For both, only H<sub>2</sub> losses are computed for the compressors when filling the storages ( $\dot{m}_{GH_2Sto,in}$ ) – no losses are assumed for storing GH<sub>2</sub> or unloading ( $\dot{m}_{GH_2Sto,out}$ ). A constant throttle valve is used for unloading at the minimum allowable storage pressure. This minimum pressure is equal to the pressure on the GH<sub>2</sub> balance which is an optimization variable (Section 5.1.2). The stored mass  $m_{GH_2Sto}$  is computed as follows (Eq. D9):

$$\frac{d}{dt} m_{GH_2Sto} = \dot{m}_{GH_2Sto,in} - \dot{m}_{GH_2Sto,out} \quad (D9)$$

Furthermore, maximum loading and unloading mass flows constraint the operation of the storages. While this is of minor importance for the aboveground tanks (several hours for full loading/unloading assumed), the mass flow into/out of the underground storage is limited to a maximum pressure change of 10 bar per day inside the cavern [155,257,367]. This equals a change of around 8% of the total mass in the storage per day. Reason for this constraint is the thermo-mechanical stress in the geological formation when loading/unloading, which has to be limited for stable operation and long lifetimes.

CAPEX functions for the storage systems (excl. compressors) are shown in Figures D2.3-4.

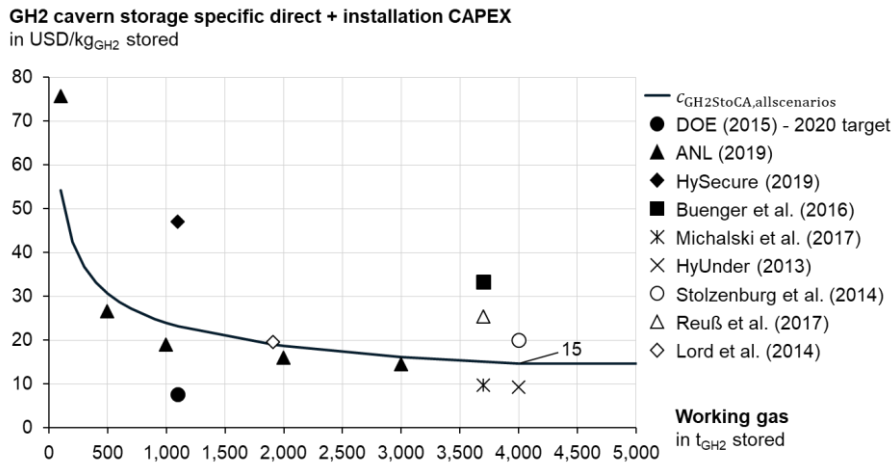


**Figure D2.3:** Direct and installation CAPEX functions for GH<sub>2</sub> cavern systems based on DOE [152], Argonne National Laboratory [263], HySecure project [273], Buenger et al. [155], Michalski et al. [160], HyUnder project [274], Stolzenburg et al. [257], Reuß et al. [106] and Lord et al. [157]

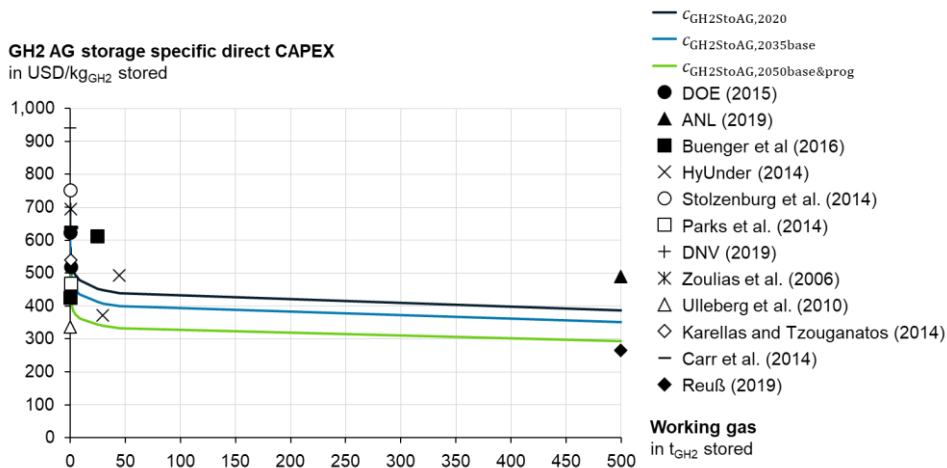


**Figure D2.4:** Direct CAPEX functions for GH<sub>2</sub> aboveground systems based on DOE [152], Argonne National Laboratory [263], Buenger et al. [155], HyUnder project [274], Stolzenburg et al. [257], Parks et al. [277], DNV [278], Zoulias et al. [279], Ulleberg et al. [268], Karellas and Tzouganatos [280], Carr et al. [281] and Reuß et al. [106]

## D2.3 Liquid hydrogen equipment

This section describes all stationary LH<sub>2</sub> equipment, the LFP and storage systems.

### Liquefaction plants

In the following, the specific energy consumption (SEC), losses and CAPEX are derived for the LFP.

The SEC depends on the ideal, minimal theoretical, liquefaction work  $w_{LFP,ideal}$  which changes with different conditions of the GH<sub>2</sub> feed and the targeted end state of LH<sub>2</sub> after the liquefaction [181]. When the GH<sub>2</sub> feed is between 1–100 bar at a temperature of 288.15 K (as in [188]) with standard saturation of ortho- to para-H<sub>2</sub> molecules, the ideal work to reach saturated LH<sub>2</sub> is between 2–3 kWh/kgLH<sub>2</sub> plus 0.625 kWh/kgLH<sub>2</sub> for the ortho- to para-H<sub>2</sub>-conversion [368]. This improvement potential also emphasizes why the optimization of the pressure on the GH<sub>2</sub> balance is of interest which feeds into the LFP. The ideal work characteristics are shown in Figure D2.5 using the regression in Eq. D10:



$$w_{\text{LFP,ideal}}(288.15 \text{ K}, p_{\text{GH2bus}}) = 4.0596 \cdot p_{\text{GH2bus}}^{-0.117} \text{ [kWh/kg}_{\text{H}_2}] \quad (\text{D10})$$

A second aspect influencing the LFP's SEC is the process design of the LFP. In this study, a very efficient Claude Cycle process with a mixed refrigerant pre-cooling cycle is selected for larger plants based on [153,369,370]. The SEC of this cycle  $e_{\text{LFP,cycle}}$  is calculated based on its coefficient of performance  $COP$  (0.46) and the ideal liquefaction work [153].

$$e_{\text{LFP,cycle}}(p_{\text{GH2bus}}) = \frac{w_{\text{LFP,ideal}}(p_{\text{GH2bus}})}{COP} \cdot (COP + 0.25 \cdot f_{\text{LFP,HEX}}(p_{\text{GH2bus}}) + 0.29) \quad (\text{D11})$$

The equation describes that the exergy losses for the liquefaction process are proportional to the change of ideal work, but not for the factor of exergy losses in the heat exchangers  $f_{\text{LFP,HEX}}$ . It decreases by 1% for a feed pressure increase from 25 to 75 bar due to smaller HEX volumes – an effect that requires the use of turbo expanders and which is limited to maximum feed pressures of 80 bar [153,174].

$$f_{\text{LFP,HEX}}(p_{\text{GH2bus}}) = 1.005 - 0.0002 \cdot p_{\text{GH2bus}} \quad (\text{D12})$$

**Ideal liquefaction work  $w_{\text{LFP,ideal}}$**   
in kWh/kg<sub>H2</sub> @ 1.3 bar

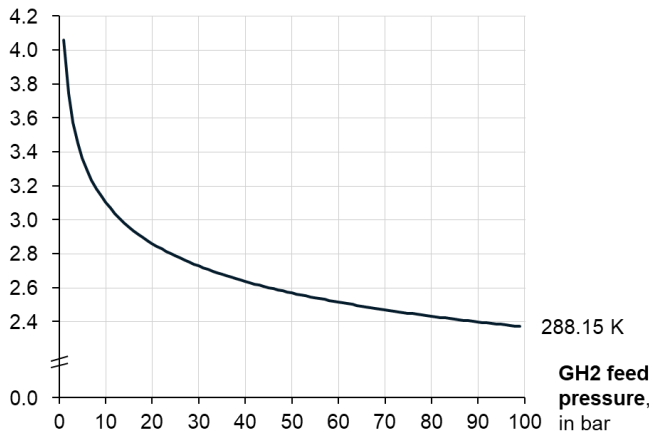


**Figure D2.5:** Ideal work for H<sub>2</sub> liquefaction depending on the pressure of the GH<sub>2</sub> feed, data from [170,371]

The SEC also depends on the size of the plant  $x_{\text{LFP}}$ . Values for  $e_{\text{LFP,size}}(x_{\text{LFP}})$  are derived from a literature overview where all process exergy calculations were adjusted to a GH<sub>2</sub> feed pressure of 30 bar, see Figure D2.6. A regression for smaller plants of 100 tpd capacity and below is shown in Eq. D13, above this threshold a fixed optimized SEC is considered.

$$e_{\text{LFP,size}}(x_{\text{LFP}}) = \begin{cases} -1.85 \cdot \ln(x_{\text{LFP}}) + 15 - 0.41 \text{ kWh/kg}_{\text{H}_2}, & \text{for } x_{\text{LFP}} \leq 100 \text{ tpd} \\ 6.1 \text{ kWh/kg}_{\text{H}_2}, & \text{for } x_{\text{LFP}} > 100 \text{ tpd} \end{cases} \quad (\text{D13})$$

The final rated specific energy consumption at full load operation is calculated with the results from Eq. D11 and Eq. D13:

$$e_{\text{LFP,rated}}(p_{\text{GH2bus}}, x_{\text{LFP}}) = \frac{e_{\text{LFP,cycle}}(p_{\text{GH2bus}})}{e_{\text{LFP,cycle}}(p_{\text{GH2bus,ref}} = 30 \text{ bar})} \cdot e_{\text{LFP,size}}(x_{\text{LFP}}) \quad (\text{D14})$$

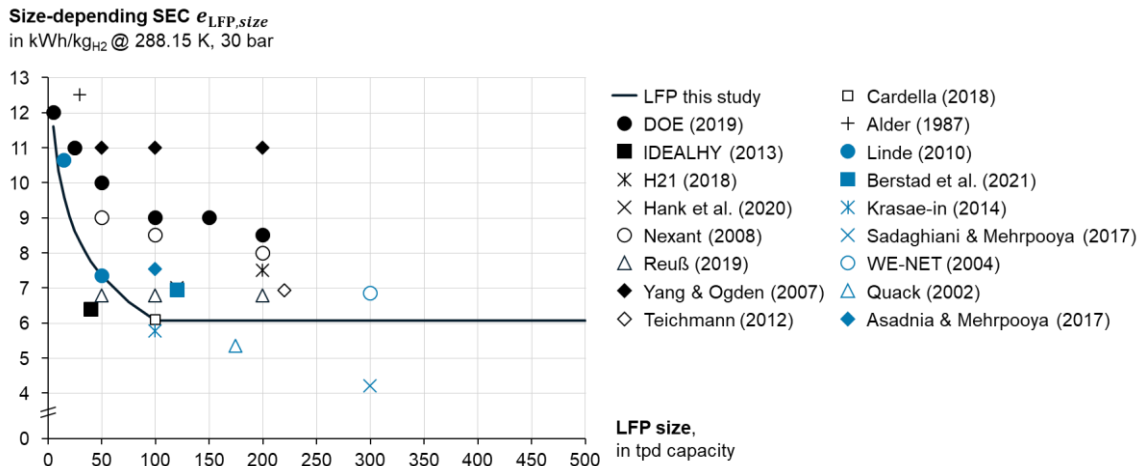


**Figure D2.6:** Size-depending SEC of LFP based on [59,153,270,271,372–376,162,184,187–189,197,198,253]

The last aspect, which is considered for the calculation of the LFP's performance is the change of efficiency when operated in part-load. Even though data on the characteristic for part-load operation is only provided by the IDEALHY project [174] and a slightly different liquefaction process design, it is assumed to be relevant and applicable for the process chosen in this study, too. The increase of SEC for each mass flow setting is shown in Figure D2.7 and described in Eq. D15:

$$e_{LFP,PL}(\dot{m}_{LFP,in}) = 1 + \left( \frac{2641}{\left( \frac{\dot{m}_{LFP,in}}{\dot{m}_{LFP,in,max}} \cdot 100 \right)^{1.154} - 12.84} \right) \cdot 0.01 \quad (D15)$$

Finally, the resulting SEC for the LFP and a given design pressure on the GH<sub>2</sub> balance, the design capacity of the LFP and the current operational point in terms of mass flow is determined:

$$e_{LFP}(p_{GH2bus}, x_{LFP}, \dot{m}_{LFP,in}) = e_{LFP,rated}(p_{GH2bus}, x_{LFP}) \cdot e_{LFP,PL}(\dot{m}_{LFP,in}) \quad (D16)$$

In a next step, losses of the LFP are considered. H<sub>2</sub> losses occur mostly in compression and expansion steps. While literature values indicate a range of 0.5–1.65% losses per kgH<sub>2</sub> feed [153,167,187], these often include losses due to a compression of H<sub>2</sub> from 1 to 30 bar. Since this study excludes this compression step from the LFP (part of the ELY), H<sub>2</sub> losses are assumed to be 1% in the 2035 and 2050 base and 0.5% in the 2050 progressive scenarios. In addition to that, losses of the mixed-refrigerant (MR) occur: 0.5% of MR per kgH<sub>2</sub> feed going through the LFP [153]. Costs for the MR are taken from [153,377] with 0.50 USD/kgMR. Seal gas losses are very small and already part of the fixed OM costs.

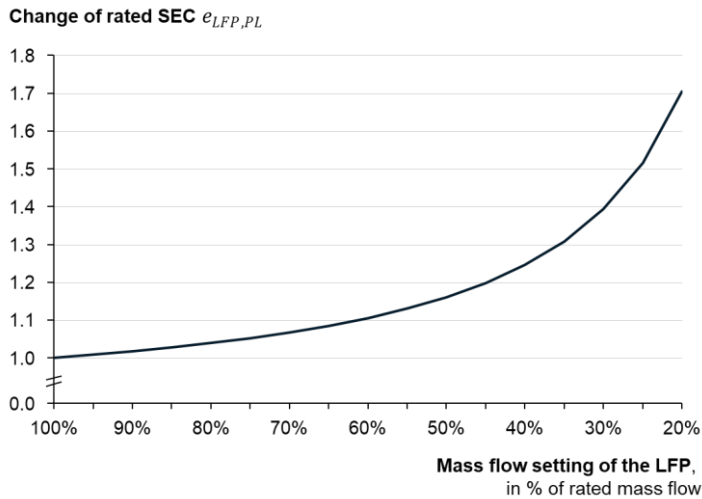


Figure D2.7: Factor for SEC change in part-load operation depending on the LFP’s mass flow setting from [174]

The specific total CAPEX  $c_{CAPEX,total,LFP,t}$  of the LFP are shown in Figure D2.8. In contrary to the CAPEX functions of other components, one additional effect has to be reflected for the LFP. The increase of the GH<sub>2</sub> feed pressure comes at a cost for more robust heat exchangers. In terms of the total CAPEX  $C_{CAPEX,LFP,i}(x_{LFP}, p_{GH2bus})$ , this causes an increase of 1.5% for a heat exchanger (HEX) in a LFP that is designed for 80 bar vs. a standard 30 bar feed pressure [153,378]. The total CAPEX for the LFP are calculated as follows with the additional cost factor for the HEX pressure adoptions  $f_{LFP,HEX}$ , which is valid for  $30 \text{ bar} \leq p_{GH2bus} \leq 80 \text{ bar}$ :

$$C_{CAPEX,LFP,i}(x_{LFP}, p_{GH2bus}) = r_{LFP,i} \cdot f_{LFP,HEX}(p_{GH2bus}) \cdot C_{CAPEX,total,LFP,2020}(x_{LFP}) \quad (D17)$$

with  $f_{LFP,HEX}(p_{GH2bus}) = 0.0003 \cdot p_{GH2bus} + 0.991 \quad (D18)$

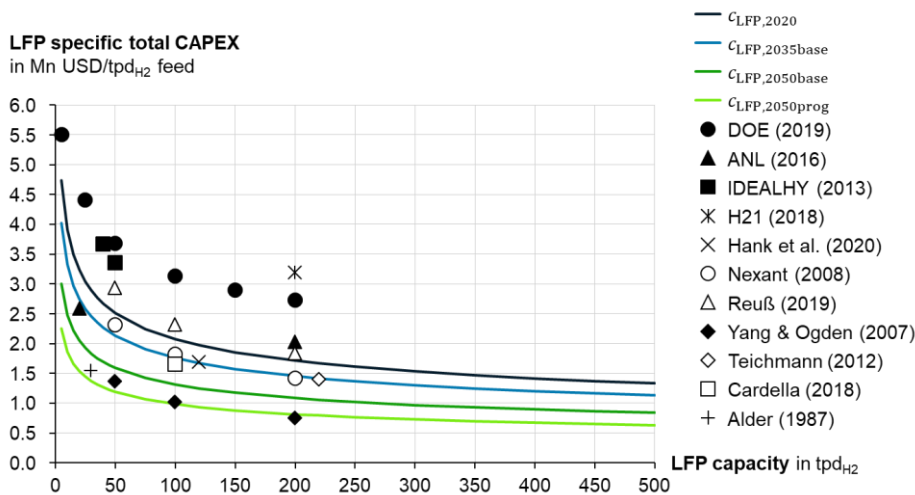


Figure D2.8: Total CAPEX function for LFP depending on the design capacity, values based on DOE [372], ANL [263], IDEALHY project [187], H21 report [253], Hank et al. [270], Nexant report [197], Reuß [198], Yang & Ogden [162], Teichmann [271], Cardella [153], Alder [59]

## Liquid hydrogen storage systems

There are different sizes and applications of LH<sub>2</sub> storages realized today. In this study, spherical shapes are considered. Such tanks come with a slightly higher ullage (not usable mass to ensure stable cryo-temperatures) of 10% compared to around 5% for cylindrical tanks (e.g., on LH<sub>2</sub> trucks) [379]. Even though the storages are double-wall vacuum insulated, boil-off occurs. The boil-off (BO), self-discharging factor  $k_{BO,LH_2Sto}$  can be calculated using this regression in dependence of the storage size (Eq. D19) which is derived from literature values shown in Figure D2.9:

$$k_{BO,LH_2Sto} = 0.014x_{LH_2Sto}^{-0.255} \quad (D19)$$

The total stored mass  $m_{LH_2Sto}$  in the LH<sub>2</sub> storages can be determined with the fill level of the storage  $F_{LH_2Sto}$ , all LH<sub>2</sub> storage mass flows and the maximum capacity of the tank  $m_{LH_2Sto,max}$ :

$$\frac{d}{dt}m_{LH_2Sto} = \dot{m}_{LH_2Sto,in} - \dot{m}_{LH_2Sto,out} - k_{BO,LH_2Sto} \cdot F_{LH_2Sto} \cdot m_{LH_2Sto,max} \quad (D20)$$

The specific direct CAPEX functions for LH<sub>2</sub> storages are shown in Figure D2.10.

For cryopumps, only limited information is available due to few realized products yet [112,115,198]. The pumps are designed based on maximum loading and unloading flow rates required for the LH<sub>2</sub> storages. They have a fixed electric energy consumption of 0.1 kWh/kgLH<sub>2</sub> flow rate and also a constant specific direct CAPEX factor of 256 USD per kg/h capacity in 2020 [106,197,198]. Due to learning effects this is assumed to decrease to 218 and 162 USD per kg/h in 2035 and both 2050 scenarios, respectively.

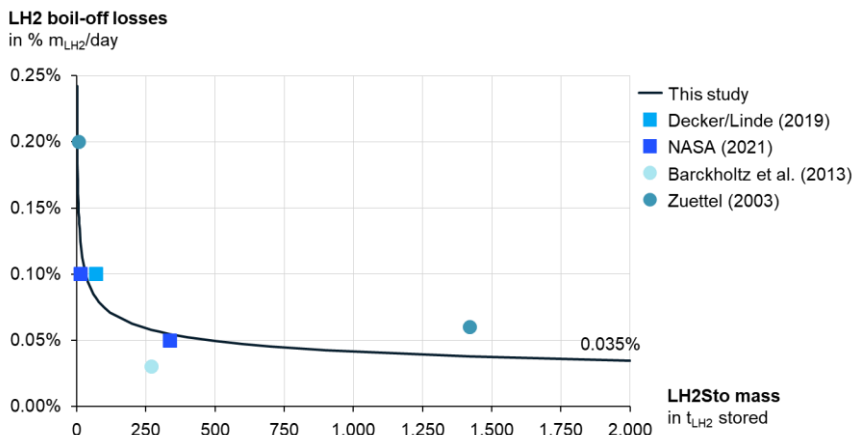


**Figure D2.9:** Boil-off losses for LH<sub>2</sub> storages depending on storage size, values from Decker [379], NASA [193], Barckholtz et al. [380] and Zuettel [381]

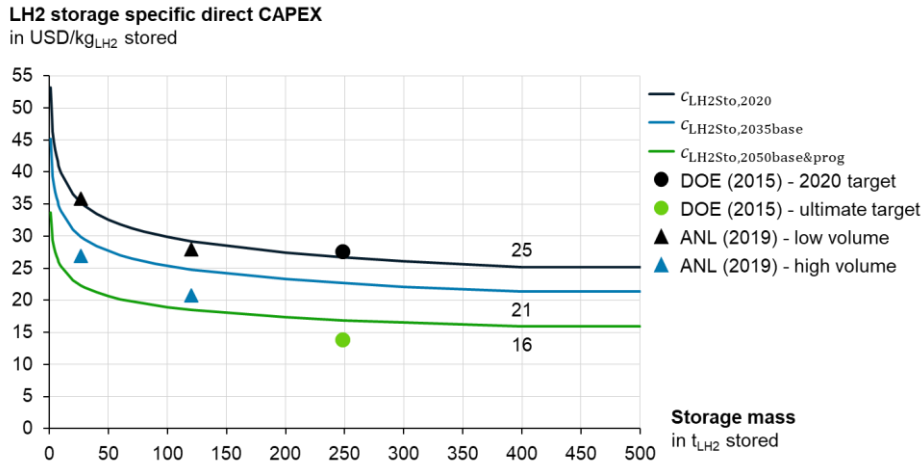


**Figure D2.10:** Direct CAPEX function for LH<sub>2</sub> storages (excl. cryopumps) based on DOE [152] and ANL [156]

## D2.4 Hydrogen transport equipment

GH<sub>2</sub> pipelines and LH<sub>2</sub> vessels in combination with LH<sub>2</sub> trucks are the main H<sub>2</sub> transport modes in scope of this study. All relevant techno-economics are derived in this section.

### GH<sub>2</sub> transport via pipelines

The GH<sub>2</sub> pipelines can be new built or retrofitted based on decommissioned natural gas pipelines. A pipeline system consists of many components – however, CAPEX are mainly caused by the pipes and the compressor stations. The number of compressor stations required for a given pipeline system is determined based on several design parameters like the mean flow speed through the pipeline  $\dot{v}_{pipe,m}$ .

The pipeline input pressure  $p_{pipe,1}$  is set to 70 bar and the final output pressure  $p_{pipe,2}$  to 30 bar, which is in line for the design of medium to larger transmission pipelines [163,164].

In a first step, the required diameter of the pipes has to be calculated with the cross-sectional area of the pipe  $A_{pipe}$ , the maximum flow rate  $\dot{m}_{pipe,in,max}$ , the mean density of H<sub>2</sub> in the pipes  $\rho_m$  and the mean flow speed (Eq. D21). The maximum flow rate is sized according to the maximum intake capacity of the LFP  $\dot{m}_{LFP,in,max}$ , while the mean flow speed must be at least 10 m/s and must not exceed 20 m/s. Further inputs for computation of the mean density is a regression from [170] in Eq. D22 and the mean pressure in the pipeline  $p_m$  (Eq. D23):

$$D_{pipe} = 2 \cdot \sqrt{\frac{A_{pipe}}{\pi}} = 2 \cdot \sqrt{\frac{\dot{m}_{pipe,in,max}}{\pi \cdot \rho_m \cdot \dot{v}_{pipe,m}}} \quad (D21)$$

with 
$$\rho_m(p_m) = -5 \cdot 10^{-5} \cdot p_m^2 + 0.0841 \cdot p_m + 0.0007 \quad (D22)$$

with 
$$p_m = \frac{2}{3} \cdot \frac{p_{pipe,1}^3 - p_{pipe,2}^3}{p_{pipe,1}^2 - p_{pipe,2}^2} \quad (D23)$$

In a second step, the maximum length between two compressor stations  $L_{\text{GH}_2\text{pipe,comp}}$  is derived in Eq. D24 (Darcy-Weisbach-equation [382]) with the friction factor  $\lambda_{\text{pipe}}$  (Eq. D25 – Nikuradse-equation [383]), mean compressibility  $K_m$  (Eq. D26, [170]) and the norm volume flow rate  $\dot{V}_n$  (Eq. D27):

$$L_{\text{pipe,comp}} = (p_{\text{pipe},1}^2 - p_{\text{pipe},2}^2) \cdot \left( \frac{D_{\text{pipe}}^5}{\lambda_{\text{pipe}}} \cdot \frac{\pi^2}{16} \cdot \frac{T_n}{T_m} \cdot \frac{1}{\rho_n \cdot p_n \cdot \dot{V}_n^2 \cdot K_m} \right) \quad (\text{D24})$$

with 
$$\lambda_{\text{pipe}} = \left( 2 \cdot \log \left( \frac{D_{\text{pipe}}}{k_{\text{pipe}}} \right) + 1.138 \right)^{-2} \quad (\text{D25})$$

with 
$$K_m = \frac{1}{Z_{\text{H}_2,n}} \frac{p_m}{\rho_m(p_m) \cdot R_s \cdot T_m} \quad (\text{D26})$$

with 
$$\dot{V}_n = \frac{\dot{m}_{\text{pipe,in,max}}}{\rho_n} \quad (\text{D27})$$

Parameters are the pipe roughness coefficient  $k_{\text{pipe}} = 0.0002$  m, the norm compressibility factor  $Z_{\text{H}_2,n} (1.0005)$ , norm and mean temperatures of GH<sub>2</sub>  $T_n$  (273.15 K),  $T_m$  (288.15 K), norm density and pressure of GH<sub>2</sub>  $\rho_n$  (0.0889 kg/m<sup>3</sup>),  $p_n$  (101,325 Pa), and the specific gas constant  $R_s$  (4,124.2 J/kgK).

In a last step, the number of required compressors  $n_{\text{pipe,comp}}$  (Eq. D28) is determined based on the total length of the pipes  $L_{\text{pipe,total}}$  and the above calculated length between compressor stations:

$$n_{\text{pipe,comp}} = \frac{L_{\text{pipe,total}}}{L_{\text{pipe,comp}}} - 1 \quad (\text{D28})$$

Then, the GH<sub>2</sub> mass losses  $\dot{m}_{\text{pipe,losses}}$  via these compressor stations are derived (Eq. D29):

$$\dot{m}_{\text{pipe,losses}} = \dot{m}_{\text{pipe,in}} - \dot{m}_{\text{pipe,in}} \cdot 0.995^{n_{\text{pipe,comp}}} \quad (\text{D29})$$

The specific total CAPEX functions for installing new pipelines (excl. compressors – see D2.2) or retrofitting existing pipelines depend on the diameter size of the pipes and are shown in Figure D2.11.

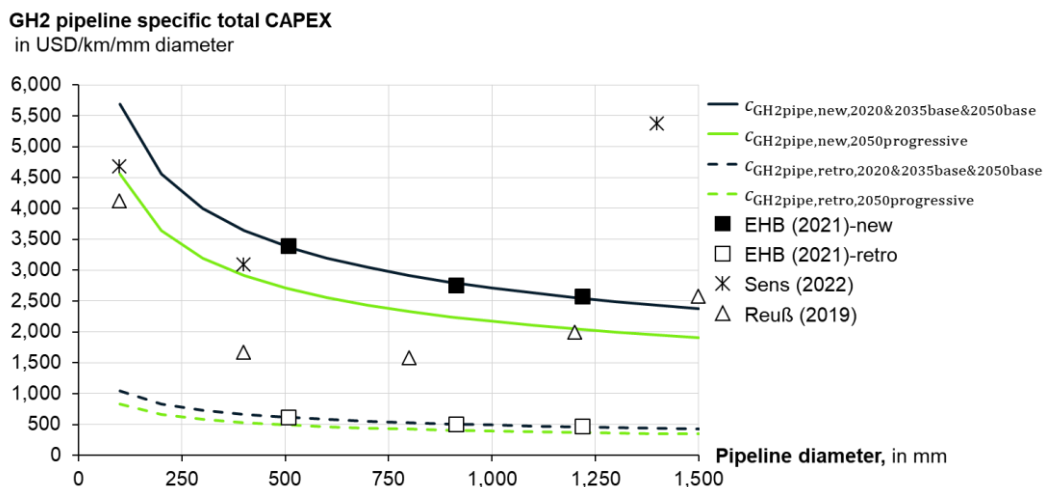


**Figure D2.11:** Total CAPEX function for GH<sub>2</sub> pipelines (excl. compressors), new-built and retrofitted based on the EHB report [164], Sens [111] and Reuß [198]

## LH<sub>2</sub> transport via vessels

The main techno-economics of LH<sub>2</sub> vessel transport depend on the number of vessels  $n_{\text{vessel}}$  required to operate the transport network (Eq. D30), the capacity of the vessels  $m_{\text{vessel}}$  (Eq. D31) and the trip characteristics.

In general, the amount of needed vessels is calculated with the number of possible annual departures  $n_{\text{vessel,departures}}$  and the number of annual trips  $n_{\text{vessel,trips}}$  that can be operated with one vessel (Eq. D32) given its trip performance (Eq. D33). The number of annual vessel departures is an optimization variable and characterizes the transport network design. As a constraint, a minimum of weekly departures is taken to ensure a supply reliability at the import-ing location. Thus, a maximum departure amount caps this optimization variable on the upper end – only sequential loading of vessels is assumed at the export terminal. With a loading and unloading time at the terminal  $t_{\text{vessel,terminal}}$  of 48 h, only 3.5 vessels can be handled per week as a maximum.

$$n_{\text{vessel}} = \frac{n_{\text{vessel,departures}}}{n_{\text{vessel,trips}}} \quad (\text{D30})$$

$$m_{\text{vessel}} = \frac{m_{\text{LH2demand}} \cdot f_{\text{LH2demand,peak}}}{n_{\text{vessel,departures}}} \quad (\text{D31})$$

The trip characteristics are determined with the availability of the vessel  $f_{\text{avail,vessel}}$  (0.91) (8,000 h per year [111,203]), the trip distance  $L_{\text{vessel,trip}}$  and the speed of the vessel  $v_{\text{vessel}} = 33.33$  km/h [111,203,204,285].

$$n_{\text{vessel,trips}} = \frac{8760 \text{ h}}{t_{\text{vessel,roundtrip}}} \cdot f_{\text{avail,vessel}} \quad (\text{D32})$$

$$\text{with } t_{\text{vessel,roundtrip}} = 2 \cdot \left( \frac{L_{\text{vessel,trip}}}{v_{\text{vessel}}} + t_{\text{vessel,terminal}} \right) \quad (\text{D33})$$

While loading the vessel, H<sub>2</sub> flash losses might occur. In the 2035 and 2050 base cases, this is assumed to be 1% of the total mass being filled into the vessel. In the 2050 progressive scenario, solutions are available to eliminate such losses. On trips, BO occurs in the storages – the GH<sub>2</sub> is used for propulsion. Due to the mobile use of the LH<sub>2</sub> tanks on the vessel, a BO rate with a factor 2.5 is assumed compared to the BO characteristics of the stationary storages (Eq. D19, Figure D2.9). This is in accordance with values from [111,203,254,282,285].

The specific total CAPEX per vessel are shown in Figure D2.12 and depend on the LH<sub>2</sub> transport capacity.

As part of the OPEX, costs are accounted for the fuel consumption (if BO mass is not sufficient), fixed OM for the vessel and other annual OPEX for crew, port or navigation fees. The fuel consumption of 0.0189 kWh/tonscapacity/km [384] and the other OPEX of 11.3 Mn USD [164,286] are for a vessel with 11,000 tLH<sub>2</sub> capacity and are computed proportionally to the changing vessel sizes.

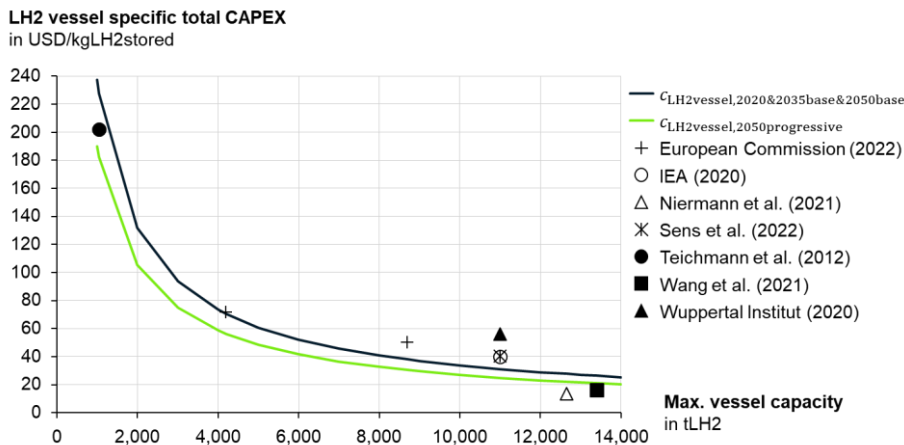


**Figure D2.12:** Total CAPEX function defined for LH<sub>2</sub> vessels with 1,000-14,000 tLH<sub>2</sub> max. capacity, data from European Commission [282], IEA [254], Niermann et al. [283], Sens et al. [111], Teichmann et al. [271], EHB report/Wang et al. [164] and the Wuppertal Institut [284]

The design and costs of the import terminals are as large as the capacity of the vessels. Techno-economics are calculated as previously described in D2.3 for LH<sub>2</sub> storages and cryopumps.

### LH<sub>2</sub> transport via trucks

The truck carries a 4.5 tLH<sub>2</sub> trailer storage and an availability of 3,500 h per year [271]. The number of trips with one LH<sub>2</sub> truck system are calculated as for the vessel in Eq. D32 and D33. The mean truck speed is assumed to be 50 km/h [106,111]. The loading and unloading takes 45 minutes each [112,115].

As for the LH<sub>2</sub> vessel loading, same size of flash losses is assumed when loading the LH<sub>2</sub> truck storages. For the BO rate of the cylindrical tank 0.1% is taken [112]. Thus, a 0.07 kgH<sub>2</sub>/km fuel consumption is chosen for the truck system [106].



## E Case study data and calculations

### E1 Data on LH<sub>2</sub> supply network

**Table E1.1:** 104 airports, country-wise interest rate for renewable energy projects based on [165,385–387], coordinates based on renewable.ninja [294,295], cavern storage availability based on [158,161,164,166,388,389]

City	IATA code	Country	Demand category	Interest rate	Coordinates for RES site	Space constraints	Cavern storage
Tirana	TIA	Albania	Small	8%	41.182, 19.507		
Sofia	SOF	Bulgaria	Medium	5%	42.647, 23.567		Yes
Prague	PRG	Czech R.	Large	6%	50.016, 14.925		Yes
Tallinn	TLL	Estonia	Small	8%	59.422, 24.994		
Budapest	BUD	Hungary	Large	5%	47.320, 18.630		Yes
Riga	RIX	Latvia	Medium	9%	57.055, 24.796		Yes
Vilnius	VNO	Lithuania	Medium	10%	54.583, 25.376		
Krakow	KRK	Poland	Medium	6%	50.171, 20.068		Yes
Warsaw	WAW	Poland	Large	6%	52.114, 20.109		Yes
Bucharest	OTP	Romania	Large	8%	44.388, 26.489		Yes
Algiers	ALG	Algeria	Medium	16%	36.615, 2.851		Yes
Zvartnots	EVN	Armenia	Small	8%	40.335, 44.473		Yes
Baku	GYD	Azerbaijan	Small	8%	40.377, 49.625		
Cairo	CAI	Egypt	Large	10%	29.754, 30.855		Yes
Erbil	EBL	Iraq	Regional	18%	36.231, 43.915		Yes
Tel Aviv	TLV	Israel	Very large	4%	31.245, 35.183		Yes
Amman	AMM	Jordan	Medium	12%	31.452, 36.305		
Beirut	BEY	Lebanon	Medium	22%	33.835, 36.013		Yes
Casablanca	CMN	Morocco	Large	9%	33.283, -8.053		Yes
Tunis	TUN	Tunisia	Medium	11%	36.418, 10.038		Yes
Billund	BLL	Denmark	Small	4%	55.747, 9.243	Yes	Yes
Copenhagen	CPH	Denmark	Very large	4%	55.766, 12.004	Yes	Yes
Birmingham	BHX	England	Large	4%	52.546, -1.634		Yes
London	LHR	England	Very large	4%	51.770, -0.853		Yes
Manchester	MAN	England	Very large	4%	53.571, -3.008		Yes
Helsinki	HEL	Finland	Very large	4%	60.374, 24.917	Yes	
Keflavik	KEF	Iceland	Medium	4%	64.035, -22.658		
Dublin	DUB	Ireland	Very large	4%	53.228, -6.212		
Bergen	BGO	Norway	Medium	4%	Grid connection	Yes	
Oslo	OSL	Norway	Very large	4%	59.629, 10.666	Yes	
Stavanger	SVG	Norway	Small	4%	58.826, 5.608	Yes	
Tromso	TOS	Norway	Small	4%	Grid connection	Yes	
Edinburgh	EDI	Scotland	Large	4%	57.489, -2.256		Yes
Glasgow	GLA	Scotland	Medium	4%	55.660, -4.783		Yes
Stockholm	ARN	Sweden	Very large	4%	59.695, 18.083		
Gothenburg	GOT	Sweden	Medium	4%	58.257, 12.877		Yes
Sarajevo	SJJ	Bosnia-Herzegovina	Regional	8%	43.979, 17.217	Yes	Yes
Dubrovnik	DBV	Croatia	Small	8%	42.567, 18.264	Yes	
Pula	PUY	Croatia	Regional	8%	44.884, 13.920		
Rijeka	RJK	Croatia	Regional	8%	45.199, 14.583		
Split	SPU	Croatia	Small	8%	43.669, 16.703		
Zadar	ZAD	Croatia	Regional	8%	44.045, 15.469		
Zagreb	ZAG	Croatia	Small	8%	45.795, 16.439		
Larnaca	LCA	Cyprus	Medium	5%	35.030, 33.892		
Athens	ATH	Greece	Very large	6%	37.939, 23.915		
Chania	CHQ	Greece	Small	6%	35.528, 24.114		
Heraklion	HER	Greece	Medium	6%	35.178, 25.312		
Mykonos	JMK	Greece	Regional	6%	37.447, 25.359	Yes	
Santorini	JTR	Greece	Small	6%	36.358, 25.434		
Kos	KGS	Greece	Small	6%	36.788, 27.085		

Rhodes	RHO	Greece	Medium	6%	35.945, 27.781		
Thessaloniki	SKG	Greece	Medium	6%	40.448, 22.892		
Bologna	BLQ	Italy	Medium	4%	44.561, 11.073		Yes
Bari	BRI	Italy	Medium	4%	40.953, 17.163		Yes
Cagliari	CAG	Italy	Small	4%	39.374, 8.982		
Catania	CTA	Italy	Large	4%	37.477, 14.867	Yes	Yes
Rome	FCO	Italy	Very large	4%	41.86, 12.221		Yes
Milan	LIN	Italy	Large	4%	45.299, 10.241		Yes
Milan	MXP	Italy	Very large	4%	45.299, 10.241		Yes
Naples	NAP	Italy	Large	4%	40.965, 14.464		Yes
Olbia	OLB	Italy	Small	4%	40.885, 9.521	Yes	
Venice	VCE	Italy	Large	4%	45.085, 11.900		Yes
Malta	MLA	Malta	Medium	5%	35.875, 14.376	Yes	
Faro	FAO	Portugal	Medium	5%	37.197, -8.307	Yes	Yes
Funchal	FNC	Portugal	Small	5%	32.809, -17.252		
Lisbon	LIS	Portugal	Very large	5%	38.676, -8.172		Yes
Porto	OPO	Portugal	Large	5%	41.267, -8.679		Yes
Belgrade	BEG	Serbia	Medium	8%	44.918, 20.992		
Ljubljana	LJU	Slovenia	Regional	5%	46.015, 14.469		
Malaga	AGP	Spain	Large	5%	36.684, -4.746		Yes
Alicante	ALC	Spain	Large	5%	38.533, -1.536		Yes
Barcelona	BCN	Spain	Very large	5%	41.332, 1.269		Yes
Bilbao	BIO	Spain	Medium	5%	42.971, -3.218		Yes
Ibiza	IBZ	Spain	Medium	5%	39.022, 1.423	Yes	
Madrid	MAD	Spain	Very large	5%	40.165, -3.244		Yes
Mahon	MAH	Spain	Small	5%	39.852, 4.234		
Palma de Mallorca	PMI	Spain	Very large	5%	39.41, 2.796		
Santiago de Compostela	SCQ	Spain	Small	5%	42.956, -8.467		
Seville	SVQ	Spain	Medium	5%	37.085, -6.619		Yes
Valencia	VLC	Spain	Medium	5%	39.505, -1.254		Yes
Istanbul	IST	Turkey	Very large	8%	41.168, 28.310		
Graz	GRZ	Austria	Regional	4%	46.965, 15.821		Yes
Salzburg	SZG	Austria	Regional	4%	47.899, 13.041		Yes
Vienna	VIE	Austria	Very large	4%	48.085, 16.745		Yes
Brussels	BRU	Belgium	Very large	4%	50.687, 3.521		Yes
Bastia	BIA	France	Regional	4%	42.191, 9.500		
Bordeaux	BOD	France	Medium	4%	44.745, -0.853		Yes
Paris	CDG	France	Very large	4%	49.033, 2.600		Yes
Lyon	LYS	France	Large	4%	45.798, 4.276		Yes
Marseille	MRS	France	Large	4%	43.517, 4.903		Yes
Nice	NCE	France	Large	4%	43.350, 6.220	Yes	Yes
Toulouse	TLS	France	Medium	4%	43.243, 1.972		Yes
Berlin	BER	Germany	Very large	4%	52.699, 13.681		Yes
Bremen	BRE	Germany	Small	4%	53.003, 8.747		Yes
Dresden	DRS	Germany	Regional	4%	51.173, 13.769		Yes
Dusseldorf	DUS	Germany	Very large	4%	51.063, 6.439		Yes
Frankfurt	FRA	Germany	Very large	4%	50.221, 8.715		Yes
Hannover	HAJ	Germany	Medium	4%	52.470, 9.561		Yes
Hamburg	HAM	Germany	Large	4%	54.016, 9.091		Yes
Munich	MUC	Germany	Very large	4%	48.474, 11.791		Yes
Stuttgart	STR	Germany	Large	4%	48.640, 8.857		Yes
Amsterdam	AMS	Netherlands	Very large	4%	52.256, 4.670		Yes
Geneva	GVA	Switzerland	Large	4%	46.693, 6.592		Yes
Zurich	ZRH	Switzerland	Very large	4%	47.573, 8.727		Yes

**Table E1.2:** 7 export hubs; same sources as in Table E1.1 for interest rates, coordinates and cavern availability

Port for export	Country	Demands	Interest rate for RES <sup>a</sup>	Coordinates for RES site	Cavern storage
Rosslare	Ireland	0.5–1.5 MtH <sub>2</sub> /a	4%	52.265, -6.620	
Aberdeen	Scotland	0.5–1.5 MtH <sub>2</sub> /a	4%	57.489, -2.256	Yes
Faro/Olhao	Portugal	0.5–1.5 MtH <sub>2</sub> /a	5%	37.459, -8.200	Yes
Alicante	Spain	0.5–1.5 MtH <sub>2</sub> /a	5%	37.804, -2.426	Yes
New	Morocco	0.5–1.5 MtH <sub>2</sub> /a	9% <sup>b</sup>	28.357, -11.291	Yes
Duba	Saudi Arabia	0.5–1.5 MtH <sub>2</sub> /a	6%	29.048, 37.169	Yes
Port Hedland	Australia	0.5–1.5 MtH <sub>2</sub> /a	5%	-25.42, 113.964	Yes

a) Interest rate 2 percentage points higher for hydrogen projects due to higher risks [239]

b) Moroccan pipeline built to connect with EHB (see Table S1.2 in the Supplementary Material of [305]) calculated with the Moroccan-specific interest rate

## E2 Data on aircraft design

Table E2 shows all performance parameters of the H<sub>2</sub>-powered aircraft modeling. The Lift-to-Drag (LoD) ratio in mid cruise conditions decreases with increasing design range due to the increasing maximum LH<sub>2</sub> tank volume and hence, the increasing fuselage length. The thrust specific fuel consumption (TSFC) in mid cruise decreases and the total propulsion efficiency increases with increasing design range due to the higher thrust requirements and engine size. The gravimetric index of the LH<sub>2</sub> tank structure and fuel systems is increasing from 42% up to 48% due to scaling effects. The thermodynamic and structural methods for the LH<sub>2</sub> tank design are described in [390,391].

**Table E2:** Hydrogen aircraft specifications – performance characteristics for four design ranges

Parameter	Unit	H2-1,500 NM	H2-2,000 NM	H2-2,500 NM	H2-3,000 NM
Lift to Drag (mid. cruise)	-	17.5	17.3	17.2	17.1
TSFC (mid. cruise)	kg/s/N	4.90e-06	4.88e-06	4.86e-06	4.84e-06
Total propulsion efficiency (mid. cruise)	-	39.2%	39.4%	39.6%	39.8%
Total thrust required (mid. cruise)	kN	37.7	39.6	41.3	43.0
Fuselage length	m	41.3	43.4	45.3	46.4
Total LH <sub>2</sub> tank volume	m <sup>3</sup>	59	75	93	110
LH <sub>2</sub> tank gravimetric index including fuel systems	-	42%	44%	46%	48%

## E3 Calculations and techno-economic assumptions for synthetic kerosene benchmark

For the benchmark in Section 6.4, synthetic kerosene produced with green H<sub>2</sub> and CO<sub>2</sub> from a direct air capture plant (DAC) is used. Therefore, techno-economic assumptions and optimization results from the LH<sub>2</sub> calculations are used (see also Table E3.1): the RES, electrolysis, GH<sub>2</sub> tanks and compressors. Then, the GH<sub>2</sub> is converted into syngas with the reverse water gas shift (RWGS) reaction. In the Fischer-Tropsch-synthesis (FT), it is advanced into long-chain hydrocarbons. These are also called syncrude and can be separated into kerosene-like jet fuel and by-products, which also result from the process. In this cost calculation, the by-products naphtha and liquid petroleum gas (LPG) are resold at a constant market price (see Table E3.2).

As the synfuel will most likely be produced at a main hub and then imported like it is currently done in the kerosene supply chain, only off-site production of synfuel is assumed in this study. The synfuel is transported via vessels and then via fuel-cell-powered trucks to the airport. Same transport cost models are used than for the LH<sub>2</sub> calculations which are described in [239]. Since the conventional refueling infrastructure can be used, fixed refueling costs of 0.01 USD/kg synfuel are assumed for this last step in the supply to the aircraft [16]. Table E3.2 shows the techno-economic assumptions for synfuel production as well as for the transportation. The TAC of the individual components  $i$  are calculated with sum of the specific CAPEX  $c_{CAPEX,i}$  multiplied by the annuity factor  $a_i$  and the specific OPEX  $c_{OPEX,i}$  with

$$c_{TAC,i} = c_{CAPEX,i} \cdot a_i + c_{OPEX,i} \cdot \quad (E1)$$

The synfuel costs are calculated analogous to the LH<sub>2</sub> models using the annuity factor from Eq. 3. The specific synfuel costs  $c_{TAC}$  are calculated as shown in Eq. E2 to E4:

$$c_{TAC} = (c_{TAC,H_2} \cdot f_{H_2} + c_{TAC,DAC} \cdot f_{CO_2} + c_{TAC,synfuel}) \cdot f_{syncrude} \quad (E2)$$

with 
$$c_{TAC,H_2} = c_{TAC,Ely} + c_{TAC,GH_2storage} + c_{TAC,H_2comp} \quad (E3)$$

and 
$$c_{TAC,synfuel} = c_{TAC,FT+RWGS} + c_{TAC,synfueltank} \quad (E4)$$

The specific costs of the H<sub>2</sub>, CO<sub>2</sub> and synfuel components  $c_{TAC,H_2}$ ,  $c_{TAC,CO_2}$  and  $c_{TAC,synfuel}$  are multiplied by the factors for the H<sub>2</sub> and CO<sub>2</sub> demand  $f_{H_2}$  and  $f_{CO_2}$  which are shown in Table E3.2. More than 1 kg syncrude has to be produced to get 1 kg synfuel because of the by-products. This effect is taken into account by the factor  $f_{syncrude}$ , which is also shown in Table E3.2. The specific energy demand for the synfuel production  $e_{synfuel}$  is calculated with

$$e_{synfuel} = (e_{Ely} \cdot f_{H_2} + e_{DAC} \cdot f_{CO_2} + e_{FT+RWGS}) \cdot f_{syncrude} \quad (E5)$$

where the energy demands for the H<sub>2</sub> and CO<sub>2</sub> production,  $e_{Ely}$  and  $e_{DAC}$ , are multiplied by the corresponding factors (Table E3.2). Then, also the energy demands of the Fischer-Tropsch and RWGS process  $E_{FT+RWGS}$  are accounted to determine the overall total specific energy demand for the syncrude production. Finally, the specific energy demand for synfuel production is derived by multiplying with the syncrude-to-synfuel-factor (Eq. E5).

It is important to note that the lower heating value of synfuel is 12.28 kWh/kg which differs slightly from conventional kerosene [392,393].

**Table E3.1:** Utilization of the synfuel components for four locations in 2035 and 2050 – results from LH<sub>2</sub> off-site system optimization

Component	Unit	Scotland		Portugal		Saudi Arabia		Australia	
		2035	2050	2035	2050	2035	2050	2035	2050
<b>Utilization</b>									
Electrolysis system	h/a	5,619	5,242	5,309	4,602	4,942	4,483	5,396	5,619
DAC	h/a	7,833	7,920	7,993	7,911	7,929	7,639	7,884	7,724
Fischer-Tropsch + RWGS	h/a	7,833	7,920	7,993	7,911	7,929	7,639	7,884	7,724
<b>Energy demand</b>									
Electrolysis system	kWh/kgH <sub>2</sub>	49.09	48.95	47.83	47.89	48.03	48.52	47.70	47.62
DAC	kWh/kgCO <sub>2</sub>	1.73	1.28	1.73	1.28	1.73	1.28	1.73	1.28
Fischer-Tropsch + RWGS	kWh/kg syn-crude	0.37	0.37	0.37	0.37	0.37	0.37	0.37	0.37
LCOE	USD/MWh	24	18	28	20	32	22	27	21

**Table E3.2:** Techno-economic assumptions for the synfuel production

Component	2035	2050	Sources
<b>DAC (low temperature)</b>			
Specific CAPEX	1 USD/kgCO <sub>2</sub> per year	0.60 USD/kgCO <sub>2</sub> per year	[394–396]
Depreciation period	25 years	25 years	[394–396]
O&M factor	4%	4%	[394–396]
Electricity consumption (electricity demand + heat demand <sup>a</sup> )	1.73 kWh/kgCO <sub>2</sub>	1.28 kWh/kgCO <sub>2</sub>	[394–398]
<b>Fischer-Tropsch + RWGS</b>			
Specific CAPEX	0.46 USD/kg syn-crude p.a.	0.40 USD/kg syn-crude p.a.	[394,399,400]
Depreciation period	30 years	30 years	[399–401]
O&M factor	4%	4%	[399,400,402]
Electricity consumption <sup>a</sup>	0.37 kWh/kg syn-crude	0.37 kWh/kg syn-crude	[392,399]
Specific H <sub>2</sub> demand $f_{H_2}$	0.48 kgH <sub>2</sub> /kg syn-crude	0.48 kgH <sub>2</sub> /kg syn-crude	[392,393]
Specific CO <sub>2</sub> demand $f_{CO_2}$	3.06 kgCO <sub>2</sub> /kg syn-crude	3.06 kgCO <sub>2</sub> /kg syn-crude	[392,393]

**Product shares**

Naphtha	24%	19%	[403]
LPG	6%	3%	[403]
Synfuel	70%	78%	[403]
Factor for synfuel production $f_{\text{syncrude}}$	1.43 kg syncrude per kg synfuel	1.28 kg syncrude per kg synfuel	
Naphtha selling price	0.50 USD/kg naphtha	0.50 USD/kg naphtha	
LPG selling price	0.50 USD/kg LPG	0.50 USD/kg LPG	

**Synfuel tank**

Specific CAPEX	0.24 USD/kg synfuel capacity	0.24 USD/kg synfuel capacity	[402]
Depreciation period	20 years	20 years	[106,402]
O&M factor	3%	3%	[402]

**Synfuel truck transport**

Total CAPEX truck	305,500 USD	305,500 USD	[106,404]
Depreciation period	12 years	12 years	[106,112,239]
Availability	40%	40%	[271]
O&M factor	3%	3%	[112,239]
Capacity	30,000 kg synfuel	30,000 kg synfuel	

**Synfuel vessel transport**

Total CAPEX vessel	48 Mn USD	48 Mn USD	[405]
Depreciation period	25 years	25 years	[405]
Availability	95%	95%	[405]
Capacity	90,000 t synfuel	90,000 t synfuel	[405]
Ullage	0.1%	0.1%	[405]
O&M	3%	3%	[405]
Other OPEX (crew etc.)	5,000 USD/d	5,000 USD/d	[405]
Specified maximum continuous rating	11,500 kW	11,500 kW	[406]
Fuel consumption	449.96 kWh/km	449.96 kWh/km	[406]
Fuel costs synthetic diesel	0.16 USD/kWh	0.16 USD/kWh	[404,407]
Speed	25.56 km/h	25.56 km/h	[406]
Loading & unloading time	48 h	48 h	[405]
Maximal distance	13,400 km	13,400 km	[405]

a) Full electric heat supply assumed – not enough excess heat in 2050

## F Publication contributor roles

Large parts of the present dissertation are adopted from four publications already released in or submitted to scientific journals. While the author of this dissertation is first author of all four articles, the intellectual properties are shared with several co-authors. For full disclosure, the “Contributor Roles Taxonomy” (CRediT) [408] is chosen to represent the roles played by the contributors of all published articles, see Table F1. This procedure is chosen to acknowledge all co-authors, but also demonstrate that the fundamental work, computational analysis, and writing were conducted by the author of this dissertation, Julian Hoelzen.

**Table F1:** CRediT contributor roles of the underlying publications

<b>Co-authors of [52]</b>	<b>Contributor roles</b>
J. Hoelzen	Conceptualization, Methodology, Investigation, Validation, Writing - Original Draft, Data Curation, Visualization
D. Silberhorn	Methodology, Software, Validation, Writing - Original Draft, Data Curation, Resources
T. Zill	Validation, Writing - Review & Editing
B. Bensmann	Methodology, Validation, Resources, Writing - Review & Editing, Project administration
R. Hanke-Rauschenbach	Writing - Review & Editing, Supervision, Funding acquisition, Project administration
<b>Co-authors of [112]</b>	<b>Contributor roles</b>
J. Hoelzen	Conceptualization, Methodology, Investigation, Validation, Writing - Original Draft, Data Curation, Visualization
M. Flohr	Methodology, Investigation, Software, Writing - Original Draft, Data Curation, Visualization
D. Silberhorn	Validation, Writing - Review & Editing
J. Mangold	Validation, Methodology, Writing - Review & Editing
A. Bensmann	Methodology, Validation, Resources, Writing - Review & Editing, Project administration
R. Hanke-Rauschenbach	Writing - Review & Editing, Supervision, Funding acquisition, Project administration
<b>Co-authors of [239]</b>	<b>Contributor roles</b>
J. Hoelzen	Conceptualization, Methodology, Investigation, Software, Validation, Writing - Original Draft, Data Curation, Visualization
L. Koenemann	Methodology, Software, Validation, Resources
L. Kistner	Software, Resources
F. Schenke	Data Curation, Validation, Writing - Review & Editing
A. Bensmann	Methodology, Validation, Resources, Writing - Review & Editing, Project administration
R. Hanke-Rauschenbach	Writing - Review & Editing, Supervision, Funding acquisition, Project administration
<b>Co-authors of [305]</b>	<b>Contributor roles</b>
J. Hoelzen	Conceptualization, Methodology, Investigation, Software, Validation, Writing - Original Draft, Data Curation, Visualization
D. Silberhorn	Methodology, Software, Validation, Data Curation, Resources
F. Schenke	Methodology, Data Curation, Validation, Writing - Original Draft
E. Stabenow	Data Curation
T. Zill	Validation, Writing - Review & Editing
A. Bensmann	Methodology, Validation, Resources, Writing - Review & Editing, Project administration
R. Hanke-Rauschenbach	Writing - Review & Editing, Supervision, Funding acquisition, Project administration

## G Curriculum Vitae

**Table G1:** Professional background

05/2018 – 10/2023	<p><b>Senior Consultant</b>, McKinsey &amp; Company in Hamburg</p> <ul style="list-style-type: none"> <li>• Consultant and project manager for strategies in the field of sustainable aviation, hydrogen technology &amp; applications, renewable energy, aircraft manufacturing, airlines and rail mobility</li> <li>• Lead of work streams and projects on CxO level at international corporations, public institutions and SMEs in Europe &amp; the Americas</li> <li>• Co-author of “Hydrogen-powered aviation”-study for European Commission Joint Undertakings (Clean Sky &amp; FCH JUs)</li> </ul>
08/2020 – 10/2023	<p><b>Research Assistant</b>, Institute for Electric Power Systems, Leibniz Universität Hannover</p> <ul style="list-style-type: none"> <li>• Research on techno-economics of (liquid) hydrogen supply chains to enable hydrogen-powered aviation including non-linear energy system modeling methodologies</li> <li>• Proposal writing and project coordination of publicly-funded research projects (national and international level), e.g., HyNEAT project</li> </ul>
05/2017 – 10/2017	<p><b>Working Student</b>, Airbus Operations in Hamburg/Bremen</p> <ul style="list-style-type: none"> <li>• Investigation of techno-economics for hybrid-electric turbo-prop aircraft for Research &amp; Technology Plateau</li> </ul>

**Table G2:** Education and scholarships

05/2022 – 09/2023	<p><b>Doctoral Scholarship</b>, Stiftung der Deutschen Wirtschaft in Berlin</p>
04/2015 – 10/2017	<p><b>M. Sc. Industrial Engineering</b>, Leibniz University Hannover</p> <ul style="list-style-type: none"> <li>• Focus on electrical engineering incl. renewable energy technologies and strategic &amp; organizational management</li> <li>• Master thesis: Techno-economic analysis of hybrid-electric propulsion systems for aircraft</li> </ul>
10/2011 – 03/2015	<p><b>B. Sc. Industrial Engineering</b>, Leibniz University Hannover</p> <ul style="list-style-type: none"> <li>• Bachelor thesis: Simulation and investigation of different concepts for the fault ride-through of a wind turbine with a fully rated converter</li> </ul>

**Table G3:** Scientific publications

<p>J. Hoelzen, Y. Liu, B. Bensmann, C. Winnefeld, A. Elham, J. Friedrichs, R. Hanke-Rauschenbach, Conceptual Design of Operation Strategies for Hybrid Electric Aircraft, <i>Energies</i> 11(1), 217 (2018)</p>
<p>J. Hoelzen, D. Silberhorn, T. Zill, B. Bensmann, R. Hanke-Rauschenbach, Hydrogen-powered aviation and its reliance on green hydrogen infrastructure – Review and research gaps, <i>International Journal of Hydrogen Energy</i> 47(5) (2022)</p>
<p>J. Hoelzen, M. Flohr, D. Silberhorn, J. Mangold, A. Bensmann, R. Hanke-Rauschenbach, H2-powered aviation at airports – Design and economics of LH2 refueling systems, <i>Energy Conversion and Management: X</i> 14 (2022)</p>
<p>J. Mangold, D. Silberhorn, N. Moebs, N. Dzikus, J. Hoelzen, T. Zill, A. Strohmayer, Refueling of LH2 Aircraft—Assessment of Turnaround Procedures and Aircraft Design Implication, <i>Energies</i> 15(7) (2022)</p>



---

S. Gronau, J. Hoelzen, T. Mueller, R. Hanke-Rauschenbach, Hydrogen-powered aviation in Germany: A macroeconomic perspective and methodological approach of fuel supply chain integration into an economy-wide dataset, *International Journal of Hydrogen Energy* 48(14) (2023)

---

F. Schenke, J. Hoelzen, C. Minke, A. Bensmann, R. Hanke-Rauschenbach, Resource requirements for the implementation of a global H<sub>2</sub>-powered aviation, *Energy Conversion and Management: X* 20 (2023)

---

J. Hoelzen, L. Koenemann, L. Kistner, F. Schenke, A. Bensmann, R. Hanke-Rauschenbach, H<sub>2</sub>-powered aviation – Design and economics of green LH<sub>2</sub> supply for airports, *Energy Conversion and Management: X* 20 (2023)

---

J. Hoelzen, D. Silberhorn, F. Schenke, E. Stabenow, T. Zill, A. Bensmann, R. Hanke-Rauschenbach, H<sub>2</sub>-powered aviation – Optimized aircraft designs and green LH<sub>2</sub> supply chains in air transport networks, in publication process (submitted, 2023)

---

D. Babuder, J. Hoelzen, Y. Lapko, D. Zingg, Impact of the Potentially Different Turnaround Times of Commercial Liquid Hydrogen Aircraft on Airline Operational Performance (submitted, 2023)

---

**Table G4:** Scientific presentations

---

J. Hoelzen, B. Bensmann, R. Hanke-Rauschenbach, H<sub>2</sub>-powered aviation and its reliance on green hydrogen infrastructure – review and research gaps, *Deutscher Luft- und Raumfahrtkongress*, online, (2021)

---

J. Hoelzen, M. Flohr, A. Bensmann, R. Hanke-Rauschenbach, Refueling of LH<sub>2</sub> aircraft – Part 1: Design and economics of LH<sub>2</sub> refueling systems at airports, *Deutscher Luft- und Raumfahrtkongress*, online, (2021)

---

J. Hoelzen, The importance of green hydrogen infrastructure for cleaner aviation, *Electric And Hybrid Aerospace Technology Symposium*, Frankfurt (2022)

---

J. Hoelzen, Hydrogen in Aviation: Opportunities and Challenges for a Carbon Neutral Aviation Industry, 2nd *Unlocking Industries – Hydrogen in Africa*, Hamburg (2023)

---

J. Hoelzen, A. Bensmann, R. Hanke-Rauschenbach, H<sub>2</sub> in der Luftfahrt: Zukünftige Bereitstellungskosten für flüssigen Wasserstoff (LH<sub>2</sub>) an Flughäfen, *Deutscher Luft- und Raumfahrtkongress*, Stuttgart (2023)

---

J. Hoelzen, Liquid hydrogen supply for H<sub>2</sub>-powered aircraft, *Electric And Hybrid Aerospace Technology Symposium*, Bremen (2023)

---

## Figures

<b>2.1</b>	Cost ranges for LH <sub>2</sub> at the dispenser derived from literature review depending on three H <sub>2</sub> cost scenarios	8
<b>2.2</b>	Overview of required components for green LH <sub>2</sub> supply	10
<b>2.3</b>	Para content of hydrogen as a function of temperature	16
<b>2.4</b>	LH <sub>2</sub> vessel design from HySTRA demonstration project lead by Kawasaki – transport between Japan and Australia	18
<b>2.5</b>	Import and export terminal design for shipping LH <sub>2</sub> via vessels	18
<b>3.1</b>	Total DOC evaluation of the reference kerosene-powered aircraft	25
<b>3.2</b>	Change of selected DOC factors for the H <sub>2</sub> -powered single-aisle aircraft due to H <sub>2</sub> propulsion technology impacting aircraft CAPEX and maintenance costs as well as fuel costs through lower energy efficiency	26
<b>4.1</b>	Airports' fuel demands: A) Considered annual fossil kerosene fuel demand in 2019 at three German airports without larger wide-body aircraft, B) average daily aircraft departures at HAM in 2019, C) monthly aircraft departures at HAM in 2019	31
<b>4.2</b>	Annual H <sub>2</sub> demand ranges for different sectors at a specific region and their projected economic viability	33
<b>4.3</b>	Topologies for LH <sub>2</sub> refueling setups at airports	34
<b>4.4</b>	Total costs of LH <sub>2</sub> at the dispenser with a truck and pipeline & hydrant refueling in 2050	35
<b>4.5</b>	Variation of main techno-economic parameters for LH <sub>2</sub> truck and pipeline & hydrant refueling for annual LH <sub>2</sub> demands between 10 to 200 ktLH <sub>2</sub>	36
<b>5.1</b>	Considered LH <sub>2</sub> supply pathways to refuel H <sub>2</sub> -powered aircraft in this study	40
<b>5.2</b>	Capacity factors of RES at chosen locations for the year 2019 (8760 hours) incl. array losses for wind parks	49
<b>5.3</b>	LH <sub>2</sub> demand profiles – left: daily profile for airports with night curfew, no night curfew, or export regions (vessel loading); right: annual demand variation for an “average” EU airport	50
<b>5.4</b>	LH <sub>2</sub> supply costs at the dispenser for on-site setups at five locations, 2050 base case scenario	51
<b>5.5</b>	Design of RES and ELY-system for five locations, 2050 base case scenario	53
<b>5.6</b>	Annual utilization of main components for five locations, 2050 base case scenario	53
<b>5.7</b>	Relative component design sizes compared to the average daily LH <sub>2</sub> demand (274 tLH <sub>2</sub> /d) for five locations, 2050 base case scenario	54
<b>5.8</b>	Total and average energy consumptions as well as total H <sub>2</sub> losses along the supply chain for five locations, 2050 base case scenario	56
<b>5.9</b>	LH <sub>2</sub> supply costs at the dispenser for on-site setups at five locations for variable annual LH <sub>2</sub> demands at the airport	58
<b>5.10</b>	Transport costs in the 2050 base case scenario for three distances (short: 1,000 km, medium: 3,000 km, long: 7,500 km) with LH <sub>2</sub> oversea vessels and a fixed 300 km truck transport on land from the importing port to the destination airport	63
<b>5.11</b>	Costs at the dispenser for receiving airport at WEAK location with LH <sub>2</sub> import (off-site) pathway over three distances compared to costs of on-site LH <sub>2</sub> production, 2050 base case scenario	64
<b>5.12</b>	Transport costs in the 2050 base case scenario for three distances (short: 1,000 km, medium: 3,000 km, long: 7,500 km) with GH <sub>2</sub> pipelines on land (new and retrofitted pipelines) from the importing site to the destination airport	65

<b>5.13</b>	Costs at the dispenser for receiving airport at WEAK location with LH <sub>2</sub> import (off-site) pathway over three distances compared to costs of on-site LH <sub>2</sub> production; two options with new built and retrofitted pipelines; 2050 base case scenario	66
<b>5.14</b>	LH <sub>2</sub> energy system costs, 2050 base case scenario	67
<b>5.15</b>	Total LH <sub>2</sub> supply costs at the dispenser for three transport distances considering only a GH <sub>2</sub> off-site supply pathway with A) new pipeline system installations (top) or B) with retrofitted pipeline systems (bottom)	68
<b>6.1</b>	Characteristics of selected air traffic network considering Lufthansa flights from Frankfurt-Main in the week of September 5th-11th 2022 and only flights of larger single-aisle aircraft (Airbus A320 family aircraft: all versions of A319, A320, A321 aircraft)	72
<b>6.2</b>	Exemplary LH <sub>2</sub> supply pathways shown for an Airport A	74
<b>6.3</b>	Optimized LH <sub>2</sub> supply costs at all selected 104 airports and 6 hubs	76
<b>6.4</b>	Cumulative frequency distribution of cost results for the best-supply-cost-pathways and LH <sub>2</sub> ON only supply	78
<b>6.5</b>	LH <sub>2</sub> costs at dispenser for three selected airports	79
<b>6.6</b>	Change of selected DOC factors excluding energy costs and energy consumption for kerosene- vs. H <sub>2</sub> -powered aircraft	81
<b>6.7</b>	H <sub>2</sub> -powered aircraft results compared to kerosene equivalent designs – A) DOC excl. energy costs comparison, B) DOC excl. energy costs comparison against best kerosene aircraft option, C) SEC comparison against best kerosene aircraft option	83
<b>6.8</b>	A) Average total DOC of kerosene-powered aircraft in a given air traffic network including different ETS-CO <sub>2</sub> -cost scenarios in USD/tCO <sub>2</sub> compared to synfuel- and H <sub>2</sub> -powered aircraft operation; B) Total DOC for H <sub>2</sub> - and synfuel-powered aircraft for each flight pair concerning kerosene-powered aircraft operation incl. 200 USD/tCO <sub>2</sub> costs	86
<b>C1</b>	Assumption-based H <sub>2</sub> aircraft fleet penetration until 2050 in A) a base case and B) an ambitious case scenario	106
<b>C2</b>	Calculated annual LH <sub>2</sub> fuel demand scenarios at A) Frankfurt airport (FRA), B) Hamburg airport (HAM), C) Bremen airport (BRE)	108
<b>D2.1</b>	Electric energy efficiency of chosen electrolysis system in dependence of the relative system power rating	114
<b>D2.2</b>	Direct CAPEX functions for GH <sub>2</sub> compressor systems	116
<b>D2.3</b>	Direct and installation CAPEX functions for GH <sub>2</sub> cavern systems	117
<b>D2.4</b>	Direct CAPEX functions for GH <sub>2</sub> aboveground systems	117
<b>D2.5</b>	Ideal work for H <sub>2</sub> liquefaction depending on the pressure of the GH <sub>2</sub> feed	118
<b>D2.6</b>	Size-depending SEC of LFP	119
<b>D2.7</b>	Factor for SEC change in part-load operation depending on the LFP's mass flow setting	120
<b>D2.8</b>	Total CAPEX function for LFP depending on the design capacity	120
<b>D2.9</b>	Boil-off losses for LH <sub>2</sub> storages depending on storage size	121
<b>D2.10</b>	Direct CAPEX function for LH <sub>2</sub> storages (excl. cryopumps)	122
<b>D2.11</b>	Total CAPEX function for GH <sub>2</sub> pipelines (excl. compressors), new-built and retrofitted	123
<b>D2.12</b>	Total CAPEX function defined for LH <sub>2</sub> vessels with 1,000-14,000 tLH <sub>2</sub> max. capacity	125

## Tables

<b>2.1</b>	Selected literature review findings mentioning LH <sub>2</sub> infrastructure for the use in aviation propulsion	5
<b>2.2</b>	Comparison of main selected water electrolysis technologies	13
<b>3.1</b>	High-level, qualitative impact on DOC factors by introducing new levers to reduce the climate impact of aviation	23
<b>3.2</b>	Conventional kerosene aircraft specifications – design criteria and outputs from modeling	24
<b>3.3</b>	Hydrogen aircraft specifications – design criteria and outputs from modeling	26
<b>4.1</b>	Overview of commercial aircraft segments referenced in this study	29
<b>4.2</b>	Calculated annual fuel demands for 2019 at selected airports and 2050 demand scenarios	32
<b>5.1</b>	Optimization variables considered in this study	43
<b>5.2</b>	Economic parameters for main components	46
<b>5.3</b>	Optimal design for five locations, 2050 base case scenario	52
<b>6.1</b>	Overview of commercial airport categories used for LH <sub>2</sub> demand calculations in this study	73
<b>6.2</b>	Future kerosene vs. H <sub>2</sub> -powered aircraft specifications for the four single-aisle (SA) designs	81
<b>6.3</b>	Comparison of fuel technologies for decarbonizing the existing air traffic network, so LH <sub>2</sub> demands at all 104 airports	88
<b>B1</b>	Hydrogen aircraft specifications – Performance characteristics	102
<b>C1</b>	Assumptions for fleet projection of H <sub>2</sub> -powered aircraft – base case	105
<b>C2</b>	Assumptions for fleet projection of H <sub>2</sub> -powered aircraft – ambitious case	105
<b>C3</b>	Efficiency factors for novel H <sub>2</sub> -powered compared to kerosene-powered aircraft used to calculate LH <sub>2</sub> demand scenarios	107
<b>D1.1</b>	Specific direct CAPEX functions in 2020 for selected components	109
<b>D1.2</b>	Overview of this study's assumptions for learning rate effects behind all components and underlying sources	110
<b>D1.3</b>	Further economic assumptions for selected supply chain component	112
<b>D2.1</b>	Coordinates for weather data sourcing via open-source tool "Renewable.ninja"	113
<b>E1.1</b>	104 airports, country-wise interest rate for renewable energy projects	126
<b>E1.2</b>	Seven export hubs: interest rates, coordinates and cavern availability	128
<b>E2</b>	Hydrogen aircraft specifications – performance characteristics for four design ranges	128
<b>E3.1</b>	Utilization of the synfuel components for four locations in 2035 and 2050 – results from LH <sub>2</sub> off-site system optimization	130
<b>E3.2</b>	Techno-economic assumptions for the synfuel production	130
<b>F1</b>	CRedit contributor roles of the underlying publications	132
<b>G1</b>	Professional background	133
<b>G2</b>	Education and scholarships	133
<b>G3</b>	Scientific publications	133
<b>G4</b>	Scientific presentations	134

**Bibliography**

- [1] S.D. Birkel, About Climate Reanalyzer, *Clim. Reanalyzer*, Clim. Chang. Institute, Univ. Maine, USA. (2023). <https://climatereanalyzer.org> (accessed July 7, 2023).
- [2] P.D. Ditlevsen, S. Ditlevsen, Warning of a forthcoming collapse of the Atlantic meridional overturning circulation, *Nat. Commun.* 14 (2023) 1–12. <https://doi.org/10.1038/s41467-023-39810-w>.
- [3] IPCC, Synthesis Report of the IPCC Sixth Assessment Report (AR6), 2023.
- [4] IATA, IATA 20-year Air Passenger Forecast, 2020.
- [5] European Commission, The European Green Deal sets out how to make Europe the first climate-neutral continent by 2050, boosting the economy, improving people’s health and quality of life, caring for nature, and leaving no one behind, Brussels, 2019.
- [6] V. Masson-Delmotte, H.-O. Pörtner, J. Skea, P. Zhai, D. Roberts, P.R. Shukla, A. Pirani, R. Pidcock, Y. Chen, E. Lonnoy, W. Moufouma-Okia, S. Connors, X. Zhou, T. Maycock, M. Tignor, C. Pean, J.B.R. Matthews, M.I. Gomis, T. Waterfield, Global warming of 1.5°C, IPCC, 2018.
- [7] B. Graver, D. Rutherford, S. Zheng, CO2 Emissions from Commercial Aviation 2013, 2018, and 2019, ICCT, Washington, 2020.
- [8] B. Pearce, COVID-19 Airline industry financial outlook update, 2021.
- [9] V. Grewe, A.G. Rao, T. Grönstedt, C. Xisto, F. Linke, J. Melkert, J. Middel, B. Ohlenforst, S. Blakey, S. Christie, S. Matthes, K. Dahlmann, Evaluating the climate impact of aviation emission scenarios towards the Paris agreement including COVID-19 effects, *Nat. Commun.* 12 (2021) 1–10. <https://doi.org/10.1038/s41467-021-24091-y>.
- [10] S. Arrowsmith, D.S. Lee, B. Owen, J. Faber, L. van Wijngaarden, O. Boucher, A. Celikel, R. Deransy, J. Fuglestvedt, J. Laukia, M.T. Lund, R. Sausen, M. Schaefer, A. Skowron, S. Stromatas, A. Watt, Updated analysis of the non-CO<sub>2</sub> climate impacts of aviation and potential policy measures pursuant to the EU Emissions Trading System Directive Article 30(4), EASA, Cologne, 2020.
- [11] D.S. Lee, D.W. Fahey, A. Skowron, M.R. Allen, U. Burkhardt, Q. Chen, S.J. Doherty, S. Freeman, P.M. Forster, J. Fuglestvedt, A. Gettelman, R.R. De León, L.L. Lim, M.T. Lund, R.J. Millar, B. Owen, J.E. Penner, G. Pitari, M.J. Prather, R. Sausen, L.J. Wilcox, The contribution of global aviation to anthropogenic climate forcing for 2000 to 2018, *Atmos. Environ.* 244 (2021) 1–29. <https://doi.org/10.1016/j.atmosenv.2020.117834>.
- [12] V. Grewe, Addressing non-CO<sub>2</sub> effects of aviation, presented at ICSA Aviation Decarbonization Forum, February, 2019.
- [13] Transport & Environment, The easy fix to air pollution linked to planes, (2023). <https://www.transportenvironment.org/discover/the-easy-fix-to-air-pollution-linked-to-planes/> (accessed July 7, 2023).
- [14] C. Voigt, J. Kleine, D. Sauer, R.H. Moore, T. Bräuer, P. Le Clercq, S. Kaufmann, M. Scheibe, T. Jurkat-witschas, M. Aigner, U. Bauder, Y. Boose, S. Borrmann, E. Crosbie, G.S. Diskin, J. Digangi, V. Hahn, C. Heckl, F. Huber, J.B. Nowak, M. Rapp, B. Rauch, C. Robinson, T. Schripp, M. Shook, E. Winstead, L. Ziemba, H. Schlager, B.E. Anderson, Cleaner burning aviation fuels can reduce contrail cloudiness, *Commun. Earth Environ.* 2 (2021) 2–11. <https://doi.org/10.1038/s43247-021-00174-y>.
- [15] EURACTIV, France unveils €15bn in aerospace aid, (n.d.). <https://www.euractiv.com/section/aerospace/news/france-unveils-e15bn-in-aerospace-aid-sets-green-goals/> (accessed April 8, 2021).
- [16] Clean Sky 2 JU, FCH 2 JU, Hydrogen-powered aviation: A fact-based study of hydrogen technology, economics, and climate impact by 2050, 2020. <https://doi.org/10.2843/766989>.
- [17] Reuters, Airbus tells EU hydrogen won’t be widely used in planes before 2050 | Reuters, (2021). <https://www.reuters.com/business/aerospace-defense/airbus-tells-eu-hydrogen-wont-be-widely-used-planes-before-2050-2021-06-10/> (accessed June 11, 2021).
- [18] Mission Possible Partnership, Making Net-Zero Aviation Possible - An industry-backed, 1.5°C-aligned transition strategy, 2022.
- [19] NLR - Royal Netherlands Aerospace Centre, SEO Amsterdam Economics, Destination 2050-A route to net zero European aviation, 2021.
- [20] International Air Transport Association, Net Zero Roadmaps - Executive Summary, Montreal, Canada, 2023.
- [21] World Economic Forum, McKinsey & Company, Target True Zero: Delivering the Infrastructure for Battery and Hydrogen-Powered Flight, 2023.
- [22] M. Hepperle, Electric Flight - Potential and Limitations, 2012.
- [23] D. Eisenhut, N. Moebs, E. Windels, D. Bergmann, I. Geiß, R. Reis, A. Strohmayer, Aircraft Requirements for Sustainable Regional Aviation, *Aerospace*. 8 (2021). <https://doi.org/10.3390/aerospace8030061>.
- [24] D.F. Finger, C. Braun, C. Bil, Impact of Battery Performance on the Initial Sizing of Hybrid-Electric General Aviation Aircraft, *J. Aerosp. Eng.* 33 (2020). [https://doi.org/10.1061/\(asce\)as.1943-5525.0001113](https://doi.org/10.1061/(asce)as.1943-5525.0001113).

- [25] J. Larsson, A. Elofsson, T. Sterner, J. Åkerman, International and national climate policies for aviation: a review, *Clim. Policy*. 19 (2019) 787–799. <https://doi.org/10.1080/14693062.2018.1562871>.
- [26] B. Kärcher, Formation and radiative forcing of contrail cirrus, *Nat. Commun.* 9 (2018) 1–17. <https://doi.org/10.1038/s41467-018-04068-0>.
- [27] V. Grewe, K. Dahlmann, J. Flink, C. Frömming, R. Ghosh, K. Gierens, R. Heller, J. Hendricks, P. Jöckel, S. Kaufmann, K. Kölker, F. Linke, T. Luchkova, B. Lührs, J. Van Manen, S. Matthes, A. Minikin, M. Niklaß, M. Plohr, M. Righi, S. Rosanka, A. Schmitt, U. Schumann, I. Terekhov, S. Unterstrasser, M. Vázquez-navarro, C. Voigt, K. Wicke, H. Yamashita, A. Zahn, H. Ziereis, Mitigating the Climate Impact from Aviation: Achievements and Results of the DLR WeCare Project, *Aerospace*. 4 (2017) 1–50. <https://doi.org/10.3390/aerospace4030034>.
- [28] Clean Aviation (CS3PG), Strategic Research and Innovation Agenda, 2020.
- [29] World Economic Forum, McKinsey & Company, Clean Skies for Tomorrow - Sustainable Aviation Fuels as a Pathway to Net-Zero Aviation - Insight Report, 2020.
- [30] S. Becken, B. Mackey, D.S. Lee, Science of the Total Environment Implications of preferential access to land and clean energy for Sustainable Aviation Fuels, *Sci. Total Environ.* 886 (2023) 163883. <https://doi.org/10.1016/j.scitotenv.2023.163883>.
- [31] C. Malins, The fat of the land - the impact of biofuel demand on the European market for rendered animal fats, 2023.
- [32] P. Schmidt, V. Batteiger, A. Roth, W. Weindorf, T. Raksha, Power-to-Liquids as Renewable Fuel Option for Aviation: A Review, *Chem. Ing. Tech.* 90 (2018) 127–140. <https://doi.org/10.1002/cite.201700129>.
- [33] F. Caiazzo, A. Agarwal, R.L. Speth, S.R.H. Barrett, Impact of biofuels on contrail warming, *Environ. Res. Lett.* 12 (2017). <https://doi.org/10.1088/1748-9326/aa893b>.
- [34] C. Pornet, Conceptual Design Methods for Sizing and Performance of Hybrid-Electric Transport Aircraft, Technische Universität München, 2018.
- [35] J. Hoelzen, Y. Liu, B. Bensmann, C. Winnefeld, A. Elham, J. Friedrichs, R. Hanke-Rauschenbach, Conceptual Design of Operation Strategies for Hybrid Electric Aircraft, *Energies*. 11 (2018) 1–26. <https://doi.org/10.3390/en11010217>.
- [36] M. Ponater, S. Marquart, L. Ström, K. Gierens, R. Sausen, G. Hüttig, On the potential of the cryoplane technology to reduce aircraft climate impact, *Proc. AAC-Conference, Friedrichshafen*. (2003) 316–321.
- [37] D. Verstraete, The Potential of Liquid Hydrogen for long range aircraft propulsion, Cranfield University, 2009.
- [38] A.J. Colozza, Hydrogen Storage for Aircraft Applications Overview, NASA, 2002.
- [39] D. Debney, S. Beddoes, M. Foster, D. James, E. Kay, O. Kay, K. Shawki, E. Stubbs, D. Thomas, K. Weider, R. Wilson, Zero-carbon Emission Aircraft Concepts, 2022.
- [40] S. Marquart, M. Ponater, L. Ström, K. Gierens, An upgraded estimate of the radiative forcing of cryoplane contrails, *Meteorol. Zeitschrift*. 14 (2005) 573–582. <https://doi.org/10.1127/0941-2948/2005/0057>.
- [41] E. Baharozu, G. Soykan, M.B. Ozerdem, Future aircraft concept in terms of energy efficiency and environmental factors, *Energy*. 140 (2017) 1368–1377. <https://doi.org/10.1016/j.energy.2017.09.007>.
- [42] Clean Sky 2 JU, FCH 2 JU, Hydrogen-powered aviation, Publications Office of the European Union, Luxembourg, 2020. <https://doi.org/10.2843/766989>.
- [43] ETC, Making Clean Electrification Possible: 30 Years to Electrify the Global Economy, 2021.
- [44] Hydrogen Council, McKinsey & Company, Hydrogen Insights - A perspective on hydrogen investment, market development and cost competitiveness, 2021.
- [45] Airbus SAS, Hydrogen - An energy carrier to fuel the climate-neutral aviation of tomorrow, 2021.
- [46] Universal Hydrogen, About Universal Hydrogen, (2021). <https://www.hydrogen.aero/about> (accessed August 9, 2021).
- [47] ZeroAvia, World First Hydrogen-Electric Passenger Plane Flight, (2020). <https://www.zeroavia.com/press-release-25-09-2020> (accessed April 8, 2021).
- [48] Choose Paris Region, H2 Hub Airport, (2021). <https://www.chooseparisregion.org/calls-for-applications/h2-hub-airport> (accessed September 8, 2021).
- [49] D. Silberhorn, G. Atanasov, J.-N. Walther, T. Zill, Assessment of Hydrogen Fuel Tank Integration At Aircraft Level, *Proc. Dtsch. Luft- Und Raumfahrtkongress*. (2019) 1–14.
- [50] P. Rompokos, A. Rolt, D. Nalianda, A.T. Isikveren, C. Senné, T. Gronstedt, H. Abedi, Synergistic technology combinations for future commercial aircraft using liquid hydrogen, *J. Eng. Gas Turbines Power*. 143 (2021). <https://doi.org/10.1115/1.4049694>.
- [51] G. Onorato, P. Proesmans, M.F.M. Hoogreef, Assessment of hydrogen transport aircraft: Effects of fuel tank integration, *CEAS Aeronaut. J.* 13 (2022) 813–845. <https://doi.org/10.1007/s13272-022-00601-6>.
- [52] J. Hoelzen, D. Silberhorn, T. Zill, B. Bensmann, R. Hanke-Rauschenbach, Hydrogen-powered aviation and its reliance on green hydrogen infrastructure - review and research gaps, *Int. J. Hydrogen Energy*. 47 (2022) 3108–3130. <https://doi.org/10.1016/j.ijhydene.2021.10.239>.
- [53] J.E. Johnson, The Economics of Liquid Hydrogen Supply for Air Transportation, *Adv. Cryog. Eng.* (1995) 12–22. [https://doi.org/10.1007/978-1-4613-9847-9\\_2](https://doi.org/10.1007/978-1-4613-9847-9_2).

- [54] G.D. Brewer, LH2 Airport Requirements study, NASA, Washington, 1976.
- [55] G.D. Brewer, Hydrogen Aircraft Technology, CRC Press, 1991. <https://doi.org/10.5772/intechopen.70078>.
- [56] P.F. Korycinski, Air terminals and liquid hydrogen commercial air transports, *Int. J. Hydrogen Energy*. 3 (1978) 231–250. [https://doi.org/10.1016/0360-3199\(78\)90021-6](https://doi.org/10.1016/0360-3199(78)90021-6).
- [57] The Boeing Commercial Airplane Company, An exploratory study to determine the integrated technological air transportation system ground requirements of liquid-hydrogen-fueled subsonic, long-haul civil air transports, 1976.
- [58] G.D. Brewer, Hydrogen usage in air transportation, *Int. J. Hydrogen Energy*. 3 (1978) 217–229. [https://doi.org/10.1016/0360-3199\(78\)90020-4](https://doi.org/10.1016/0360-3199(78)90020-4).
- [59] H.P. Alder, Hydrogen in Air Transportation - Feasibility Study for Zurich-Airport, Switzerland, *Int. J. Hydrogen Energy*. 12 (1987) 571–585. [https://doi.org/10.1016/0360-3199\(87\)90016-4](https://doi.org/10.1016/0360-3199(87)90016-4).
- [60] A. Contreras, S. Yiğit, K. Özyay, T.N. Veziroğlu, Hydrogen as aviation fuel: A comparison with hydrocarbon fuels, *Int. J. Hydrogen Energy*. 22 (1997) 1053–1060. [https://doi.org/10.1016/s0360-3199\(97\)00008-6](https://doi.org/10.1016/s0360-3199(97)00008-6).
- [61] U. Schmidtchen, E. Behrend, H.W. Pohl, N. Rostek, Hydrogen Aircraft and Airport Safety, *Renew. Sustain. Energy Rev.* 1 (1997) 239–269. [https://doi.org/10.1016/S1364-0321\(97\)00007-5](https://doi.org/10.1016/S1364-0321(97)00007-5).
- [62] Airbus Deutschland GmbH, Cryoplane: Liquid Hydrogen Fuelled Aircraft - Final Technical Report, 2003.
- [63] M.J. Sefain, Hydrogen Aircraft Concepts & Ground Support, Cranfield University, 2000.
- [64] F. Svensson, Potential of reducing the environmental impact of civil subsonic aviation by using liquid hydrogen, Cranfield University, 2005.
- [65] F. Haglind, A. Hasselrot, R. Singh, Potential of reducing the environmental impact of aviation by using hydrogen Part III: Optimum cruising altitude and airport implications, *Aeronaut. J.* 110 (2006) 553–565. <https://doi.org/10.1017/s0001924000013853>.
- [66] B. Khandelwal, A. Karakurt, P.R. Sekaran, V. Sethi, R. Singh, Hydrogen powered aircraft: The future of air transport, *Prog. Aerosp. Sci.* 60 (2013) 45–59. <https://doi.org/10.1016/j.paerosci.2012.12.002>.
- [67] C. Stiller, P. Schmidt, Airport liquid hydrogen infrastructure for aircraft auxiliary power units, *Proceeding 18th World Hydrog. Energy Conf. Essen, Ger.* 78 (2010) 422–429.
- [68] M. Janić, Greening commercial air transportation by using liquid hydrogen (LH2) as a fuel, *Int. J. Hydrogen Energy*. 39 (2014) 16426–16441. <https://doi.org/10.1016/j.ijhydene.2014.08.011>.
- [69] P. Stadler, Cost evaluation of large scale hydrogen production for the aviation industry, Ecole Polytechnique Federale De Lausanne, 2014.
- [70] M. Marksel, A.P. Brdink, R. Kamnik, L. Trainelli, C.E. Riboldi, A.L. Rolando, MAHEPA D10 .1: Ground infrastructure investment plan, 2019.
- [71] M. Marksel, A.B. Prapotnik, R. Kamnik, K. Hanžič, T. Letnik, S. Božičnik, Adaption of Airport Infrastructure for Operation of ICE-Hybrid and Fuel-Cell Aircraft, *Proc. Th ICTS, Portoroz.* (2020) 1–8.
- [72] C. Amy, A. Kunycky, Hydrogen as a renewable energy carrier for commercial aircraft, *ArXiv Prepr. ArXiv1910.05632.* (2019) 1–41.
- [73] R. Fusaro, V. Vercella, D. Ferretto, N. Viola, J. Steelant, Economic and environmental sustainability of liquid hydrogen fuel for hypersonic transportation systems, *CEAS Sp. J.* 12 (2020) 441–462. <https://doi.org/10.1007/s12567-020-00311-x>.
- [74] L. Jones, C. Wuschke, T.Z. Fahidy, Model of a Cryogenic Liquid-Hydrogen Pipeline For an Airport Ground Distribution System, *Int. J. Hydrogen Energy*. 8 (1983) 623–630. [https://doi.org/10.1016/0360-3199\(83\)90231-8](https://doi.org/10.1016/0360-3199(83)90231-8).
- [75] F.W. Armstrong, J.E. Allen, R.M. Denning, Fuel-related issues concerning the future of aviation, *Proc. Inst. Mech. Eng. Part G J. Aerosp. Eng.* 211 (1997) 1–11. <https://doi.org/10.1243/0954410971532451>.
- [76] C.M. Benson, P.G. Holborn, A.M. Rolt, J.M. Ingram, E. Alexander, Combined hazard analyses to explore the impact of liquid hydrogen fuel on the civil aviation industry, in: *Proc. ASME Turbo Expo 2020 - Turbomach. Tech. Conf. Expo. London, Engl., 2020*: pp. 1–12. <https://doi.org/10.1115/GT2020-14977>.
- [77] ISO, ISO/PAS 15594:2004 (E) - Airport hydrogen fuelling facility operations, 2004.
- [78] S. Rondinelli, R. Sabatini, A. Gardi, Challenges and Benefits offered by Liquid Hydrogen Fuels in Commercial Aviation, *Proc. Pract. Responses to Clim. Chang. 2014 (PRCC 2014)*, Barton, Aust. (2014) 1–11. <https://doi.org/10.13140/2.1.2658.9764>.
- [79] J.S. Schutte, A.P. Payan, S.I. Briceno, D.N. Mavris, Hydrogen-Powered Aircraft, *Encycl. Aerosp. Eng.* (2015). <https://doi.org/10.1002/9780470686652.eae1024>.
- [80] IRENA, Renewable Power Generation Costs in 2019, International Renewable Energy Agency, Abu Dhabi, 2020.
- [81] W. Burmeister, Hydrogen Project at Munich Airport, 2000.
- [82] K. Pehr, P. Sauermann, O. Traeger, M. Bracha, Liquid hydrogen for motor vehicles - The world's first public LH2 filling station, *Int. J. Hydrogen Energy*. 26 (2001) 777–782. [https://doi.org/10.1016/S0360-3199\(00\)00128-2](https://doi.org/10.1016/S0360-3199(00)00128-2).
- [83] E. Testa, C. Giammusso, M. Bruno, P. Maggiore, Analysis of environmental benefits resulting from use of hydrogen technology in handling operations at airports, *Clean Technol. Environ. Policy.* 16 (2014) 875–890. <https://doi.org/10.1007/s10098-013-0678-3>.

- [84] J.A. Stockford, C. Lawson, Z. Liu, Benefit and performance impact analysis of using hydrogen fuel cell powered e-Taxi system on A320 class airliner, *Aeronaut. J.* 123 (2019) 378–397. <https://doi.org/10.1017/aer.2018.156>.
- [85] C. Andrieux, X. Roboam, C. Turpin, B. Sareni, Energy modelling of a hydrogen hub (electricity, heat, transport vehicle) for future airports, *Symp. Génie Electrique, Univ. Lorraine, Nancy*. (2018). <https://doi.org/hal-02981850>.
- [86] J. Ochoa Robles, M. Giraud Billoud, C. Azzaro-Pantel, A.A. Aguilar-Lasserre, Optimal Design of a Sustainable Hydrogen Supply Chain Network: Application in an Airport Ecosystem, *ACS Sustain. Chem. Eng.* 7 (2019) 17587–17597. <https://doi.org/10.1021/acssuschemeng.9b02620>.
- [87] Y. Xiang, H. Cai, J. Liu, X. Zhang, Techno-economic design of energy systems for airport electrification: A hydrogen-solar-storage integrated microgrid solution, *Appl. Energy*. 283 (2021) 1–33. <https://doi.org/10.1016/j.apenergy.2020.116374>.
- [88] D.G. Victor, Liquid hydrogen aircraft and the greenhouse effect, *Int. J. Hydrogen Energy*. 15 (1990) 357–367. [https://doi.org/10.1016/0360-3199\(90\)90186-3](https://doi.org/10.1016/0360-3199(90)90186-3).
- [89] M. Janic, The potential of liquid hydrogen for the future “carbon-neutral” air transport system, *Transp. Res. Part D Transp. Environ.* 13 (2008) 428–435. <https://doi.org/10.1016/j.trd.2008.07.005>.
- [90] M. Janic, Is liquid hydrogen a solution for mitigating air pollution by airports?, *Int. J. Hydrogen Energy*. 35 (2010) 2190–2202. <https://doi.org/10.1016/j.ijhydene.2009.12.022>.
- [91] I. Yilmaz, M. Ilbaş, M. Taştan, C. Tarhan, Investigation of hydrogen usage in aviation industry, *Energy Convers. Manag.* 63 (2012) 63–69. <https://doi.org/10.1016/j.enconman.2011.12.032>.
- [92] I. Dincer, C. Acar, A review on potential use of hydrogen in aviation applications, *Int. J. Sustain. Aviat.* 2 (2016) 74–100. <https://doi.org/10.1504/ijsa.2016.076077>.
- [93] C. Penke, C. Falter, V. Batteiger, Pathways and environmental assessment for the introduction of renewable hydrogen into the aviation sector, *Sustain. Prod. Life Cycle Eng. Manag.* (2021) 41–52. [https://doi.org/10.1007/978-3-030-50519-6\\_4](https://doi.org/10.1007/978-3-030-50519-6_4).
- [94] A. Godula-Jopek, A. Westenberger, Hydrogen-fueled aeroplanes, *Compend. Hydrog. Energy*. (2016) 67–85. <https://doi.org/10.1016/b978-1-78242-364-5.00004-x>.
- [95] R. Merino-Martinez, F. Yin, E. Smeets, J. Aalders, The Cryo-V: Silent and Climate-Neutral Medium Range Aircraft Final DSE Report, TU Delft, 2020. <https://doi.org/10.13140/RG.2.2.31363.94241>.
- [96] L. Kotzur, L. Nolting, M. Hoffmann, T. Groß, A. Smolenko, J. Priesmann, H. Büsing, R. Beer, F. Kullmann, B. Singh, A. Praktijnjo, D. Stolten, M. Robinius, A modeler’s guide to handle complexity in energy system optimization, *Renew. Sustain. Energy Rev.* (2020).
- [97] N. Cooper, C. Horend, F. Röben, A. Bardow, N. Shay, A framework for the design & operation of a large-scale wind-powered hydrogen electrolyzer hub, *Int. J. Hydrogen Energy*. 47 (2022) 8671–8686. <https://doi.org/https://doi.org/10.1016/j.ijhydene.2021.12.225>.
- [98] M. Raab, R. Körner, R.U. Dietrich, Techno-economic assessment of renewable hydrogen production and the influence of grid participation, *Int. J. Hydrogen Energy*. 47 (2022) 26798–26811. <https://doi.org/10.1016/j.ijhydene.2022.06.038>.
- [99] P.M. Heuser, D.S. Ryberg, T. Grube, M. Robinius, D. Stolten, Techno-economic analysis of a potential energy trading link between Patagonia and Japan based on CO<sub>2</sub> free hydrogen, *Int. J. Hydrogen Energy*. 44 (2019) 12733–12747. <https://doi.org/10.1016/j.ijhydene.2018.12.156>.
- [100] S. Oliva H., M. Garcia G., Investigating the impact of variable energy prices and renewable generation on the annualized cost of hydrogen, *Int. J. Hydrogen Energy*. (2023). <https://doi.org/10.1016/j.ijhydene.2022.12.304>.
- [101] A. Hofrichter, D. Rank, M. Heberl, M. Sterner, Determination of the optimal power ratio between electrolysis and renewable energy to investigate the effects on the hydrogen production costs, *Int. J. Hydrogen Energy*. 48 (2023) 1651–1663. <https://doi.org/10.1016/j.ijhydene.2022.09.263>.
- [102] W. Maurer, P. Rechberger, M. Justl, R. Keuschnigg, Parameter study for dimensioning of a PV optimized hydrogen supply plant, *Int. J. Hydrogen Energy*. 47 (2022) 40815–40825. <https://doi.org/https://doi.org/10.1016/j.ijhydene.2022.09.183>.
- [103] P.M. Heuser, T. Grube, H. Heinrichs, M. Robinius, D. Stolten, Worldwide Hydrogen Provision Scheme Based on Renewable Energy, (2020) 1–27.
- [104] M. Robinius, P. Markewitz, P. Lopion, F. Kullmann, P.-M. Heuser, K. Syranidis, S. Cerniauskas, T. Schöb, M. Reuß, S. Ryberg, L. Kotzur, D. Caglayan, L. Welder, J. Linßen, T. Grube, H. Heinrichs, P. Stenzel, D. Stolten, Wege für die Energiewende - Kosteneffiziente und klimagerechte Transformationsstrategie für das deutsche Energiesystem bis zum Jahr 2050, Forschungszentrum Jülich GmbH, 2020.
- [105] M. Reuß, T. Grube, M. Robinius, D. Stolten, A hydrogen supply chain with spatial resolution: Comparative analysis of infrastructure technologies in Germany, *Appl. Energy*. 247 (2019) 438–453. <https://doi.org/10.1016/j.apenergy.2019.04.064>.
- [106] M. Reuß, T. Grube, M. Robinius, P. Preuster, P. Wasserscheid, D. Stolten, Seasonal storage and alternative carriers: A flexible hydrogen supply chain model, *Appl. Energy*. 200 (2017) 290–302. <https://doi.org/10.1016/j.apenergy.2017.05.050>.
- [107] J.O. Robles, S.D.L. Almaraz, C. Azzaro-Pantel, Optimization of a Hydrogen Supply Chain Network



- Design by Multi-Objective Genetic Algorithms, Elsevier Masson SAS, 2016. <https://doi.org/10.1016/B978-0-444-63428-3.50139-9>.
- [108] S. De-León Almaraz, C. Azzaro-Pantel, L. Montastruc, M. Boix, Deployment of a hydrogen supply chain by multi-objective/multi-period optimisation at regional and national scales, *Chem. Eng. Res. Des.* 104 (2015) 11–31. <https://doi.org/10.1016/j.cherd.2015.07.005>.
- [109] S. De-León Almaraz, C. Azzaro-Pantel, L. Montastruc, S. Domenech, Hydrogen supply chain optimization for deployment scenarios in the Midi-Pyrénées region, France, *Int. J. Hydrogen Energy.* 39 (2014) 11831–11845. <https://doi.org/10.1016/j.ijhydene.2014.05.165>.
- [110] J.O. Robles, S.D.L. Almaraz, C. Azzaro-Pantel, Hydrogen supply chain design: Key technological components and sustainable assessment, 2018. <https://doi.org/10.1016/B978-0-12-811197-0.00002-6>.
- [111] L. Sens, Y. Piguel, U. Neuling, S. Timmerberg, K. Wilbrand, M. Kaltschmitt, Cost minimized hydrogen from solar and wind – Production and supply in the European catchment area, *Energy Convers. Manag.* 265 (2022) 115742. <https://doi.org/10.1016/j.enconman.2022.115742>.
- [112] J. Hoelzen, M. Flohr, J. Mangold, A. Bensmann, R. Hanke-Rauschenbach, H<sub>2</sub>-powered aviation at airports – Design and economics of LH<sub>2</sub> refueling systems, *Energy Convers. Manag.* X. 14 (2022) 100206. <https://doi.org/10.1016/j.ecmx.2022.100206>.
- [113] IATA, IATA - Fuel Price Monitor, (n.d.). <https://www.iata.org/en/publications/economics/fuel-monitor/> (accessed April 8, 2021).
- [114] U.S. Energy Information Administration, Annual Energy Outlook 2021, 2021.
- [115] J. Mangold, D. Silberhorn, N. Moebis, N. Dzikus, J. Hoelzen, T. Zill, A. Strohmayer, Refueling of LH<sub>2</sub> Aircraft—Assessment of Turnaround Procedures and Aircraft Design Implication, *Energies.* 15 (2022) 2475. <https://doi.org/10.3390/en15072475>.
- [116] Mott MacDonald, Connected Places Catapult, Feasibility of Zero Emissions Airport Operations in England by 2040, 2022.
- [117] Connected Places Catapult, Zero Emission Flight Infrastructure Standards Action Plan, 2023.
- [118] G. Le Bris, L.-G. Nguyen, B. Tagoe, P. Jonat, C.Y. Justin, E. Reindel, K.B. Preston, P.J. Ansell, Preparing Your Airport for Electric Aircraft and Hydrogen Technologies, The National Academies Press, Washington DC, 2022. <https://doi.org/10.17226/26512>.
- [119] M. Scott, H. Clarke, Analysing the costs of hydrogen aircraft, Brussels, 2023.
- [120] A. Prapotnik Brdnik, R. Kamnik, S. Bozicnik, M. Marksel, Ground infrastructure investments for operation of hybrid-electric aircraft, *IOP Conf. Ser. Mater. Sci. Eng.* 1226 (2022) 012073. <https://doi.org/10.1088/1757-899x/1226/1/012073>.
- [121] P. Ansell, K. Haran, P. Laskaridis, Hydrogen-Electric Aircraft Technologies, 2022.
- [122] A. Postma-Kurlanc, H. Leadbetter, C. Pickard, Hydrogen Infrastructure and Operations - Airports, Airlines and Airspace, 2022. [https://doi.org/10.1007/978-4-431-56042-5\\_40](https://doi.org/10.1007/978-4-431-56042-5_40).
- [123] D. Silberhorn, K. Dahlmann, A. Görtz, F. Linke, J. Zanger, B. Rauch, T. Methling, C. Janzer, J. Hartmann, Climate Impact Reduction Potentials of Synthetic Kerosene and Green Hydrogen Powered Mid-Range Aircraft Concepts, *Appl. Sci.* 12 (2022). <https://doi.org/10.3390/app12125950>.
- [124] K. Dahal, S. Brynolf, C. Xisto, J. Hansson, M. Grahn, T. Grönstedt, M. Lehtveer, Techno-economic review of alternative fuels and propulsion systems for the aviation sector, *Renew. Sustain. Energy Rev.* 151 (2021). <https://doi.org/10.1016/j.rser.2021.111564>.
- [125] D. Silberhorn, J. Hartmann, N. Dzikus, G. Atanasov, T. Zill, J.C. Gomez Trillos, M. Oswald, U. Brand, T. Vogt, W. Grimme, The air-vehicle as a complex system of air transport energy systems, *Aiaa Aviat. 2020 Forum.* (2020) 1–25. <https://doi.org/10.2514/6.2020-2622>.
- [126] K. Kossarev, A.E. Scholz, M. Hornung, Comparative environmental life cycle assessment and operating cost analysis of long-range hydrogen and biofuel fueled transport aircraft, *CEAS Aeronaut. J.* (2022). <https://doi.org/10.1007/s13272-022-00627-w>.
- [127] F. Troeltsch, M. Engelman, F. Peter, J. Kaiser, M. Hornung, A.E. Scholz, Hydrogen Powered Long Haul Aircraft with Minimized Climate Impact, *Aiaa Aviat. 2020 Forum.* (2020) 14. <https://doi.org/10.2514/6.2020-2660>.
- [128] J. Mukhopadhaya, D. Rutherford, Performance Analysis of Evolutionary Hydrogen-Powered Aircraft, Washington DC, 2022.
- [129] J. Cole, W. McClintock, L. Powis, Market Forecasts & Strategy, 2022. [https://doi.org/10.1016/0140-3664\(90\)90181-f](https://doi.org/10.1016/0140-3664(90)90181-f).
- [130] Project Napkin, Making Zero-carbon Emission Flight a Reality in the UK Final Report - Project NAPKIN, 2022.
- [131] Hydrogen Council, Hydrogen decarbonization pathways - A life-cycle assessment, 2021.
- [132] European Commission, Commission delegated regulation (EU) of 10.2.2023, Brussels, 2023.
- [133] IEA - International Energy Agency, Renewables 2022 - Analysis forecast to 2027, Paris, 2022. <https://www.iea.org/reports/renewables-2022>; License: CC BY 4.0.
- [134] IRENA, Renewable Power Generation Costs in 2021, Abu Dhabi, 2022.
- [135] S. Afanasyeva, D. Bogdanov, C. Breyer, Relevance of PV with single-axis tracking for energy scenarios,

- Sol. Energy. 173 (2018) 173–191. <https://doi.org/10.1016/j.solener.2018.07.029>.
- [136] R. Wiser, M. Bolinger, B. Hoen, D. Millstein, J. Rand, G. Barbose, N. Darghouth, W. Gorman, S. Jeong, B. Paulos, Land-based wind market report: 2022 edition, 2022.
- [137] Global Wind Energy Council, GWEC Global Wind Report 2022, Brussels, 2022.
- [138] W. Musial, P. Spitsen, P. Duffy, P. Beiter, M. Marquis, R. Hammond, M. Shields, Offshore Wind Market Report: 2022 Edition, 2022.
- [139] T.M. Gür, Review of electrical energy storage technologies, materials and systems: Challenges and prospects for large-scale grid storage, *Energy Environ. Sci.* 11 (2018) 2696–2767. <https://doi.org/10.1039/c8ee01419a>.
- [140] P. Denholm, W. Cole, A.W. Frazier, K. Podkaminer, N. Blair, Storage Futures Study - The Challenge of Defining Long-Duration Energy Storage, 2021.
- [141] IRENA, Innovations landscape brief: Utility-Scale Batteries, Abu Dhabi, 2019.
- [142] Hydrogen Council, Path to hydrogen competitiveness - A cost perspective, 2020.
- [143] A. Buttler, H. Spliethoff, Current status of water electrolysis for energy storage, grid balancing and sector coupling via power-to-gas and power-to-liquids: A review, *Renew. Sustain. Energy Rev.* 82 (2018) 2440–2454. <https://doi.org/10.1016/j.rser.2017.09.003>.
- [144] T. Smolinka, N. Wiebe, P. Sterchele, A. Palzer, F. Lehner, M. Jansen, S. Kiemel, R. Mieke, S. Wahren, F. Zimmermann, Studie IndWEde, Bundesministerium für Verkehr und digitale Infrastruktur (BMVI), 2018.
- [145] IRENA, Green Hydrogen Cost Reduction: Scaling up Electrolysers to meet the 1.5°C Climate Goal, Abu Dhabi, 2020.
- [146] S.M. Saba, M. Mu, M. Robinius, D. Stolten, The investment costs of electrolysis - A comparison of cost studies from the past 30 years, *Int. J. Hydrogen Energy.* 43 (2018) 1209–1223. <https://doi.org/10.1016/j.ijhydene.2017.11.115>.
- [147] J. Proost, State-of-the art CAPEX data for water electrolysers, and their impact on renewable hydrogen price settings, *Int. J. Hydrogen Energy.* 44 (2018) 4406–4413. <https://doi.org/10.1016/j.ijhydene.2018.07.164>.
- [148] L. Bertuccioli, A. Chan, D. Hart, F. Lehner, B. Madden, E. Standen, Development of Water Electrolysis in the European Union, 2014.
- [149] F. Schenke, J. Hoelzen, C. Minke, A. Bensmann, R. Hanke-Rauschenbach, Resource requirements for the implementation of a global H<sub>2</sub>-powered aviation, *Energy Convers. Manag.* X. 20 (2023) 100435. <https://doi.org/10.1016/j.ecmx.2023.100435>.
- [150] C. Minke, M. Suermann, B. Bensmann, R. Hanke-Rauschenbach, Is iridium demand a potential bottleneck in the realization of large-scale PEM water electrolysis?, *Int. J. Hydrogen Energy.* 46 (2021) 23581–23590. <https://doi.org/10.1016/j.ijhydene.2021.04.174>.
- [151] G. Sdanghi, G. Maranzana, A. Celzard, V. Fierro, Review of the current technologies and performances of hydrogen compression for stationary and automotive applications, *Renew. Sustain. Energy Rev.* 102 (2019) 150–170. <https://doi.org/10.1016/j.rser.2018.11.028>.
- [152] Hydrogen and Fuel Cell Technologies Office, 3.2 Hydrogen Delivery, 2015.
- [153] U.F. Cardella, Large-scale hydrogen liquefaction under the aspect of economic viability, Technische Universität München, 2018.
- [154] Concepts NREC, Development Of A Centrifugal Hydrogen Pipeline Gas Compressor - Final Report, 2015.
- [155] U. Büniger, J. Michalski, F. Crotonino, O. Kruck, Large-scale underground storage of hydrogen for the grid integration of renewable energy and other applications, Elsevier Ltd., 2016. <https://doi.org/10.1016/b978-1-78242-364-5.00007-5>.
- [156] R.K. Ahluwalia, D.D. Papadimas, J.-K. Peng, H.S. Roh, System Level Analysis of Hydrogen Storage Options, 2019.
- [157] A.S. Lord, P.H. Kobos, D.J. Borns, Geologic storage of hydrogen: Scaling up to meet city transportation demands, *Int. J. Hydrogen Energy.* 39 (2014) 15570–15582. <https://doi.org/10.1016/j.ijhydene.2014.07.121>.
- [158] F. Crotonino, S. Donadei, U. Büniger, H. Lindinger, Large-Scale Hydrogen Underground Storage for Securing Future Energy Supplies, 18th World Hydrog. Energy Conf. 2010. 78 (2010) 10.
- [159] A.S. Lord, P.H. Kobos, G.T. Klise, D.J. Borns, A life cycle cost analysis framework for geologic storage of hydrogen: A user's tool, Albuquerque, 2011.
- [160] J. Michalski, U. Büniger, F. Crotonino, S. Donadei, G.S. Schneider, T. Pregger, K.K. Cao, D. Heide, Hydrogen generation by electrolysis and storage in salt caverns: Potentials, economics and systems aspects with regard to the German energy transition, *Int. J. Hydrogen Energy.* 42 (2017) 13427–13443. <https://doi.org/10.1016/j.ijhydene.2017.02.102>.
- [161] G. Hévin, Underground storage of Hydrogen in salt caverns, 2019.
- [162] C. Yang, J. Ogden, Determining the lowest-cost hydrogen delivery mode, *Int. J. Hydrogen Energy.* 32 (2007) 268–286. <https://doi.org/10.1016/j.ijhydene.2006.05.009>.
- [163] A. Wang, K. Van der Leun, D. Peters, M. Buseman, European Hydrogen Backbone, 2020.

- [164] A. Wang, J. Jens, D. Mavins, M. Moultak, M. Schimmel, K. Van der Leun, D. Peters, M. Buseman, European Hydrogen Backbone - Analysing future demand, supply, and transport of hydrogen, 2021.
- [165] N. Pieton, H. Abdel-Khalek, M. Graf, B. Drechsler, V. Lenivova, C. Nolden, E. Bergup, M. Fuhad Anwar Sinha, J. Fragoso, K. Franke, C. Kleinschmitt, V.P. Müller, M. Wietschel, M. Holst, F. Weise, C. Voglstätter, Export Potentials of Green Hydrogen – Methodology for a Techno-Economic Assessment, 2023.
- [166] J. Jens, A. Wang, K. van der Leun, D. Peters, M. Buseman, Extending the European Hydrogen Backbone, 2021.
- [167] M. Reuß, T. Grube, M. Robinius, D. Stolten, A hydrogen supply chain with spatial resolution: Comparative analysis of infrastructure technologies in Germany, *Appl. Energy*. 247 (2019) 438–453. <https://doi.org/10.1016/j.apenergy.2019.04.064>.
- [168] D. Krieg, Konzept und Kosten eines Pipelinesystems zur Versorgung des deutschen Straßenverkehrs mit Wasserstoff, 2012.
- [169] G. Wilson, P. Rowley, Flexibility in Great Britain 's gas networks: analysis of linepack and linepack flexibility using hourly data, *UK Energy Res. Cent.* May (2019). <https://doi.org/10.5286/ukerc.edc.000947>.
- [170] J.W. Leachman, R.T. Jacobsen, S.G. Penoncello, E.W. Lemmon, Fundamental equations of state for parahydrogen, normal hydrogen, and orthohydrogen, *J. Phys. Chem. Ref. Data*. 38 (2009) 721–748. <https://doi.org/10.1063/1.3160306>.
- [171] G.E. McIntosh, Applications of ortho-para hydrogen catalyst, *IOP Conf. Ser. Mater. Sci. Eng.* 101 (2015) 1–5. <https://doi.org/10.1088/1757-899X/101/1/012079>.
- [172] G.E. Schmauch, Technical aspects of ortho-parahydrogen conversion, *Ind. Eng. Chem.* 56 (1964) 20–31. <https://doi.org/10.1021/ie50653a003>.
- [173] E. Tzimas, C. Filiou, S.D. Petevs, J. Veyret, Hydrogen Storage : State-of-the-Art and Future Perspective, 2003.
- [174] J. Essler, C. Haberstroh, H.T. Walnum, D. Berstad, P. Nekså, J. Stang, S.A. Energi, L. Decker, P. Treite, L.A. Kryotechnik, Report on Technology Overview and Barriers to Energy- and Cost-Efficient Large Scale Hydrogen Liquefaction, 2012.
- [175] T. Zhang, J. Uratani, Y. Huang, L. Xu, S. Griffiths, Y. Ding, Hydrogen liquefaction and storage: Recent progress and perspectives, *Renew. Sustain. Energy Rev.* 176 (2023) 113204. <https://doi.org/10.1016/j.rser.2023.113204>.
- [176] H. Eichseder, M. Klell, Speicherung und Transport, in: *Wasserst. Der Fahrzeugtechnik*, Vieweg+Teubner, Wiesbaden, 2008: pp. 85–138. [https://doi.org/10.1007/978-3-8348-9503-5\\_5](https://doi.org/10.1007/978-3-8348-9503-5_5).
- [177] M. Aasadnia, M. Mehrpooya, Large-scale liquid hydrogen production methods and approaches: A review, *Appl. Energy*. 212 (2018) 57–83. <https://doi.org/10.1016/j.apenergy.2017.12.033>.
- [178] M. Aasadnia, M. Mehrpooya, Conceptual design and analysis of a novel process for hydrogen liquefaction assisted by absorption precooling system, *J. Clean. Prod.* 205 (2018) 565–588. <https://doi.org/10.1016/j.jclepro.2018.09.001>.
- [179] A.B. Fradkov, V.F. Troitskii, Liquefier with two-stage conversion to obtain 98 per cent parahydrogen, *Cryogenics (Guildf)*. 5 (1965) 136–137. [https://doi.org/10.1016/0011-2275\(65\)90004-4](https://doi.org/10.1016/0011-2275(65)90004-4).
- [180] R.M. Bliesner, Parahydrogen-Orthohydrogen Conversion for Boil-Off Reduction From Space Stage, (2013).
- [181] H. Quack, J. Essler, C. Haberstroh, P. Nekså, D. Berstad, M. Drescher, J. Stang, H.T. Walnum, L. Decker, P. Treite, Boundary Conditions and assumptions Influencing the Power Needed to Liquefy Hydrogen, 2012.
- [182] K. Stolzenburg, R. Mubbala, Integrated Design for Demonstration of Efficient Liquefaction of Hydrogen (IDEALHY), Fuel Cells and Hydrogen Joint Undertaking, 2013.
- [183] W. Peschka, Liquid Hydrogen, Springer Vienna, Vienna, 1992. <https://doi.org/10.1007/978-3-7091-9126-2>.
- [184] M. Aasadnia, M. Mehrpooya, A novel hydrogen liquefaction process configuration with combined mixed refrigerant systems, *Int. J. Hydrogen Energy*. 42 (2017) 15564–15585. <https://doi.org/10.1016/j.ijhydene.2017.04.260>.
- [185] H. Rezaie, K. Nasir, M. Ziabasharhagh, A review of hydrogen liquefaction, current situation and its future, (2021). <https://www.researchgate.net/publication/349483353>.
- [186] U. Cardella, L. Decker, H. Klein, Roadmap to economically viable hydrogen liquefaction, *Int. J. Hydrogen Energy*. 42 (2017) 13329–13338. <https://doi.org/10.1016/j.ijhydene.2017.01.068>.
- [187] K. Stolzenburg, D. Berstad, L. Decker, A. Elliott, C. Haberstroh, C. Hatto, M. Klaus, N.D. Mortimer, R. Mubbala, O. Mwabonje, P. Nekså, H. Quack, J.H.R. Rix, I. Seemann, H.T. Walnum, Efficient Liquefaction of Hydrogen: Results of the IDEALHY Project, *Proc. Energy. – Symp. Stralsund/Germany*, Novemb. (2013) p.1-8.
- [188] D. Berstad, G. Skaugen, Ø. Wilhelmsen, Dissecting the exergy balance of a hydrogen liquefier: Analysis of a scaled-up claudé hydrogen liquefier with mixed refrigerant pre-cooling, *Int. J. Hydrogen Energy*. 46 (2021) 8014–8029. <https://doi.org/10.1016/j.ijhydene.2020.09.188>.

- [189] M.S. Sadaghiani, M. Mehrpooya, Introducing and energy analysis of a novel cryogenic hydrogen liquefaction process configuration, *Int. J. Hydrogen Energy*. 42 (2017) 6033–6050. <https://doi.org/10.1016/j.ijhydene.2017.01.136>.
- [190] Airports Council International, Aerospace Technology Institute, Integration of Hydrogen Aircraft into the Air Transport System, 2021.
- [191] M. Kuhn, Storage Density of Hydrogen under certain pressure and temperature conditions, (2015).
- [192] W.U. Notardonato, A.M. Swanger, J.E. Fesmire, K.M. Jumper, W.L. Johnson, T.M. Tomsik, Zero boil-off methods for large-scale liquid hydrogen tanks using integrated refrigeration and storage, *IOP Conf. Ser. Mater. Sci. Eng.* 278 (2017). <https://doi.org/10.1088/1757-899X/278/1/012012>.
- [193] J.E. Fesmire, A. Swanger, DOE / NASA Advances in Liquid Hydrogen Storage Workshop, 2021.
- [194] M. Klell, Handbook of Hydrogen Storage - 1 Storage of Hydrogen in the Pure Form, Wiley-VCH Verlag GmbH & Co. KGaA, Weinheim, 2010. <https://doi.org/10.1002/9783527629800.ch1>.
- [195] G. Petitpas, A.J. Simon, J. Moreno-blanco, S.M. Aceves, Liquid Hydrogen Infrastructure Analysis, DOE Hydrog. Fuel Cells Annu. Merit Rev. Washingt. D.C. June 6th, 2017. (2017).
- [196] Cryostar, Hydrogen Expanders and Pumps, (2019).
- [197] Nexant, Air Liquide, Argonne National Laboratory, Chevron Technology Venture, Gas Technology Institute, The National Renewable Energy Laboratory, Pacific Northwest National Laboratory, TIAX LLC, H2A Hydrogen Delivery Infrastructure Analysis Models and Conventional Pathway Options Analysis Results, 2008.
- [198] M.E. Reuß, Techno-ökonomische Analyse alternativer Wasserstoffinfrastruktur, Schriften, Forschungszentrum Jülich GmbH Zentralbibliothek, Verlag, 2019.
- [199] S. Kamiya, World's first ocean going liquid hydrogen carrier, 2021.
- [200] Kawasaki Heavy Industries Ltd., Kawasaki Technical Review, Special Issue on Hydrogen Energy Supply Chain, No. 182. (2021).
- [201] D. Berstad, S. Gardarsdottir, S. Roussanaly, M. Voldsund, Y. Ishimoto, P. Neksa, Liquid hydrogen as prospective energy carrier: A brief review and discussion of underlying assumptions applied in value chain analysis, *Renew. Sustain. Energy Rev.* 154 (2022) 111772. <https://doi.org/10.1016/j.rser.2021.111772>.
- [202] NCE Maritime Cleantech, Norwegian future value chains for liquid hydrogen, 2019.
- [203] Y. Ishimoto, M. Voldsund, P. Neksa, S. Roussanaly, D. Berstad, S.O. Gardarsdottir, Large-scale production and transport of hydrogen from Norway to Europe and Japan : Value chain analysis and comparison of liquid hydrogen and ammonia as energy carriers, *Int. J. Hydrogen Energy*. 45 (2020) 32865–32883. <https://doi.org/10.1016/j.ijhydene.2020.09.017>.
- [204] A.N. Alkhaledi, S. Sampath, P. Pilidis, A hydrogen fuelled LH2 tanker ship design, *Ships Offshore Struct.* 17 (2021) 1555–1564. <https://doi.org/10.1080/17445302.2021.1935626>.
- [205] G.D. Brewer, LH2 Airport Requirements Study, 1976.
- [206] V. Vercella, M. Fioriti, N. Viola, Towards a methodology for new technologies assessment in aircraft operating cost, *Proc. Inst. Mech. Eng. Part G J. Aerosp. Eng.* 235 (2020) 879–892. <https://doi.org/10.1177/0954410020964675>.
- [207] M.A. Camilleri, Aircraft Operating Costs and Profitability, in: *Travel Mark. Tour. Econ. Airl. Prod.*, Springer Nature, Cham (Switzerland), 2018: pp. 191–204.
- [208] NASA, Technology Facts: Winglets, 2004.
- [209] J. Thorbeck, DOC-Assessment Method, TU Berlin, 2013. [https://www.fzt.haw-hamburg.de/pers/Scholz/Aero/TU-Berlin\\_DOC-Method\\_with\\_remarks\\_13-09-19.pdf](https://www.fzt.haw-hamburg.de/pers/Scholz/Aero/TU-Berlin_DOC-Method_with_remarks_13-09-19.pdf) (accessed April 8, 2021).
- [210] A. Bain, Sourcebook for Hydrogen Applications, TISEC, 1998.
- [211] German Airports Association (ADV), ADV Monthly Traffic Report, Berlin, 2020.
- [212] Hamburg Airport, Starts 2019 - Linien- und Touristikverkehr, 2021.
- [213] Boeing, Commercial market outlook 2020-2039, 2020.
- [214] V. Grewe, A.G. Rao, T. Grönstedt, C. Xisto, F. Linke, J. Melkert, J. Middel, B. Ohlenforst, S. Blakey, S. Christie, S. Matthes, K. Dahlmann, Supplementary material: Grewe et al., Evaluating the climate impact of aviation emission scenarios towards the Paris Agreement including COVID-19 effects, *Nat. Commun.* (2021) 1–42. <https://doi.org/10.1038/s41467-021-24091-y>.
- [215] F. Ueckerdt, C. Bauer, A. Dirnacher, J. Everall, R. Sacchi, G. Luderer, Potential and risks of hydrogen-based e-fuels in climate change mitigation, *Nat. Clim. Chang.* 11 (2021) 384–393. <https://doi.org/10.1038/s41558-021-01032-7>.
- [216] I. Staffell, D. Scamman, A. Velazquez Abad, P. Balcombe, P.E. Dodds, P. Ekins, N. Shah, K.R. Ward, The role of hydrogen and fuel cells in the global energy system, *Energy Environ. Sci.* 12 (2019) 463–491. <https://doi.org/10.1039/c8ee01157e>.
- [217] H2MOBILITY, Overview Hydrogen Refuelling for Heavy Duty Vehicles, 2021.
- [218] Alstom, Weltweit erste Wasserstofftankstelle für Passagierzüge entsteht in Bremervörde, 2020.

- [219] DB AG, Deutsche Bahn Daten & Fakten 2019, 2019.
- [220] Energy Transitions Commission, Making the Hydrogen Economy Possible, 2021.
- [221] L. Van Hoecke, L. Laffineur, R. Campe, P. Perreault, S.W. Verbruggen, S. Lenaerts, Challenges in the use of hydrogen for maritime applications, *Energy Environ. Sci.* 14 (2021) 815–843. <https://doi.org/10.1039/d0ee01545h>.
- [222] C.J. McKinlay, S.R. Turnock, D.A. Hudson, Route to zero emission shipping: Hydrogen, ammonia or methanol?, *Int. J. Hydrogen Energy.* 46 (2021) 28282–28297. <https://doi.org/10.1016/j.ijhydene.2021.06.066>.
- [223] Wirtschaftsvereinigung Stahl, Fakten zur Stahlindustrie in Deutschland 2020, 2020.
- [224] A. Otto, M. Robinius, T. Grube, S. Schiebahn, A. Praktiknjo, D. Stolten, Power-to-Steel : Reducing CO 2 through the Integration of Renewable Energy and Hydrogen into the German Steel Industry, *Energies.* 10 (2017). <https://doi.org/10.3390/en10040451>.
- [225] L. Welder, D.S. Ryberg, L. Kotzur, T. Grube, M. Robinius, D. Stolten, Spatio-temporal optimization of a future energy system for power-to-hydrogen applications in Germany, *Energy.* 158 (2018) 1130–1149. <https://doi.org/10.1016/j.energy.2018.05.059>.
- [226] C. Kurrer, The potential of hydrogen for decarbonising steel production, 2020.
- [227] Ammonia Energy Association, Yara and Nel collaborate to reduce electrolyzer costs; announce green ammonia pilot in Norway by 2022, (2019). <https://www.ammoniaenergy.org/articles/yara-and-nel-collaborate-to-reduce-electrolyzer-costs-announce-green-ammonia-pilot-in-norway-by-2022/> (accessed June 5, 2021).
- [228] Cirium, Diio Mi airline schedule database, 2021.
- [229] D. Teichmann, W. Arlt, P. Wasserscheid, R. Freymann, A future energy supply based on Liquid Organic Hydrogen Carriers (LOHC), *Energy Environ. Sci.* 4 (2011) 2767–2773. <https://doi.org/10.1039/c1ee01454d>.
- [230] N.J. Ashford, S. Mumayiz, P.H. Wright, *Airport Engineering: Planning, Design, and Development of 21st Century Airports: Fourth Edition*, 2011. <https://doi.org/10.1002/9780470950074>.
- [231] National Academies of Science Engineering and Medicine, *Overview of Airport Fueling Operations*, The National Academies Press, Washington DC, 2015. <https://doi.org/10.17226/22141>.
- [232] M. Hromádka, A. Cíger, Hydrant refueling system as an optimisation of aircraft refuelling, *Transp. Probl.* 10 (2015) 61–71. <https://doi.org/10.21307/tp-2015-035>.
- [233] C. Ozores, *Planning of Aviation Fuel Concessions*, 2014.
- [234] International Civil Aviation Organization, *ICAO's Policies on Charges for Airports and Air Navigation Services*, 2004.
- [235] International Civil Aviation Organization, *Manual on Civil Aviation Jet Fuel Supply*, 2012.
- [236] OJ L 197, Directive 2012/18/EU of the European Parliament and of the Council of 4 July 2012 on the control of major-accident hazards involving dangerous substances, amending and subsequently repealing Council Directive 96/82/EC Text with EEA relevance, *Off. J. Eur. Union.* (2012) 1–37.
- [237] OJ L 96, Directive 2014/34/EU of the European Parliament and of the Council of 26 February 2014 on the harmonisation of the laws of the Member States relating to equipment and protective systems intended for use in potentially explosive atmospheres (recast) Text w, *Off. J. Eur. Union.* (2014) 309–356.
- [238] OJ L 334, Directive 2010/75/EU of the European Parliament and of the Council of 24 November 2010 on industrial emissions (integrated pollution prevention and control) Text with EEA relevance, *Off. J. Eur. Union.* (2010) 17–119.
- [239] J. Hoelzen, L. Koenemann, L. Kister, F. Schenke, A. Bensmann, R. Hanke-Rauschenbach, H2-powered aviation – Design and economics of green LH2 supply for airports, *Energy Convers. Manag.* X. August (2023). <https://doi.org/10.1016/j.ecmx.2023.100442>.
- [240] S. Gronau, J. Hoelzen, T. Mueller, R. Hanke-Rauschenbach, Hydrogen-powered aviation in Germany: A macroeconomic perspective and methodological approach of fuel supply chain integration into an economy-wide dataset, *Int. J. Hydrogen Energy.* 48 (2023) 5347–5376. <https://doi.org/10.1016/j.ijhydene.2022.10.168>.
- [241] T. Mueller, S. Gronau, Fostering Macroeconomic Research on Hydrogen-Powered Aviation: A Systematic Literature Review on General Equilibrium Models, *Energies.* 16 (2023) 109–134. <https://doi.org/10.3390/en16031439>.
- [242] M. Janic, Modelling the full costs of an intermodal and road freight transport network, *Transp. Res. Part D Transp. Environ.* 12 (2007) 33–44. <https://doi.org/10.1016/j.trd.2006.10.004>.
- [243] Bloomberg, *Airbus Warns Lack of Infrastructure May Delay Hydrogen Plane*, (2022). <https://www.bloomberg.com/news/articles/2022-11-30/airbus-warns-lack-of-infrastructure-may-delay-hydrogen-aircraft> (accessed December 1, 2022).
- [244] C. Kost, S. Shammugam, V. Fluri, D. Peper, A.D. Memar, T. Schlegl, *Stromgestehungskosten Erneuerbare Energien*, 2021.
- [245] N.R.E.L. (NREL), *2022 Annual Technology Baseline (ATB) Cost and Performance Data for Electricity Generation Technologies [data set]*, 2022. <https://doi.org/10.25984/1871952>.

- [246] FCHEA, Roadmap to a US Hydrogen Economy, 2021.
- [247] European Technology & Innovation Platform PV, Fact sheets about photovoltaics: PV the cheapest electricity source almost everywhere, 2020.
- [248] L. Sens, U. Neuling, M. Kaltschmitt, Capital expenditure and levelized cost of electricity of photovoltaic plants and wind turbines – Development by 2050, *Renew. Energy*. 185 (2022) 525–537. <https://doi.org/10.1016/j.renene.2021.12.042>.
- [249] R. Wiser, J. Rand, J. Seel, P. Beiter, E. Baker, E. Lantz, P. Gilman, Expert elicitation survey predicts 37% to 49% declines in wind energy costs by 2050, *Nat. Energy*. 6 (2021) 555–565. <https://doi.org/10.1038/s41560-021-00810-z>.
- [250] M. Ram, D. Bogdanov, A. Aghahosseini, A. Gulagi, S.A. Oyewo, M. Child, U. Caldera, K. Sadovskaia, J. Farfan, L.S.N.S. Barbosa, M. Fasihi, S. Khalili, C. Breyer, Global Energy System based on 100% Renewable Energy – Power, Heat, Transport and Desalination Sectors. Study by Lappeenranta University of Technology and Energy Watch Group, Lappeenranta, Berlin, 2019.
- [251] W. Cole, A.W. Frazier, C. Augustine, Cost Projections for Utility-Scale Battery Storage: 2021 Update, 2021.
- [252] C. van Leeuwen, A. Zauner, Innovative large-scale energy storage technologies and Power-to-Gas concepts after optimisation - D8.3, 2018.
- [253] D. Sadler, H.S. Anderson, M. Sperrink, A. Cargill, M. Sjøvoll, K.I. Asen, J.E. Finnesand, T. Melien, R. Thorsen, L. Hagesaether, P. Ringrose, B. Nazarian, H.H. Kvadsheim, H21 North Of England, 2018.
- [254] IEA, IEA G20 Hydrogen report: Assumptions annex, 2020.
- [255] M. Deutsch, S. Andreaola, C. Menos-Aikateriniadis, A. Paxton, H. Preißler, H. Miebling, M. Rehn, R. Sarsfield-Hall, B. Unger, G. Flis, No-regret hydrogen. Charting early steps for H<sub>2</sub> infrastructure in Europe, 2021.
- [256] S. Bruce, M. Temminghoff, J. Hayward, E. Schmidt, C. Munnings, D. Palfreyman, P. Hartley, National Hydrogen Roadmap, 2018.
- [257] K. Stolzenburg, R. Hamelmann, M. Wietschel, F. Genoese, J. Michaelis, J. Lehmann, A. Miede, S. Krause, C. Sponholz, S. Donadei, F. Crotogino, A. Acht, P.-L. Horvath, Integration von Wind-Wasserstoff-Systemen in das Energiesystem - Abschlussbericht, 2014.
- [258] International Energy Agency, Global Hydrogen Review 2021, 2021. <https://doi.org/10.1787/39351842-en>.
- [259] B. James, W. Colella, J. Moton, G. Saur, T. Ramsden, PEM Electrolysis H2A Production Case Study Documentation, 2013.
- [260] DNV, Hydrogen Forecast to 2050 - Energy Transition Outlook 2022, 2022.
- [261] International Energy Agency, Hydrogen in North-Western Europe.: A vision towards 2030, 2021.
- [262] H.A. Khan, R. Daiyan, Z. Han, M. Hablutzel, N. Haque, R. Amal, Designing optimal integrated electricity supply configurations for renewable hydrogen generation in Australia, *IScience*. 24 (2021) 102539. <https://doi.org/10.1016/j.isci.2021.102539>.
- [263] K. Reddi, A. Elgowainy, D.R. Brown, Hydrogen Delivery Infrastructure Analysis, 2016. <https://doi.org/10.13140/RG.2.1.5159.8964>.
- [264] W. Krewitt, S. Schmid, CASCADE Mints - D1.1 Fuel cell technologies and H2 production/distribution options, 2005.
- [265] A. Léon, Hydrogen Technology - Mobile and Portable Applications, Springer-Verlag Berlin Heidelberg GmbH, 2008.
- [266] C. Yang, J.M. Ogden, Analyzing Natural Gas Based Hydrogen Infrastructure - Optimizing Transitions from Distributed to Centralized H2 Production, 2005.
- [267] E.L. Broerman, N. Shade, K. Brun, J. Bennett, N. Poerner, D. Strickland, J. Helffrich, S. Coogan, A. Rimpel, P. Bueno, Hydrogen Compression Application of the Linear Motor Reciprocating Compressor (LMRC), 2015.
- [268] Ø. Ulleberg, T. Nakken, A. Eté, The wind/hydrogen demonstration system at Utsira in Norway: Evaluation of system performance using operational data and updated hydrogen energy system modeling tools, *Int. J. Hydrogen Energy*. 35 (2010) 1841–1852. <https://doi.org/10.1016/j.ijhydene.2009.10.077>.
- [269] S. Song, H. Lin, P. Sherman, X. Yang, C.P. Nielsen, X. Chen, M.B. McElroy, Production of hydrogen from offshore wind in China and cost-competitive supply to Japan, *Nat. Commun*. 12 (2021) 10–17. <https://doi.org/10.1038/s41467-021-27214-7>.
- [270] C. Hank, A. Sternberg, N. Köppel, M. Holst, T. Smolinka, A. Schaadt, C. Hebling, H.M. Henning, Energy efficiency and economic assessment of imported energy carriers based on renewable electricity, *Sustain. Energy Fuels*. 4 (2020) 2256–2273. <https://doi.org/10.1039/d0se00067a>.
- [271] D. Teichmann, W. Arlt, P. Wasserscheid, Liquid Organic Hydrogen Carriers as an efficient vector for the transport and storage of renewable energy, *Int. J. Hydrogen Energy*. 37 (2012) 18118–18132. <https://doi.org/10.1016/j.ijhydene.2012.08.066>.
- [272] R. d'Amore-Domenech, T.J. Leo, B.G. Pollet, Bulk power transmission at sea: Life cycle cost comparison of electricity and hydrogen as energy vectors, *Appl. Energy*. 288 (2021) 116625. <https://doi.org/10.1016/j.apenergy.2021.116625>.

- [273] R. Stevenson, A. Leadbetter, L. Day, Project HySecure Phase 1 Summary Sept 2019, 2019.
- [274] O. Kruck, F. Crotochino, R. Prelicz, T. Rudolph, Overview on all Known Underground Storage Technologies for Hydrogen, 2013.
- [275] Deutsches Zentrum für Luft- und Raumfahrt, Ludwig Bölkow Systemtechnik, Fraunhofer ISE, KBB Underground Technologies, Studie über die Planung einer Demonstrationsanlage zur Wasserstoff-Kraftstoffgewinnung durch Elektrolyse mit Zwischenspeicherung in Salzkavernen unter Druck, 2014.
- [276] A. Le Duigou, A.-G. Bader, J.-C. Lanoix, L. Nadau, Relevance and costs of large scale underground hydrogen storage in France, *Int. J. Hydrogen Energy*. 42 (2017) 22987–23003. <https://doi.org/10.1016/j.ijhydene.2017.06.239>.
- [277] G. Parks, R. Boyd, J. Cornish, R. Remick, Hydrogen Station Compression, Storage, and Dispensing - Technical Status and Costs, 2014.
- [278] R. van Gerwen, M. Eijgelaar, T. Bosma, Hydrogen in the electricity value chain, 2019.
- [279] E.I. Zoulias, R. Glockner, N. Lymberopoulos, T. Tsoutsos, I. Vosseler, O. Gavalda, H.J. Mydske, P. Taylor, Integration of hydrogen energy technologies in stand-alone power systems analysis of the current potential for applications, *Renew. Sustain. Energy Rev.* 10 (2006) 432–462. <https://doi.org/10.1016/j.rser.2004.10.001>.
- [280] S. Karellas, N. Tzouganatos, Comparison of the performance of compressed-air and hydrogen energy storage systems: Karpathos island case study, *Renew. Sustain. Energy Rev.* 29 (2014) 865–882. <https://doi.org/10.1016/j.rser.2013.07.019>.
- [281] S. Carr, G.C. Premier, A.J. Guwy, R.M. Dinsdale, J. Maddy, Hydrogen storage and demand to increase wind power onto electricity distribution networks, *Int. J. Hydrogen Energy*. 39 (2014) 10195–10207. <https://doi.org/10.1016/j.ijhydene.2014.04.145>.
- [282] R. Ortiz Cebolla, F. Dolci, E. Weidner, Assessment of Hydrogen Delivery Options: Feasibility of Transport of Green Hydrogen within Europe, 2022. <https://doi.org/10.2760/869085>.
- [283] M. Niermann, S. Timmerberg, S. Drünert, M. Kaltschmitt, Liquid Organic Hydrogen Carriers and alternatives for international transport of renewable hydrogen, *Renew. Sustain. Energy Rev.* 135 (2021) 110171. <https://doi.org/10.1016/j.rser.2020.110171>.
- [284] F. Merten, A. Scholz, C. Krüger, S. Heck, Y. Girard, M. Mecke, M. George, Bewertung der Vor- und Nachteile von Wasserstoffimporten im Vergleich zur heimischen Erzeugung, Wuppertal, 2020.
- [285] G. Brändle, M. Schönfisch, S. Schulte, Estimating long-term global supply costs for low-carbon hydrogen, *Appl. Energy*. 302 (2021) 117481. <https://doi.org/10.1016/j.apenergy.2021.117481>.
- [286] M. Al-breiki, Y. Bicer, Comparative cost assessment of sustainable energy carriers produced from natural gas accounting for boil-off gas and social cost of carbon, *Energy Reports*. 6 (2020) 1897–1909. <https://doi.org/10.1016/j.egyr.2020.07.013>.
- [287] Chemical Engineering, The Chemical Engineering Plant Cost Index, (2022). <https://www.chemengonline.com/pci-home> (accessed August 8, 2022).
- [288] U. Caldera, C. Breyer, Assessing the potential for renewable energy powered desalination for the global irrigation sector, *Sci. Total Environ.* 694 (2019) 133598. <https://doi.org/10.1016/j.scitotenv.2019.133598>.
- [289] IRENA, Renewable Power Generation Costs in 2020, Abu Dhabi, 2021.
- [290] Danish Energy Agency, Deutsche Energie-Agentur, China National Renewable Energy Centre, Distributed Wind and PV in Denmark and Germany, 2019.
- [291] A. Shepherd, S. Roberts, G. Sünnerberg, A. Lovett, A.F.S. Hastings, Scotland's onshore wind energy generation, impact on natural capital & satisfying no-nuclear energy policy, *Energy Reports*. 7 (2021) 7106–7117. <https://doi.org/10.1016/j.egyr.2021.10.063>.
- [292] European Environment Agency, Europe's onshore and offshore wind energy potential, 2009.
- [293] 4C Offshore, Global Offshore Renewable Map, (2022). <https://map.4coffshore.com/offshorewind/> (accessed December 21, 2022).
- [294] I. Staffell, S. Pfenninger, Using bias-corrected reanalysis to simulate current and future wind power output, *Energy*. 114 (2016) 1224–1239. <https://doi.org/10.1016/j.energy.2016.08.068>.
- [295] S. Pfenninger, I. Staffell, Long-term patterns of European PV output using 30 years of validated hourly reanalysis and satellite data, *Energy*. 114 (2016) 1251–1265. <https://doi.org/10.1016/j.energy.2016.08.060>.
- [296] E. Gaertner, J. Rinker, L. Sethuraman, B. Anderson, F. Zahle, G. Barter, N. Abbas, F. Meng, P. Bortolotti, W. Skrzypinski, G. Scott, R. Feil, H. Bredmose, K. Dykes, M. Shields, C. Allen, A. Viselli, Definition of the IEA 15-Megawatt Offshore Reference Wind Turbine, 2020.
- [297] National Renewable Energy Laboratory, Onshore Wind Turbine Documentation: 2020ATB\_NREL\_Reference\_7MW\_200, (2020). [https://nrel.github.io/turbine-models/2020ATB\\_NREL\\_Reference\\_7MW\\_200.html#references](https://nrel.github.io/turbine-models/2020ATB_NREL_Reference_7MW_200.html#references) (accessed November 12, 2022).
- [298] R. Wiser, M. Bolinger, B. Hoen, Land-based wind market report: 2022 edition, 2022.
- [299] C. Lohr, F. Peterssen, M. Schlemminger, A. Bensmann, R. Niepelt, R. Brendel, R. Hanke-Rauschenbach, Multi-criteria energy system analysis of onshore wind power distribution in climate-neutral Germany, SSRN. (2023). <https://doi.org/10.2139/ssrn.4367164>.

- [300] M. Bolinger, G. Bolinger, Land Requirements for Utility-Scale PV : An Empirical Update on Power and Energy Density, *IEEE J. Photovoltaics*. 12 (2022) 589–594. <https://doi.org/10.1109/JPHOTOV.2021.3136805>.
- [301] D.G. Caglayan, N. Weber, H.U. Heinrichs, J. Linßen, M. Robinus, P.A. Kukla, D. Stolten, Technical potential of salt caverns for hydrogen storage in Europe, *Int. J. Hydrogen Energy*. 45 (2020) 6793–6805. <https://doi.org/10.1016/j.ijhydene.2019.12.161>.
- [302] IRENA, Global hydrogen trade to meet the 1.5 °C climate goal: Part I – Trade outlook for 2050 and way forward, Abu Dhabi, 2022.
- [303] BloombergNEF, Hydrogen Economy Outlook - Key messages, 2020.
- [304] IRENA, Global hydrogen trade to meet the 1.5 °C climate goal: Part II – Technology review of hydrogen carriers, Abu Dhabi, 2022.
- [305] J. Hoelzen, D. Silberhorn, F. Schenke, E. Stabenow, A. Bensmann, T. Zill, R. Hanke-Rauschenbach, H<sub>2</sub>-powered aviation – Optimized aircraft designs and green LH<sub>2</sub> supply chains in air transport networks, *Publ. Process.* (2023).
- [306] M. Alderighi, A. Cento, P. Nijkamp, P. Rietveld, Assessment of new hub-and-spoke and point-to-point airline network configurations, *Transp. Rev.* 27 (2007) 529–549. <https://doi.org/10.1080/01441640701322552>.
- [307] EUROCONTROL, European Aviation Overview - 9th February 2023, 2023.
- [308] Flightradar24, Live Flight Tracker, (2023). <https://www.flightradar24.com/> (accessed February 2, 2023).
- [309] A. Bensmann, J. Brandt, T. Iversen, C. Eckert, F. Peterssen, B. Bensmann, M. Beer, H. Weyer, R. Hanke-Rauschenbach, Cost and competitiveness of green hydrogen in Europe: Effects of the European Union regulatory framework, *Res. Sq. in publica* (2023). <https://doi.org/10.21203/rs.3.rs-3164444/v1> License:
- [310] International Energy Agency, Norway 2022 - Energy Policy Review, 2022.
- [311] D. Bogdanov, M. Ram, A. Aghahosseini, A. Gulagi, A.S. Oyewo, M. Child, U. Caldera, K. Sadovskaia, J. Farfan, L. De Souza Noel Simas Barbosa, M. Fasihi, S. Khalili, T. Traber, C. Breyer, Low-cost renewable electricity as the key driver of the global energy transition towards sustainability, *Energy*. 227 (2021) 120467. <https://doi.org/10.1016/j.energy.2021.120467>.
- [312] G. Kakoulaki, I. Kougias, N. Taylor, F. Dolci, J. Moya, A. Jäger-Waldau, Green hydrogen in Europe – A regional assessment: Substituting existing production with electrolysis powered by renewables, *Energy Convers. Manag.* 228 (2021). <https://doi.org/10.1016/j.enconman.2020.113649>.
- [313] IRENA, Geopolitics of the Energy Transformation: The Hydrogen Factor, Abu Dhabi, 2022.
- [314] D. Bogdanov, M. Child, C. Breyer, Reply to 'Bias in energy system models with uniform cost of capital assumption,' *Nat. Commun.* 10 (2019) 1–2. <https://doi.org/10.1038/s41467-019-12469-y>.
- [315] EUROCONTROL, Fuel Tankering: economic benefits and environmental impact, 2019.
- [316] Umweltbundesamt, Deutsche Emissionshandelsstelle, Emissionshandel im Luftverkehr, Berlin, 2023.
- [317] A. van Velzen, Environmental and economic impacts of EU ETS and CORSIA policy scenarios for European aviation, Utrecht, 2022.
- [318] IRENA, Accelerating Hydrogen Deployment in the G7: Recommendations for the Hydrogen Action Pact, Abu Dhabi, 2022.
- [319] T. Bollerhey, M. Exenberger, F. Geyer, K. Westphal, H<sub>2</sub>GLOBAL – Idea, Instrument and Intentions, Hamburg, 2023.
- [320] M. Beltramo, D. Trapp, B. Kimoto, D. Marsh, Parametric Study of Transport Aircraft Systems Cost and Weight, NASA, 1977.
- [321] L.R. Jenkinson, P. Simpkin, D. Rhodes, Civil Jet Aircraft Design, Arnold, a member of the Hodder Headline Group, London, 1999.
- [322] M. Mottschall, P. Kasten, S. Kühnel, L. Minnich, Sensitivitäten zur Bewertung der Kosten verschiedener Energieversorgungsoptionen des Verkehrs bis zum Jahr 2050 - Abschlussbericht, 2019.
- [323] D. Seider, M. Litz, M. Mischke, P. Kroll, RCE: Distributed, Collaborative Problem Solving Environment, 2012.
- [324] S. Woehler, G. Atanasov, D. Silberhorn, B. Fröhler, T. Zill, Preliminary Aircraft Design within a Multidisciplinary and Multifidelity Design Environment, in: *Proc. Aerosp. Eur. Conf. Bordeaux (France)*, Febr., 2020.
- [325] M. Alder, E. Moerland, J. Jepsen, B. Nagel, Recent Advances in Establishing a Common Language for Aircraft Design with CPACS, *Proc. Aerosp. Eur. Conf.* (2020) 1–14. <https://elib.dlr.de/134341/>.
- [326] Airbus SAS, Airbus A320 - Aircraft Characteristics, Airport and Maintenance Planning, 2020.
- [327] R. O'Hayre, S.-W. Cha, W.G. Colella, F.B. Prinz, Fuel Cell Fundamentals, 3rd Editio, John Wiley & Sons, New Jersey, 2016.
- [328] C. Winnefeld, T. Kadyk, R. Hanke-Rauschenbach, Modelling and Designing Cryogenic Hydrogen Tanks for Future Aircraft Applications, *Energies*. 11 (2018) 1–23. <https://doi.org/10.3390/en11010105>.
- [329] Fraport AG, Frankfurt Airport Luftverkehrsstatistik 2019, Frankfurt am Main, 2020.



- [330] A.B. Graver, K. Zhang, D. Rutherford, CO2 Emissions from Commercial Aviation , 2018, 2019.
- [331] European Environment Agency, 1.A.3.a Aviation 1 Master emissions calculator 2019, (2019).
- [332] Embraer Commercial Aviation, Market outlook 2020, 2020.
- [333] Airfleets.net, Production list of aircraft, (2021). <https://www.airfleets.net> (accessed August 3, 2021).
- [334] Aviation Week Intelligence Network, AWIN Market Analysis - Commercial Aviation, August 2021, 2021.
- [335] Airbus SAS, Global Market Forecast 2019-2038, 2019.
- [336] K. Seeckt, D. Scholz, Jet versus prop, hydrogen versus kerosene for a regional freighter aircraft, Dtsch. Luft- Und Raumfahrtkongress 2009. (2009).
- [337] C. Wilson, Up-scaling , formative phases , and learning in the historical diffusion of energy technologies, *Energy Policy*. 50 (2012) 81–94. <https://doi.org/10.1016/j.enpol.2012.04.077>.
- [338] J.A. Hayward, P.W. Graham, A global and local endogenous experience curve model for projecting future uptake and cost of electricity generation technologies, *Energy Econ*. 40 (2013) 537–548. <https://doi.org/10.1016/j.eneco.2013.08.010>.
- [339] E.S. Rubin, I.M.L. Azevedo, P. Jaramillo, S. Yeh, A review of learning rates for electricity supply technologies, *Energy Policy*. 86 (2015) 198–218. <https://doi.org/10.1016/j.enpol.2015.06.011>.
- [340] F. Pieper, Das Konzept von Lernkurven im Energiesektor — Beschreibung , Modellierung und Aggregation Diplomarbeit, (2003).
- [341] IEA, Experience Curves for Energy Technology Policy, 2000.
- [342] Hydrogen Council and McKinsey & Company, Hydrogen for Net-Zero: A critical cost-competitive energy vector, 2021.
- [343] P. Graham, J. Hayward, J. Foster, L. Havas, GenCost 2021-22: Final report, 2022.
- [344] A. Mayyas, M. Ruth, B. Pivovar, G. Bender, K. Wipke, Manufacturing Cost Analysis for Proton Exchange Membrane Water Electrolyzers, 2019.
- [345] M. Fette, C. Brandstaett, L. Kimmer, C. Rickert, I. Roller, H.C. Gils, H. Gardian, T. Pregger, F. Cebulla, E. Meyer, J. Schaffert, E. Tali, N. Bruecken, M. Koepcke, N. Duenne, S. von Berg, Multi-Sektor-Kopplung - Modellbasierte Analyse der Integration Erneuerbarer Stromerzeugung durch die Kopplung der Stromversorgung mit dem Wärme, Gas- und Verkehrssektor, 2020.
- [346] E. Rinne, H. Holttinen, J. Kiviluoma, S. Rissanen, Effects of turbine technology and land use on wind power resource potential, *Nat. Energy*. 3 (2018) 494–500. <https://doi.org/10.1038/s41560-018-0137-9>.
- [347] R.J. Barthelmie, L.E. Jensen, Evaluation of wind farm efficiency and wind turbine wakes at the Nysted offshore wind farm, *Wind Energy*. 13 (2010) 573–586. <https://doi.org/10.1002/we.408>.
- [348] H. Yang, K. Xie, H.M. Tai, Y. Chai, Wind Farm Layout Optimization and Its Application to Power System Reliability Analysis, *IEEE Trans. Power Syst*. 31 (2016) 2135–2143. <https://doi.org/10.1109/TPWRS.2015.2452920>.
- [349] P. Gebraad, J.J. Thomas, A. Ning, P. Fleming, K. Dykes, Maximization of the annual energy production of wind power plants by optimization of layout and yaw-based wake control, *Wind Energy*. 20 (2017) 97–107. <https://doi.org/10.1002/we.1993>.
- [350] S. Krohn, P.-E. Morthorst, S. Awerbuch, The Economics of Wind Energy, 2009. <https://doi.org/10.1111/j.1745-6622.2009.00231.x>.
- [351] M. Wagner, F. Neumann, U.O. Reilly, Optimizing the Layout of 1000 Wind Turbines Massachusetts Institute of Technology, *Eur. Wind Energy Assoc. Annu. Event*. (2011) 10. <https://domino.mpi-sb.mpg.de/intranet/ag1/ag1publ.nsf/0/08f2e8f1d20ab7fec125785d00343a1b?OpenDocument>.
- [352] T. Sørensen, P. Nielsen, M.L. Thøgersen, Recalibrating wind turbine wake model parameters - Validating the wake model performance for Large offshore Wind Farms, *Eur. Wind Energy Conf. Exhib*. 2006, EWEC 2006. 2 (2006) 1660–1665.
- [353] Y.K. Wu, Y.S. Su, T.Y. Wu, Z.J. Lee, Estimation of wake losses in an offshore wind farm by WAsP - A real project case study in Taiwan, *IET Semin. Dig*. 2015 (2015). <https://doi.org/10.1049/ic.2015.0264>.
- [354] A. Penã, K. Schaldemose Hansen, S. Ott, M. Paul Van Der Laan, On wake modeling, wind-farm gradients, and AEP predictions at the Anholt wind farm, *Wind Energy Sci*. 3 (2018) 191–202. <https://doi.org/10.5194/wes-3-191-2018>.
- [355] S. Rehman, A.B. Mohammed, L. Alhems, A heuristic approach to siting and design optimization of an onshore wind farm layout, *Energies*. 13 (2020). <https://doi.org/10.3390/en13225946>.
- [356] P. Härtel, T.K. Vrana, T. Hennig, M. von Bonin, E.J. Wiggelinkhuizen, F.D.J. Nieuwenhout, Review of investment model cost parameters for VSC HVDC transmission infrastructure, *Electr. Power Syst. Res*. 151 (2017) 419–431. <https://doi.org/10.1016/j.epsr.2017.06.008>.
- [357] W. Gorman, A. Mills, R. Wiser, Improving estimates of transmission capital costs for utility-scale wind and solar projects to inform renewable energy policy, *Energy Policy*. 135 (2019). <https://doi.org/10.1016/j.enpol.2019.110994>.
- [358] P. Godron, J. Neubarth, M. Soyah, V. Asceri, G. Callegari, B. Cova, F. Banez, L. Olmos, A. Ramos, M. Rivier, *Desert Power: Getting connected*, 2014.
- [359] A. Mills, R. Wiser, K. Porter, The cost of transmission for wind energy in the United States: A review of transmission planning studies, *Renew. Sustain. Energy Rev*. 16 (2012) 1–19.

- <https://doi.org/10.1016/j.rser.2011.07.131>.
- [360] B. Miao, L. Giordano, S.H. Chan, Long-distance renewable hydrogen transmission via cables and pipelines, *Int. J. Hydrogen Energy*. 46 (2021) 18699–18718. <https://doi.org/10.1016/j.ijhydene.2021.03.067>.
- [361] M. Fasihi, C. Breyer, Baseload electricity and hydrogen supply based on hybrid PV-wind power plants, *J. Clean. Prod.* 243 (2020) 118466. <https://doi.org/10.1016/j.jclepro.2019.118466>.
- [362] K. Schaber, F. Steinke, P. Mühlich, T. Hamacher, Parametric study of variable renewable energy integration in Europe: Advantages and costs of transmission grid extensions, *Energy Policy*. 42 (2012) 498–508. <https://doi.org/10.1016/j.enpol.2011.12.016>.
- [363] S. Lauria, M. Schembari, F. Palone, M. Maccioni, Very long distance connection of gigawattsize offshore wind farms: Extra high-voltage AC versus high-voltage DC cost comparison, *IET Renew. Power Gener.* 10 (2016) 713–720. <https://doi.org/10.1049/iet-rpg.2015.0348>.
- [364] D. Schönberger, P2G durch Elektrolyse – eine flexible Speicherlösung, 2016.
- [365] M. Holst, S. Aschbrenner, T. Smolinka, C. Voglstätter, G. Grimm, Cost Forecast for Low Temperature Electrolysis - Technology Driven Bottom-up Prognosis for PEM and Alkaline Water Electrolysis Systems, 2021.
- [366] F. Saravia, F. Graf, S. Schwarz, F. Gröschl, Genügend Wasser für die Elektrolyse - Wieviel Wasser wird für die Erzeugung von grünem Wasserstoff benötigt und gibt es ausreichende Ressourcen?, n.d.
- [367] R. Groenenberg, J. Juez-Larré, C. Goncalvez, L. Wasch, H. Dijkstra, B. Wassing, B. Orlic, K. Van Der Valk, T.H. Van Der Meulen, K. Kranenburg-Bruinsma, *Techno-Economic Modelling of Large-Scale Energy Storage Systems*, Utrecht, 2020.
- [368] M.R. Gardiner, Energy requirements for hydrogen gas compression and liquefaction as related to vehicle storage needs, 2009.
- [369] U. Cardella, L. Decker, J. Sundberg, H. Klein, Process optimization for large-scale hydrogen liquefaction, *Int. J. Hydrogen Energy*. 42 (2017) 12339–12354. <https://doi.org/10.1016/j.ijhydene.2017.03.167>.
- [370] U. Cardella, L. Decker, H. Klein, Economically viable large-scale hydrogen liquefaction, *IOP Conf. Ser. Mater. Sci. Eng.* 171 (2017). <https://doi.org/10.1088/1757-899X/171/1/012013>.
- [371] I.H. Bell, J. Wronski, S. Quoilin, V. Lemort, Pure and pseudo-pure fluid thermophysical property evaluation and the open-source thermophysical property library coolprop, *Ind. Eng. Chem. Res.* 53 (2014) 2498–2508. <https://doi.org/10.1021/ie4033999>.
- [372] E. Connelly, M. Penev, A. Elgowainy, C. Hunter, DOE Hydrogen and Fuel Cells Program Record 19001, Department of Energy - United States of America, 2019.
- [373] K. Ohlig, L. Decker, The latest developments and outlook for hydrogen liquefaction technology, *AIP Conf. Proc.* 1573 (2014) 1311–1317. <https://doi.org/10.1063/1.4860858>.
- [374] S. Krasae-in, ScienceDirect Optimal operation of a large-scale liquid hydrogen plant utilizing mixed fluid refrigeration system, *Int. J. Hydrogen Energy*. 39 (2014) 7015–7029. <https://doi.org/10.1016/j.ijhydene.2014.02.046>.
- [375] K. Ohira, A Summary of Liquid Hydrogen and Cryogenic Technologies in Japan's WE-NET Project, *AIP Conf. Proc.* 710 (2004). <https://doi.org/10.1063/1.1774663>.
- [376] H. Quack, Conceptual design of a high efficiency large capacity hydrogen liquefier, *AIP Conf. Proc.* 613 (2002). <https://doi.org/10.1063/1.1472029>.
- [377] U.S. Energy Information Administration, Hydrocarbon gas liquids explained - prices for hydrocarbon gas liquids, (2022). <https://www.eia.gov/energyexplained/hydrocarbon-gas-liquids/prices-for-hydrocarbon-gas-liquids.php> (accessed January 2, 2023).
- [378] M.T. Syed, S.A. Sherif, T.N. Veziroglu, J.W. Sheffield, An Economic Analysis of Three Hydrogen Liquefaction Systems, *Int. J. Hydrogen Energy*. 23 (1998) 565–576.
- [379] L. Decker, Liquid Hydrogen Distribution Technology - HYPER closing seminar, 2019.
- [380] T. Barckholtz, A. Burgunder, D. Casey, S. Dillich, A. Elgowainy, J. Merritt, G. Parks, S. Pawel, J. Simnick, H. Soto, E. Sutherland\*, *Hydrogen Delivery Technical Team Roadmap*, Washington DC, 2013. <https://doi.org/https://doi.org/10.2172/1220133>.
- [381] A. Züttel, Materials for hydrogen storage, *Mater. Today*. 6 (2003) 24–33. [https://doi.org/10.1016/S1369-7021\(03\)00922-2](https://doi.org/10.1016/S1369-7021(03)00922-2).
- [382] J. Mischner, H.-G. Fasold, J. Heymer, *Systemplanerische Grundlagen der Gasversorgung*, 2015.
- [383] J. Mischner, Fluidynamische Berechnung von Hochdruckgasleitungen, in: H.-B. Horlacher, U. Helbig (Eds.), *Rohrleitungen 2 Einsatz, Verlegung, Berechnung, Rehabil.*, Springer Vieweg, Heidelberg, 2018: pp. 587–622. [https://doi.org/10.1007/978-3-662-50355-3\\_103](https://doi.org/10.1007/978-3-662-50355-3_103).
- [384] M. Schmied, W. Knörr, *Carbon Footprint - Teilgutachten "Monitoring für den CO<sub>2</sub>-Ausstoß in der Logistikkette*, 2012.
- [385] A. Roth, R. Brückmann, M. Jimeno Mak Đukan, L. Kitzing Barbara Breitschopf, A. Alexander-Haw Ana Lucia Amazo Blanco, G. Resch, D5.2, *Renewable energy financing conditions in Europe: survey and impact analysis*, 2021.
- [386] IRENA, *The cost of financing for renewables*, Abu Dhabi, 2023.

- [387] J. Terrapon-Pfaff, M. Prantner, S.R. Ersoy, Risikobewertung und Risikokostenanalyse der MENA-Region. MENA-Fuels: Teilbericht 8 des Wuppertal Instituts an das Bundesministerium für Wirtschaft und Klimaschutz (BMWK), Wuppertal, Stuttgart, Köln, Saarbrücken, 2022.
- [388] J. Simon, A.M. Ferriz, L.C. Correias, HyUnder - Hydrogen underground storage at large scale: Case study Spain, *Energy Procedia*. 73 (2015) 136–144. <https://doi.org/10.1016/j.egypro.2015.07.661>.
- [389] J. Cihlar, D. Mavins, K. van der Leun, Picturing the value of underground gas storage to the European hydrogen system, 2021.
- [390] T. Burschky, Y. Cabac, D. Silberhorn, Liquid hydrogen storage design trades for a short-range aircraft concept, Dtsch. Luft- Und Raumfahrtkongress 2021. (2021).
- [391] T. Burschky, D. Silberhorn, J. Wehrspohn, T. Zill, Scenario-based implications of liquid hydrogen storage tank insulation quality for a short-range aircraft concept, *AIAA Aviat. 2023 Forum*. (2023) 1–21. <https://doi.org/10.2514/6.2023-3522>.
- [392] F.G. Albrecht, T. Van Nguyen, Prospects of electrofuels to defossilize transportation in Denmark – A techno-economic and ecological analysis, *Energy*. 192 (2020) 116511. <https://doi.org/10.1016/j.energy.2019.116511>.
- [393] S. Schemme, J.L. Breuer, M. Köller, S. Meschede, F. Walman, R.C. Samsun, R. Peters, D. Stolten, H<sub>2</sub>-based synthetic fuels: A techno-economic comparison of alcohol, ether and hydrocarbon production, *Int. J. Hydrogen Energy*. 45 (2020) 5395–5414. <https://doi.org/10.1016/j.ijhydene.2019.05.028>.
- [394] M. Cames, S. Chaudry, K. Gockeler, P. Kasten, S. Kurth, E-Fuels versus DACCS, 2021.
- [395] M. Ozkan, S.P. Nayak, A.D. Ruiz, W. Jiang, Current status and pillars of direct air capture technologies, *IScience*. 25 (2022) 103990. <https://doi.org/10.1016/j.isci.2022.103990>.
- [396] M. Fasihi, O. Efimova, C. Breyer, Techno-economic assessment of CO<sub>2</sub> direct air capture plants, *J. Clean. Prod.* 224 (2019) 957–980. <https://doi.org/10.1016/j.jclepro.2019.03.086>.
- [397] K. Madhu, S. Pauliuk, S. Dhathri, F. Creutzig, Understanding environmental trade-offs and resource demand of direct air capture technologies through comparative life-cycle assessment, *Nat. Energy*. 6 (2021) 1035–1044. <https://doi.org/10.1038/s41560-021-00922-6>.
- [398] D. Heß, M. Klumpp, R. Dittmeyer, Nutzung von CO<sub>2</sub> aus Luft als Rohstoff für synthetische Kraftstoffe und Chemikalien, 2020.
- [399] D.H. König, Techno-ökonomische Prozessbewertung der Herstellung synthetischen Flugturbinentreibstoffes aus CO<sub>2</sub> und H<sub>2</sub>, Universität Stuttgart, 2016.
- [400] S. Brynolf, M. Taljegard, M. Grahn, J. Hansson, Electrofuels for the transport sector: A review of production costs, *Renew. Sustain. Energy Rev.* 81 (2018) 1887–1905. <https://doi.org/10.1016/j.rser.2017.05.288>.
- [401] S. Drünert, U. Neuling, T. Zitscher, M. Kaltschmitt, Power-to-Liquid fuels for aviation – Processes, resources and supply potential under German conditions, *Appl. Energy*. 277 (2020) 115578. <https://doi.org/10.1016/j.apenergy.2020.115578>.
- [402] P. Runge, C. Sölch, J. Albert, P. Wasserscheid, G. Zöttl, V. Grimm, Economic comparison of different electric fuels for energy scenarios in 2035, *Appl. Energy*. 233–234 (2019) 1078–1093. <https://doi.org/10.1016/j.apenergy.2018.10.023>.
- [403] Haldor Tapsoe, Sasol, Expect more... by turning green energy into fuels G2LTM eFuels – a business ready solution, 2021.
- [404] L. Sens, U. Neuling, K. Wilbrand, M. Kaltschmitt, Conditioned hydrogen for a green hydrogen supply for heavy duty-vehicles in 2030 and 2050 – A techno-economic well-to-tank assessment of various supply chains, *Int. J. Hydrogen Energy*. (2022). <https://doi.org/10.1016/j.ijhydene.2022.07.113>.
- [405] M. Fasihi, D. Bogdanov, C. Breyer, Techno-Economic Assessment of Power-to-Liquids (PtL) Fuels Production and Global Trading Based on Hybrid PV-Wind Power Plants, *Energy Procedia*. 99 (2016) 243–268. <https://doi.org/10.1016/j.egypro.2016.10.115>.
- [406] MAN Energy Solutions, Propulsion trends in tankering, Copenhagen, 2021.
- [407] M. Pfennig, N. Gerhardt, C. Pape, D. Böttger, Mittel- und langfristige Potenziale von PtL- und H<sub>2</sub>-Importen aus internationalen EE-Vorzugsregionen. Teilbericht im Rahmen des Projektes: KLIMAWIRKSAMKEIT ELEKTROMOBILITÄT - Entwicklungsoptionen des Straßenverkehrs unter Berücksichtigung der Rückkoppl., (2017).
- [408] NISO, CRediT: Contributor Roles Taxonomy, (2023). <https://credit.niso.org/> (accessed August 8, 2023).